Linking ageing and arthritis: The role of the longevity-related SIRT1 molecule in age-related cartilage degeneration and osteoarthritis



Pradeep Kumar Sacitharan

University College

Supervisors

Dr James Edwards

Professor Tonia Vincent

A thesis submitted for the degree of

Doctor of Philosophy in Molecular and Cellular Medicine

Acknowledgments

The last four years in Oxford have been some of the best of my life. I have grown as an individual and more importantly built a strong foundation to be scientist. My growth and success over these would not be possible without the support, encouragement and mentorship from so many individuals.

I feel privileged to have worked with both my academic supervisors. I am indebted to Professor Tonia Vincent for all her guidance and support. I have learnt a great deal from her critical and analytical approach to scientific thinking and from her vast experience in the field. I am also equally indebted to Dr James Edwards for all his guidance and support from whom I have learnt the art of creativity, efficiency and planning in science. Both supervisors have always given me freedom to express my thoughts and articulate my ideas to wide audiences which has been truly enjoyable. In addition, I would like to thank Professor Claire Edwards too for her support over the years. I also have been lucky to have worked in two lab groups consisting of great individuals whom have supported me over the years and I would like to thank them wholeheartedly.

I would like to thank the Kennedy Trust for funding my D.Phil and Arthritis Research UK for funding the Osteoarthritis Centre of Pathogenesis. I have been privileged to work at The Kennedy Institute of Rheumatology and Nuffield Department of Orthopaedics Rheumatology and Musculoskeletal Sciences both which are filled with talented and kind individuals from a wide array of specialities. Collaborations and conversations with everyone at the department made me think laterally about science and broaden my outlook in life. In my time here, I have

also met senior leading scientists and role models whom have inspired me greatly. All these experiences have been invaluable.

My thanks to my friends who have always challenged me, supported me and made me a better person. I feel very lucky to have met three of the brightest, kindest and most talented individuals and my dearest friends in my life; Dr Geoffrey Lee, Dr Anand Segar and Philippos Demetriou … 'the dream team'. Our amazing conversations during curry nights and ice cream evenings have spanned from science to philosophy to politics to the nature of this universe and cannot ever be measured up too.

Finally I would like to thank my family; my brother Vinoth, my mum, my dad, Pooja and her family and my family around the world and especially in Sri Lanka. I thank them for all their support and love over the years. You have supported my dreams and believed in me even when all the odds were against me. Thank you for all your sacrifices. I have only come so far because you were at my side. I hope to make you proud and celebrate more successes with you in the future. I love you all very much.

For my loved ones…

“Dream big, never give in, fight against all the odds and what society denies you , do not listen to the nay sayers or pessimists, believe in a bigger goal, find your talent, then find your passion, ask what you can do for the world and then out work the whole world to achieve your dreams. You have one life make sure you die with no regrets! Greatness is within all of us and greatness awaits you.”

Pradeep Kumar Sacitharan (2016)

Abstract

Linking ageing and arthritis: The role of the longevity-related SIRT1 molecule in age-related cartilage degeneration and osteoarthritis

A thesis submitted for the degree of

Doctor of Philosophy in Molecular and Cellular Medicine

Pradeep Kumar Sacitharan

University College

Hilary Term 2016

Osteoarthritis (OA) is the most common form of arthritis worldwide and is characterised by the progressive degradation of articular cartilage. Ageing is the primary risk factor associated with OA. However, the roles of ageing-related mechanisms in cartilage homeostasis are poorly understood. The class three histone deacetylase, Silent mating type information regulation 2 homolog (SIRT1) has been extensively shown to regulate lifespan in lower organisms and signalling pathways linked to mammalian ageing. My thesis explores the role of Sirtuin 1 in cartilage homeostasis and OA.

I used *in vitro* experiments with chondrocyte cell lines, human clinical samples, novel genetically modified cartilage specific and whole body SIRT1 deficient mice alongside molecular biological tools to investigate my research questions.

Human OA cartilage showed decreased SIRT1 compared to healthy cartilage. Mice with cartilage-specific SIRT1 deletion showed greater cartilage degradation during ageing and in an experimental OA model. *In vitro* and *in vivo* studies showed SIRT1 to directly regulate autophagy in chondrocytes. More importantly, the activation of autophagy using spermidine protected against experimental OA in wild-type mice but not in cartilage-specific SIRT1 deficient mice. In addition, my data revealed whole body SIRT1 deficient mice had increased early joint inflammation in repose to injury but displayed less cartilage loss over time in an experimental OA model.

Together I have shown that SIRT1 declines with age and contributes to OA due to dysregulated autophagy. However, chronic low grade inflammation caused by SIRT1 loss was protective. My data suggest these pathways can be targeted to treat OA.

Statement of Originality

All the work presented in this thesis is my own, except where it has been stated otherwise.

TABLE OF CONTENTS

List of figures xv

List of tables xvii

Abbreviations xviii

1 Introduction 1

1.1 Structure of articular cartilage 2

1.1.1 Histomorphological organization of articular cartilage 2

1.1.2 Chondrocytes 3

1.1.3 Collagens 5

1.1.4 Proteoglycans 6

1.1.5 Other components of articular cartilage 7

1.2 Osteoarthritis 9

1.2.1 Pathophysiology of OA 10

1.2.2 Cytokines 11

1.2.2.1 Proinflammatory cytokines 11

1.2.3 Transforming Growth Factor beta 12

1.2.4 Insulin-like Growth Factor 1 13

1.2.5 MMPs 14

1.2.6 ADAMTS 15

1.2.7 Tissue Inhibitor of Metalloproteinases 16

1.2.8 Mechanical forces 16

1.3 OA disease models 17

1.3.1 Destabilization of medial meniscus 19

1.3.2 Transgenic mice in OA research 20

1.3.3.1 Cre/Lox system 21

1.3.3.2 Inducible Cre/Lox system 21

1.4 Clinical aspects of OA 23

1.4.1 Current treatments for OA 24

1.5 Risk factors of OA 25

1.5.1 Genetics 25

1.5.2 Dietary factors 26

1.5.3 Obesity 28

1.5.4 Gender 28

1.5.5 Mechanical injury 29

1.5.6 Age 29

1.6 Cellular Aging Pathways in OA 31

1.6.1 Sirtuins 32

1.6.2 SIRT1 33

1.6.3 Regulation of SIRT1 34

1.6.3.1 Transcriptional regulation of the SIRT1 gene 34

1.6.3.2 Posttranscriptional regulation of SIRT1 mRNA 35

1.6.3.3 Posttranscriptional regulation of SIRT1 protein 35

1.6.4 SIRT1 Targets 36

1.6.5 SIRT1 and inflammation 38

1.6.6 SIRT1 and aging diseases 38

1.6.6.1 Longevity 38

1.6.6.2 Type 2 Diabetes Mellitus 39

1.6.6.3 Neurological disorders 39

1.6.6.4 Cardiovascular disease 40

1.6.6.5 SIRT1 and OA 40

1.6.7 Autophagy 42

1.6.7.1 Molecular pathway of autophagy 43

1.6.7.2 Autophagy and OA 45

1.6.7.3 Autophagy and SIRT1 46

1.7 Research hypothesis 47

1.8 Research aims 47

2.0 Methods 48

2.1 Isolation of human chondrocytes 49

2.2 Cell culture 49

2.3 SIRT1 small inferencing Ribonucleic Acid transfection 50

2.4 RNA extraction from cell cultures 50

2.5 RT-PCR and quantitative PCR 51

2.6 TaqMan Low Density Array microfluidic cards 51

2.7 Western blot analysis 53

2.8 Drug Treatment 54

2.9 Cell viability assay 54

2.10 Fluorescence-activated cell sorting 55

2.11 Mice and ethics 55

2.12 Generation of cartilage-specific SIRT1 KO mice 55

2.13 Generation of whole body SIRT1 KO mice 56

2.14 Induction of Cre-LoxP recombination 56

2.15 Genotyping of Mice 56

2.16 Validation of Cre expression using ROSA26 reporter mice 57

2.17 RNA extraction from murine tissue 58

2.18 Protein extraction from murine hip avulsion 59

2.19 DMM 59

2.20 Histology 60

2.21 Modified Osteoarthritis Research Society International disease scoring 61

2.22 Synovitis scoring 63

2.23 Spermidine treatment 65

2.24 LC3-GFP Studies 65

2.25 Electron Microscopy 66

2.26 Immunoprecipitation 67

2.27 Immunohistochemistry 67

2.28 Data analysis 68

3. The role of SIRT1 in chondrocytes: *in vitro* 70

3.1 Introduction 71

3.2 Hypothesis 71

3.3 Results 73

3.3.1 Validation of SIRT1 protein expression and optimisation of SIRT1 antibodies in human and mouse cell lines 72

3.3.2 SIRT1 protein expression in isolated chondrocytes from human samples 73

3.3.3 Optimisation of SIRT1 silencing using siRNA in HTB-94 cells....75

3.3.4 Effects of SIRT1 mRNA silencing on cartilage and ECM markers....76

3.3.5 Optimisation of SIRT1 drug concentrations....78

3.3.6 Validation of SIRT1 drugs in HTB-94 cells....80

3.3.7 Effects of pharmacologically manipulating SIRT1 activity on cartilage and ECM markers....82

3.4 Discussion....84

4. Generation and validation of SIRT1 conditional knockout mice....87

4.1 Introduction....88

4.2 Hypothesis....88

4.3 Results....89

4.3.1 Validation of Cre expression....89

4.3.2 Generation of SIRT1 cKO mice lines....91

4.3.3 Validation of knockout of SIRT1 mRNA expression in murine tissue....93

4.3.4 Optimisation of SIRT1 protein detection from murine hips....95

4.3.5 Validation of knockout of SIRT1 protein expression in murine cartilage....96

4.3.6 *In vivo* effects of SIRT1 knockout on cartilage and ECM markers....97

4.3.7 Age related effects of SIRT1 KO *in vivo*....99

4.4 Discussion....100

5. The regulation of chondrocyte autophagy by SIRT1....103

5.1 Introduction....104

5.2 Hypothesis....104

5.3 Results 105

5.3.1 Autophagy protein expression in isolated chondrocytes from human samples 106

5.3.2 Effects of SIRT1 mRNA silencing on autophagy markers 107

5.3.3 Effects of pharmacologically manipulating SIRT1 activity on autophagy markers 108

5.3.4 Effects of manipulating SIRT1 on chondrocyte autophagy markers *in vivo* 111

5.3.5 Effects of manipulating SIRT1 activity on LC3-GFP *ex vivo* 114

5.3.6 The functional effect of SIRT1 deletion on chondrocyte autophagy *in vivo* 116

5.3.7 *In vivo* effects of SIRT1 knockout on autophagy in ageing murine cartilage 118

5.3.8 The direct regulation of autophagy proteins by SIRT1 in chondrocytes 119

5.3.9 Targeting SIRT1-autophagy interaction in chondrocytes *in vivo* 126

5.3.10 Targeting SIRT1-autophagy interaction in an experimental OA model 128

5.4 Discussion 132

6. The regulation of joint inflammation by SIRT1 138

6.1 Introduction 139

6.2 Hypothesis 140

6.3 Results 141

6.3.1 Effect of whole body vs cartilage specific SIRT1 deficiency on the gene expression of cartilage and OA markers 141

6.3.2 Effect of whole body vs cartilage specific SIRT1 deficiency on the gene expression of cartilage and OA markers 6hrs, 24hrs and 72hrs post DMM 143

6.3.3 Effect of whole body vs cartilage specific SIRT1 deletion on synovitis 24hrs post DMM..... 149

6.3.4 Effect of pan tissue vs cartilage specific SIRT1 deficiency on cartilage degradation 8 and 12 weeks post DMM 151

6.4 Discussion 153

7. Final discussion 157

8. Awards and Publications 166

8.1 Publications 167

8.2 Awards 167

9. References 168

List of figures

Figure 1.1: Histomorphological organization of articular cartilage 3

Figure 1.2: Components of the cartilage ECM 9

Figure 1.3: Factors involved in OA pathogenesis 10

Figure 1.4: Anatomy of the right knee joint of the mouse 20

Figure 1.5: Chondrocyte specific deletion of SIRT1 using Aggrecan CreER^{T2} mice 23

Figure 1.6: Cellular aging mechanisms 32

Figure 1.7: Mechanism of action of sirtuins 33

Figure 1.8: SIRT1 Targets 37

Figure 1.9: Mammalian autophagic pathway 44

Figure 2.1: Histological Safranin-O chondropathy grading scores 63

Figure 3.1: Validation of SIRT1 protein expression in cell lines by western blotting 73

Figure 3.2: SIRT1 protein expression form HACs 74

Figure 3.3: Optimisation of SIRT1 siRNA in HTB-94 cell line 75

Figure 3.4: Effects of SIRT1 mRNA silencing on cartilage and ECM markers 77

Figure 3.5: Optimisation of SIRT1 drug concentrations 79

Figure 3.6: Validation of SIRT1 drugs in HTB-94 cells 81

Figure 3.7: Effects of pharmacologically manipulating SIRT1 activity on cartilage and ECM markers 83

Figure 4.1: Validation of Cre specificity by ROSA26 reporter mice 89

Figure 4.2: Genotyping of the different generations of SIRT cKO mice 91

Figure 4.3: Validation of knockout of SIRT1 mRNA expression in murine tissue 94

Figure 4.4: Optimisation of SIRT1 protein expression from murine hips 95

Figure 4.5: Validation of knockout of SIRT1 protein expression in murine cartilage 96

Figure 4.6: *In vivo* effects of SIRT1 knockout on cartilage and ECM markers 98

Figure 4.7: Age related effects of SIRT1 KO *in vivo* 99

Figure 5.1: Autophagy protein expression in HACs 106

Figure 5.2: Effects of SIRT1 mRNA silencing on autophagy markers 107

Figure 5.3: Effects of pharmacologically manipulating SIRT1 activity on autophagy markers 109

Figure 5.4: Effect of pharmacologically manipulating SIRT1 activity on LC3 II 110

Figure 5.5: Effects of manipulating SIRT1 on P62 and LC3 in chondrocytes *in vivo* 113

Figure 5.6: Effect of manipulating SIRT1 activity on LC3-GFP *ex vivo* 114

Figure 5.7: The effect of SIRT1 loss on autophagosomes count in murine chondrocytes 117

Figure 5.8: Effect of SIRT1 loss on chondrocyte autophagy in aging murine cartilage 118

Figure 5.9: The direct regulation of autophagy proteins by SIRT1 in chondrocytes 119

Figure 5.10: SIRT1 interaction and functional modification of BECLIN 1. 121

Figure 5.11: SIRT1 interaction and functional modification of ATG5 122

Figure 5.12: SIRT1 interaction and functional modification of ATG7 123

Figure 5.13: SIRT1 interaction and functional modification of LC3 I and LC3 II 125

Figure 5.14: Targeting SIRT1-autophagy interaction in chondrocytes *in vivo* 127

Figure 5.15: Targeting SIRT1-autophagy interaction in an experimental OA model 129

Figure 5.16: LC3 protein expression in mice treated with spermidine in an experimental OA model 131

Figure 6.1: Synovitis scoring in SIRT1 cKO murine lines 150

Figure 6.2: OARSI scoring of SIR1 cKO mice 8 and 12 weeks post DMM. 152

List of Tables

Table 1.1: Animal models used to study OA 19

Table 2.1: TaqMan Gene Expression Assay primers/probe mixes 52

Table 2.2: Primers used for genotyping of mice and q-PCR experiments 57

Table 2.3: OARSI chondropathy grading scale 62

Table 2.4: Scoring system for synovial hyperplasia 64

Table 2.5: Scoring system for synovial inflammation 64

Table 5.1: Gene Expression changes of autophagy-related genes in $SIRT1^{Agg}$ KO mice 111

Table 6.1: Gene expression of inflammatory markers in $SIRT1^{fl/fl}$, $SIRT1^{ROSA}$ and $SIRT1^{Agg}$ murine knee joints at 10 weeks of age 142

Table 6.2: Gene expression of inflammatory markers in $SIRT1^{fl/fl}$, $SIRT1^{ROSA}$ and $SIRT1^{Agg}$ murine knee joints at 6hrs post DMM. 144

Table 6.3: Gene expression of inflammatory markers in $SIRT1^{fl/fl}$, $SIRT1^{ROSA}$ and $SIRT1^{Agg}$ murine knee joints at 24hrs post DMM. 146

Table 6.4: Gene expression of inflammatory markers in $SIRT1^{fl/fl}$, $SIRT1^{ROSA}$ and $SIRT1^{Agg}$ murine knee joints at 72hrs post DMM. 148

Abbreviations

ER	Endoplasmic reticulum
ECM	Extracellular matrix
ACAN	Aggrecan gene name
ADAMTS	A disintegrin and metalloproteinase with thrombospondin motif
Aggrecan CreER^{T2}	Inducible Aggrecan Cre ER^{T2}
ANOVA	One-way analysis of variance
AROS	Active regulator of SIRT1
ATDC-5	Teratocarcinoma AT805 derived mouse cell line)
ATG	Autophagy-related
ATP	Adenosine triphosphate
BAF	Bafilomycin A1
BECN1	Beclin1
CD	Cluster differentiation
cDNA	Complementary DNA
cKO	Conditional knockout
COL10	Type X collagen
COL2	Type II collagen
COL2A1	Collagen 2(α1)
COL2A1 CreER^{T2}	Inducible COL2A1 Cre
COMP	Cartilage oligomeric matrix protein
COX-2	Cyclooxygenase-2

CREB	cyclic adenosine monophosphate response element binding protein
CS	Chondroitin sulfate
CTGF	Connective tissue growth factor
DBC-1	Deleted in breast cancer-1
DMEM	Dulbecco's modified Eagle's medium
DMM	Destabilization of medial meniscus
DMOADs	Disease-modifying OA drugs
DMSO	Dimethyl Sulfoxide
DMT2	Type 2 diabetes mellitus
DNA	Deoxyribonucleic acid
DYRK	Dual-specificity tyrosine phosphorylation-regulated kinase
EDTA	Ethylenediaminetetraacetic acid
EM	Electron Microscopy
FABP	Fatty acid binding protein
FACS	Fluorescence-activated cell sorting
FCS	Foetal calf serum
FOXO	Forkhead box protein O
GAG	Glycosaminoglycan
GDF5	Growth and differentiation factor 5 gene
GFP	Green fluorescent protein
HACs	Human articular chondrocytes
HEK293	Human Embryonic Kidney 293 cell line
HEPES	(4-(2-hydroxyethyl)-1-piperazineethanesulfonic acid

HRP	Horseradish peroxidase
hsp90	Heat shock protein 90
HTB-94	Chondrosarcoma cell line
IGF-1	Insulin-like growth factor 1
IgG	Immunoglobulin G
IL18	Interleukin 18
IL-1β	Interleukin 1-beta
IL6	Interleukin 6
iNOS	Inducible nitric oxide synthase
JNK	c-Jun N-terminal kinase
LC3	Microtubule-associated protein 1A/1B-light chain 3
LBD	Ligand binding domain
LXR	Liver X receptor
MEFs	Murine embryonic fibroblasts
MFI	Mean fluorescence intensity
miR	mircoRNA
MMPs	Matrix metalloproteinases
mRNA	messenger ribonucleic acid
MT-MMPs	Membrane type MMPs
mTOR	Mammalian target of rapamycin
MTT	3-(4,5-dimethylthiazol-2-yl)-2,5-diphenyltetrazolium bromide
NAD^+	Nicotinamide adenine dinucleotide
NaDC3	Na^+-dependent dicarboxylate cotransporter

NADH	Nicotinamide adenine dinucleotide reduced
NF-κB	Nuclear factor kappa-light-chain-enhancer of activated B cells
NO	Nitric oxide
OA	Osteoarthritis
OARSI	Osteoarthritis Research Society International
PARP	Poly(ADP-ribose) polymerase
PBS	Phosphate buffer saline
PGC-1α	Peroxisome proliferator activated receptor-gamma co-activator-1alpha
PGE2	Prostaglandin E2
PIPES	Piperazine-N,N'-bis(2-ethanesulfonic acid)
RA	Rheumatoid arthritis
RIPA	Radioimmunoprecipitation assay
RNase	Ribonuclease
RT-qPCR	Quantitative reverse transcription polymerase chain reaction
S.E.M	Standard error of mean
Sir2	Silent information regulator 2
siRNA	small inferencing Ribonucleic Acid
SIRT	Silent mating type information regulation 2 homolog
SIRT1$^{fl/fl}$	SIRT1 floxed mice
SIRT^{Agg}	SIRT1$^{fl/fl}$; Aggrecan CreER^{T2+} mice
SIRT^{ROSA}	SIRT1$^{fl/fl}$; ROSA CreER^{T2+} mice
SOX-9	SRY (sex determining region Y)-box 9

SQSTM1	Sequestosome 1
TFEB	Transcription factor EB
TGFβ	Transforming Growth Factor beta
TIMPs	Tissue inhibitor of metalloproteinases
TLDA	TaqMan® Low Density Array microfluidic cards
TLR	Toll like receptor
TLV	Low Viscosity Resin
TNFα	Tumour Necrosis Factor-alpha
TSG6	Tumor necrosis factor-inducible gene 6
TX	Tamoxifen
ULK1	Unc-51 Like Autophagy Activating Kinase 1
WB	Western blot
WT	Wild type
x g	Relative centrifugal force
β-actin	Beta-actin
β-gal	Beta-galactosidase

1. Introduction

1 Introduction

1.1 Structure of articular cartilage

Articular cartilage is located on the surfaces of joints which are involved in mechanical movement and is avascular and aneural (Pearle *et al*. 2005). Its key role is to provide a smooth surface which results in frictionless articulation to absorb and distribute loads (Buckwalter and Mankin 1998). Articular cartilage is mainly composed of water, collagen, proteoglycans and chondrocytes (the only resident cells) (Pearle *et al*. 2005). It also contains other minor collagens (type VI, IX and XI) and several non-collagenous proteins and glycoproteins (Heinegård and Saxne 2011). These components make up extensive hydrated extracellular matrix (ECM). Both cell content and matrix synthesis of cartilage decrease with age and the organization of articular cartilage reflects its functional role (Buckwalter and Mankin 1998).

1.1.1 Histomorphological organization of articular cartilage

Cartilage can be divided into four zones (Figure 1.1). The superficial zone, which is closest to the articular surface and comprises of collagen fibres, which are densely packed around flattened ellipsoid shaped chondrocytes (Stockwell 1978). The morphology of the superficial zone provides high tensile strength of cartilage to accommodate the forces generated during joint loading and articulation (Buckwalter and Mankin 1998). The collagen fibres in the middle zone of articular cartilage are randomly arranged with chondrocytes spherical in shape and at times found in pairs (Pearle *et al.* 2005). The deep zone of articular cartilage comprises of columns of ellipsoid shaped chondrocytes distributed between radially oriented collagen fibres that extend into the calcified zone (Stockwell 1978). The calcified zone of articular cartilage contains chondrocytes expressing a hypertrophic phenotype which synthesise

calcified matrix providing an interface between uncalcified cartilage and the underlying subchondral bone (Stockwell 1991).

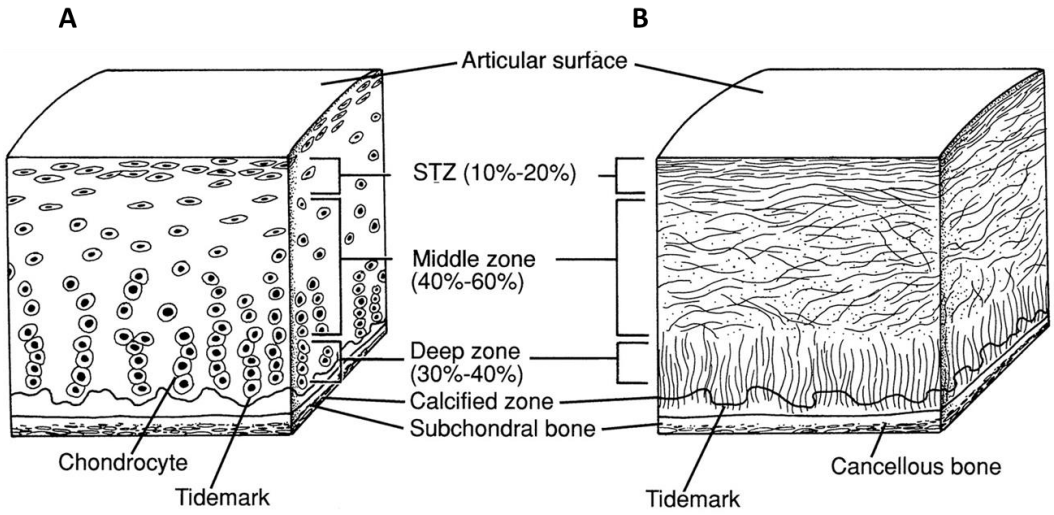

Figure 1.1: Histomorphological organization of articular cartilage. Structure and arrangement of **(A)** chondrocytes and **(B)** collagen fibres in the different zones of articular cartilage. Adapted from Jazrawi *et al.* (2011).

1.1.2 Chondrocytes

Chondrocytes are responsible for maintaining a balanced cartilage turnover and respond to changes induced by joint loading, cytokines, growth factors and the presence of fragmented matrix molecules in the ECM of cartilage (Stockwell 1978; Wieland *et al*. 2005). During embryogenesis, chondrocytes are responsible for the longitudinal bone growth within the epiphyseal growth plate (Hall and Miyake 1992; Archer and Francis-West 2003). Chondrocytes differentiate from colony-forming unit-fibroblast and later mesenchymal stem cells and initially express collagen type I prior to differentiation into foetal chondrocytes (Goldring 2012). Foetal chondrocytes switch to the expression of chondrocyte specific type II collagen (COL2) (Ryan and Sandell 1990; Sandell *et al.* 1991) in addition to type IX and XI

collagens, while levels of type I collagen expression are significantly inhibited (Luo *et al*. 1995). During postnatal bone growth, foetal chondrocytes in growth plates enlarge (chondrocyte hypertrophy) which results in terminal differentiation (Drissi *et al*. 2005). Hypertrophic chondrocytes increase in volume and express high levels of collagen X (COL10) and calcium deposition within the matrix (Alvarez *et al.* 2001). Differentiated chondrocytes (mature) do not exhibit proliferation potential (Buckwalter and Mankin 1998; Drissi *et al.* 2005). As cartilage is avascular in nature, chondrocytes exist in hypoxic conditions and rely on nutrients obtained from the articular surface by diffusion as well as signals obtained by the extracellular ionic environment and ECM interactions (Stockwell 1991). The transcription factor SRY (sex determining region Y)-box 9 (SOX-9) is a key regulator of chondrocyte differentiation in both mesenchymal stem cells and foetal chondrocytes (Bell *et al*. 1997; DeLise *et al*. 2000). SOX-9 expression level remains elevated in differentiated chondrocytes (DeLise *et al*. 2000). The expression of chondrocyte-specific genes including COL2 is tightly regulated by SOX-9 transcription factor (De Crombrugghe *et al*. 2000). Mutations in SOX-9 lead to skeletal malformation syndromes such as Campomelic Dysplasia (Sock *et al*. 2003).

Substantial loss of chondrocytes by necrosis or apoptosis is observed in the superficial and middle zones of cartilage throughout osteoarthritis (OA) progression (Lotz and Caramés 2011). Chondrocyte apoptosis may be the result of various inflammatory mediators, decreased cellular metabolism and decreased protection from mechanical force (Heinegård and Saxne 2011; Lotz and Caramés 2011). The loss of chondrocytes reduces cartilage volume and effective ECM turnover which in turn increases cartilage loss leading to OA (Stockwell 1991; Buckwalter and Mankin 1998).

1.1.3 Collagens

Collagens account for around 10% of the wet and over 50% of the dry weight of articular cartilage (Sophia Fox *et al*. 2009). Each molecule of collagen comprises of three α polypeptide chains coiled into a rigid helical structure either in homotrimers or heterotrimers states (Shoulders and Raines 2010). A repeating tripeptide motif, G-X-Y, within the polypeptide chains allows collagens to form into a triple helix formation (Shoulders and Raines 2010). There are four types of collagens in articular cartilage: fibrillar, fibrillar-associated collagens, fibrillar-associated collagens with interrupted triple helices and non-fibrillar collagens (Thomas *et al*. 1994).

Types II and XI collagen are fibril forming collagens (Thomas *et al*. 1994). COL2 accounts for 90 to 95 per cent of the collagen in articular cartilage and forms the primary component of cross-banded fibrils (Buckwalter and Mankin 1998). COL2 is composed of three α1 (II)-chains which are arranged to form a triple helix (Thomas *et al.* 1994). Covalent cross-links between individual collagen molecules lead to formation of fibrils, with many fibrils forming fibres which provide the cartilage with tensile strength (Buckwalter and Mankin 1998). COL2 is synthesized as a procollagen molecule with N- and C-propeptides and both propeptides are cleaved before the collagen is embedded into the matrix (Thomas *et al*. 1994). In contrast, Type XI collagen retains its N-propeptide domain and is formed as a heterotrimer of three different α-chains (α1, α2, α3), which then form the core of COL2 fibrils (Thomas *et al.* 1994). Type IX collagen is heterotrimeric molecule consisting of three different α-chains (α1(IX), α2(IX), and α3(IX)) with domains interrupted with short-non helical regions (Thomas *et al*. 1994). Type IX collagen alongside type XI collagen is thought to bind covalently to the surface of COL2 fibrils in antiparallel directions, which stabilizes the collagen network (Thomas *et al*.

1994). COL10 is a homotrimeric collagen with a large C-terminal, a short N-terminal domain. It is normally secreted by hypertrophic chondrocytes, plays a role in endochondral ossification and matrix calcification and in articular cartilage it is expressed in the calcified zone (Pearle *et al*. 2005). Type VI is a monomer which is a heterotrimer consisting of three distinct α chains (α1, α2 and α3). Type VI is found in the pericelluar matrix (surrounds individual chondrocytes) and binds to other components of cartilage such as biglycan, hyaluron, decorin and fibronectin (Heinegård and Saxne 2011).

1.1.4 Proteoglycans

Proteoglycans found in the ECM of articular cartilage enable the tissue to cope with dynamic swelling pressures to resist compressive loads (Maroudas and Bullough 1968). Proteoglycans consist of a core protein which is covalently attached to glycosaminoglycan (GAG) side chains (Ferguson *et al*. 2009). The core protein can also be attached to chondroitin sulphate, dermatan sulphate, keratan sulphate or heparan sulphate both alone or in combination (Heinegård and Saxne 2011). These side chains can be sulphated which leads to a high negative charge that is responsible for the hydrophilic properties of the ECM (Heinegard *et al*. 1987).

Aggrecan (gene name ACAN) comprises about 90% of the total ECM proteoglycan weight (Sophia Fox *et al*. 2009). The aggrecan core protein has three globular domains G1, G2 and G3 (Knudson and Knudson 2001). A long GAG chain covalently bound to keratan sulphate separates the G1 and G2 domains (Knudson and Knudson 2001). Whereas, the G1 domain of aggrecan interacts with GAG hyaluronan; this interaction is stabilised by a link protein (Knudson and Knudson 2001). Both interactions of aggrecan to hyaluronan and the link

protein forms the proteoglycan aggregates (Knudson and Knudson 2001). Hyaluronan also has the ability to bind to the cluster differentiation (CD) 44, integrin receptor located on the chondrocyte (Knudson *et al*. 1996). Versican is the other large proteoglycan in articular cartilage which also contains chondroitin sulfate (CS) but is much less abundant than aggrecan (Olin *et al*. 2001).

Decorin and biglycan proteoglycans are similar in structure and contain an N-terminal domain that is substituted with one or two dermatan sulphate/CS side chains respectively (Knudson and Knudson 2001). Decorin is found in the interterritorial matrix and binds to COL2 fibrils (Sophia Fox *et al*. 2009). In comparison, Biglycan is found in the pericellular matrix and binds to type VI collagen (Knudson and Knudson 2001). Lumican and fibromodulin proteoglycans are also found in articular cartilage and are primarily substituted with keratan sulphate chains (Chakravarti 2002). Fibromodulin attaches to COL2 fibres and with decorin and biglycan may play a role in regulating collagen fibril organisation and cartilage stiffness (Knudson and Knudson 2001). Other proteoglycans in articular cartilage include epiphycan, basement membrane proteoglycan perlecan, cell surface proteoglycans such as the syndecans and the phosphatidylinositol linked heparan sulfate proteoglycan and glypican (Knudson and Knudson 2001).

1.1.5 Other components of articular cartilage

The ECM of articular cartilage also contains proteins which are neither collagens nor proteoglycans, but are critical for ECM function and maintenance (Figure 1.2; Heinegård and Saxne 2011). Fibronectin is a high molecular weight found in the pericellular and territorial matrix of articular cartilage (Rees *et al*. 1987). Fibronectin is upregulated in OA tissue but is

expressed at low levels in normal, healthy cartilage (Rees *et al*. 1987). Cleaved fibronectin fragments can activate toll like receptor (TLR) 4 signalling, which can increase inflammatory cytokine expression, up-regulate matrix metalloproteinases (MMPs) and induce proteoglycan loss and enhance COL2 cleavage in cultured cartilage explants (Okamura *et al.* 2001). Cartilage oligomeric matrix protein (COMP), also termed thrombospondin-5, is another abundant macromolecule in cartilage (Oldberg *et al*. 1992). It is expressed at high levels in proliferating chondrocytes located in the growth plate and in the pericellular matrix of mature cartilage (Carlsén *et al*. 1998). COMP is able to bind to collagens I and II in a zinc-dependent manner and it is involved in collagen fibril organization (Rosenberg *et al*. 1998). Tenascin-C is another large glycoprotein composed of six subunits and is expressed in normal articular cartilage, upregulated in OA and following stimulation with Interleukin 1-beta (IL-1β), and mechanical loading (Järvinen *et al*. 1999; Pfander *et al*. 2004). Another structural glycoprotein present in cartilage is fibrillin-1 (Ferguson *et al*. 2009). Fibrillin-1 is localized in the pericellular matrix and constitutes the structural backbone of microfibrils which in turn provide a scaffold for the deposition of elastin (Keene *et al*. 1997). The formation of elastin fibers gives elasticity and resilience to cartilage (Rock et al. 2004). However, unlike collagen fibrils, fibrillin-1 microfibrils do not have well-defined patterns of organization (Keene *et al*. 1997).

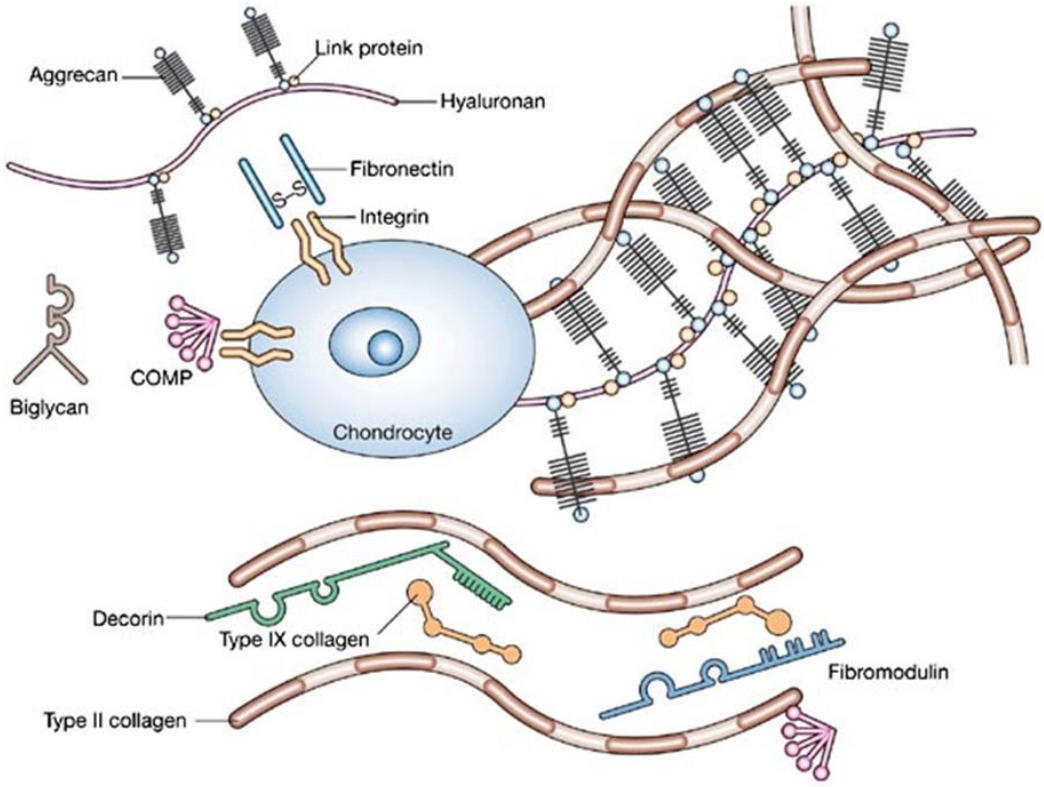

Figure 1.2: Components of the cartilage ECM. Adapted from Chen *et al*. (2006)

1.2 OA

OA is the most common form of arthritis worldwide (Woolf and Pfleger 2003; Glyn-Jones *et al*. 2015). OA mostly affects the joints of the hand, knee and hip, and is characterized by the progressive degradation of articular cartilage with secondary synovitis (Vincent and Watt 2014). Increased age is a primary risk factor for the development of OA, along with obesity, genetic predisposition and joint injury (Figure 1.3; Bijlsma *et al*. 2011). Among older adults, OA is one of the most common causes of chronic disability (Loeser 2012a). Functional impairment and pain can lead to severe distress and depression in these patients (Bijlsma *et al*. 2011). The increase in the lifespan of the global population is set to increase the prevalence of the disease (Woolf and Pfleger 2003; Glyn-Jones *et al*. 2015).

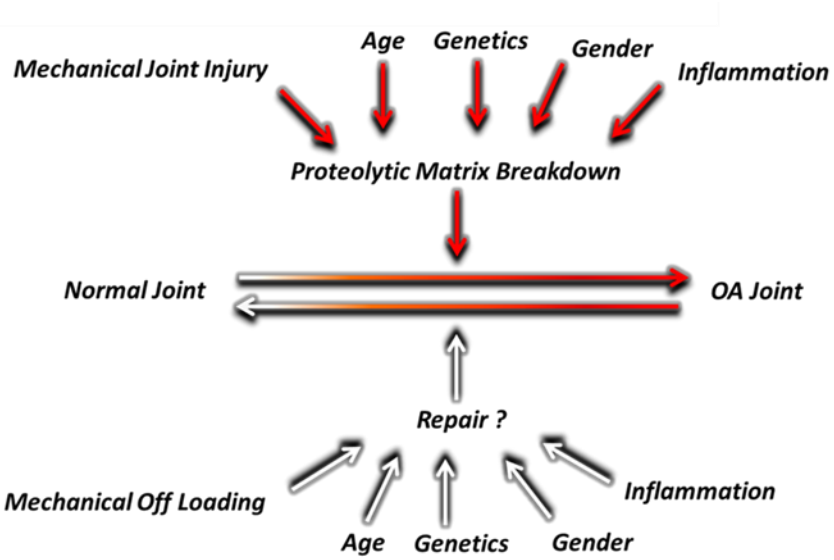

Figure 1.3: Factors involved in OA pathogenesis.

1.2.1 Pathophysiology of OA

The degradation of articular cartilage is caused by principle matrix degrading enzymes such as members of the 'a disintegrin and metalloproteinase with thrombospondin motif' (ADAMTS) family and the MMPs; which degrade aggrecan (ADAMTS) and collagen (MMPs) respectively (Nagase *et al.* 2006). OA chondrocytes secrete higher levels of cytokines such as IL-1β and Tumour Necrosis Factor-alpha (TNFα) that are capable of inducing and activating these catabolic enzymes (Goldring and Otero 2011). The significance of joint inflammation in contributing to tissue breakdown is unclear. Infiltration of mononuclear cells into the synovial membrane is observed in human OA (Scanzello and Goldring 2012) and there is much evidence to support activation of the innate immune system in disease (Orlowsky and Kraus, 2015). Inflammation, when present, will exacerbate tissue breakdown and contribute to painful episodes of disease.

1.2.2 Cytokines

Cytokines regulate cellular activities and cell-cell interactions (Hsu 2008). Cytokines are secreted and can act in an autocrine, paracrine or in some instances endocrine action (Hsu 2008). They can be secreted in a cascade and have overlapping functions which can result in catabolic or anabolic events or may inhibit either of these processes (Hsu 2008).

1.2.2.1 Proinflammatory cytokines

The role of catabolic or proinflammatory cytokines such as IL-1 and TNFα in the pathophysiology of rheumatoid arthritis (RA) is well established (McInnes and Schett 2007). Blockade of these cytokines, especially TNF-α has resulted in effective treatments of RA (Feldmann and Maini 2001). However, the roles of proinflammatory cytokines in OA are still being addressed. IL-1 was originally termed 'Catabolin' and initially purified from pig synovium (Saklatvala 1981). Subsequently, IL-1 has been demonstrated to be upregulated in OA cartilage and both IL-1 and TNF-α are detected in OA synovial fluid (Smith *et al.* 1997). Immunohistochemical staining of IL-1β showed its expression in the superficial layers of OA cartilage (Melchiorri *et al.* 1998). Studies in animal models demonstrated intra-articular IL-1 injections induce an OA-like disease (Pettipher *et al.* 1986) and interleukin-1 receptor antagonist decreased cartilage loss in animal models of OA (Pelletier *et al.* 1997). Experiments inhibiting the IL-1 receptor in humans have still not been carried out. However, IL-1 antagonists have showed low efficacy in patients (Calich *et al.* 2010). Treatment of chondrocytes with TNFα also results in the release of matrix degrading enzymes and suppression of matrix synthesis (Saklatvala 1986; Nagase *et al.* 2006). TNFα is expressed in the middle and deep zones of cartilage explants from OA knee joints (Moos *et al.* 1999). Both TNFα and TNFα-converting enzyme messenger ribonucleic acid (mRNA) is upregulated in OA

(Amin 1999). Only a few experimental trials have investigated the efficacy of TNFα in OA and showed that blockade of the cytokine had modest decreases in disease (Calich *et al.* 2010). IL-1β inhibition in clinical trials have shown significant benefit in knee and hand OA patients (Chevalier et al. 2013). Blockade of IL-1 receptor improved pain and global disability during a in hand and knee OA patients but patients did display upper respiratory tract infections (Chevalier et al. 2013) . These promising studies have not yet been followed up with larger controlled trials.

Both IL-1 and TNFα directly upregulate the expression of Cyclooxygenase-2 (COX-2) and inducible nitric oxide synthase (iNOS) which in turn induce chondrocytes to synthesise prostaglandin E2 (PGE2) and nitric oxide (NO) (Goldring and Berenbaum, 2004). COX-2 and iNOS are elevated in OA cartilage compared to normal human cartilage (Amin and Abramson 1998). Nitric oxide (NO) is a cytotoxic free radical and mediates a number of processes associated with OA including endoplasmic reticulum stress and apoptosis (Amin and Abramson 1998). In addition, PGE2 has been shown to oppose the effects of IL-1 on cartilage matrix synthesis by stimulating COL2 expression which could be a counteractive mechanism to IL-1 induced chondrocyte dedifferentiation (Melchiorri *et al.* 1998).

1.2.3 Transforming Growth Factor beta (TGF-β)

TGF-β is a large family of growth factors, which plays a critical role in embryonic development cell proliferation, differentiation, apoptosis and cell migration (Massagué 2012). There are three isotypes of TGF-β: TGF-β -1, -2 and -3, which share a conserved homology of around 90% and are differentially expressed in different tissues and cell populations (Massagué 2012). High TGF-β levels have been detected in the synovial fluid of OA patients and the

correlation between the genetic variants of TGF-β signalling pathway components and OA is also reported in patients (Blom *et al.* 2004; Shen *et al.* 2014). Both TGF-β isoforms and TGF-β receptors are broadly expressed in cartilage, bone and synovial tissues and play different roles in these tissues. Hence, the role of TGF-β in OA pathogenesis is unclear (Shen *et al.* 2014). Transgenic mice that overexpress the dominant-negative type II TGF-β receptor in skeletal tissue exhibit progressive skeletal degeneration (Serra *et al.* 1997; Hiramatsu *et al.* 2011). Global and cartilage specific deletion of SMAD3, a key downstream signalling molecule of TGF-β, causes increased cartilage tissue, articular cartilage fibrillation, clefting, subchondral bone sclerosis and osteophyte formation (Yang *et al.* 2001; Wu *et al.* 2009). In addition, deletion of TGF-β Receptor type II in articular chondrocytes also leads to a progressive OA-like phenotype in mice (Shen *et al.* 2013). Moreover, overexpression of TGF-β1 in osteoblastic cells in mice leads to spontaneous OA and subchondral bone sclerosis whereas inhibition of TGF-β activity in subchondral bone, stabilizes the subchondral bone microarchitecture and decreases OA pathology in mice (Zhen *et al.* 2013). In addition, inducible knockout of the TGF-β type II receptor in Nestin-positive MSCs leads to fewer changes in the subchondral bone and less articular cartilage degeneration (Zhen *et al.* 2013). Blaney Davidson *et al* (2007) also showed that the cells in the outer layer of osteophytes strongly express TGF-β1 to activate the TGF-β signalling pathway in the experimental OA murine models; which further illustrates the diverse role of TGF-β in OA.

1.2.4 Insulin-like Growth Factor 1 (IGF1)

IGF1 was identified by Salmon and Daughaday (1957) and originally named as “sulphation factor” because of its ability to stimulate 35-sulphate incorporation into rat cartilage. Exogenous IGF1, when added to monolayers of bovine chondrocytes or cartilage explants,

increases proteoglycan synthesis (Sah *et al* 1994). Furthermore, a combination of IGF1 and TGFβ has been shown to regulate proliferation and differentiation of periosteal mesenchymal cells during chondrogenesis (Fukumoto *et al.* 2003). However, addition of IGF1 alone did not have the same effect on chondrogenesis (Fukumoto *et al.* 2003). This result validates the experiments conducted by Tsukazaki *et al.* (1994) who showed the ability of TGFβ1 to increase the number of IGF1 receptors in chondrocytes without changing their affinity. IGF1 deficient rats developed articular cartilage lesions (Ekenstedt *et al.* 2006) and in murine and equine models addition of IGF1 to chondrocyte grafts enhanced chondrogenesis in cartilage defects (Fortier *et al.* 2002; Goodrich *et al.* 2007). These studies further support the need for IGF1 to maintain articular cartilage integrity. Several studies have demonstrated that the ability of chondrocytes to respond to IGF1 decreases with age and in OA (Loeser *et al.* 2000; Morales 2008).

1.2.5 MMPs

MMPs are a family of proteinases in humans with a major role in regulating ECM turnover (Nagase *et al.* 2006). All of the MMPs share three domains: the pro-peptide, the catalytic domain which is linked to a third similar domain the haemopexin-like C-terminal domain (Nagase *et al.* 2006). All the MMPs contain a zinc atom in the catalytic domain and are synthesised as inactive proenzymes that require activation (Nagase *et al.* 2006). The MMPs can be classified into four main groups: collagenases, stromelysins, gelatinases and membrane type MMPs (MT-MMPs) (Verma and Hansch 2007). Gelatinases (MMP-2 and MMP-9) degrade partially denatured collagen and have been implicated in angiogenesis and neurogenesis (Singh *et al.* 2015). Stromelysins (MMP-3, MMP-10, MMP-11, and MMP-7) are small proteases that degrade segments of the extracellular matrix (Nagase *et al.* 2006).

Stromelysins have a broad range of substrates including proteoglycans, laminin and fibronectin, and they are believed to play central role in the activation of other MMPs through cleavage of their pro-peptide domains (Nagase *et al.* 2006). MT-MMPs (MMP-14 to 17 and 24) activate a few proteases and are involved in the synthesis of components at the cell surface (Page-McCaw *et al.* 2007). Collagenases are the main type of MMPs involved in cartilage biology and OA (Heinegård and Saxne 2011). These collagenases cleave fibrillar collagens at a single point in collagen strands (Nagase *et al.* 2006). MMP-13 preferentially cleaves COL2 over collagen type I and III whereas MMP-1 preferentially cleaves type III and MMP-8 type I collagen (Nagase *et al.* 2006). Overexpression of MMP-13 in the mouse leads to an OA phenotype (Neuhold *et al.* 2001) and MMP-13 knockout mice are protected from surgically induced osteoarthritis (Little *et al.* 2009). Zymogens (pro-MMPs) are expressed in normal cartilage tissue but MMP-2, -9, -13, -14, -16 and -28 are overexpressed in osteoarthritic cartilage and synovial tissue. Expression of MMP-1, -3 and -10 are down regulated in disease (Hofmann *et al.* 1992).

1.2.6 ADAMTS

The ADAMTS are a family of (ADAMTS1-ADAMTS19) metalloproteinases.(Stanton *et al.* 2011). ADAMTS have at least one thrombospondin type 1 sequence motif familiar with ECM proteins and similarly to MMPs they contain a zinc-binding sequence within their catalytic domain (Nagase and Kashiwagi 2003). ADAMTS can also cleave matrix proteins such as decorin, fibromodulin and COMP (Heinegård and Saxne 2011). Aggrecanase activity was first observed in bovine articular cartilage treated with IL-1 (Westling *et al.* 2002). Subsequently, ADAMTS4 (Tortorella *et al.* 1999) and ADAMTS5 (Thirunavukkarasu *et al.* 2007) were identified in cartilage. It has since been established that ADAMTS5 is the main enzyme active in mouse

cartilage (Glasson *et al.* 2004), as deletion of ADAMTS5, but not ADAMTS4, protects against cartilage degradation and inflammatory arthritis. ADAMTS16, -2, -14 and -12 are up regulated in diseased cartilage whereas ADAMTS1, -9, -5 and -15 are down regulated (Milner *et al.* 2006).

1.2.7 Tissue Inhibitor of Metalloproteinases (TIMPs)

The regulation of the activity of MMPs and ADAMTS is controlled by TIMPs (Nagase *et al.* 2006). TIMPs (1-4) are endogenous inhibitors of MMPs and ADAMTSs and are thought to regulate proteolytic activity (Nagase *et al.* 2006). TIMP-3 has been identified as a potent inhibitor of ADAMTS4 and ADAMTS5 *in vitro* (Kashiwagi *et al.* 2001). TIMP-3 can also inhibit aggrecanase-mediated aggrecan degradation from cartilage explants stimulated with IL-1 or retinoic acid (Gendron *et al.* 2003).

1.2.8 Mechanical forces

Some researchers consider all OA to be secondary to abnormal mechanical loading or the failure of the joint to cope with regular mechanical stresses (Cicuttini and Wluka 2014). Joint structures including cartilage, menisci, ligament and subchondral bone are subject to daily mechanical stress and load (Brandt *et al.* 2009). Occupational associated OA such as 'miners knee' (McMillan and Nichols 2005) or 'foundry workers elbow' (Mintz and Fraga 1973) and the predisposition of OA after knee injury (Nelson *et al.* 2006; Stefan *et al.* 2007) contributed to the idea that OA was due to 'wear and tear' (Jensen and Eenberg 1996). Mechano-protective mechanism such as muscle hypertrophy declines in elderly populations and is very likely to contribute to loss of joint protection during the normal gait cycle with age (Brook *et al.* 2015). This is amplified by loss of gait reflexes whereby deceleration of movement upon

heel strike would normally occur in a younger individual but is lost in the elderly (Brandt *et al.* 2009). In addition, proteases and aggrecanases have been shown to be induced rapidly upon surgical joint destabilization in a highly mechano-sensitive manner; gene regulation and disease is abrogated if the joint is immobilized following surgery. This suggests that mechanical factors can also initiate pathogenic pathways (Burleigh *et al.* 2012). These findings accord well with epidemiological evidence that OA may principally be driven by mechanical joint overload and injury (Brandt *et al.* 2009).

1.3 OA disease models

Pritzker described an animal model as 'a homogeneous set of animals which have an inherited, naturally acquired, or experimentally induced biological process, amenable to scientific investigation, that in one or more aspects resembles the disease in humans (Pritzker 1994). Although animal models cannot entirely mimic human disease they represent an extremely powerful tool for investigating the pathophysiology of a complex condition such as OA.

There are many established models of OA in species such as the rabbit, dog, cat, rat and mouse (Table 1.1**;** Ameye and Young 2006). These models are broadly classified into two groups, either spontaneous (naturally occurring/ageing) or induced (Vincent *et al.* 2012). The occurrence of OA in spontaneous models is often unpredictable with variable onset and severity depending on the strain type and sex (Fang and Beier 2014). However, these spontaneous OA animal models are the closest to mimicking OA disease progression with age. In contrast, induced models include chemically induced models and surgical (mechanical) destabilisation models (Vincent *et al.* 2012). Chemically induced models elicit pathological characteristics of OA by intra-articular injection of agents such as iodoacetate (iodoacetic

acid), trypsin, papain and collagenase type VII (Little and Smith 2008). Chemical induced models are more indicative of inflammatory arthritis with secondary effects on articular cartilage (Little and Smith 2008). Surgically induced models are more reminiscent of human post-traumatic OA but require a greater degree of technical skill (Little and Smith 2008). Surgical models induce instability of the joint by transection of specific ligaments (anterior cruciate ligament transection or medial collateral ligament) or by partial or total meniscectomy (Fang and Beier 2014).

Table 1.1: Animal models used to study OA. Adapted from (Ameye and Young 2006).

Type of Model	Species
Spontaneous	
• SRT/ort	Mouse
• Natural ageing	Mouse and Rat
Enzyme/chemically induced	
• Collagenase	Mouse
• TGF-β	Mouse
• Iodoacetate	Mouse
Surgically induced	
• Anterior cruciate ligament transection	Mouse, Rat, Rabbit, Dog and Cat
• Meniscectomy	Mouse, Guinea Pig, Rat
• Destabilisation of the medical Meniscus	Mouse
• Ovariectomy	Mouse and Rat
• Cartilage defect	Mouse, Rat and Rabbit
• Injury	Dog

1.3.1 Destabilization of medial meniscus

Destabilization of medial meniscus (DMM) is now the most commonly used surgical model for OA in mice (Fang and Beier 2014). The procedure was first described by Clements (Clements *et al.* 2003) and was further modified by Glasson (Glasson *et al.* 2004). Transection of the medial menisco-tibial ligament (Figure 1.4) causes the displacement of the meniscus increasing the mechanical load at the area of direct contact between femoral and tibial

surfaces (Glasson *et al.* 2007). DMM is minimally traumatic and yields a slower predictable progression of cartilage degeneration compared to other described models (Little and Smith 2008). Hence, the DMM model has increased reliability, reproducibility, structural similarity to human OA (Little and Hunter 2013). Osteophyte formation, subchondral bone sclerosis and pain are also observed in the DMM model (Fang and Beier 2014).

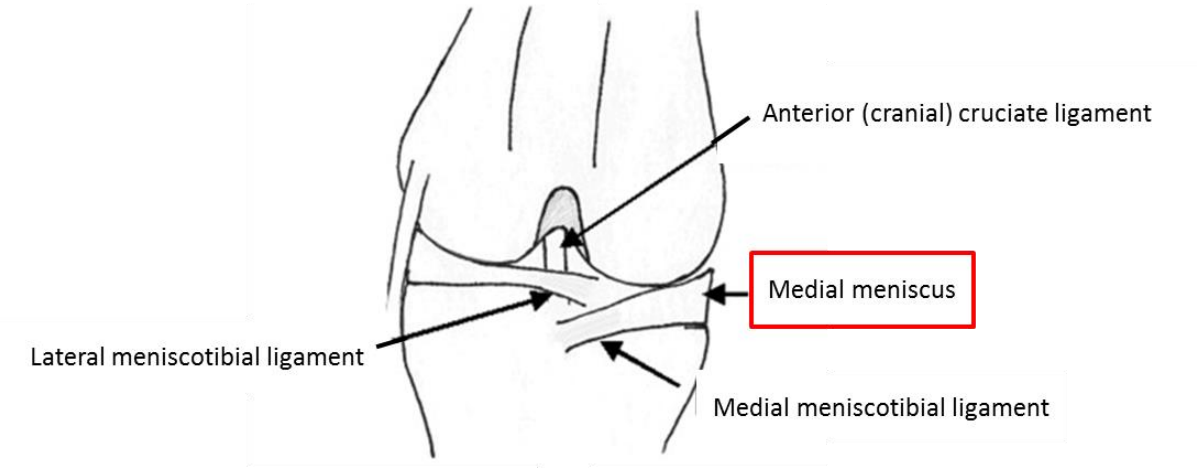

Figure 1.4: Anatomy of the right knee joint of the mouse. Adapted from Glasson *et al.* 2007.

1.3.2 Transgenic mice in OA research

The use of transgenic mice in OA research has been increasing at a rapid rate (Little and Smith 2008) . Transgenic mice are generated to examine whether deleting or overexpressing a certain gene is important in a biological setting (Miller 2011). In OA research, transgenic mice are commonly used in a disease model or aged to examine if OA disease progression increases compared to control mice (Little and Smith 2008). Transgenic mice have been engineered typically using the Cre/Lox system to delete target genes of interest in a whole body or cartilage specific manner (Fang and Beier 2014).

1.3.3.1 Cre/Lox system

Cre/Lox is a site-directed bacterial recombination system (Lewandoski 2001)**.** Cre belongs to the integrase family of site-specific deoxyribonucleic acid (DNA) recombinases and is derived from P1 bacteriophage (Hamilton and Abremski 1984). Cre recognizes the 34-bp loxP site by binding to its 13-bp inverted repeat elements that flank an 8-bp asymmetric core sequence (Sauer and Henderson 1989). This results in the deletion of the intervening sequence due to the loss of the circular reaction product (Sauer and Henderson 1989). Therefore, the Cre/Lox system allows genetic manipulation with spatial precision because a recombination event can only take place in cells where both Cre protein and Cre targeting sequences are present (Lewandoski 2001) . To achieve conditional gene inactivation by the Cre/Lox system in the mouse, a part of the gene of interest is loxP flanked ("floxed") by molecular cloning (Feil *et al.* 2009a). The mouse line carrying the floxed allele is then bred with a Cre carrying line mouse (Feil *et al.* 2009a). In their offspring, the floxed allele will be excised in the cells where Cre recombinase is active (Feil *et al.* 2009a). To achieve cell-type specificity to Cre recombinase activity cell or tissue, specific promoters are used to drive Cre expression (El Marjou *et al.* 2004). For example in OA research to achieve chondrocyte/cartilage specific genetic manipulation a COL2A1 or aggrecan ACAN promoter drives Cre expression (Fang and Beier 2014). However, it is important to note that deleting certain genes using constitutive (from embryogenesis) COL2A1 Cre mice leads to developmental problems or experimental caveats (Fang and Beier 2014). Therefore, to circumvent these problems an inducible Cre system has to be generated.

1.3.3.2 Inducible Cre/Lox system

Several design strategies have been pursued to control the temporal dimension of Cre

expression (Figure 1.5; Lewandoski 2001). Most of these strategies fuse the Cre recombinase to a steroid receptor ligand binding domain ((LBD); Kellendonk *et al.* 1996). This takes advantage of the nuclear localization capability LDB when bound to its ligand (Feil *et al.* 2009a). The Cre-LBD fusion protein is synthesized in the endoplasmic reticulum and remains in the cytoplasm due its binding to heat shock protein 90 (hsp70) which precludes translocation into the nucleus (Feil *et al.* 2009b). The Cre-LDB complex dissociates from hsp90 only when the LDB ligand is introduced, which enables the Cre-LDB complex to translocate to the nucleus (Feil *et al.* 2009b). Hence, Cre mediated DNA recombination can occur because the Cre recombinase and target gene floxed by the LoxP sites are now all located in the same subcellular compartment (Feil *et al.* 2009b). Fusion of a three point mutant estrogen receptor to the c-terminus of Cre recombinase is the most common form of LBD used in inducible Cre/Lox systems (Feil *et al.* 1997). The mutated estrogen receptor ($CreER^{T2}$) cannot bind endogenous estrogen but has a high affinity to tamoxifen a selective estrogen-receptor modulator (Feil *et al.* 1997). Tamoxifen can be administered to animals systemically but the optimal amount and length of treatment depends on Cre line and the experimental question (Lewandoski 2001). In OA research typically COL2A1 $CreER^{T2}$ (inducible COL2A1 Cre; Chen *et al.* 2007) or aggrecan $CreER^{T2}$ (inducible aggrecan Cre; Henry *et al.* 2009; Lo Cascio *et al.* 2014) mice are used to conditionally delete target genes of interest in articular cartilage at a desired time especially in adulthood to avoid any adverse developmental phenotypes (Fang and Beier 2014).

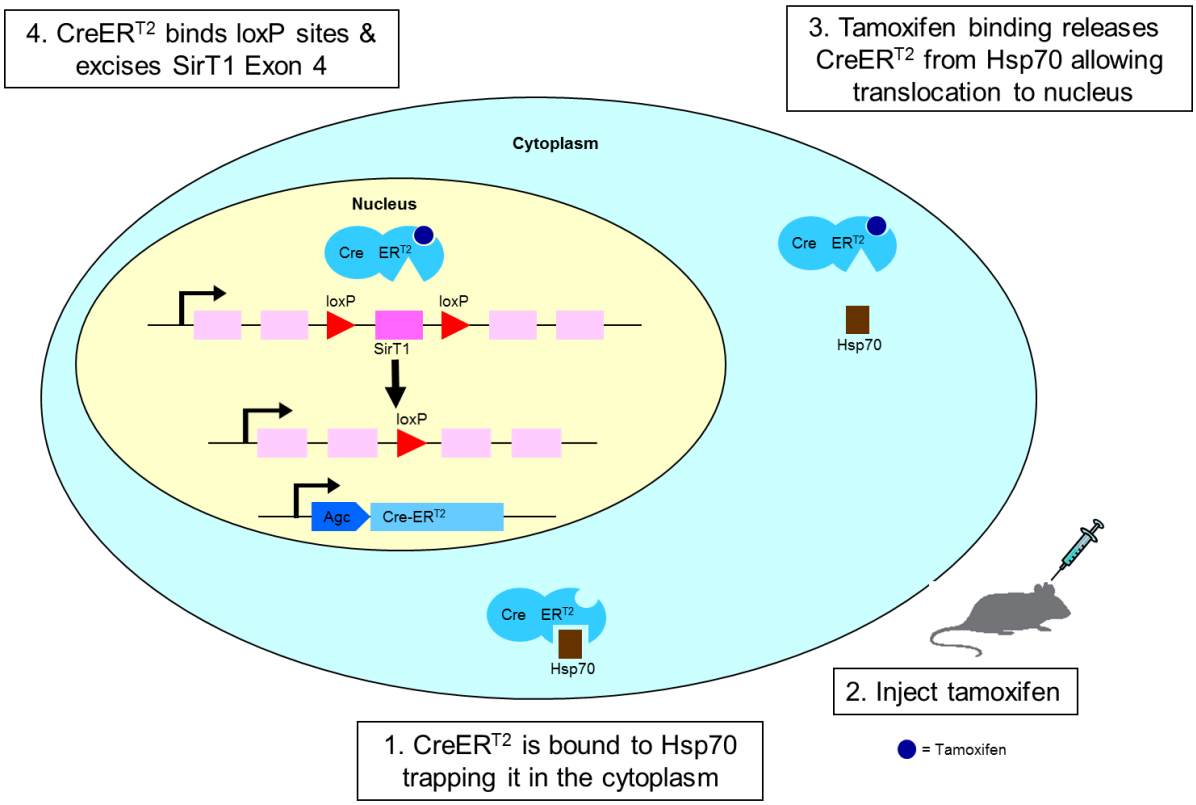

Figure 1.5: Chondrocyte specific deletion of a gene using AggrecanCreER^{T2} mice.

1.4 Clinical aspects of OA

OA affects an estimated 10% of men and 18% of women over 60 years of age and the socioeconomic burden is large, costing between 1·0% and 2·5% of gross domestic product (Woolf and Pfleger 2003; Hiligsmann *et al.* 2014). OA can present as mono- or polyarticular with clinical presentation usually occurring late in disease; associated with pain, stiffness, decreased mobility, deformity and at times with depression (Vincent and Watt 2014). Symptomatic joints display chronic pain with radiographic joint space narrowing indicating cartilage loss, bone cysts and osteophyte formation and subchondral sclerosis (Bijlsma *et al.* 2011). The diagnosis of OA can be based on clinical criteria and symptom-based case definitions such as those recommended by the American Rheumatism Association (Hochberg *et al.* 2012), or on radiological criteria, such as the Kellgren-Lawrence grading of plain joint

radiography (Kellgren and Lawrence 1957). This overall joint scoring system grades OA in five levels from 0 to 4, defining OA by the presence of a definite osteophyte (Grade≥2), and more severe grades by the appearance of joint space narrowing, sclerosis, cysts, and deformity (Kellgren and Lawrence 1957; Neogi and Zhang 2013). More sensitive imaging methods such as magnetic resonance imaging can visualize multiple structures in a joint however are very expensive for general clinical use (Glyn-Jones *et al.* 2015).

1.4.1 Current treatments for OA

Depending on the severity of OA, patients are first advised to lose weight and modify their lifestyles (Glyn-Jones *et al.* 2015). Weight loss in overweight and obese patients reduces the risk of symptomatic osteoarthritis and improves symptoms once evidence of disease is found (Gudbergsen *et al.* 2013). In addition, exercises to improve muscle strength and aerobic capacity decrease OA symptoms and have benefits in cardiovascular health and all-cause mortality (Uthman *et al.* 2013; Glyn-Jones *et al.* 2015). Current pharmacological treatments for OA aim to alleviate pain and target joint inflammation (Hunter 2011). Use of supplements including glucosamine and chondroitin has been widely recommended and shown to be safe; however, the efficacy of these supplements remains controversial (Wieland *et al.* 2005). Non-steroidal anti-inflammatory drugs such as aspirin and ibuprofen are prescribed to reduce inflammation and pain (Cheng and Visco 2012). Another form of treatment is the local administration of corticosteroids via intra-articular injections to reduce the production of pro-inflammatory mediators and the infiltration of mononuclear cells into the synovium (Buckingham 2006). The current strategy of pharmaceutical companies is to develop disease-modifying OA drugs (DMOADs) which include inhibitors of cyclooxygenases, MMPs, cytokines and NO (Wieland *et al.* 2005). However, with poor results in clinical trials and low efficacy of

DMOADs, the current endpoint treatment for OA still remains joint replacement surgery (Hunter 2011).

1.5 Risk factors of OA

OA can be caused by a complex interplay between systemic and local factors due to multiple risk factors (Neogi and Zhang 2013). For example, an inherited predisposition to develop OA may only initiate in old age or if an insult to the joint has occurred (Neogi and Zhang 2013). The significance of risk factors may vary for different joints, for different stages of the disease, or even for the development as opposed to the progression of disease (Reynard and Loughlin 2012). These risk factors include genetics, diet and obesity, gender, mechanical injury and age (Glyn-Jones *et al.* 2015).

1.5.1 Genetics

Many studies have investigated the association between genetics and OA (Peach *et al.* 2005). Twin and familial studies have identified hereditary factors as a component of primary OA development (Spector *et al.* 1996). 10-30% of knee OA is estimated to be hereditary and 50% of hip OA and 70% of hand OA is estimated to be hereditary (Hunter *et al.* 2004; Peach *et al.* 2005). There is also evidence that suggests the joint which might develop OA in a person has hereditary link too (Valdes and Spector 2009).

Genome wide association and linkage studies have identified candidate genes and susceptibility gene loci for OA (Loughlin 2005). These studies identified regions with OA susceptibility on chromosomes 2p, 4q, 7p, 8q, 9p, 9q, 10p and 16p (Valdes and Spector 2014). Moreover, genes on chromosomes 2, 4, and 16 are likely to be the strongest candidates for

hereditary OA onset and progression (Loughlin 2001). Some of these gene candidates include IL-1 cluster genes at chromosome 2p11.2-q13 associated with increased susceptibility for knee and hip OA; IL4 receptor chain at 16p12.1 and frizzled related protein 3 gene at 2q32.1 associated with increased susceptibility to hip OA; missense mutation in Matrilin 3 gene at 2p24.1 associated with hand OA and Metalloproteinase gene ADAM12 at 10q26.2 associated with knee OA alone (reviewed in Reynard and Loughlin 2012). In addition, severe osteoarthritis of the hand has been associated with variants within the ALDH1A2 gene at 15q22 (Styrkarsdottir *et al.* 2014).

Out of approximately 80 published genes only one gene has shown consistent and robust evidence of genetic association: growth and differentiation factor 5 gene (GDF5); Reynard and Loughlin 2012). A single nucleotide polymorphism rs143383, located in the 3' untranslated region of the GDF5 gene is associated with OA (Miyamoto *et al.* 2007). GDF5 is an extracellular signalling molecule and a member of the TGFβ superfamily and participates in the development, maintenance and repair of synovial joint tissues (Reynard *et al.* 2011). Many studies have found that the genetic deficit in GDF5 is not restricted to cartilage but is found in all of the joint tissues so far examined in OA patients (Reynard and Loughlin 2012). Mouse studies have confirmed that a reduction in GDF5 mRNA and protein can result in an OA-like phenotype (Daans *et al.* 2011).

1.5.2 Dietary factors

Dietary factors such as vitamin supplementation are the subject of considerable interest and debate in OA. The Framingham Study demonstrated subjects in the lowest (<27 ng/ml) and middle (27.0 – 33.0 ng/ml) tertile of serum 25- hydroxyvitamin D had a 3-fold increased risk

for progressive knee OA compared with those in the highest tertile. However, no such effect was observed for the risk of developing hip OA (McAlindon *et al.* 1996a). In contrast, in the Study of Osteoporotic Fractures, women in the middle (23-29 ng/mL) and lowest (8-22 ng/mL) tertiles of serum 25-vitamin D were 3 times as likely to develop incident hip OA, compared to those in the highest tertile (30-72 ng/mL) (Lane *et al.* 1999). Low vitamin C dietary intake was associated with an increased risk of progression, but not incidence, of knee OA among the participants in the Framingham Study (McAlindon *et al.* 1996b). Neogi *et al.* (2008) showed high serum vitamin K was associated with a low prevalence of radiographic hand OA and the presence of large osteophytes but the relation of serum vitamin K levels to knee radiographic OA was less clear. However, a placebo-controlled trial of vitamin K supplementation did not confirm a protective effect of vitamin K on the severity of radiographic hand OA (Neogi and Zhang 2013). In areas of China and Eastern Asia the prevalence of Kashin-Beck Disease, an early onset of osteoarthropathy is high (Fang *et al.* 2003; Moreno-Reyes *et al.* 2003). In these areas, the levels of selenium (a non-metal element with anti-oxidative properties) are low in soil (Moreno-Reyes *et al.* 2003). Interestingly, supplementation of selenium decreased the incidence of this disease (Moreno-Reyes *et al.* 2003). However, others have reported that high selenium intake is associated with increased risk of both hip and knee OA (Neogi *et al.* 2008). Studies on dietary factors such as the ones outlined above and other studies in the past focusing on nutritional supplementation such as glucosamine or chondroitin have been conflicting and produced poor clinical efficacy (McAlindon *et al.* 1996b; Hunter 2011; Neogi and Zhang 2013).

1.5.3 Obesity

Being obese or overweight are potent risk factors for OA, especially OA of the knee (King *et al.* 2013). The increase load caused by obesity and being overweight might be a leading cause of knee or hip OA by placing undue stress on joint and supporting structures (Neogi and Zhang 2013). The Framingham Study showed that women who lose approximately 5 kg had a 50% reduction in the risk of development of symptomatic knee OA and a strong association with a reduced risk of radiographic knee OA (Felson *et al.* 1992). Losing weight has also been shown to decrease pain and disability in established knee OA patients (Messier *et al.* 2004). Interestingly, a clinical trial showed patients who combined weight loss with exercise were effective in decreasing pain and improving function (Messier *et al.* 2004). However, exercise and/or weight loss alone did not improve pain and functional outcomes (Messier *et al.* 2004). Meta-analysis of the study demonstrated the effects of weight loss on pain were not consistent but weight reduction by about 5% was associated with an improvement of physical function (Christensen *et al.* 2007). The association of being overweight and hip OA is inconsistent and weaker than knee OA (Neogi *et al.* 2008); however, obesity has been shown to increase the risk of bilateral radiographic as well as symptomatic hip OA (Tepper and Hochberg 1993). High body mass index, especially at a young age has been also associated with an increased risk of total hip replacement therapy (Karlson *et al.* 2003).

1.5.4 Gender

Women are more likely to have OA than men (Srikanth *et al.* 2005). There is an increase in the prevalence of OA in women around the time of menopause (Wluka *et al.* 2000; Srikanth *et al.* 2005). This raises the question of whether hormonal factors might play a role in the development of OA. However, there has been conflicting observational data to support the

positive effect of estrogen, either endogenous or exogenous, in OA (Neogi and Zhang 2013). No significant difference was found in the prevalence of knee pain or its associated disability between those taking estrogen plus progestin therapy or those taking placebo (Nevitt *et al.* 2001). In contrast, Women's Health Initiative showed women on estrogen replacement therapy were 15% less likely to require total knee or hip arthroplasty than those not taking such therapy (Cirillo *et al.* 2006).

1.5.5 Mechanical injury

Numerous studies have shown that knee injury is a major risk factor for OA. Injury to the structures of a joint, particularly a trans-articular fracture, meniscal tear requiring meniscectomy, or anterior cruciate ligament injury increases the prevalence of OA (Neogi and Zhang 2013). In the Framingham Study the prevalence of meniscal damage was much higher among subjects with radiographic knee OA (82%) than those without OA (25%) (Englund *et al.* 2008). A systemic review of studies involving patients with anterior cruciate ligament injury, either isolated or combined with medial collateral ligament, reported the prevalence of OA was up to 48% in subjects with anterior cruciate ligament and additional meniscal injury (Øiestad *et al.* 2009). In addition, Stefan *et al.* (2007) reported that 50% of those with a diagnosed anterior cruciate ligament or meniscus tear develop osteoarthritis with associated pain and functional impairment 10 to 20 years after the original diagnosis.

1.5.6 Age

Age is the strongest risk factor for OA in all joints (Shane Anderson and Loeser 2010). The increased prevalence and incidence of OA with age may be a consequence of cumulative exposure to various risk factors and biological changes that occur with ageing (Lotz and Loeser

2012). The Framingham Osteoarthritis Study showed the prevalence of radiographic OA increased with each decade of life from 33% among those aged 60–70 to 43.7% among those over 80 years of age, whereas, the prevalence of symptomatic knee OA in all subjects was 9.5% and increased with age in women but not men (Felson *et al.* 1987). In addition, a population-based cohort of 3,000 study participants conducted in the United States of America (USA) showed the incidence of radiographic knee OA rose from 26.2% in the 55–64 year range to nearly 50% in the 75+ group (Jordan *et al.* 2009). Likewise the prevalence of symptomatic knee OA increased from 16.3% to 32.8% between these groups (Jordan *et al.* 2009). The Chingford Women's study, which is a community-based cohort living in the United Kingdom (UK), showed that at baseline, when the median age was 53 years, 13.7% of the patients had radiographic knee osteoarthritis; by a median age of 68 years the incidence of radiographic knee osteoarthritis increased to 47.8% (Leyland *et al.* 2012).

Hip OA is less common in the ageing population than knee OA but is still quite prevalent (Shane Anderson and Loeser 2010). The prevalence of primary radiographic hip OA increased from 0.7% in the 40–44 age group to 14% in the 85+ age group in a systematic review which examined the prevalence of primary hip OA (Dagenais *et al.* 2009). An American cohort study demonstrated a higher prevalence of symptomatic hip OA in their population with age: of 5.9% in the 45–54 age groups increasing to 17% in the 75+ age group (Jordan *et al.* 2009). Moreover, a study of a cohort of patients with osteoporotic fractures reported an increase in the prevalence and incidence of hip OA in women over age 65 (Arden *et al.* 2009).

The hand is probably the joint most commonly affected by OA in the ageing population (Loeser 2012b). However, hand OA is not as disabling as OA of the knee or hip (Shane

Anderson and Loeser 2010) . The Zoetermeer survey found that radiographic involvement of the distal interphalangeal joint affected more than half of men over the age of 65 and more than half of women over the age of 55 (van Saase *et al.* 1989). The Framingham study found 13% of men and 26% of women over the age of 70 have symptomatic hand OA involving at least one joint (Zhang *et al.* 2002). The Fallon Community Health Plan reported that yearly incidence rates for hand OA were 0.35% and 0.21% for men and women respectively over the age of 60 and the incidence rates younger than 60 years were much lower (Oliveria *et al.* 1995).

1.6 Cellular Ageing Pathways in OA

The mechanisms by which age affects cartilage health are multiple and varied but probably not simply due to accumulated 'wear and tear' over time. It is well established that COL2 has negligible turnover during the normal adult lifetime but becomes biochemically modified (crosslinked) with age (Bank, Bayliss, Lafeber, Maroudas and TeKoppele, 1998). Cartilage proteoglycan, whilst having a much shorter half-life, is also modified with age (Hickery *et al.*, 2003; Lauder, Huckerby, Brown, Bayliss and Nieduszynski, 2001). Collectively this significantly changes the stiffness of the matrix (Bank *et al.*, 1998) and is likely to affect not only its 'brittleness', making it more susceptible to fracture, but also the ability of chondrocytes to sense and respond to mechanical load. Interestingly, Loeser *et al.* (2013) used a surgical OA model in 12-week-old and 12-month-old male mice. Not only did the older mice exhibit increased OA disease scores, but gene expression profiles were also significantly different in the aged mice (Loeser *et al.* 2013). One significant advance over the past decade or so has been the characterization of the cellular metabolic pathways that are affected by ageing (Figure 1.6). Largely these pathways have been defined in other model systems and in recent

years studied in the joint.

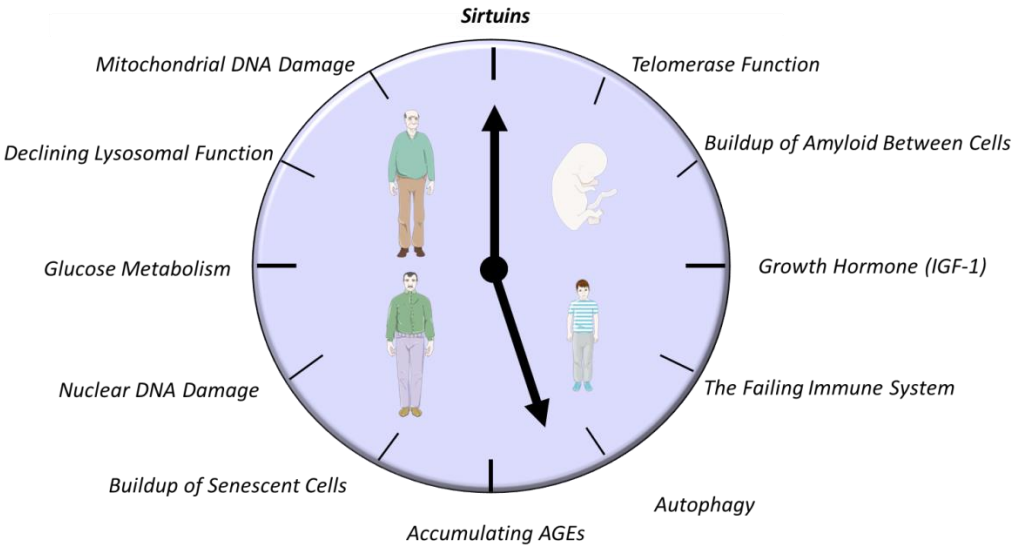

Figure 1.6: Cellular ageing mechanisms.

1.6.1 Sirtuins

The well-conserved sirtuin gene family has been strongly associated with longevity since Sir2 (Silent information regulator 2) was shown to extend lifespan in budding yeast, worms, flies and mice (Giblin *et al.* 2014). In mammals, the sir2 homologs are known as sirtuin(s) (silent mating type information regulation 2 homolog (SIRT)), a seven member family (SIRT1-7) of nicotinamide adenine dinucleotide (NAD^+) dependent deacetylases (Figure 1.7), with SIRT4 and SIRT6 also demonstrating ADP-ribosyltransferase activity (Verdin 2014). SIRT1 is found in the cytosol and nucleus, whereas SIRT2 is predominately located in the cytosol. SIRT3, SIRT4 and SIRT5 are found in the mitochondria, SIRT6 in the nucleus and SIRT7 in the nucleolus (Nakagawa and Guarente 2011a). The sirtuins are involved in a wide range of physiological systems and cellular functions including cell metabolism, apoptosis, growth and development, inflammatory and stress responses (Sacitharan *et al.* 2012; Morris 2013). The

diverse roles of the sirtuin family have resulted in them being studied extensively over the past decade in the fields of age-related pathologies (Giblin *et al.* 2014).

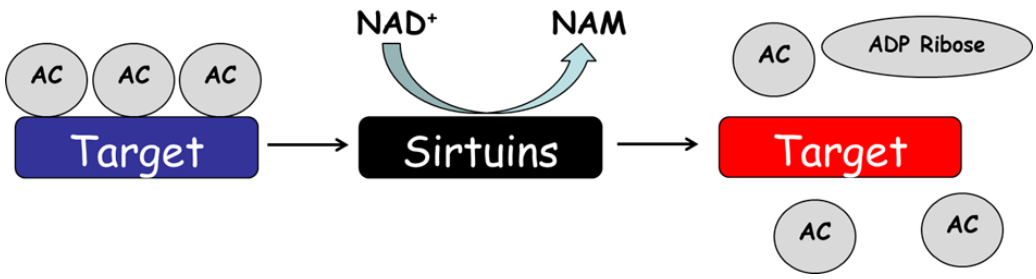

Figure 1.7: Mechanism of action of sirtuins.

1.6.2 SIRT1

The closest mammalian homologue to Sir2 is SIRT1 (Frye 1999). SIRT1, 110 Kd in molecular weight, is found in the nucleus in most cell types but can be also found in the cytoplasm under some conditions (Tanno *et al.* 2007). The three-dimensional structure of SIRT1 has modeled indicating that SIRT1 has a globular core and two large unordered structural regions at N- and C- terminals (Autiero *et al.* 2009). Moreover, the N- and C-terminal regions of SIRT1 are positioned behind the catalytic core. Between the N- terminal and the catalytic core, there is an allosteric site to regulate enzymatic activity (Autiero *et al.* 2009). The N-terminal sequence contains functional nuclear localization sequences and the nuclear exporting sequences are located in the catalytic domain (Tanno *et al.* 2007). The C and N terminals of SIRT1 have different functional elements which would be disrupted after cleavage for example a 75kD cleaved SIRT1 peptide has been shown to block apoptosis in osteoarthritic chondrocytes (Oppenheimer *et al.* 2012).

1.6.3 Regulation of SIRT1

1.6.3.1 Transcriptional regulation of the SIRT1 gene

Several transcription factors have been shown to modulate transcription of SIRT1. Under conditions of oxidative stress it has been demonstrated that the transcriptional suppressor hypermethylated in cancer 1 forms a complex with SIRT1 promotor and suppresses the transcription of SIRT1 (Huffman *et al.* 2007). In addition, the nuclear transcription factor EVI-1 required for embryogenesis has also been shown to bind to the promoter region of SIRT1, causing the transcriptional upregulation of the gene (Pradhan *et al.* 2011). Furthermore, E2F Transcription Factor 1 which activates transcription of genes within the apoptosis pathway targets the SIRT1 promoter under conditions of oxidative stress (Wang *et al.* 2006). This mechanism upregulates SIRT1 gene expression causing a negative feedback loop in which SIRT1 inhibits the action of E2F-1 (Wang *et al.* 2006). SIRT1 transcriptional regulation can also be regulated by nutrient availability (Houtkooper *et al.* 2012). For example, SIRT1 mRNA levels increased in serum starved conditions in Henrietta Lacks cells and this effect was abrogated when Forkhead box protein O (FOXO) 3a was silenced (Nemoto *et al.* 2004). Similarly, FOXO1 has been shown to interact with the SIRT1 promoter and increase SIRT1 mRNA levels (Xiong *et al.* 2011). In addition, it has been reported that nutrient deprivation activates cyclic adenosine monophosphate response element binding protein (CREB) which also binds to the SIRT1 promoter region and upregulates SIRT1 expression (Jeong *et al.* 2012). This action is counterbalanced by the suppression of SIRT1 expression by the carbohydrate response element binding protein responsible for promoting energy storage with increased nutrient availability (Wang *et al.* 2010). In the process of adipogenesis CCAAT/enhancer binding protein increases the levels of SIRT1 expression to inhibit further synthesis of adipose tissue (Jin *et al.* 2010).

1.6.3.2 Post transcriptional regulation of SIRT1 mRNA

Multiple mircoRNA (miRNAS; denoted with miR accessions) have been observed to influence SIRT1 regulation to date (Yamakuchi 2012). Downregulation of SIRT1 in endothelial cells leading to cellular senescence (miR-217; Menghini *et al.* 2009); downregulation of SIRT1 in endothelial progenitor cells inhibiting angiogenesis (mIR-34a; Zhao *et al.* 2010); downregulation of SIRT1 leading to apoptosis in cardiomyocytes (mIR-34a; Zhu *et al.* 2011) and downregulation of SIRT1 mRNA levels in high embryonic mouse stem cells (miR-9; miR-135a; miR-199b; miR-204; miR-181a and b Saunders *et al.* 2010). Conversely, upregulation of SIRT1 mRNA levels results in the transformation of mammary epithelial cells in breast cancer (miR-200a; Eades *et al.* 2011).

1.6.3.3 Post translational regulation of SIRT1 protein

Sumoylation of the SIRT1 protein at K734 by small ubiquitin-related modifiers activates SIRT1 under normal physiological conditions (Yang *et al.* 2007). The desumoylase Sentrin-specific protease 1 inactivates SIRT1 during acute DNA damage which activates the apoptotic pathway (Yang *et al.* 2007). Phosphorylation sites have been identified at threonine and serine residues within the SIRT1 protein sequence (Sasaki *et al.* 2006). Phosphorylation of the SIRT1 protein by casein kinase 2 has been reported at S154, S649, S651 and S683 resulting in SIRT1 activation and increased substrate binding in response to DNA damage (Kang *et al.* 2009). The dual specificity tyrosine phosphorylation-regulated kinases dual-specificity tyrosine phosphorylation-regulated kinase (DYRK) 1A and 3 regulate neuronal development, cell proliferation and apoptosis (Guo *et al.* 2010). Both DYRK1A and DYRK3 have been shown to phosphorylate SIRT1 at tyrosine 522, serine 530, serine 531 and serine 532 (Guo *et al.* 2010). In addition, c-Jun N-terminal kinase (JNK) 1 and 2 family, which induce signalling cascades in

response to cellular stress, also phosphorylate SIRT1 (Ng and Tang 2013). JNK1 phosphorylates SIRT1 at serine 47 and tyrosine 530 promoting resistance to cellular stress (Nasrin *et al.* 2009). JNK2 phosphorylates SIRT1 at serine 27 and stabilises the protein (Ford *et al.* 2008).

Active regulator of SIRT1 (AROS) and deleted in breast cancer-1 (DBC-1), activate and reduce SIRT1 deacetylase activity respectively (Dang and Le 2012). AROS protein has been shown to directly bind with amino acids 114 – 217 in the SIRT1 protein to enhance deacetylation activity (Kim *et al.* 2007). Conversely, DBC-1 binds at amino acids 243-268, a region in the catalytic core of the SIRT1 protein, to confer reduced deacetylase activity (Kim *et al.* 2008). In addition, it must be noted that the dependence of SIRT1 on the availability of the NAD^+ cofactor has profound effects on downstream SIRT1-mediated responses (Imai and Yoshino 2013). Na^+-dependent dicarboxylate cotransporter (NaDC3) is required for the transport of Krebs' cycle intermediates thus affecting NAD^+/nicotinamide adenine dinucleotide reduced (NADH) ratio within the cell (Liu *et al.* 2010). Overexpression of NaDC3 in embryonic lung fibroblasts increased Krebs' cycle intermediates and decreased intercellular NAD^+ levels which downregulated SIRT1 activity (Liu *et al.* 2010). Similarly, overexpression of nicotinamide mononucleotide adenylyltransferase 1, a central enzyme in NAD^+ biosynthesis, increased NAD^+ biosynthesis thus increasing SIRT1 activity in transgenic mice (Song *et al.* 2013).

1.6.4 SIRT1 Targets

SIRT1 has multiple histone and non-histone targets (Figure 1.8). SIRT1 regulates chromatin via deacetylation of histones which silences DNA transcription in times of stress, and allows for chromatin stabilisation or DNA repair (Imai *et al.* 2000a). The first major substrate of SIRT1

to be shown was Histone 4 lysine 16 (Hajji *et al.* 2010) which controls the cell cycle in breast and colon cancer cells (Pruitt *et al.* 2006). Other histone targets for deacetylation include lysine residues at positions 9 and 26 of histone 1, 14 of histone 3, and 16 of histone 4 (Imai *et al.* 2000b). Moreover, SIRT1 has been extensively shown to have other non-histone targets (Nakagawa and Guarente 2011b). These include p300 (Bouras *et al.* 2005), Peroxisome proliferator activated receptor-gamma co-activator-1alpha (PGC-1α; Amat *et al.* 2009), p53 (Kim *et al.* 2007), FOXO transcription factors (Brunet *et al.* 2004), transcription factors hairy and enhancer of split-1 and -2 (Takata and Ishikawa 2003), peroxisome proliferator-activated receptor-γ (Han *et al.* 2010) and nuclear factor kappa-light-chain-enhancer of activated B cells (NF-κB) (Rothgiesser *et al.* 2010).

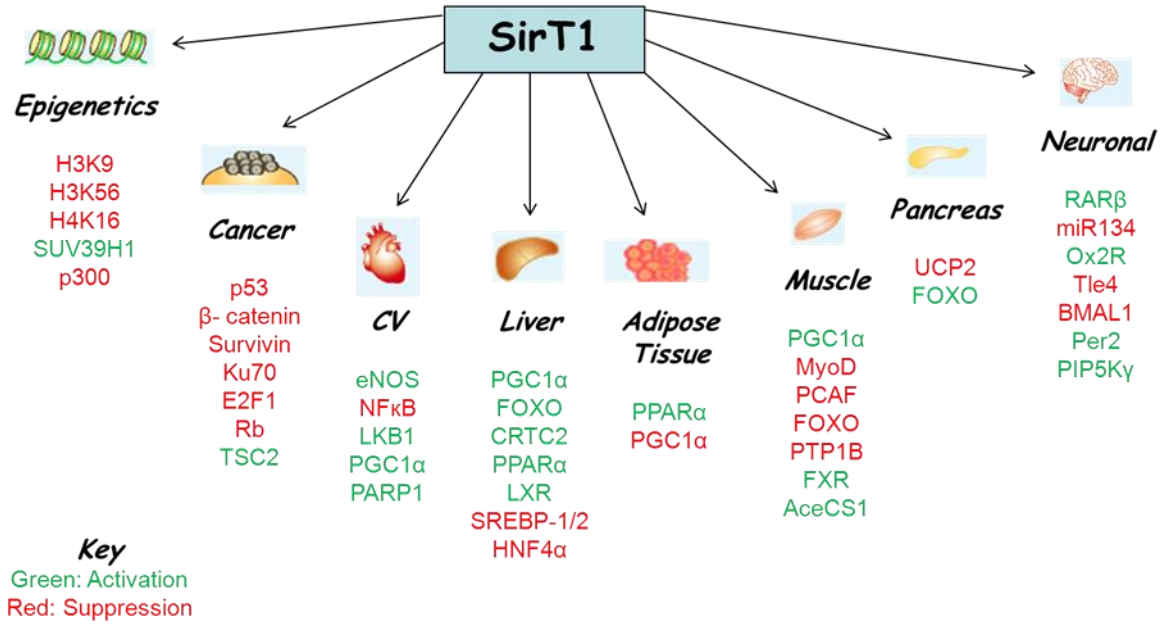

Figure 1.8: SIRT1 Targets. Deacetylation by SIRT1 either increases or decreases the physiological activity of its targets. Adapted from Guarente *et al* 2011.

1.6.5 SIRT1 and inflammation

SIRT1 plays a role in inflammation by regulating NF-κB. It has been shown that SIRT1 deacetylates lysine 310 on the RelA/p65 subunit of NF-κB, thereby inhibiting its translocation into the nucleus and reducing the expression of its target genes (Rothgiesser *et al.* 2010). Interestingly, cigarette smoke extracts increase pro-inflammatory responses mediated by NF-κB by decreasing the interaction between SIRT1 and RelA/p65 resulting in increased acetylation and activation of NF-κB (Hwang *et al.* 2010). SIRT1 is expressed at higher levels in calorie restricted rodents which also show decreased inflammatory responses (Chen *et al.* 2008). In addition, SIRT1 activating compounds also were shown to have anti-inflammatory effects (Nayagam *et al.* 2006).

1.6.6 SIRT1 and ageing diseases

1.6.6.1 Longevity

Initial research showed deletion of the Sir2 gene in Saccharomyces cerevisiae reduced life span. However, insertion of an extra copy of Sir2 increased lifespan by up to 30% (Kaeberlein *et al.* 1999). Moreover, overexpression of Sir2 in both the nematode worm and fruit fly also resulted in an increase in lifespan (Tissenbaum and Guarente 2001; Rogina and Helfand 2004) Therefore, SIRT1 was believed to hold the same capacity in mammals. However, overexpressing SIRT1 in mice resulted in no lifespan expansion (Herranz *et al.* 2010). Interestingly, supplementation of SRT1720, an activator of SIRT1, extended lifespan of mice and reduced risk factors for metabolic disease such has low fat mass, low insulin sensitivity, low muscle composition and high inflammatory gene expression (Mitchell *et al.* 2014). In addition, SIRT1 levels increased in calorie restricted mice which have increased lifespan compared to mice on standard diet (Chen *et al.* 2005). Despite the conflicting data on SIRT1

increasing lifespan in mammals it has been shown to have crucial roles in the etiology of age-related human diseases (Nakagawa and Guarente 2011b).

1.6.6.2 Type 2 Diabetes Mellitus

In type 2 diabetes mellitus (DMT2) insulin production is normal but the sensitivity is lost. In the liver SIRT1 has been implicated to affect gluconeogenesis and DMT2 in two distinct mechanisms. On one hand the direct deacetylation of PGC-1α and FOXO1 appears to favor glucose production by increasing the insulin signalling cascade (Rodgers *et al.* 2005). Conversely, CREB activation by SIRT1 suppresses glucose production (Liu *et al.* 2008). In addition, following supplementation of the SIRT1 activator resveratrol reduced circulating glucose levels in a genetic model of murine obesity (the leptin-deficient *ob/ob* mouse) model (Guarente 2011). SIRT1 overexpression in mice also prevented DMT2 by increasing insulin sensitivity (Bordone *et al.* 2007; Banks *et al.* 2008).

1.6.6.3 Neurological disorders

SIRT1 function has been implicated in protecting against neurodegenerative disorders such as Parkinson's and Alzheimer's diseases (Guarente 2011). β-Amyloid peptide gives rise to a protein aggregate of plaques in the brain of patients of both diseases (Guarente 2011). Donmez *et al* (2010) showed SIRT1 increases the Notch signalling pathway, which suppresses β-amyloid production, thus decreasing β-amyloid production. In addition, β-amyloid peptide and the level of plaques were reduced in mice that overexpress SIRT1 (Huang *et al.* 2008). In a separate study in mice, SIRT1 was shown to directly deacetylate tau protein to destabilize it and reduce tangles (Min *et al.* 2010). Interestingly, SIRT1 has been shown to activate brain-derived neurotrophic factor resulting in increased benefits of learning and memory in mice

(Gao *et al.* 2010; Michán *et al.* 2010). These studies indicate activation of SIRT1 as a potential method to treat common neurodegenerative disorders.

1.6.6.4 Cardiovascular disease

SIRT1 has been reported to have cardiovascular protective properties (Morris 2013). For example, transgenic mice that overexpress SIRT1 in the heart had decreased cardiac hypertrophy (Alcendor *et al.* 2007). SIRT1 also protects smooth muscle by directly inhibiting the expression of the angiotensin receptor AT1 which reduces reactive oxygen species and oxidative stress (Li *et al.* 2011). Alongside the effect on AT1, SIRT1 has been reported to activate endothelial nitric oxide synthase, a potent vasodilator which reduces blood pressure. SIRT1 has also been shown to regulate fat and cholesterol homeostasis (Ota *et al.* 2008). SIRT1 activates the nuclear receptor liver X receptor (LXR) by direct deacetylation which activates Adenosine triphosphate (ATP)-binding cassette transporter A1 and increases cholesterol uptake in cells (Li *et al.* 2007). LXR activation also increases the expression of the gene encoding the sterol regulatory element-binding protein 1 which increases fat and cholesterol synthesis in the liver (Denechaud *et al.* 2008). Mice overexpressing SIRT1 or mice administered with SIRT1 activators also showed decreased cholesterol levels (Zhang *et al.* 2008; Mitchell *et al.* 2014). The cardiovascular protective properties of SIRT1 could also be explained by its function in the kidney and in the control of blood pressure (He *et al.* 2010). Kidney specific SIRT1 overexpression prevented senescence of tubular epithelium cells and decreased blood pressure in mice (He *et al.* 2010).

1.6.6.5 SIRT1 and OA

Most sirtuin focussed OA research to date has been around SIRT1. SIRT1 expression is

decreased in human articular chondrocytes in response to nutritional, catabolic or mechanical stress (Takayama *et al.* 2009). Dvir-Ginzberg *et al.* (2008) showed that overexpression of SIRT1 in chondrocytes isolated from articular cartilage of human joints resulted in an increase in cartilage specific gene expression of collagen 2(α1) (COL2A1) through the deacetylation of SOX-9 (Dvir-Ginzberg *et al.* 2008). Similarly, decreased expression of aggrecan, COL2A1 and collagen 9(α1) was observed in SIRT1 siRNA treated human knee chondrocytes (Fujita *et al.* 2011). Conversely, decreasing SIRT1 resulted in the upregulation of collagen 10(α1) and ADAMTS5 gene expression (Fujita *et al.* 2011).

During the course of this thesis Gabay *et al.* (2012) demonstrated that SIRT1 constitutive whole body knockout mice had increased OA disease scores and exhibited low levels of COL2A1, ACAN, GAG release and high protein levels of MMP-13. These studies were performed at 3 weeks of age as constitutive SIRT1 KO mice only survive for a few weeks post-partum. The same group generated mice in which a point mutation renders SIRT1 inactive. These mice displayed increased levels of apoptotic chondrocytes and increased OA disease scores when compared with age-matched (9 months) wild type (WT) control mice (Gabay *et al.* 2013). Matsuzaki *et al.* (2013) generated cartilage specific SIRT1 conditional knockout (cKO) mice using an inducible COL2A1 Cre recombinase (COL2A1 Cre ER^{T2}). SIRT1-cKO mice showed accelerated OA progression at 2 and 4 (but surprisingly not 8) weeks post joint destabilisation. In addition, spontaneous OA scores were significantly higher in 1 year old SIRT1-cKO mice than in control mice (Matsuzaki *et al.* 2013). Together, these studies to date suggest that SIRT1 may have a protective role in cartilage. The specific targets of SIRT1 and precise mechanisms of action in chondrocytes are as yet unclear.

1.6.7 Autophagy

Autophagy is a cellular homeostasis mechanism for the removal of dysfunctional organelles and proteins (Boya *et al.* 2013). There are three main types of autophagy; microautophagy, chaperone-mediated autophagy and macroautophagy (Boya *et al.* 2013). Microautophagy sequesters cytoplasmic components, and delivers them for degradation to the lysosomal or vacuolar membrane (Glick *et al.* 2010). During chaperone-mediated autophagy a chaperone protein binds to a target protein, causing it to unfold, allowing for direct transport across the lysosomal membrane (Glick *et al.* 2010). Macroautophagy, hereafter referred to as autophagy, is the most well characterized process of the three (Glick *et al.* 2010).

Autophagy is initially induced by the isolation membrane (phagophore) derived from lipid bilayer contributed by the endoplasmic reticulum (ER) and/or the trans-Golgi and endosomes (Mizushima *et al.* 2010). This phagophore expands to engulf intra-cellular cargo, such as protein aggregates, organelles and ribosomes, thereby forming a double-membraned autophagosome (Mizushima *et al.* 2010). The mature autophagosome fuses with the lysosome promoting the degradation of autophagosomal contents by lysosomal acid proteases (Mizushima *et al.* 2010). By-products and recycled amino acids after degradation are exported by lysosomal permeases and transporters out to the cytoplasm and can be reused for building macromolecules and for metabolism (Salminen and Kaarniranta 2009a). Hence, autophagy not only degrades and recycles unwanted proteins but is also involved in ATP generation and energy metabolism (Rubinsztein *et al.* 2011).

1.6.7.1 Molecular pathway of autophagy

The molecular pathway of autophagy is complex and involves several conserved autophagy-related (ATG) proteins (Figure 1.9; (Jaeger and Wyss-Coray 2009)). The induction and phagophore formation can be activated by various stimuli such as nutrient starvation, and leads to the formation of the phagophore, a step that involves two protein complexes (Hansen and Johansen 2011). At first a complex that includes the serine/threonine kinase ATG11/ Unc-51 Like Autophagy Activating Kinase 1 (ULK1) positively regulates autophagosome formation thereby activating another complex containing class III phosphatidylinositol 3-kinases/Vacuolar Protein Sorting 34, ATG6/Beclin1, ATG14 and Vps15/p150.73 (Tanida 2011). Thereafter, the elongation of the phagophore forms the characteristic double-membrane autophagosome (Tanida 2011). This step requires two key ubiquitin-like conjugation pathways (Glick *et al.* 2010). The first ubiquitin-like pathway leads to the conjugation of Atg5-Atg12 and Atg16L complex which associates with the outer membrane of the extending phagophore (Glick *et al.* 2010). The second ubiquitin-like pathway processes microtubule-associated protein 1A/1B-light chain 3 (LC3) which is encoded by the Atg8. Upon autophagy induction, LC3B is cleaved by Atg4 to generate LC3B-I (Hansen and Johansen 2011). LC3B-I is activated by Atg7 and then conjugated to phosphatidylethanolamine in the membrane to generate processed LC3B-II (Hansen and Johansen 2011). Processed LC3B-II binds onto the growing phagophore and it is found on both the inner and outer surfaces of the autophagosome, enabling the expansion and completion of the autophagic membrane (Hansen and Johansen 2011). After the autophagic membrane closes, the Atg16-Atg5-Atg12 complex dissociates from the vesicle but not LC3B-II (Hansen and Johansen 2011). Therefore, LC3B-II is used as a classical marker to monitor the level of autophagy in cells (Mizushima *et al.* 2010). The fusion between the autophagosome and the

lysosome requires the lysosomal membrane protein 2 and the small GTPase Rab7 (Mizushima 2007). After fusion, a series of acid hydrolases are degraded the sequestered cytoplasmic cargo (Glick *et al.* 2010).

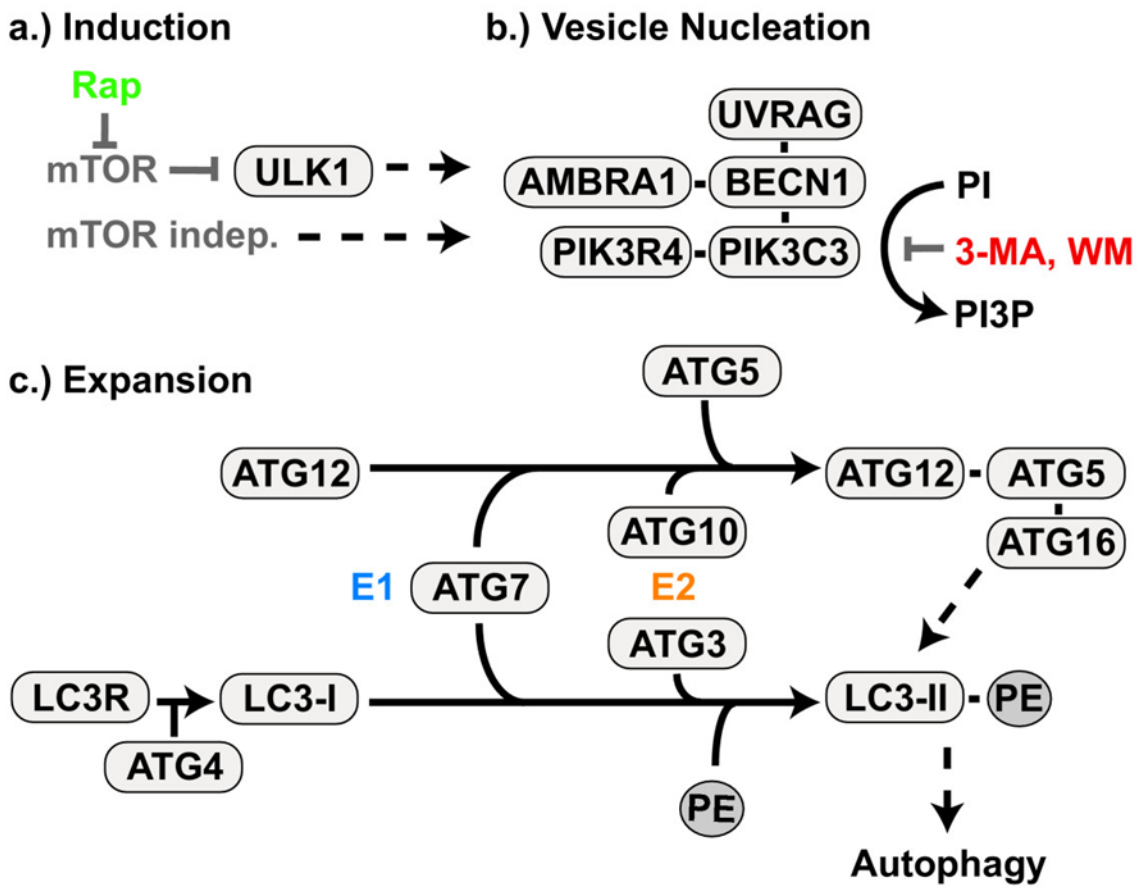

Figure 1.9: Mammalian autophagic pathway. Adapted from Jaeger and Wyss-Coray (2009).

Autophagy also plays a role in development (Mizushima and Levine 2010), immunity (Deretic *et al.* 2013), and ageing (Rubinsztein *et al.* 2011) and is involved in several human pathologies including cancer (Kenific and Debnath 2015), cardiovascular disease (Choi *et al.* 2013), diabetes (Jung and Lee 2010) and neurodegenerative disorders such as Alzheimer's and Parkinson's diseases (Wong and Cuervo 2010). Recent observations indicate that this process is compromised in ageing cartilage (Lotz and Caramés 2011).

1.6.7.2 Autophagy and OA

Caramés *et al* (2010) initially examined key autophagy proteins in human and murine cartilage. These key autophagy markers were ULK1, Beclin1, and LC3 (Lotz and Caramés 2011). ULK1, Beclin1, and LC3 protein expression was reduced in human OA chondrocytes and cartilage (Caramés *et al.* 2010). In mouse knee joints, protein expression of ULK1, Beclin1, and LC3 decreased together with glycosaminoglycans (GAG) loss at ages 9 months and 12 months and in the DMM OA disease model, 8 weeks after surgery (Caramés *et al.* 2010). However, Poly(ADP-ribose) polymerase (PARP) p85 (a marker for apoptosis) expression was increased at these time points (Caramés *et al.* 2010). A further study by Caramés *et al* (2015) showed 28-month-old mice had significant reduction in the total number of autophagic vesicles per cell and in the total area of vesicles per cell in articular cartilage compared to young 6-month-old mice. With increasing age, the expression of ATG5 and LC3 decreased in these mice, and this was followed by a reduction in cartilage cellularity, OA disease score and an increase in PARP p85 (Caramés *et al.* 2015). Interestingly, Bouderlique *et al.* (2015) generated cartilage specific ATG5 conditional KO (ATG5cKO) mice which developed severe osteoarthritis when aged and also displayed increased cell death, cleaved caspase 3 and cleaved caspase 9 (Bouderlique *et al.* 2015). Surprisingly, no difference in the development of post-traumatic osteoarthritis was observed between Atg5 cKO mice and control mice post DMM (Bouderlique *et al.* 2015).

Studies have also examined the role of mammalian target of rapamycin (mTOR) signalling which when activated inhibits ULK1 which in turn inhibits autophagy. Zhang *et al.* (2014) reported that upregulation of mTOR expression correlates with increased chondrocyte apoptosis and reduced expression of key autophagy genes in human OA tissue. In addition,

inducible cartilage-specific mTOR KO mice displayed increased autophagy signalling and significant protection from DMM induced OA associated with a significant reduction in the apoptosis and synovial fibrosis (Zhang *et al.* 2014). In another study, Carames *et al.* (2012) used rapamycin to pharmacologically inhibit mTOR in mice. The severity of cartilage degradation was significantly reduced in the rapamycin-treated group compared with the control group and this was associated with a significant decrease in synovitis 10 weeks post DMM (Carames *et al.* 2012). Rapamycin treatment also maintained cartilage cellularity and decreased ADAMTS5 and IL-1β expression in articular cartilage (Carames *et al.* 2012). These results suggest that rapamycin, at least in part by autophagy activation, reduces the severity of experimental osteoarthritis. However, further studies are required to investigate if other key regulators of autophagy exist in ageing cartilage apart from the classical mTOR/ULK1 signalling cascade.

1.6.7.3 Autophagy and SIRT1

The role of SIRT1 in the regulation of autophagy has also been reported. Embryonic fibroblasts isolated from SIRT1 KO mice had decreased autophagy during starvation (Lee *et al.* 2008). Lee *et al.* (2008) also demonstrated that the absence of SIRT1 leads to markedly elevated acetylation of ATG5, ATG7, and ATG8 in both cultured cells (Henrietta Lacks cells) and in embryonic and neonatal tissues. In addition, the same study showed that SIRT1 KO mice partially resemble ATG5 KO mice, including the accumulation of damaged organelles and early perinatal mortality (Lee *et al.* 2008). Morselli *et al.* (2010) also showed that knockout of SIRT1 prevented the induction of autophagy in human colon carcinoma cells by nutrient deprivation and by dietary restriction in C.*elegans*. SIRT1 inhibition has also been shown to increase smoke induced autophagy in lung epithelial, fibroblasts and macrophages cell lines (Hwang

et al. 2010). In addition, manipulating NAD^+/NADH ratio through the addition of nicotinamide increases SIRT1 level in cultured fibroblasts and stimulates mitophagy (Jiang *et al.* 2014). The role of SIRT1 in the regulation of autophagy in chondrocytes and OA is still unknown.

1.7 Research hypothesis

My D.Phil hypothesis is that the loss of SIRT1 in ageing dysregulates normal chondrocyte biology and may predispose to osteoarthritis.

1.8 Research aims

1) To generate a ubiquitous and a cartilage specific inducible SIRT1 knockout mouse line.

2) To determine the physiological effect of cartilage specific and ubiquitous SIRT1 deletion in ageing mice and in an *in vivo* model of OA.

3) To investigate if SIRT1 regulates autophagy in chondrocyte biology and to determine if loss of this pathway leads to accelerated cartilage ageing and OA.

2. Methods

2.1 Isolation of human articular chondrocytes (HACs)

Healthy or OA knee/hip articular cartilage was obtained from patients at the Royal National Orthopedic Hospital (Stanmore, U.K) or Oxford Musculoskeletal Biobank (Oxford, U.K). Healthy, normal cartilage was obtained from patients who underwent surgery for tumours of the lower leg in which the knee joint was not affected. The age of the patients ranged from 21-86 years old. Tissue samples were collected with informed donor consent in full compliance with national and institutional ethical requirements, the UK Human Tissue Act, and the Declaration of Helsinki (License 12217 and Oxford REC C 09/H0606/11). Dissected cartilage pieces were incubated overnight in Dulbecco's modified Eagle's medium (DMEM) with 1mg/ml/g Collagenase A (Roche Pharmaceuticals, Hertfordshire, U.K.) at 37 Celsius (°C) for 5-6 hrs (hours). Thereafter, the digest was strained and centrifuged at 1200 × g (relative centrifugal force) for 5 min. The cell pellets were subsequently washed three times with DMEM and resuspended in DMEM containing 10% FCS. Cells were plated at 50% confluence in 15 centimeter (cm) culture dishes. Cells used in experiments were at passage 1.

2.2 Cell culture

HTB-94 (human chondrosarcoma cell line) or ATDC-5 (teratocarcinoma AT805 derived mouse cell line) cells were obtained from the American Type Culture Collection (Manassas, U.S.A), cultured in (DMEM) containing 4.5g/l of glucose and L-glutamine (Lonza, Verviers, Belgium). DMEM was supplemented, unless stated otherwise with 10% fetal calf serum (FCS) (PAA Laboratories, Pasching, Germany), 1% Penicillin and Streptomycin (Cambrex, Maryland, USA), Amphotericin B (Gibco, New York, USA) and 2% (4-(2-hydroxyethyl)-1-piperazineethanesulfonic acid (HEPES) solution (Cambrex, Maryland, USA). Cells were

maintained under sterile conditions in a humidified atmosphere of 37°C containing 95% oxygen and 5% (v/v) carbon dioxide unless stated otherwise. All plastics for cell culture were purchased from Beckton-Dickinson (Oxford, U.K).

2.3 SIRT1 small inferencing Ribonucleic Acid (siRNA) transfection

Cells (density of 250,000 cells/well) were wet reverse transfected with Dharmacon ON-TARGETplus SMARTpool (4 oligos) human SIRT1 siRNA (L-003540-00-0005) (Dharmacon Technologies, Fisher Scientific, Schwerte, Germany) at a final concentration of 25nM in 6 well plates. A scrambled oligo sequence (D-001810-01-05) (Dharmacon Technologies) was used as control at a final concentration of 25nM. All the oligos were transfected into cells using DharmaFECT 1 transfection reagent (Dharmacon Technologies). At first the cells were incubated for 24 or 48hrs in DMEM containing 10% FCS with no antibiotics or HEPES solutions. 48hrs was chosen as the ideal time point for efficient genetic suppression of SIRT1 after quantitative reverse transcription polymerase chain reaction (RT-qPCR) and protein validation. Thereafter, all siRNA experiments were carried out with a 48hrs wet reverse transfection of the smart-pool siRNA and scrambled control.

2.4 RNA extraction from cell cultures

Prior to RNA extraction from cells, media from wells was removed and the cell layer was washed with phosphate buffered saline (PBS). The cell layer was lysed and total RNA was isolated using RNeasy Mini Kit (Qiagen, Clawley, U.K) as per the manufacturer's instructions. RNA was eluted in 40 microliters (µl) of Ribonuclease (RNase) free water and its concentration was determined by measuring the absorbance at 260 nanometers and 280 nanometers.

2.5 RT-PCR and quantitative PCR

Complementary DNA (cDNA) was generated from 500ng of isolated RNA from either cell cultures or murine tissue using a High Capacity reverse transcription cDNA kit (Applied Biosystems, Paisley, U.K) according to the recommendations of the manufacturer. Briefly, a total of 20µl mixture containing 10µl of RNA, 2µl of 10 x reverse transcriptase buffer, 2µl of random primer, 0.8 deoxyribonucleotides, 1µl RNase inhibitor, 1µl reverse transcriptase and 3.2µl of RNase free water was used per reaction (Bio-Rad, Hertfordshire, U.K). A programme of 25°C for 10min, 37°C for 120min and finally 85°C for 5min was used for reverse transcription. A total of 10µl of reaction mixture containing 1µl cDNA template, 5µl of TaqMan 2× Universal PCR Master Mix (Applied Biosystems), 0.5µl of TaqMan primers (Table 2.1) and 3.5µl of nuclease-free water was added to each well of a 384 well plate. The plate was sealed and centrifuged. RT-qPCR was carried out on a ViiA™ 7 Real-Time PCR System (Applied Biosystems). Relative gene expression was analysed by the $^{\Delta\Delta}$Ct method using *18S* ribosomal RNA (*18S)* as an endogenous control gene.

2.6 TaqMan Low Density Array microfluidic cards (TLDA)

TLDA cards were custom designed and purchased from Applied Biosystems. A total of 100µl reaction mixture containing 50µl cDNA template (500ng starting RNA) in nuclease-free water and 50µl of TaqMan 2x Universal PCR Master Mix was briefly vortexed and centrifuged prior to addition to each TLDA loading port. The TLDA card was then centrifuged twice for 1min each at 1200 r.p.m, sealed and then ran on a ViiA™ 7 RT-qPCR System (Applied Biosystems). The thermocycling conditions were: hold at 50°C for 2min for optimal activity of UNGerase enzyme, then denaturation at 94.5°C for 10min followed by 40 cycles of denaturation at 97°C for 30s and an annealing/ extension step at 59.7°C for 1min.

Table 2.1: TaqMan Gene Expression Assay primers/probe mixes. Used in TaqMan Low Density Array microfluidic cards and single RTq-PCR experiments.

Gene	Human	Murine
18S	Hs03003631_g1	Mm02601776_g1
ACAN	Hs00153936_m1	Mm00545794_m1
ADAMTS1	-	Mm00477355_m1
ADAMTS15	-	Mm01176187_m1
ADAMTS4	-	Mm00556068_m1
ADAMTS5	Hs00199841_m1	Mm00478620_m1
Atg10	-	Mm00470550_m1
ATG12	-	Mm00503201_m1
ATG13	-	Mm00521135_m1
ATG14	-	Mm00553733_m1
ATG16	-	Mm00513085_m1
ATG4	-	Mm04214755_s1
ATG5	-	Mm00504340_m1
ATG7	-	Mm00512209_m1
ATG9	-	Mm01264420_m1
Beclin 1 (BECN1)	Hs00177504_m1	Mm01265461_m1
COL2A1	Hs00264051_m1	Mm01309565_m1
Connective tissue growth factor (CTGF)	-	Mm00515790_g1
Interleukin-18 (IL18)	-	Mm00802090_m1
IL1β	-	Mm01336189_m1
Interleukin-6 (IL6)	-	Mm99999064_m1
LC3A	Hs01076567_g1	Mm00458724_m1
LC3B	-	Mm00782868_sH
MMP-13	Hs00233992_m1	Mm00439491_m1
SIRT1	Hs01009005_m1	Mm00490758_m1
SOX-9	Hs01001343_g1	Mm00448840_m1
Sequestosome 1 (SQSTM1)	-	Mm00448091_m1
TIMP1	-	Mm00441818_m1
Tumor necrosis factor-inducible gene 6 (TSG6)	-	Mm00493736_m1
ULK1	Mm00437238_m1	Mm00437238_m1

2.7 Western blot (WB) analysis

Tissue samples were homogenized in radioimmunoprecipitation assay (RIPA) lysis buffer (Sigma-Aldrich), Ethylenediaminetetraacetic acid (EDTA)-free protease inhibitor (Roche Pharmaceuticals) and Phosphatase inhibitor cocktail 2 and 3 (Sigma-Aldrich). Thereafter, protein levels were quantified by bicinchoninic acid assay (Thermo Fisher Scientific, Northumberland, UK). Cell extracts containing 20–50 microgram (μg) of proteins were placed in denaturing buffer (Life technologies, Paisley, U.K) and reducing buffer (Life technologies). Samples were then subjected to sodium dodecyl sulfate polyacrylamide gel electrophoresis and then transferred to nitrocellulose membranes using the Trans-Blot® Turbo™ Blotting System (Bio-Rad). The membranes were blocked with Tris(hydroxymethyl)aminomethane (Tris)-buffered saline and tween 20 buffer (20mM Tris–chlorine, pH 7.5, 150mM sodium chloride and 0.2% tween 20) containing 5% bovine serum albumin. Thereafter, membranes were probed overnight with a primary antibody: Human SIRT1 (#9475; 1:1000; Cell Signalling Technology, MA, U.S.A), Mouse SIRT1 (07-131; 1:1000; Millipore, Massachusetts, U.S.A) or Beta-actin (β-actin) (A2228; 1:20000; Sigma-Aldrich), COL2A1 (SAB4500366; 1:1000; Sigma-Aldrich), SOX-9 (ab26414; 1:1000; Abcam, Cambridge, U.K.), ULK1 (NBP2-24738; 1:1000; Novus Biologicals, Cambridge, UK), Beclin1 (NB500-249; 1:1000; Novus Biologicals), LC3 (NB100-2220; 1:1000; Novus Biologicals), ATG5 (#12994; 1:1000; Cell Signalling Technology); ATG7 (#8558; 1:1000; Cell Signalling Technology), Acetyl-Lysine Antibody (#9441; 1:1000; Cell Signalling Technology), P62/SQSTM1 (NBP1-48320; 1:1000; Novus Biologicals). Secondary horseradish peroxidase (HRP)-conjugated anti-rabbit (#7074; 1:5000; Cell Signalling Technology), Secondary HRP-conjugated anti-mouse (#7076; 1:5000; Cell Signalling Technology) antibodies were subsequently used to detect protein expression via enhanced chemiluminescence (Select™; Amersham Biosciences, Buckinghamshire, UK). Densitometric

analysis was carried out using ImageJ (National Institutes of Health, Bethesda, Maryland, USA) software.

2.8 Drug Treatment

Cells were seeded at 300,000 cells per well in 6 well plates in complete DMEM media. Cells were left for 24hr to settle and adhere. Thereafter, the complete DMEM media was removed and cells were treated with DMEM media containing antibiotics and HEPES solutions but no FCS for 1hr. After serum starvation media in the wells was removed and replaced with complete media containing EX-527 (inhibitor of SIRT1; 100nM; E7034; Sigma-Aldrich), SRT1720 (activator of SIRT1; 500nM; S1129; Selleckchem, Boston, Massachusetts, U.S.A) or the solvent control of Dimethyl Sulfoxide (DMSO).

2.9 Cell viability assay

Cell viability after drug treatments at each time point (1, 2, 4, and 24hrs) was quantified colorimetrically by measuring the reduction of the tetrazolium salt via 3-(4,5-dimethylthiazol-2-yl)-2,5-diphenyltetrazolium bromide (MTT) assay (Sigma-Aldrich, Dorset, UK), to formazan by mitochondrial dehydrogenases. Briefly, media was removed from wells and replaced with 100µl serum free DMEM media containing MTT (1mg/ml) per well. Cells were incubated for 30mins and the media was removed and plates were left overnight to dry. Wells were treated with 100µl of DMSO and the absorbance was measured at 570 nanometers on a FluoStar Omega (BMG Labtech, Aylesbury, U.K) plate reader.

2.10 Fluorescence-activated cell sorting (FACS)

Autophagy was also measured by quantifying LC3-II mean fluorescence intensity (MFI) using the FlowCellect Autophagy LC3 Antibody-based Assay Kit (FCCH100171, Merck-Millipore, MA, USA) according to the manufacturer's instructions after treating the cells with either containing EX-527 (100nM), SRT1720 (500nM), the vehicle control of DMSO, Bafilomycin A1 (BAF; B1793; 10nM Sigma-Aldrich). Untreated cell were also used as a negative control. Use of this kit includes a step where cytosolic LC3-I is washed from the cell, leaving only membrane bound LC3-II prior to staining.

2.11 Mice and ethics

All animal procedures were approved by the British Home Office, under the UK Animal (Scientific Procedures) Act 1986 (Project license 70/7289). Mice weighed 18 – 25g and were maintained in cages under controlled temperatures (19 – 23°C) and lights (12-hr light, 12-hr dark cycle, lights on at 0700 hrs). All mice had *ad libitum* access to water and chow (RM1 diet; Special Diet Services, Devon, UK).

2.12 Generation of cartilage-specific SIRT1 KO mice

Mice carrying a floxed SIRT1 allele, in which exon 4 of SIRT1 was flanked by LoxP sites ($SIRT1^{fl/fl}$) were purchased from the Jackson Laboratory (Maine, U.S.A). Aggrecan $CreER^{T2}$ mice were generated and donated by Professor George Bou-Gharios (University of Liverpool). Homozygote Aggrecan $CreER^{T2}$ mice were bred with $SIRT1^{fl/fl}$ mice to generate homozygote double transgenic $SIRT1^{fl/fl}$; Aggrecan $CreER^{T2+}$ mice ($SIRT1^{Agg}$) mice. $SIRT1^{Agg}$ mice were obtained at the expected Mendelian ratio with no adverse phenotypic side effects. $SIRT1^{fl/fl}$ mice were used as control mice.

2.13 Generation of whole body SIRT1 KO mice

Reverse Orientation Splice Acceptor (ROSA) Cre mice were purchased from the Jackson Laboratory. ROSA-Cre mice were bred with $SIRT1^{fl/fl}$ mice to generate homozygote $SIRT1^{fl/fl}$; ROSA $CreER^{T2+}$ mice ($SIRT1^{ROSA}$) mice were obtained at the expected Mendelian ratio with no adverse phenotypic side effects. $SIRT1^{fl/fl}$ mice were used as control mice.

2.14 Induction of Cre-LoxP recombination

Free base tamoxifen (TX) (50 milligram (mg)) (T5648; Sigma-Aldrich) was suspended in 500ml of 100% ethanol which was then diluted in 4,500ml of sunflower oil. Thereafter the solution was thoroughly sonicated until all of the TX was dissolved. The final concentration was 10mg/ml. Adult mice were administered intraperitoneal doses of 2 mg three times, every other day at 8 week of age. Young mice were (used so cartilaginous hips can be avulsed) administered intraperitoneal doses of 2mg three times, every other day at 8 week of age. Pregnant female mice were given a single dose 20 milligram/kilogram (mg/kg).

2.15 Genotyping of Mice

Genomic DNA was extracted from ear biopsies of mice using RedExtract-N-Amp Tissue PCR Kit (Sigma-Aldrich). The extraction of genomic DNA was done as per the manufactures instruction. The PCR mixture contained 4µl of REDExtract-N-Amp™ 0.5 micromolar (µM) of each primer (Table 2.2), and 1µl of the DNA template in a total volume of 10µl. Thereafter, agarose gel electrophoresis (1% Tris-acetate-EDTA) was conducted to determine the genotype of the mice. The internal control of fatty acid binding protein (FABP) was used.

Table 2.2: Primers used for genotyping of mice and q-PCR experiments

Gene	*Primer Sequence*
SIRT1	Forward: GGTTGACTTAGGTCTTGTCTG
	Reverse: CGTCCCTTGTAATGTTTCCC
Internal Control	Forward: GCATTACCGGTCGATGCAACGAGTGATGAG
	Reverse: GAGTGAACGAACCTGGTCGAAATCAGTGCG
Cre	Forward: TGGACAGGACTGGACCTCTGCTTTCCTAGA
	Reverse: TAGAGCTTTGCCACATCACAGGTCATTCAG

2.16 Validation of Cre expression using ROSA26 reporter mice

SIRT1^{Agg} were bred with ROSA26 reporter mice to test the tissue/cellular expression pattern of ROSA CreER^{T2} and Aggrecan CreER^{T2} transgenic mice (purchased from the Jackson Laboratory). ROSA26 reporter mice have a loxP-flanked DNA STOP sequence preventing expression of the downstream β-galactosidase gene. When crossed with a Cre transgenic strain and TX is administered the STOP sequence is removed and β-galactosidase is expressed in cells/tissues where Cre is expressed. Staining of embryos with the 5-bromo-4-chloro-3-indolyl b-Dgalactopyranoside the substrate of β-galactosidase will yield a blue precipitate. This will confirm the expression of the Cre. SIRT1^{Agg} mice not carrying the Cre allele were used as controls. At day 14 of gestation, pregnant female mice were injected with TX. Thereafter, at day 15.5 of gestation pregnant female mice were sacrificed, the yolk sacs removed and the embryos were collected. Embryos were fixed in 2% formaldehyde, 0.2% glutaraldehyde in PBS at room temperature for 1hr. Thereafter embryos were rinsed twice in PBS and stained for β-

galactosidase overnight in the dark at room temperature in PBS containing Potassium Ferrocyanide, (Sigma-Aldrich), Potassium Ferricyanide (Sigma-Aldrich) and 1 mg/ml 5-bromo-4-chloro-3-indolyl b-Dgalactopyranoside. The following day embryos were washed twice in PBS and fixed in 4% formaldehyde overnight. Embryos were photographed using a Stereo Microscope (Model M165 C, Leica Microsystems Buffalo, U.S.A) the magnification of x1.6 was used for normal embryo pictures and the magnification of x3.5 for close up embryo pictures. The microscope was fitted with a ProgRes® CFscan camera (Jenoptik, Massachusetts, U.S.A) for increased resolution (12 megapixels). ProgRes® CapturePro software (Jenoptik) was used to analyse and capture images.

2.17 RNA extraction from murine tissue

Mice were injected with TX at week 8 and culled at week 10. Microdissected cartilage (cartilage from 4 mouse knee joints were pooled to give n=1) was at first was collected in RNAlater® Stabilization solution (Life technologies). Thereafter samples were placed in TRIzol® (Life technologies) and was homogenised using PowerGen™ Model 125 Homogenizer (Fisher Scientific). Homogenised samples were shaken for 10mins at room temperature and then centrifuged at 13000 × g for 10mins at 4°C. Supernatants were diluted in an equal amount of 1-Bromo-3-chloropropane (Sigma-Aldrich), vortexed and centrifuged 13000 × g for 15 min at 4°C. The upper aqueous phase was removed and placed in new eppendorfs. Thereafter the RNeasy Mini Kit protocol was followed to isolate RNA. RNA was eluted in 40µl of RNase free water and its concentration was determined by measuring the absorbance at 260nm and 280nm. Reverse transcription was performed on the collected RNA as described above.

2.18 Protein extraction from murine hip avulsion

Mice were injected with TX at week 5 and culled at week 7. Young hips were used due to their cartilaginous nature and an adequate amount of protein can be extracted. Hips were avulsed and placed in ice cold protein lysis buffer (as described above). Thereafter, samples were shaken for 2hrs at 4°C. The samples were then centrifuged at 13,000 × g for 5mins at 4°C and the supernatants were collected for experiments. Immunoblotting was performed on the collected supernatants as described above.

2.19 DMM

10 week old male mice were anaesthetized by intra-peritoneal injection of a 1:1:2 mixture of Hypnorm (0.315mg/ml fentanyl citrate and 10mg/ml fluanisone; VetaPharma Limited company (Ltd), Leeds, UK), Hypnovel (5mg/ml midazolam; Roche), and sterile water for injection, at a dose of 10 millilitre/kilogram body weight. Mice undergoing surgery for later time points were anaesthetized by inhalation of Isoflurane (3% induction and 1.5-2% maintenance) in 1.5-2 L/min oxygen. All animals received a subcutaneous injection of Vetergesic (0.05mg/kg buprenorphine hydrochloride in sterile water; Alstoe Animal Heath Ltd, York, UK) post-surgery. The ventral portion of the right (Ipsilateral) knee was shaved and swabbed with iodine to prepare a sterile surgical field. The surgical procedure was carried out with the aid of a dissecting microscope. A midline incision over the ventral aspect of the knee was made with a no.15 scalpel (Swann Morton, Sheffield, U.K.) and the medial compartment entered via a medial para-patellar approach to avoid damage to the medial collateral ligament and minimizing trauma to the quadriceps. Mild hemorrhage from the fat pad upon dissection was controlled by pressure from absorption spears or swabs. The medial menicus was identified and the attachments of its anterior horn to the tibial plateau cut using a 3 millimeter

15 ophthalmic scalpel (Swann Morton). Care was taken to avoid injury to the anterior cruciate ligament and the cartilage surfaces. The medial meniscus was grasped by its anterior horn with a jeweler's forcep and its mobility confirmed. The para-pateller window was closed using an absorbable 6/0 Vicryl suture (W9575; New Jersey, Ethilon, USA) and a round-bodied needle to avoid tissue damage. The skin was closed using a 5/0 Ethilon suture (W1601T; Ethilon) with reverse cut needle (Ethilon). For sham control limbs, the mice were anaesthetized and prepared as before. The right knee was opened using the same medial para-patellar approach and the meniscus identified but the menisco-tibial ligament was not released (i.e capsulotomy alone). The incision was closed and the mice recovered as before. Left (contralateral) knees for both DMM and sham operations were left as un-operated controls. DMM surgeries were performed by Dr Jadwiga Miotla Zarebska (University of Oxford).

2.20 Histology

Following euthanasia by carbon dioxide or cervical dislocation, mouse knees were harvested by excising at the proximal femur and distal tibia. The skin and surrounding muscles were then removed without disturbing the joint and its associated ligaments. The knee specimens were fixed in 10% Neutral Buffered Formalin (Cellpath, Newtown, UK) for at least 24hrs before any further processing. The specimens were decalcified in 20% formic acid for 14 days. The knees were then processed as per standard protocol: 2 changes of formalin (40°C) followed by 70% alcohol (40°C), 90% alcohol (40°C), 3 changes of absolute alcohol (40°C), 4 changes of xylene (40°C) and 4 changes of paraffin wax (60°C) with each change lasting 1.5hrs. The knees were then embedded in paraffin wax. 4µm coronal or sagittal sections were obtained using a MICROM HM325 microtome (Microm UK Ltd, Oxford, UK), at 80 µm intervals, i.e., every 20th section, for staining with Safranin-O. Safranin-O staining was

performed in a Leica autostainer XL (Leica Microsystems, Wetzlar, DE). Sections were re-hydrated in 2 changes of absolute alcohol and then washed in tap watered. Nuclei were stained with Heamotoxylin for 5mins followed by washing in running tap water. The stain was differentiated in 0.5% acid alcohol (70% alcohol) for 30s and washed in tap water. Sections were then immersed in ammoniated water (1% ammonia in tap water) for 2mins and washed again with tap water. Finally the sections were dehydrated, cleared and mounted and coverslipped using Leica CV5030 (Leica) glass coverslipper. Each change or wash unless stated lasted 1min. Histology was performed by Dr Byrony, Stott, Dr Ida Parisi and Marcia Curtinha (University of Oxford).

2.21 Modified Osteoarthritis Research Society International (OARSI) disease scoring

A modified OARSI OA grading system (Table 2.4; Figure 2.1; Chia *et al.* 2009) was used to grade chondropathy in aged mice or mice which were subjected to DMM. Coronal sections stained for Safranin-O were scored blindly by two individual scorers. A minimum of 6 sections were scored per joint. All four quadrants of the knee were individually scored (medial femoral condyle and tibial plateau, lateral femoral condyle and tibial plateau). The summed score was calculated from the sum of the three highest scoring section totals (obtained from the sum of all four quadrants per section). This provides an indication of both severity and extent of OA damage within the joint.

Table 2.3: OARSI chondropathy grading scale

Grade	Features of Cartilage Damage
0	No Damage
0.5	Mild Proteoglycan (Safranin-O staining) loss
1	Roughened articular surface and small fibrillations
2	Fibrillation down to the layer immediately below the superficial layer and some loss of surface lamina
3	Mild loss of cartilage, with no loss of calcified cartilage i.e. Down to the tidemark.
5	Moderate loss of cartilage, involving loss of calcified cartilage
6	Severe loss (more than 80% thickness) of cartilage i.e Down to the subchondral bone

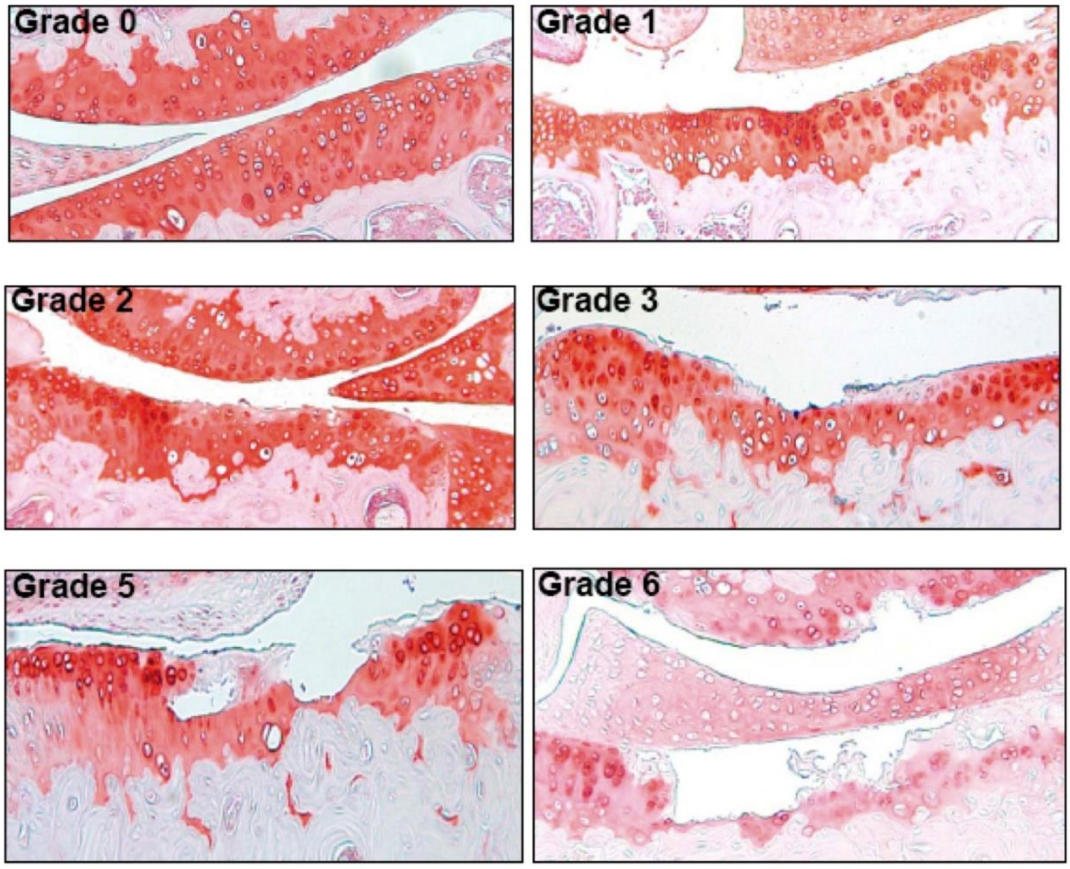

Figure 2.1: Histological Safranin-O chondropathy grading scores. Adapted from Glasson (2007).

2.22 Synovitis scoring

Sagittal sections (exposes more of the synovium) from mice knee joints were stained for Safranin-O and scored blindly by two individual scorers. The summed score was calculated from the sum of the three highest scoring section totals. A minimum of 3 sections were scored per joint. Usually, the most axial slide i.e. near intercondylar fossa/cruciate ligaments was scored. Occasionally, depending on the embedding and cutting, if this slide is too axial a slide a few sections further back was used – the slide needs to be in an area where in the posterior aspect of the joint there is a only a small area of meniscus still visible. Two different types of scoring were used; Synovial hyperplasia (Table 2.4) and Sub-synovial inflammation (Table 2.5).

Table 2.4: Scoring system for synovial hyperplasia

Grade	Severity of Synovial Hyperplasia
0	Normal= 1 cell thick
1	Mild= 2-3 cells thick
2	Moderate= 4-5 cells thick
3	Severe = >5 cells thick

Only the posterior aspect which is superior to the meniscal remnant of the joint was scored to avoid issues of effects of the surgical incision. The area attached to the tibia or femur of the surface of the meniscus was not scored.

Table 2.5: Scoring system for synovial inflammation

Grade	Severity of Inflammation
0	No inflammatory cells
1	Occasional scattered inflammatory cells - perivascular
2	Focal areas of dense sub-synovial white blood cells infiltrate - but still predominantly normal sub-synovial areolar connective tissue present
3	Widespread dense sub-synovial white blood cells infiltrate – markedly reduced or little/no normal areolar connective tissue evident or lymphoid follicle formation – distinct accumulations of mononuclear cells organised into rounded masses reminiscent of lymph nodules

Only the posterior aspect which is superior to the meniscal remnant of the joint was scored to avoid issues of effects of the surgical incision. The area attached to the tibia or femur of the surface of the meniscus was not scored. The infiltration of inflammatory cells (neutrophils, macrophages and/or lymphocytes) is scored.

2.23 Spermidine treatment

Mice were administered spermidine (S2626; Sigma-Aldrich) in the drinking water from the day of DMM surgery. Spermidine was added at a concentration of 5mM from a 1M aqueous stock. Spermidine-containing drinking water was replenished every 2–3 days.

2.24 LC3-Green fluorescent protein (GFP) Studies

Hips from LC3-GFP mice (donated by Professor Katja Simon, University of Oxford) were avulsed and placed in DMEM media containing either EX-527 (100nM) or SRT1720 (500nM) or DMSO. For positive controls, serum free DMEM containing either EX-527 (100nM) or SRT1720 (500nM) or DMSO was used. After an incubation of 2hrs, hips were embedded in Optimal Cutting Temperature (CellPath, Powys, U.K) and snap-frozen. Thereafter, samples were cryosectioned (CM1900UV Cyrostat, Leica, Nussloch, Germany) at 10µm and mounted (ProLong Diamond Antifade Mountant, Thermo Fisher Scientific) to slides. Fluorescence images were taken by the Olympus FLUOVIEW FV1200 confocal microscope (Olympus, Tokyo, Japan) using an excitation wavelength of 473 nanometers and a band-path of 490−540 nanometers. Bright filed images were obtained using scattering wavelength of 635 nanometers. A maximum of 54 images of confocal z stacks were imaged with a PLAPON OSC2 60x oil-immersion objective, with a z-step of 0.35µm, and a scanning resolution of 2048x2048 pixels (pixel size 69nanometers). The cells were segmented in bright filed and GFP intensity was measured in fluorescent channel. Intensity of background was subtracted from intensities of individual cells and divided by intensity of background in order to normalise and score cells. The number of LC3 puncta per cell was counted throughout each z stacks by two blinded operators. Confocal microcopy analysis was conducted with the help of Dr Volodymyr Nechyporuk-Zloy (University of Oxford).

2.25 Transmission Electron Microscopy (TEM)

Microdissected cartilage from $SIRT^{fl/fl}$ or $SIRT1^{Agg}$ mice were fixed using 2.5% glutaraldehyde (G5882; Sigma-Aldrich) + 4% paraformaldehyde (stock solutions both from Agar Scientific) in 0.1M piperazine-N,N'-bis(2-ethanesulfonic acid) (PIPES; P6757; Sigma-Aldrich) buffer at pH 7.2. Samples were incubated at room temperature in the fume hood for approx. 1-2hrs stored at 4°C overnight. Samples were rinsed with 0.1M PIPES buffer (3 changes of fresh buffer, 10-15mins each), then with 50mM glycine in 0.1M PIPES (to quench free aldehydes) for 15mins, and again with 0.1M PIPES for 10-15 mins. Secondary fixation was carried out using 1% osmium tetroxide (TAAB Laboratories, Reading, U.K.) in 0.1 M PIPES buffer at 4 °C for 2hrs with gentle rotation. Samples were then rinsed in Milli-Q water (3-5 changes of fresh water, 10-15mins each). Tertiary fixation was carried out using 0.2% Uranyl acetate (Agar Scientific, Stansted, U.K.) aqueous overnight at 4 °C in the dark. Samples were rinsed with water for 5-10mins. Samples were dehydrated in 30%, 70% 50%, 80%, 90%, 95% ethanol, each for 15mins at 4 °C with rotation/agitation then in 100% dry ethanol at 4 °C for 3x 90mins. Thereafter, Epoxy resin infiltration was carried out incubating samples with 2:1 100% dry ethanol: Low Viscosity Resin (TLV; from TAAB Laboratories) for 1-2hrs, then 1:1 100% dry ethanol: TLV resin for 2-3hrs, and 1:2 100% dry ethanol:TLV resin for 1-2hrs in the fume hood with rotation. Samples were then incubated in 100% TLV resin overnight at room temperature and then embedded in Beem capsules filled with fresh 100% TLV resin. Samples were cut semi-thin sections (0.5µm) as required using a diamond knife (Diatome, Biel, Switzerland) on an ultramicrotome (UC7, Leica). Transmission electron microscopies were imaged at 120 kilovolt on the FEI Tecnai 12 (Oregon, U.S.A) using the Gatan US1000 charge-coupled device camera (Pleasanton, U.S.A) with Digital Micrograph software (Pleasanton, U.S.A). Autophagosomes

from images were counted by two blinded operators. EM capturing was conducted by Dr Erin Johnson and Dr Anna Pielach (University of Oxford).

2.26 Immunoprecipitation

We performed immunoprecipitation using magnetic Beads (Pierce, Rockford, U.S.A) SIRT1 or autophagy antibodies (mentioned above) were incubated with magnetic beads at room temperature for 1hr. Thereafter the bead and antibody complex were washed for 3 times with RIPA lysis buffer. The bead and antibody complex were thereafter incubated with extract volumes of protein supernatant from respective experiments at 4°C overnight. The supernatant was then removed and the bead-antibody complex was then washed for 3 times with RIPA lysis buffer. Total Acetyl lysine or autophagy targets for the respective experiments were then detected by western blotting. Rabbit Immunoglobulin G (IgG) (#2729; Cell Signalling Technology) was used as negative control.

2.27 Immunohistochemistry

Paraffin embedded sections were heated in an oven maintained at 60°C for 30 mins overnight then dewaxed in xylene for 10 mins followed by submersion in 100% alcohol (3 x 5 mins). Heat mediated antigen retrieval was performed on sections. Sections were submerged in 0.01M, pH 6.0, citric acid buffer (C9999; Sigma-Aldrich) warmed in a water bath at 100°C for 20mins. Slides were then rinsed in PBS and blocking of non-specific binding sites was achieved by incubation for 2hrs at room temp with 10% normal serum and 0.5% bovine serum albumin in PBS. The appropriate concentration of primary antibody solution (made in blocking solution) was added to sections which were then incubated overnight at 4°C. LC3 (Novus) antibody was used at the dilution of 1:200. IgG control (D1415; Santa Cruz Biotechnology,

Dallas, U.S.A) was used at 1:200 as well. Sections were washed in PBS (2 x 10 mins) and then in incubated with biotinylated rabbit secondary antibody (1:100; BA-1000; Vector Laboratories, Peterborough, U.K) for 1hr at room temp. Following this, sections were washed in PBS and then incubated with an avidin-biotin-peroxidase complex solution (PK-6100; Vector Laboratories, Peterborough, U.K) at room temp for a period of 1hr. Sections were washed in PBS (2 x 10 mins) and then incubated with 3'3'diaminobenzidine (D12384; Sigma-Aldrich) solution to visualise antibody binding. The colour reaction was stopped after 3mins by immersion of sections in running water (10 mins). Sections were then counter stained with Mayers Haematoxylin (MHS1; Sigma-Aldrich) for 1min then followed by 5mins in running tap water. Sections were then dehydrated through a series of alcohols; 70% (2mins), 90% (2mins.), 100% (2 x 5 mins) and then xylene (10 mins) before being mounted and coverslipped in DPX mounting media (44581; Sigma). Slides were imaged using a light microscope (Olympus BX51, Olympus) at the magnification of x20. Quantification of LC3 positive cells/total cells in the medial femoral condyle and tibial plateau of $SIRT1^{fl/fl}$ mice or $SIRT1^{Agg}$ mice or $SIRT1^{ROSA}$ mice were counted by two blinded operators.

2.28 Data analysis

All data are expressed as mean ± standard error of mean (S.E.M) of n observations. Experiments were statistically analysed utilising the Students unpaired t-test for parametric data with independent groups compared with their specific controls or time-matched controls. One-way analysis of variance (ANOVA) with the Bonferroni post hoc test or ANOVA Tukeys multiple comparison test was used to compare 3 or more groups. A significant difference was accepted when $p \leq 0.05$, $p \leq 0.01$, $p \leq 0.001$ or $p \leq 0.0001$ represented in all

tables and figures as *, **, *** or **** respectively. Data analysis was performed using GraphPad Prism® 5.0 (GraphPad Software, California, U.S.A).

3. The role of SIRT1 in chondrocytes: *in vitro*

3.1 Introduction

OA is the most common form of arthritis worldwide characterized by the degradation of articular cartilage (Glyn-Jones *et al.* 2015). Increased age is a primary risk factor for the development of OA (Vincent and Watt 2014). However, the roles of ageing mechanisms in chondrocytes, the only resident cell in cartilage are not well understood. The class three histone deacetylase, SIRT1 has been extensively shown to regulate lifespan in lower organisms, pathways linked to mammalian ageing and age-related diseases (Sacitharan et al. 2012). Hence, investigating the expression and role of SIRT1 in chondrocytes will provide insight to how they are dysregulated over time which may lead to OA and the loss of cartilage integrity during ageing.

3.2 Hypothesis

SIRT1 expression decreases in ageing and OA cartilage compared to young cartilage and this dysregulates chondrocyte biology.

3.3 Results

3.3.1 Validation of SIRT1 protein expression and optimisation of SIRT1 antibodies in human and mouse cell lines

Initial experiments were conducted to validate SIRT1 expression in the human HTB-94 cell line that will be used throughout this thesis. These experiments also allowed the opportunity to optimise antibodies for both human and mouse species for future experiments (Figure 3.1).

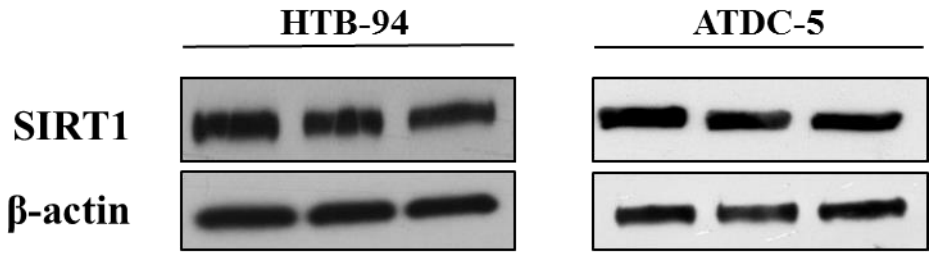

Figure 3.1: Validation of SIRT1 protein expression in cell lines by western blotting. SIRT1: 110 kilodalton (kDa); β-actin (42 kDa) was used as loading control. Repeats are from three different experiments (*n*=3).

3.3.2 SIRT1 protein expression in isolated chondrocytes from human samples

Using the optimised human SIRT1 antibody, the protein expression of SIRT1 in HACs was examined (Figure 3.2 A and B). SIRT1 protein expression decreased by 61.23% in old healthy HACs compared to young healthy HACs (*P*=0.0001) (Figure 3.2 A and B). Moreover, SIRT1 protein expression decreased by 72.73% in OA HACs compared to young healthy HACs (*P*=0.0002) (Figure 3.2 A and B). There was a 29.64% decrease in SIRT1 protein expression in OA HACs compared to old healthy HACs (*P*=0.002) (Figure 3.2 A and B).

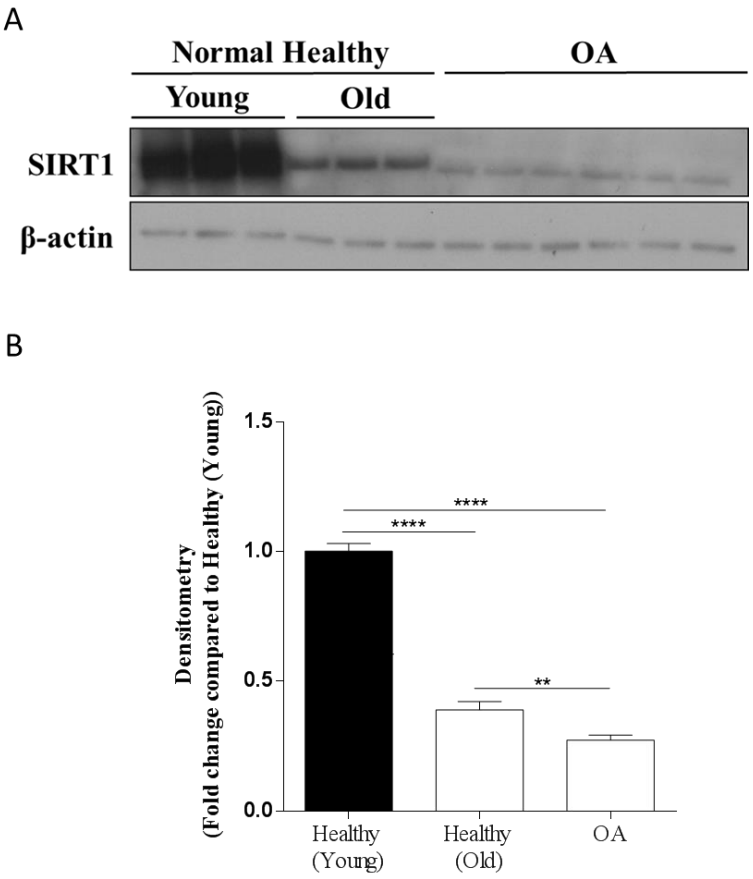

Figure 3.2: SIRT1 protein expression from HACs. (A) SIRT1 protein expression in isolated chondrocytes from young (21-37yrs) (*n*=3), old (62-68yrs) (*n*=3) and OA (49-86yrs) (*n*=6) knee joints. SIRT1: 110 kDa. β-actin: 42 kDa **(B)** Densitometry quantification of SIRT1 protein expression from HACs. Graphs show the mean ± S.E.M.; ANOVA Tukeys multiple comparison test; ** *P*< 0.01 or **** *P*<0.0001.

3.3.3 Optimisation of SIRT1 silencing using siRNA in HTB-94 cells

After observing a decrease in SIRT1 protein expression in OA chondrocytes, the cellular effects of decreasing *SIRT1* mRNA expression in chondrocytes was explored using SIRT1 siRNA. SIRT1 protein and mRNA expression was assessed at 24h and 48h post siRNA transfection. After 48h of transfection, SIRT1 silencing of 88% (*P*=0.0001) was achieved, whereas 24h post-transfection only silenced *SIRT1* by 54% (*P*=0.002) (Figure 3.3 A and B). In addition, SIRT1 expression on the protein level was efficiently knocked down (Figure 3.3 A and B).

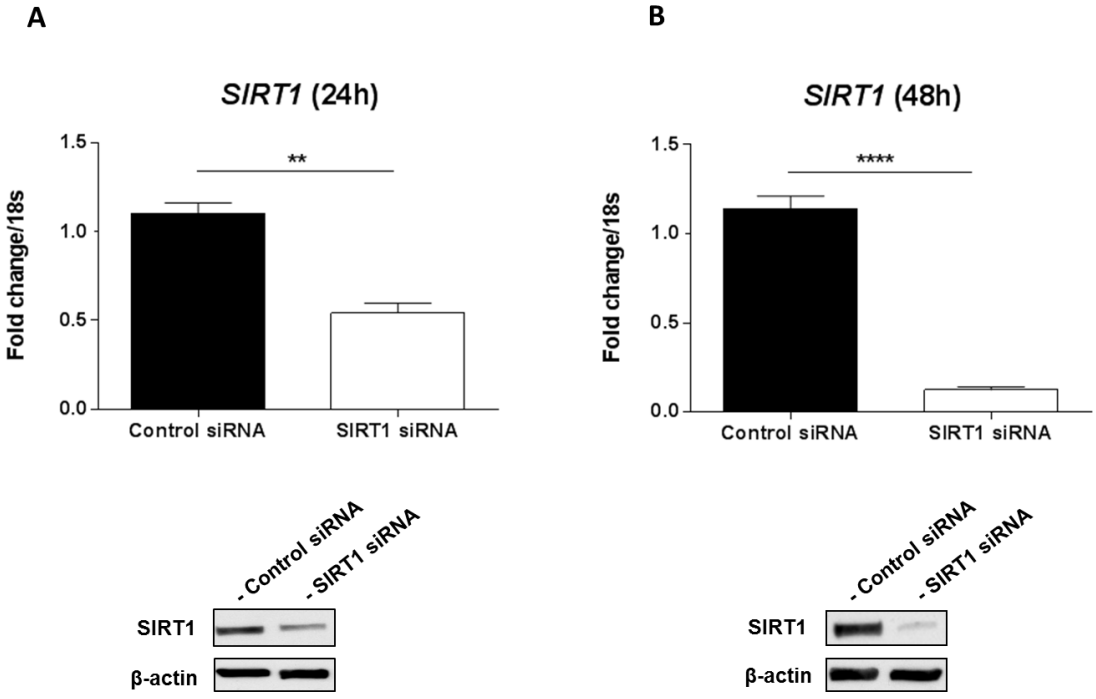

Figure 3.3: Optimisation of SIRT1 siRNA in HTB-94 cell line. RT-qPCR analysis for *SIRT1* mRNA silencing at **(A)** 24hrs and **(B)** 48hrs post transfection compared to scrambled siRNA treated cells at each time point. Data normalised to the endogenous level of *18S*. Graphs show the mean ± S.E.M. (*n*=3); unpaired t-test; ** p≤ 0.01 or **** p≤ 0.0001. Lower panels of each graph contains the WB analysis for SIRT1 protein silencing at 24hrs and 48hrs post transfection (respectively) compared to scrambled siRNA treated cells at each time point. β-actin was used as loading control. SIRT1: 110 kDa; β-actin: 42 kDa.

3.3.4 Effects of SIRT1 mRNA silencing on cartilage and ECM markers

After successfully optimising SIRT1 siRNA transfection, I went on to examine the effect of silencing SIRT1 on cartilage and OA markers in HTB-94 cells. I examined the mRNA expression of the main cartilage components *COL2A1* and *ACAN* and the chondrocyte differentiation factor of *SOX-9*. *COL2A1* (58.12%; *P*=0.002), *ACAN* (42.84%; *P*=0.004) and *SOX-9* (37.32% *P*=0.006) significantly decreased when SIRT1 (88.98%; *P*=0.0001) was silenced (Figure 3.4 A). However, the gene expression of *MMP-13* (4.12%; *P*=0.825) and *ADAMTS5* (+10%; *P*=0.305) the main matrix degrading proteases involved in OA did not alter significantly (Figure 3.4 A). The protein expression of COL2A1 (34.75%; *P*=0.03) and SOX-9 (39.03%; *P*=0.03) significantly decreased when SIRT1 (45.14%; *P*=0.02) was silenced (Figure 3.4 B and C).

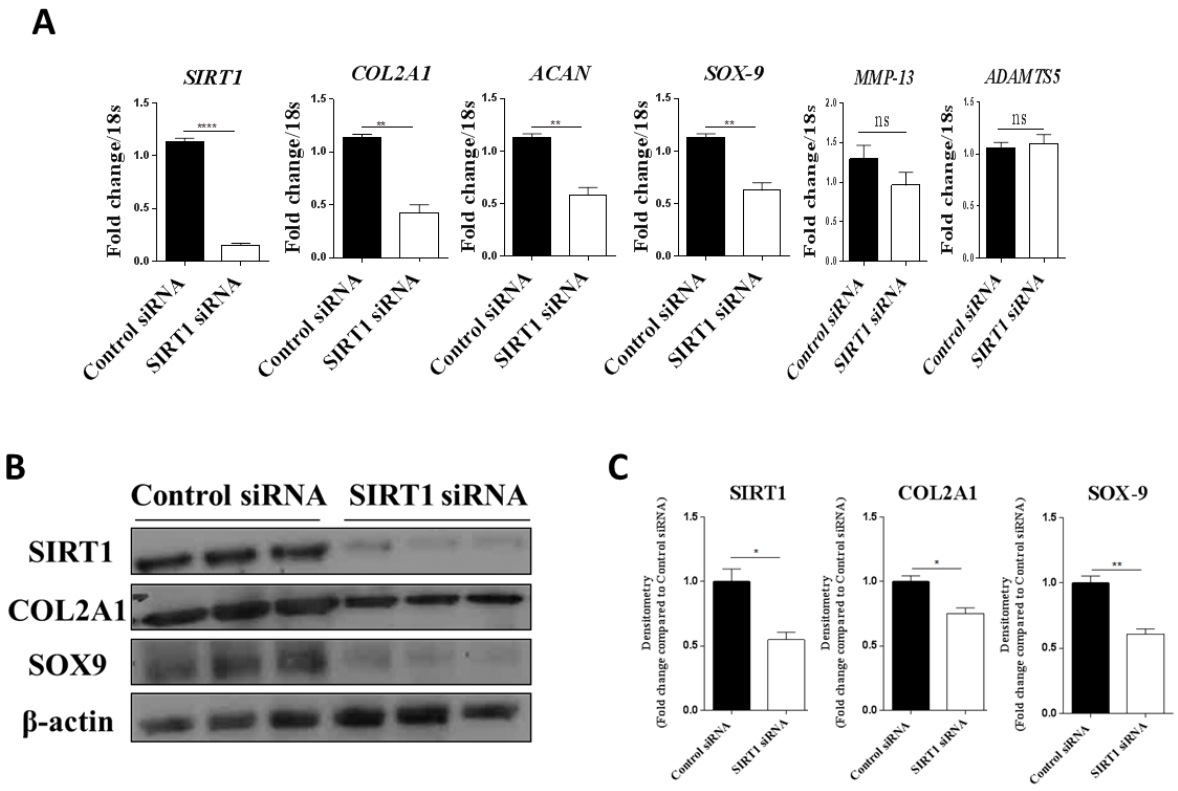

Figure 3.4: Effects of SIRT1 mRNA silencing on cartilage and ECM markers. (A) RT-qPCR analysis of cartilage marker expressions in HTB-94 chondrocytic cells following SIRT1 siRNA or control siRNA transfection (*n*=3). Data normalised to the endogenous level of *18S*. **(B)** Protein expression of cartilage markers in HTB-94 cells transfected with SIRT1 siRNA or control siRNA (*n*=3). **(C)** Densitometry quantification of protein expression of cartilage markers in HTB-94 cells transfected with SIRT1 siRNA or control siRNA (*n*=3). SIRT1: 110 kDa; COL2A1: 141 kDa; SOX-9: 60 kDa; β-actin: 42 kDa. Graphs show the mean ± S.E.M; unpaired t-test; ns=non-significant, * *P*< 0.05, ** *P*< 0.01 or **** *P*<0.0001.

3.3.5 Optimisation of SIRT1 drug concentrations

After observing the effects of *SIRT1* mRNA silencing, the effects of targeting SIRT1 activity pharmacologically in chondrocytes was investigated. Drugs which inhibit (EX-527) or activate (SRT1720) SIRT1 were selected. An MTT cell viability assay was used to determine the correct dose and time point for future experiments. Concentrations above 10 micromolar (μM) of EX-527 yielded below 55% cell viability across all time points whereas 1μM EX-527 yielded a cell viability of 89% at 1hr and 71% at 2hr (Figure 3.5 A). The concentration of 100 nanomolar (nM) of EX-527 at 2hr will be used in future experiments due to the high cell viability of 90% and the longer length of time the drug will have for efficacy (Figure 3.5 A).

Concentrations of above 10μM of SRT1720 at all-time points resulted in low cell viability (Figure 3.5 B). In addition, at the 24hr time point (data not shown) all the cells seeded were dead. The concentration of 1μM of SRT1720 yielded cell viabilities of 79% and 53% at 1hr and 2hr time points respectively (Figure 3.5 B). The concentration of 500nM of SRT1720 at 2hr will be used in future experiments due to the high cell viability of 91% (Figure 3.5 B).

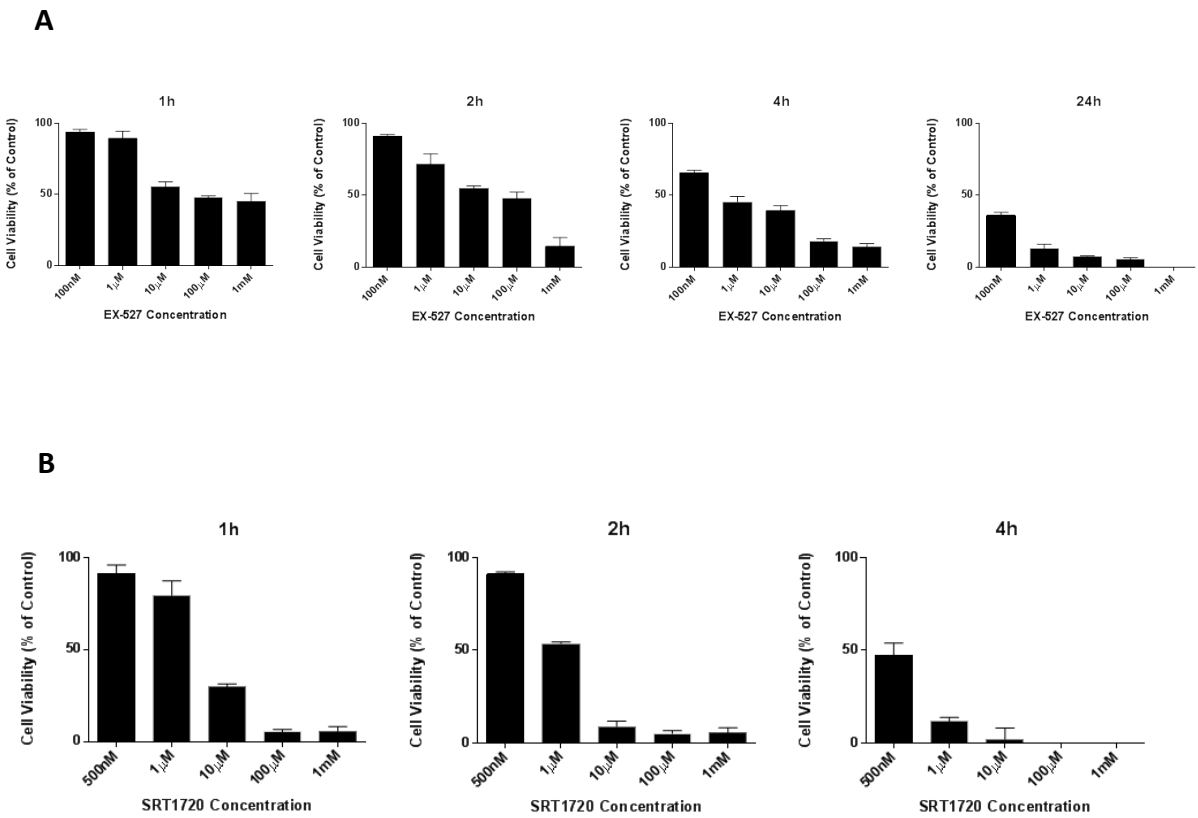

Figure 3.5: Optimisation of SIRT1 drug concentrations. Cell viability of HTB-94 cells after **(A)** EX-527 and **(B)** SRT1720 treatment. 24hrs treatment of SRT1720 resulted in total cell death at all-time points. Graph shows cell viability as a percentage of the control of DMSO. Data presented as mean ± SEM (*n*=3).

3.3.6 Validation of SIRT1 drugs in HTB-94 cells

After optimising a safe concentration of SIRT1 drugs to use in HTB-94 cells the change of SIRT1 activity was checked after drug treatment. SIRT1 catalyses the deacetylation of acetyl-lysine residues proteins (Bouras *et al.* 2005). Thus, total acetyl lysine protein expression in cells can be probed to check SIRT1 activity. Inhibiting SIRT1 activity with EX-527 significantly decreased SIRT1 protein expression in HTB-94 cells (-29.21%; *P*=0.001) (Figure 3.6 A and B). Conversely, activating SIRT1 activity with SRT1720 significantly increased SIRT1 protein expression in HTB-94 cells (+34.46%; *P*=0.001) (Figure 3.6 A and B). Inhibiting SIRT1 activity with EX-527 significantly increased total acetyl lysine expression in HTB-94 cells (+62.79%; *P*=0.01) (Figure 3.6 A and B). Conversely, activating SIRT1 activity with SRT1720 significantly decreased total acetyl lysine expression in HTB-94 cells (-42.96%; *P*=0.05) (Figure 3.6 A and B).

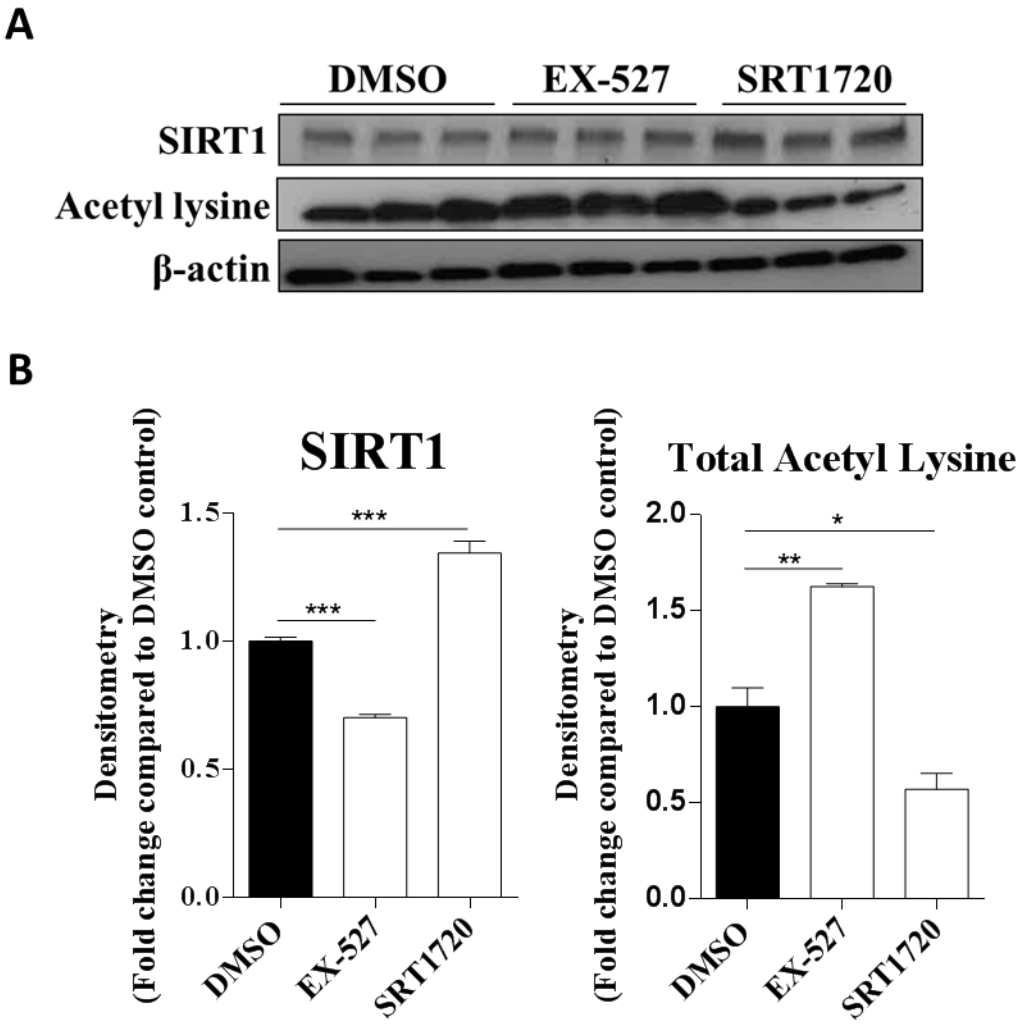

Figure 3.6: Validation of SIRT1 drugs in HTB-94 cells. (A) Protein expression of total acetyl lysine in HTB-94 cells treated with DMSO control or EX-527 (100nM) or SRT1720 (500nM) (*n*=3). **(B)** Densitometry quantification of protein expression of total acetyl lysine in HTB-94 cells treated with DMSO control or EX-527 (100nM) or SRT1720 (500nM) (*n*=3). SIRT1: 110 kDa; Acetyl lysine: 76 kDa; β-actin: 42 kDa. Graphs show the mean ± S.E.M.; ANOVA Tukeys multiple comparison test; * $P< 0.05$, ** $P< 0.01$ or *** $P<0.001$.

3.3.7 Effects of pharmacologically manipulating SIRT1 activity on cartilage and ECM markers

The gene expressions of cartilage markers *COL2A1* (70.40%; *P*=0.05), *ACAN* (65.16%; *P*=0.01) and *SOX-9* (67.96%; *P*=0.05) significantly decreased when SIRT1 activity was inhibited (61.28%; *P*=0.05) by EX-527 (Figure 3.7 A). However, *MMP-13* (12.09%; *P*=0.088) and *ADAMTS5* (24.23%; *P*=0.2275) expression did not significantly change (Figure 3.7 A). Protein expression of COL2A1 (31.03%; *P*<0.001) and SOX-9 (34.04%; *P*=0.001) also significantly decreased when SIRT1 activity was inhibited (63.98%; *P*=0.001) by EX-527 (Figure 3.7 B and C). In comparison, the gene expressions of *COL2A1* (71.46%; *P*=0.05), *ACAN* (71.62%; *P*=0.01), *SOX-9* (54.11%; *P*=0.05) significantly increased when SIRT1 activity was stimulated (86.99%; *P*=0.05) by SRT1720 (Figure 3.7 A). However, *MMP-13* (10.09%; *P*=0.6533) and *ADAMTS5* (7.12%; *P*=0.6918) gene expressions did not significantly alter (Figure 3.7 A). Protein expression of COL2A1 (28.90%; *P*=0.001) and SOX-9 (25.28%; *P*=0.001) also significantly increased when SIRT1 activity was increased (66.07%; *P*=0.001) by SRT1720 (Figure 3.7 B and C).

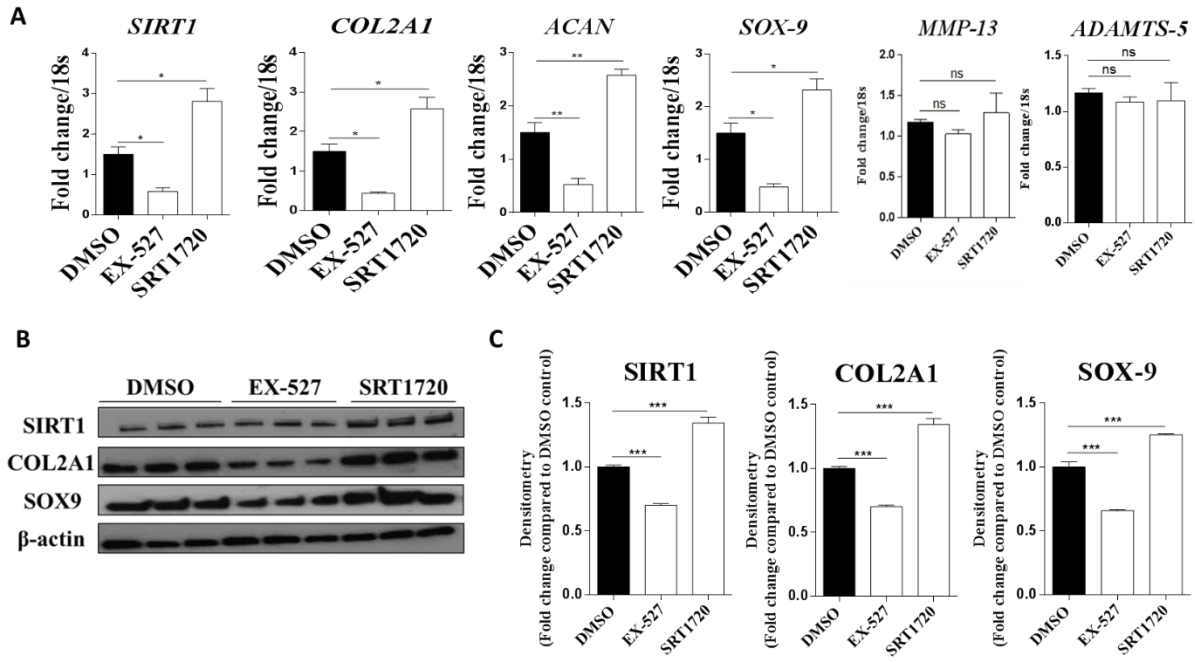

Figure 3.7: Effects of pharmacologically manipulating SIRT1 activity on cartilage and ECM markers. (A) RT-qPCR analysis of cartilage marker expressions in HTB-94 cells treated with DMSO control or EX-527 (100nM) or SRT1720 (500nM) (*n*=3). **(B)** Protein expression of cartilage marker expressions in HTB-94 cells with DMSO control or EX-527 (100nM) or SRT1720 (500nM) (*n*=3). **(C)** Densitometry quantification of protein expression SIRT1, COL2A1 and SOX-9 in HTB-94 cells treated with DMSO control or EX-527 (100nM) or SRT1720 (500nM) (*n*=3). SIRT1: 110 kDa; COL2A1: 141 kDa; SOX-9: 60 kDa; β-actin: 42 kDa. Graphs show the mean ± S.E.M.; ANOVA Tukeys multiple comparison test; ns=non-significant, * $P< 0.05$, ** $P< 0.01$ or *** $P<0.001$.

3.4 Discussion

The role of SIRT1 in ageing biology has been well established but the protective role which this essential histone deacetylase may play in OA remains unclear. At first I conducted experiments in HACs and found SIRT1 protein expression decreased in healthy aged samples compared to healthy young HACs. SIRT1 protein expression further decreased in OA HACs compared to healthy HACs. This finding confirmed previous reports describing a decrease in SIRT1 in aged and OA HACs (Gagarina *et al.* 2010; Fujita *et al.* 2011). Thereafter, I wanted to examine the cellular effects of decreasing SIRT1 expression in chondrocytes *in vitro* having observed the decrease in SIRT1 in OA HACs.

Silencing SIRT1 in HTB-94 chondrosarcoma cell line decreased COL2A1, ACAN and SOX-9 gene and protein expressions. Fujita and colleagues (2010) also showed HACs treated with SIRT1 siRNA had decreased *COL2A1* and *ACAN* gene expressions. However, in contrast to previous studies (Takayama *et al.* 2009; Fujita *et al.* 2011; Matsushita *et al.* 2013), I did not observe a significant up regulation in *MMP-13* or *ADAMTS5* gene expressions when SIRT1 was knock down. Similarly, Matsushita *et al* (2012) also observed no significant increase in MMP-13 and ADAMTS5 when SIRT1 was silenced. However, SIRT1 siRNA alongside IL-1β treatment did increase MMP-13 and ADAMTS5 gene expression. Increasing the activity of NF-κB by SIRT1 silencing alongside IL-1β treatment could explain elevated *MMP-13 and ADAMTS5* gene expressions noticed in previous studies (Takayama *et al.* 2009; Fujita *et al.* 2011; Matsushita *et al.* 2013). Furthermore, Oppenheimer and colleagues (2014) recently demonstrated the possible direct regulation of *COL2A1* gene expression by SIRT1 deacetylation. Hence, an inflammatory response or an increase in protease activity might not be required to decrease

COL2A1 gene expression. This may account for the decreased *COL2A1* gene expression without any alternation in *MMP-13* and *ADAMTS5* gene expressions when SIRT1 was silenced.

To validate my findings in SIRT1 silenced chondrocytes I used drugs to inhibit or activate SIRT1 activity. No studies to date have used EX-527 and SRT1720 in chondrocytes. Total acetyl lysine protein level increased or decreased when HTB-94 cells were treated using EX-527 and SRT1720 respectively. This indicated the drugs to have a robust effect on the deacetylation activity of SIRT1. The drugs have been used previously in other cells types. For example EX-527 has been shown to inhibit SIRT1 deacetylation of LC3 and increase acetyl lysine residues on LC3 protein in Human Embryonic Kidney 293 cell line (HEK293). Conversely, another study showed increasing the deacetylation activity of SIRT1 with SRT1720 treatment decreases total acetyl lysine residues on PGC-1α (Funk *et al.* 2010).

Inhibiting SIRT1 activity in HTB-94 cells significantly decreased COL2A1, ACAN and SOX-9 gene and protein expression but had no effect on MMP-13 or ADAMTS5 expressions. These results paralleled and supported my earlier findings achieved using siRNA knocked down. Interestingly, sirtinol, a first generation SIRT1 inhibitor has been previously demonstrated to increase apoptosis of human chondrocytes (Takayama *et al.* 2009). Likewise, inhibiting SIRT1 with EX-527 did significantly decrease cell viability of HTB-94 cells. Interestingly, Bar Oz *et al.* (2016) cultured human chondrocytes with EX-527 and reported decreased SOX-9 nuclear localization which could explain my results of decreased SOX-9 mRNA and protein expression.

HTB-94 cells treated with SRT1720 demonstrated increased gene expressions of COL2A1, ACAN and SOX-9 gene and protein expression level. However, consistent with earlier findings,

there was no significant change in *MMP-13 or ADAMTS5* gene expression following SRT1720 treatment. Resveratrol, a phenolic SIRT1 activating compound has previously been shown to increase the gene expression of *COL2A1*, *ACAN* and *SOX-9* (Kim *et al.* 2014). In addition, Moon and colleagues (2013) showed resveratrol dose dependently decreased MMP-13 activity in HACs treated with TNF-α. Hence, this could explain why a pro-inflammatory stimulus alongside SIRT1 loss is required to increase protease expression *in vitro*.

In summary, work described in this chapter shows SIRT1 expression decreases in aged and OA HACs compared to young HACs and the loss of SIRT1 decreases key cartilage and chondrocyte markers *in vitro*; which can be rescued by increasing SIRT1 activity. These data suggest that the loss of SIRT1 during ageing and OA possibly dysregulates chondrocyte biology and facilitates OA development.

4. Generation and validation of SIRT1 conditional knockout mice

4.1 Introduction

I sought to explore the chondroprotective nature of SIRT1 *in vivo*, after observing the loss of SIRT1 dysregulated chondrocyte markers *in vitro*. Previous studies have reported whole body SIRT1 KO mice die prenatally or during the postnatal period from neurological and cardiac malformations or display developmental phenotypes (Mcburney *et al.* 2003; Coussens *et al.* 2008). Many researchers have generated inducible SIRT1 cKO mice to circumvent developmental problems and investigate the tissue specific role of SIRT1 (Vinciguerra *et al.* 2010). For example, SIRT1 liver-specific knockout mice displayed increased fatty liver disease (Purushotham *et al.* 2009); SIRT1 myeloid-specific knockout mice displayed increased inflammation in white adipose tissue (Schug *et al.* 2010); and SIRT1 brain-specific knockout mice displayed increased glucose intolerance associated with ageing (Cohen *et al.* 2009). Hence, to investigate the *in vivo* physiological effects of SIRT1 loss in chondrocytes and to avoid adverse developmental phenotypes I generated two inducible cKO; a cartilage specific cKO ($SIRT1^{Agg}$) and a whole body cKO ($SIRT1^{ROSA}$).

4.2 Hypothesis

Inducible SIRT1 cKO will not display adverse developmental phenotypes and a loss of SIRT1 in cartilage will dysregulate ECM markers leading to cartilage degradation.

4.3 Results

4.3.1 Validation of Cre expression

Both the ROSA and Aggrecan Cre mice lines were crossed with ROSA26 reporter mice to demonstrate the robust specificity of Cre expression. As expected ROSA CreER^{T2} mice crossed with ROSA26 reporter mice produced strong whole body stained embryos (Figure 4.1 A). In comparison, Aggrecan Cre CreER^{T2} mice crossed with reporter mice produced embryos with specific areas of staining in cartilaginous regions such as in the developing clavicles, humerus, radius, ulna, digits, dorsal ribs and the vertebra of spine and tail (Figure 4.1 B).

A

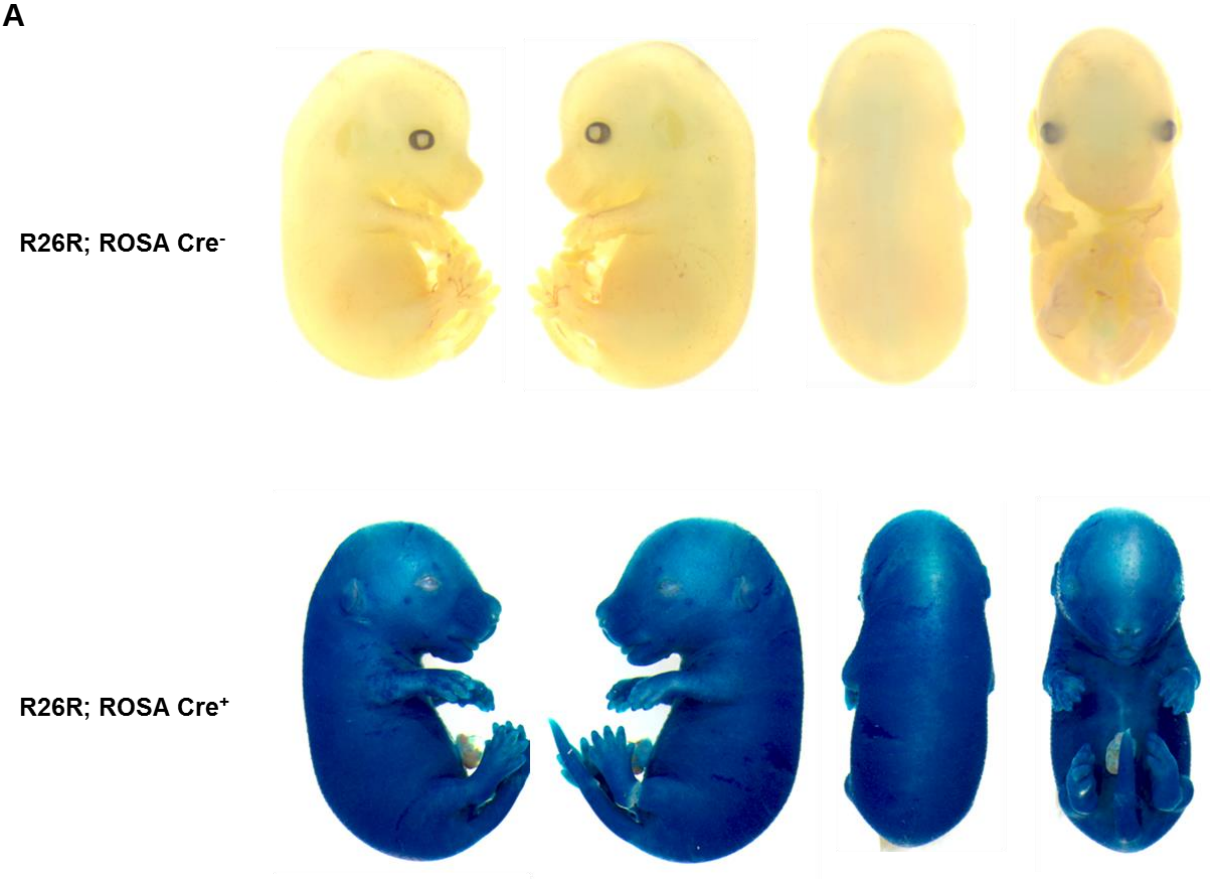

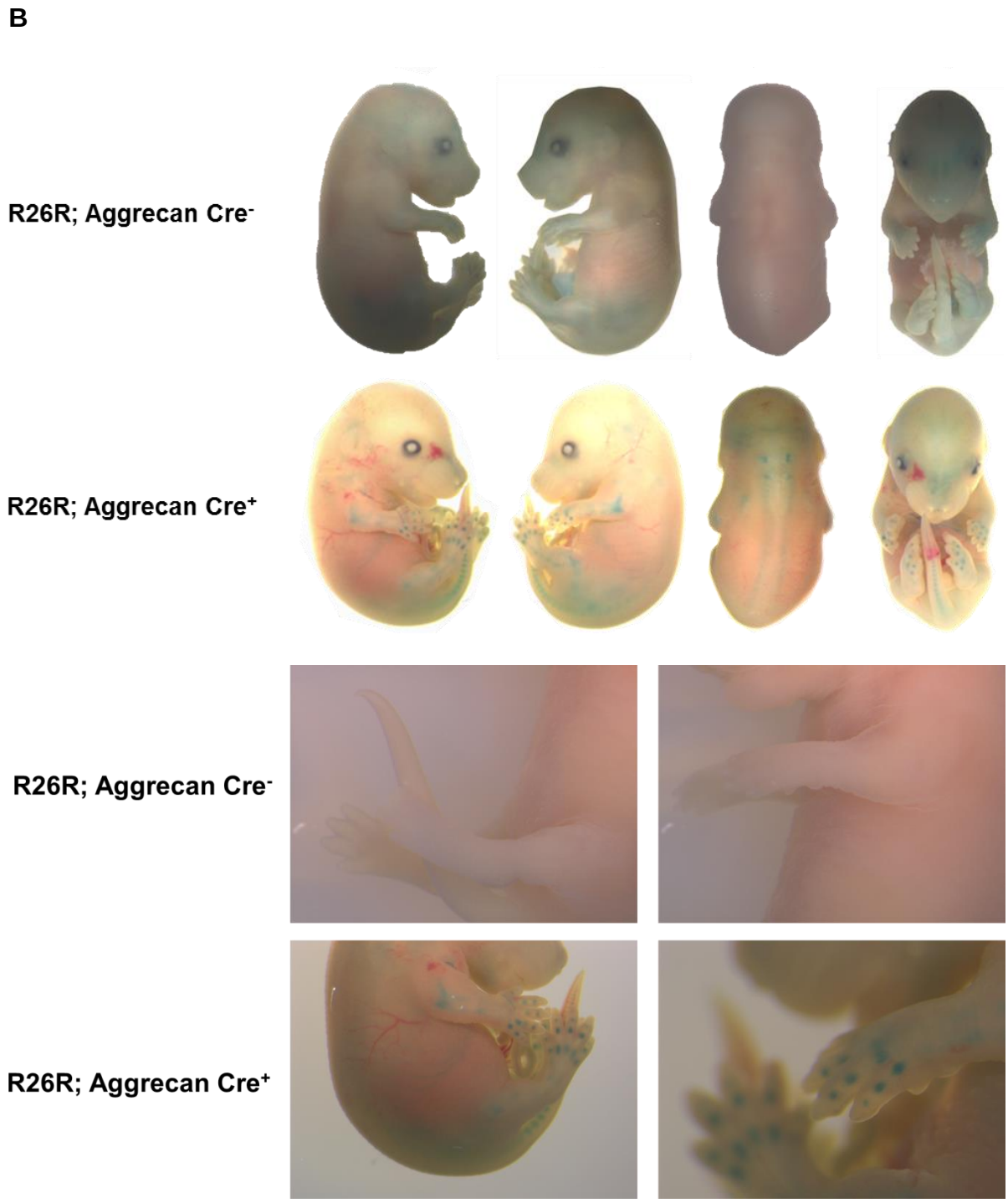

Figure 4.1: Validation of Cre specificity by ROSA26 reporter mice. A) ROSA Cre^{+} or **B)** Aggrecan Cre^{+} expressing mice; Cre^{-} mice from respective lines were used as control. Representative images of β-galactosidase staining (blue) in Cre expressing areas (*n*=4).

4.3.2 Generation of SIRT1 cKO mice lines

SIRT1$^{fl/fl}$ mice were bred with in house ROSA and Aggrecan Cre lines, to obtain homozygote mice carrying both the SIRT1$^{fl/fl}$ allele and ROSA Cre^{+} allele (Figure 4.2 A) or Aggrecan Cre^{+} allele (Figure 4.2 B).

A

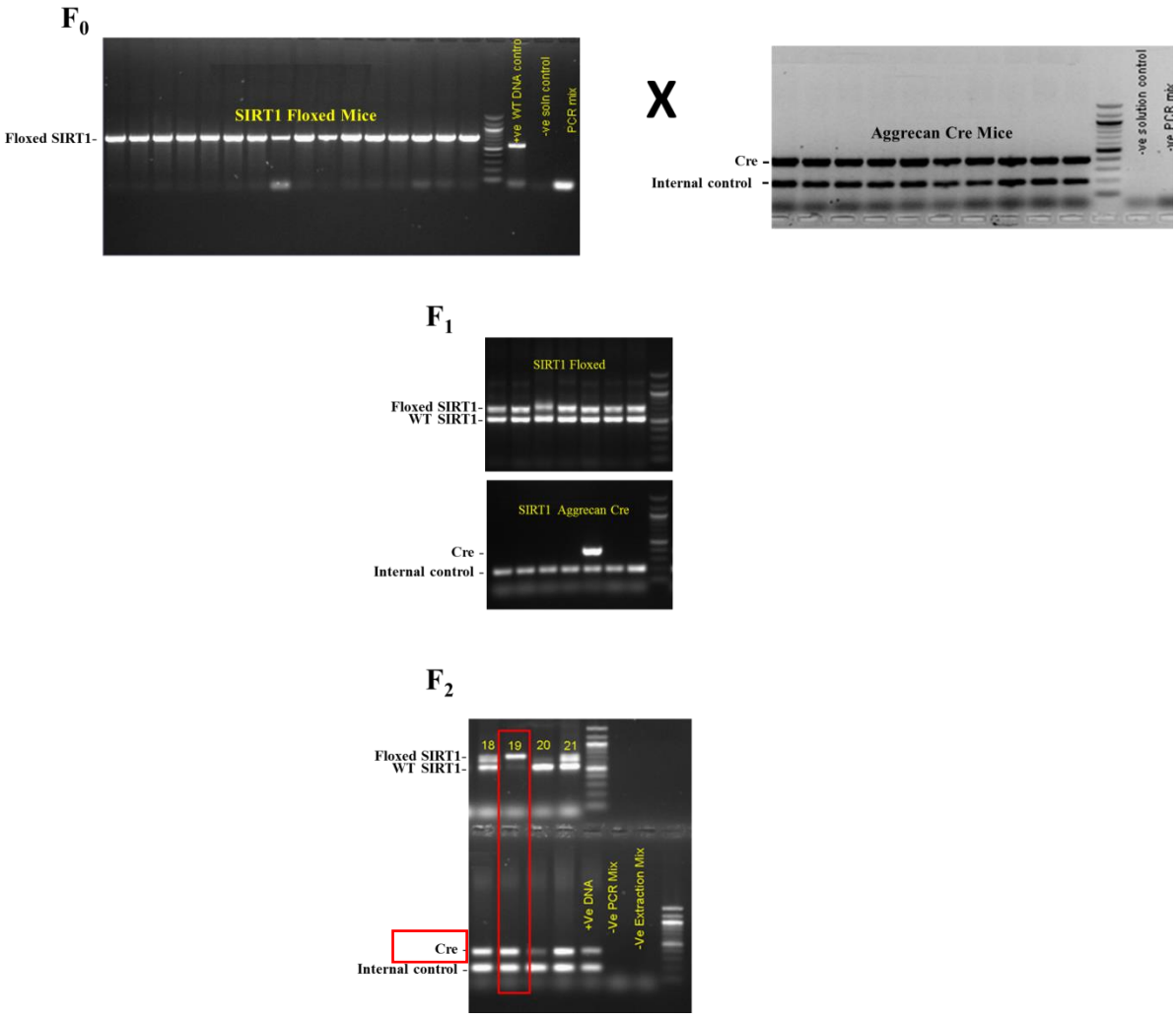

B

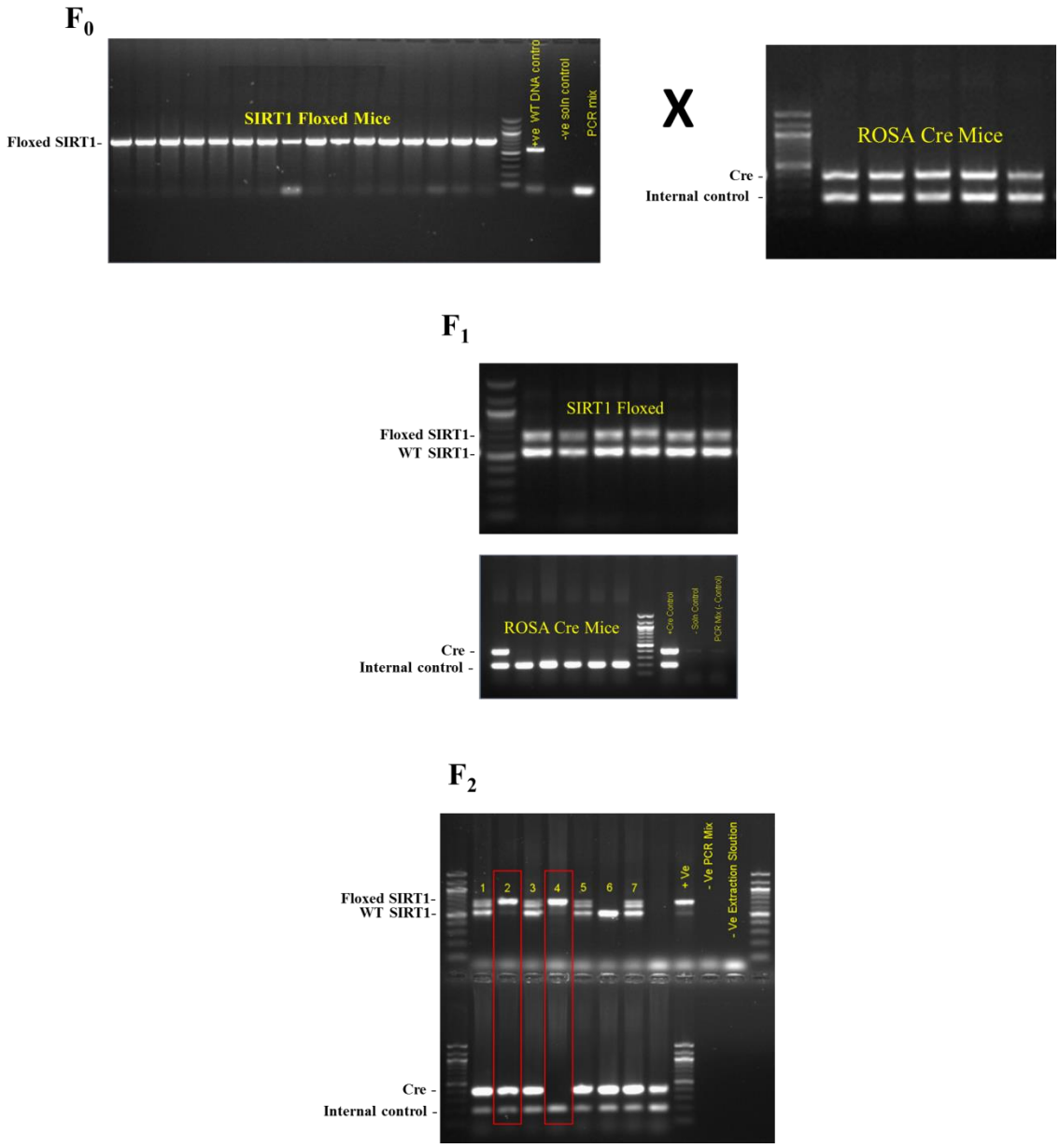

Figure 4.2: Genotyping of the different generations of SIRT cKO mice. A) SIRT1^{Agg} and **B)** SIRT1^{ROSA} mice. SIRT1$^{fl/fl}$ Homozygote (750bp); WT SIRT1 (550bp); SIRT1$^{fl/fl}$ Heterozygote (Both 750bp and 550bp); Cre (408bp); FABP (208bp). Positive controls of mouse DNA and negative controls of PCR and extraction buffer mixes were used. Red marked lines indicate the genotype of mice that will be used in experiments which are homozygote SIRT1$^{fl/fl}$ and Cre^{+}.

4.3.3 Validation of knockout of SIRT1 mRNA expression in murine tissue

To confirm knockout efficiency in both lines of mice, *Sirt1* mRNA gene expression was analysed in kidney, tibia, fibula and knee joint tissues obtained from control mice ($SIRT1^{fl/fl}$) and cKO mouse lines. *Sirt1* mRNA expression was significantly reduced in the kidney (99.43%; *P*=0.0001), tibia and fibula (97.21%; *P*=0.0003) and knee joint (96.11%; *P*=0.0001) tissues obtained $SIRT1^{ROSA}$ mice compared to control mice ($SIRT1^{fl/fl}$) (Figure 4.3 A). As expected there was no significant reduction in *Sirt1* mRNA expression in kidney (12.21%; *P*=0.7053), tibia and fibula (0.00%; *P*=0.8874) and knee joint (4.73%; *P*=0.8471) tissues obtained from $SIRT1^{Agg}$ mice compared to control mice ($SIRT1^{fl/fl}$) (Figure 4.3 B). Thereafter, microdissected cartilage from the knee joints of both cKO mouse lines was analysed to confirm *Sirt1* knockout efficiency in articular cartilage. *Sirt1* mRNA expression was significantly reduced in microdissected cartilage from $SIRT1^{Agg}$ (93.21%; *P*=0.0001) and $SIRT1^{ROSA}$ (79.66%; *P*=0.0001) mice (Figure 4.3 C).

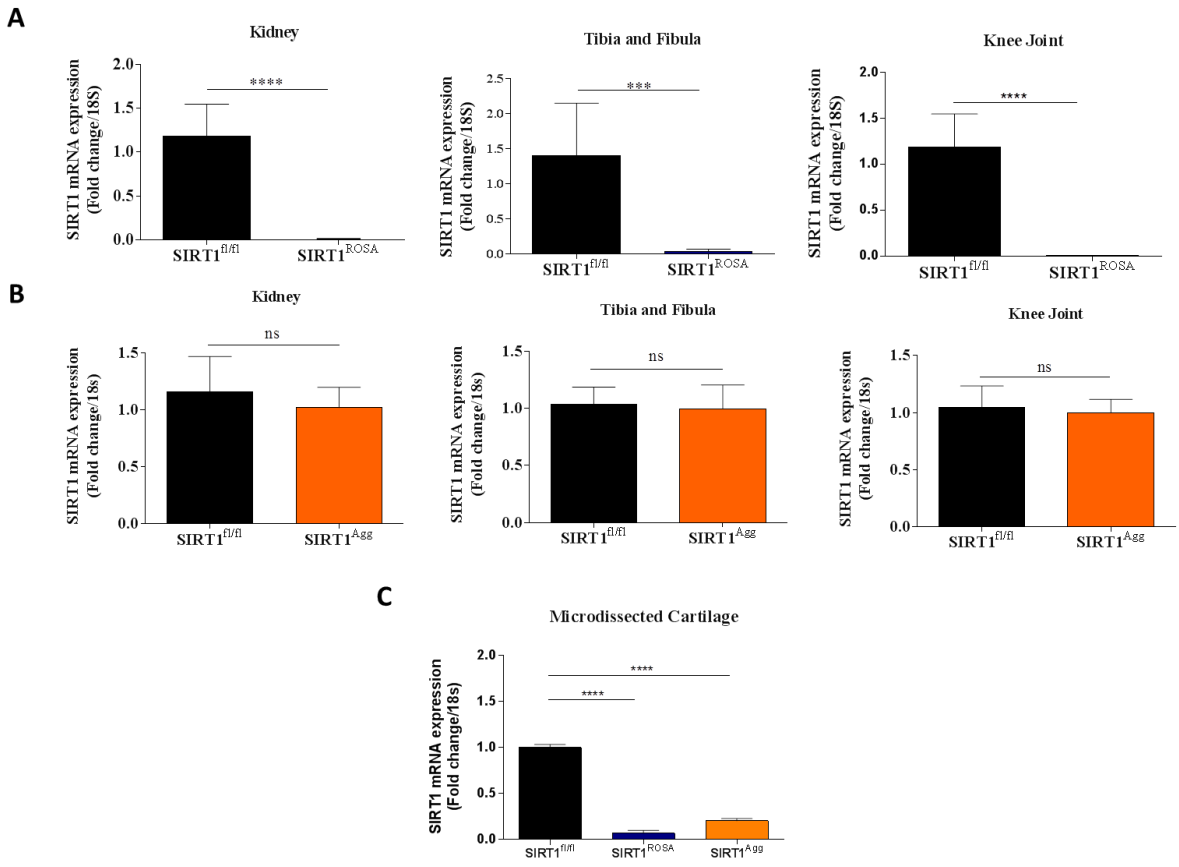

Figure 4.3: Validation of knockout of SIRT1 mRNA expression in murine tissue. Mice were injected with TX at the age of week 8 and culled at week 10. RNA was isolated from the kidneys, tibias, fibulas and knee joints and RT-qPCR analysis was conducted. SIRT1 mRNA expression in **(A)** $SIRT1^{ROSA}$ and **(B)** $SIRT1^{Agg}$ mice. **(c)** SIRT1 mRNA expression in microdissected articular cartilage from knees joints obtained from both $SIRT1^{ROSA}$ and $SIRT1^{Agg}$ mice. Data was normalised to the endogenous level of *18S* and the relative value from both sets of mice are shown as the mean ± S.E.M. (*n*=4); unpaired t-test or ANOVA Tukeys multiple comparison test; ns = not significant, *** p≤ 0.001 or **** p≤ 0.0001.

4.3.4 Optimisation of SIRT1 protein detection from murine hips

A preliminary experiment was conducted to determine the number of hips I required in future experiments to probe SIRT1 protein expression. This study confirmed that a minimum of 3 hips would be required (Figure 4.4). Hereafter all *ex vivo* protein experiments were performed using 4 hips pooled together.

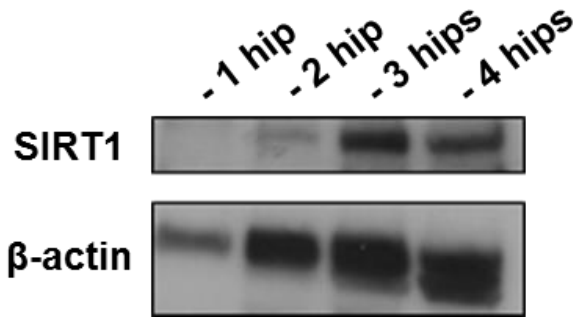

Figure 4.4: **Optimisation of SIRT1 protein expression from murine hips.** Validation of SIRT1 protein expression in different number of hips from wild type mice (aged week 6). SIRT1: 110 kDa; β-actin: 42 kDa.

4.3.5 Validation of knockout of SIRT1 protein expression in murine cartilage

Cartilaginous young hips were avulsed to validate SIRT1 knockout at the protein level. SIRT1 protein expression was significantly decreased in cartilage from $SIRT1^{Agg}$ (94.48%; *P*=0.0002) and $SIRT1^{ROSA}$ mice (78.59%; *P*=0.0001) (Figure 4.5).

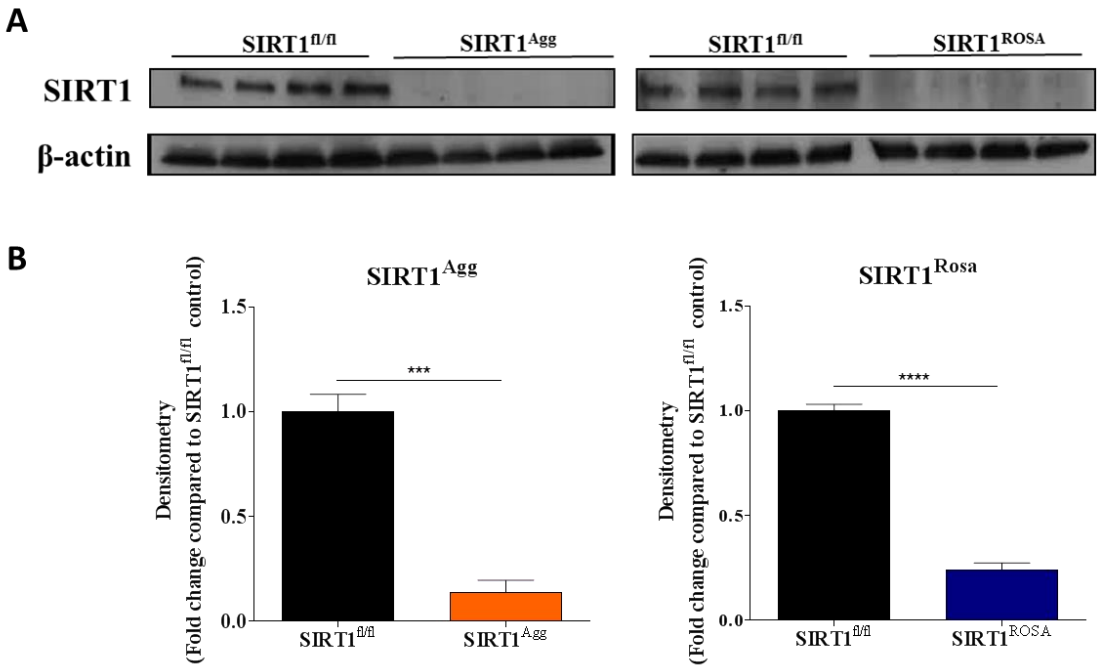

Figure 4.5: Validation of knockout of SIRT1 protein expression in murine cartilage. (A) Protein expression of SIRT1 from cartilaginous hips avulsed from young (6 week) mice (*n*=4). **(B)** Densitometry quantification of protein expression of SIRT1 from cartilaginous hips avulsed from young (6 week) mice (*n*=4). SIRT1: 110 kDa; β-actin: 42 kDa. Graphs show the mean ± S.E.M; unpaired t-test; *** *P*<0.001 or **** *P*<0.0001.

4.3.6 In vivo effects of SIRT1 knockout on cartilage and ECM markers

After successfully validating SIRT1 knocked down in articular cartilage, I went on to examine the effect of SIRT1 loss on cartilage and OA markers *in vivo* were examined. *Col2a1* (91.18%; *P*=0.0001), *Acan* (79.66%; *P*=0.0001) and *Sox-9* (61.97% *P*=0.01) were significantly decreased when *Sirt1* (79.66%; *P*<0.0001) was knocked down (Figure 4.6 A). However, *Mmp-13* (8.05%; *P*=0.267) and *Adamts5* (-0.08%; *P*=0.988) were not altered significantly (Figure 4.6 A). The protein expression of COL2A1 (-37.59%; *P*=0.007) and SOX-9 (-34.54%; *P*=0.04) were significantly decreased when SIRT1 (-94.48%; *P*=0.0002) was knocked down (Figure 4.6 B and C).

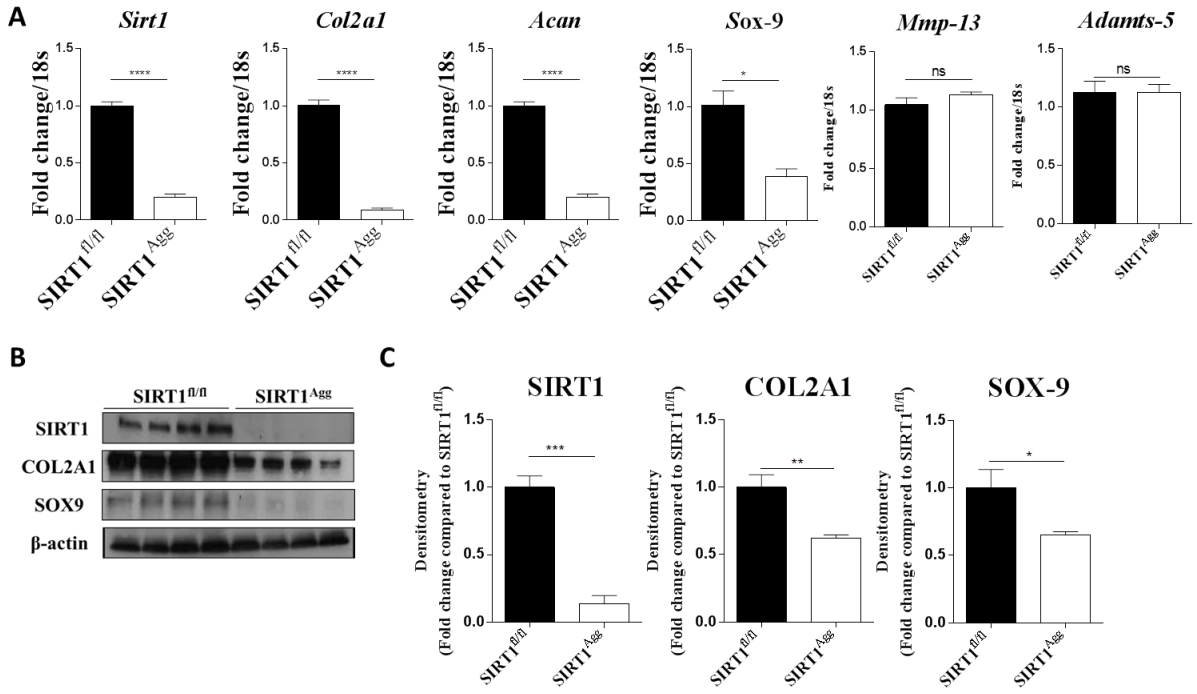

Figure 4.6: *In vivo* effects of SIRT1 knockout on cartilage and ECM markers. (A) RT-qPCR analysis of cartilage marker expressions in SIRT1^{Agg} mice compared to SIRT1$^{fl/fl}$ mice (*n*=4). Data normalised to the endogenous level of *18S*. **(B)** Protein expression of cartilage markers in cartilaginous hips avulsed from young (6 week) SIRT1^{Agg} mice compared to SIRT1$^{fl/fl}$ mice (*n*=4). **(C)** Densitometry quantification of protein expression of cartilage markers in cartilaginous hips avulsed from young (6 week) SIRT1^{Agg} mice compared to SIRT1$^{fl/fl}$ mice (*n*=4). SIRT1: 110 kDa; COL2A1: 141 kDa; SOX-9: 60 kDa; β-actin: 42 kDa. Graphs show the S.E.M; unpaired t-test; ns=non-significant, * *P*< 0.05, ** *P*< 0.01, *** *P*<0.0001 or **** *P*<0.0001.

4.3.7 *Age related effects of SIRT1 KO in vivo*

After observing the loss of cartilage and ECM markers in young SIRT1^{Agg} mice, I sought to determine whether premature cartilage degradation occurred in aged SIRT1^{Agg} mice compared to SIRT1$^{fl/fl}$ mice. Quantitation of joint disease using the OARSI scoring system confirmed acceleration of osteoarthritis in SIRT1^{Agg} mice at 2 months (5.12 ± 0.58 versus (vs) 3.125 ± 0.23; *P*=0.015), 6 months (10.17 ± 1.01 vs 7.86 ± 1.248; *P*=0.0001) and 12 (24.60 ± 2.58 vs 3.93 ± 0.41; *P*=0.0002) months compared to SIRT1$^{fl/fl}$ mice (Figure 4.7 A and B).

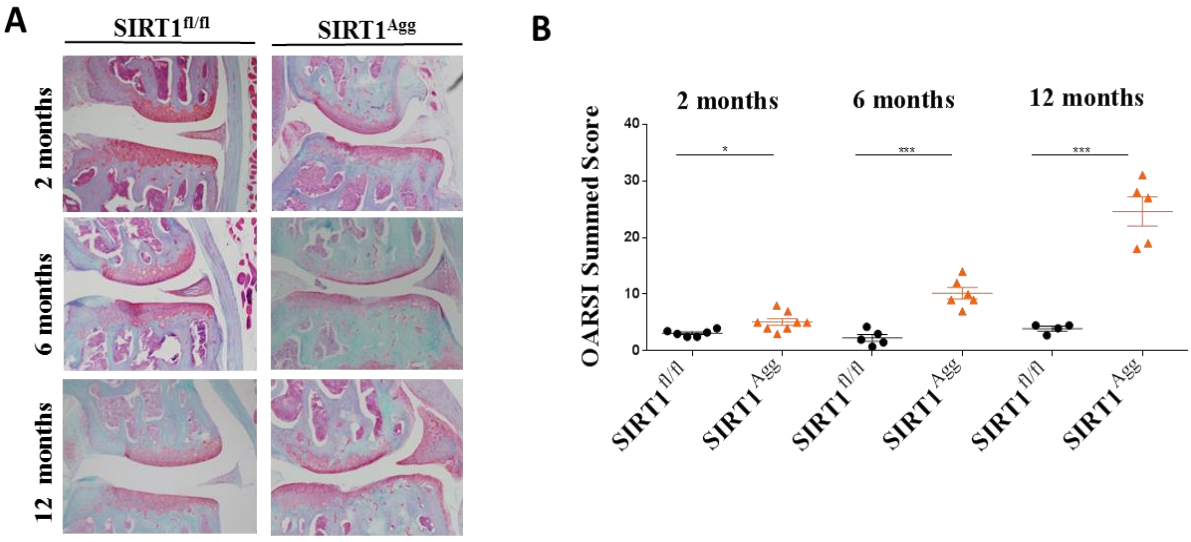

Figure 4.7: Age related effects of SIRT1 KO *in vivo*. (A) Representative images of Safranin-O fast green staining of the medial femoral condyle and tibial plateau of control SIRT1$^{fl/fl}$ or SIRT1^{Agg} mice at 2 months, 6 months and 12 months age **(B)** OARSI disease scores assessed by two blinded operators (*n*=4-8). All data are expressed as mean ± S.E.M of *n* observations. ANOVA with Bonferroni post hoc test was used for disease score analysis. * *P*<0.05 or *** *P*<0.001.

4.4 Discussion

SIRT1 cKO mice were generated to explore the chondroprotective nature of SIRT1 *in vivo*. I successful generated SIRT1^{ROSA} and SIRT1^{Agg} cKO mice lines which displayed no adverse developmental effects reported in constitutive SIRT1 KO mice lines such as exencephaly, defects in bone growth and autoimmune phenotype (Mcburney *et al.* 2003; Coussens *et al.* 2008; Sequeira *et al.* 2008). I decided to use the Aggrecan CreER^{T2} based on previous studies which have shown that the expression of the *Acan* gene was not significantly different in joints post DMM and ACL injury models compared to sham controls (Appleton *et al.* 2007; Loeser *et al.* 2013). Several other Cre lines have been used to target chondrocyte progenitor cells such as Prx1-Cre (Logan *et al.* 2002), Gdf5-Cre (Rountree *et al.* 2004), and SOX-9-Cre (Akiyama *et al.* 2005), whereas Col2a1-Cre (Sakai *et al.* 2001), Col10a1-Cre (Hilton *et al.* 2007), and Col11a2-Cre (Fujimaki *et al.* 2005) have been used to target chondrocytes. However, a severe drawback of these Cre lines is the lack of chondrocyte specific Cre expression, especially during development. In addition, the COL2A1 CreER^{T2} mice have been reported to display low expression in articular cartilage of adult animals (Nakamura *et al.* 2006).

ROSA26 reporter studies demonstrated the ROSA CreER^{T2} have excellent Cre activity resulting in full body staining. Likewise, ROSA26 reporter studies showed the Aggrecan-CreER^{T2} activity and expression in cartilage specific regions such as fore and hind limbs, developing ribs, the nasal, the head region at the base of the trachea, developing vertebrae, tail, and the developing bones of the forelimbs, such as the humerus radius, ulna and digits. Similar staining was also previously reported using the Aggrecan-CreER^{T2} (Lo Cascio *et al.* 2014). Validation of SIRT1 deletion was assessed after breeding mice to obtain homozygote mice carrying both the SIRT1$^{fl/fl}$ allele and ROSA-CreER^{T2} and Aggrecan-CreER^{T2} allele. SIRT1 mRNA

and protein expression were significantly decreased in knee joint, micro-dissected cartilage and young avulsed hips indicating CRE recombination and activation post TX administration.

After validating SIRT1 deletion, I next examined the effect of SIRT1 loss on key cartilage and chondrocyte markers in murine articular cartilage. In accordance with the *in vitro* results, chondrocyte markers and matrix protein expression (COL2A1, SOX-9 and ACAN) were also decreased in mRNA and protein lysates from avulsed femoral heads of young SIRT1^{Agg} mice. In accordance with Gabay *et al.* (2012) used constitutive SIRT1 heterozygous mice and showed at 1 month and 9 months of age these mice had decreased COL2A1 and aggrecan protein in articular cartilage sections from the medial tibial plateau compared to wildtype controls. In addition, mice homozygous for an allele carrying a point mutation that encodes a SIRT1 protein with no enzymatic activity showed reduced COL2A1 and aggrecan in cartilage tissue sections at 6 months of age compared to wild-type mice (Gabay *et al.* 2013). Further studies using SIRT1 COL2A1 CreER^{T2} mice reported less COL2A1 staining in articular cartilage from knee joints compared to wild type mice 8 weeks post DMM (Matsuzaki *et al.* 2013). Hence my findings alongside other studies suggest loss of SIRT1 may result in the dysregulation of normal chondrocyte homeostasis and may predispose to cartilage degradation and OA.

To determine whether premature cartilage degradation occurred after SIRT1 deletion, joints were examined histologically at 2, 6 and 12 months of age. Quantitation of joint disease confirmed acceleration of osteoarthritis in SIRT1^{Agg} mice compared to control mice. In agreement with my results, other studies have reported SIRT1 transgenic mice had increased cartilage degradation in knee joints at 6 months, 9 months and 12 months compared to wild-

type mice (Gabay *et al.* 2012a; Gabay *et al.* 2013; Matsuzaki *et al.* 2013). These data suggest declining SIRT1 levels during ageing impairs chondrocyte biology contributing to OA. However, the $SIRT1^{ROSA}$ mice were generated at a later date than $SIRT1^{AGG}$ mice. Hence, I could not determine cartilage marker expression and cartilage degradation in aged $SIRT1^{ROSA}$ mice during my DPhil. If conducted these studies possibly would have confirmed the findings from the $SIRT1^{Agg}$ mice.

In summary, in this chapter I have demonstrated the successful generation and validation of two novel SIRT1 cKO mice lines. I have also revealed the loss of SIRT1 in articular cartilage *in vivo* decreases key cartilage and chondrocyte markers leading to aged related cartilage loss. These data suggest the critical role of SIRT1 in chondrocyte homoeostasis and a protective role in OA. However, further *in vitro* and *in vivo* studies are required to assess the mechanism by which SIRT1 controls chondrocyte homeostasis.

5. The regulation of chondrocyte autophagy by SIRT1

5.1 Introduction

My data indicated that SIRT1 has a protective role in OA. Therefore I next explored how SIRT1 might maintain chondrocyte biology and cartilage integrity over time. I postulated that SIRT1 may be controlling other age-related mechanisms known to contribute to chondrocyte biology and cartilage integrity. The well-conserved cellular process of autophagy (self-eating), where unwanted or dysfunctional cytoplasmic constituents are isolated, degraded and recycled, decreases with age, leading to an accumulation of toxic and non-functional protein elements (Rubinsztein *et al.* 2011). Key autophagy proteins ULK1, BECLIN1 and LC3 have been shown to decrease in human ageing cartilage, OA samples and murine knee joints post DMM (Caramés *et al.* 2010) . In addition, mice deficient in the key autophagy protein ATG5, have been shown to develop premature OA (Bouderlique *et al.* 2015). However, how autophagy is regulated in chondrocytes is still unknown. The role of SIRT1 in the regulation of autophagy has also been reported in other cell types (Salminen and Kaarniranta 2009b). Embryonic fibroblast deficient in SIRT1 displayed decreased autophagy (Lee *et al.* 2008), SIRT1 inhibition in human colon carcinoma cells lead to decreased in autophagy (Qiu *et al.* 2015) and knocked down of SIRT1 decreased autophagy in HEK293 cell lines (Huang *et al.* 2015). Hence, I wanted to investigate if SIRT1 controls autophagy in cartilage and if the loss of both these ageing mechanisms will lead to OA.

5.2 Hypothesis

The loss of SIRT1 impairs autophagy which dysregulates chondrocyte biology and predisposes to OA.

5.3 Results

5.3.1 Autophagy protein expression in isolated chondrocytes from human samples

At first I wanted to determine if autophagy decreases in ageing and OA HACs. I measured the protein expression of three key autophagy markers; ULK1, BECLIN 1 and LC3 in HACs. ULK1 protein expression decreased by 45.31% in old healthy HACs compared to young healthy HACS (*P*=0.01) (Figure 5.1 A and B). ULK1 protein expression decreased by 59.21% in OA HACs compared to young healthy HACs (*P*=0.0001) (Figure 5.1 A and B). There was a 13.90% but not a significant decrease in ULK1 protein expression in OA HACs compared to old healthy HACs (*P*=0.065) (Figure 5.1 A and B).

BECLIN 1 protein expression decreased by 42.34% in old healthy HACs compared to young healthy HACs (*P*=0.01) (Figure 5.1 A and B). BECLIN 1 protein expression decreased by 65.12% in OA HACs compared to young healthy HACs (*P*=0.0001) (Figure 5.1 A and B). There was a 22.79% decrease in BECLIN 1 protein expression in OA HACs compared to old healthy HACs (*P*=0.05) (Figure 5.1 A and B).

Conversion of LC3 I to LC3 II indicates the formation of autophagosomes and increased autophagy. LC3 I to LC3 II protein conversion decreased by 45.90% in old healthy HACs compared to young healthy HACs (*P*=0.0001) (Figure 5.1 A and C). LC3 I to LC3 II protein conversion decreased by 67.80% in OA HACs compared to young healthy HACs (*P*=0.0001) (Figure 5.1 A and C). There was a 21.90% decrease in LC3 I to LC3 II protein conversion in OA HACs compared to old healthy HACs (*P*=0.001) (Figure 5.1 A and C).

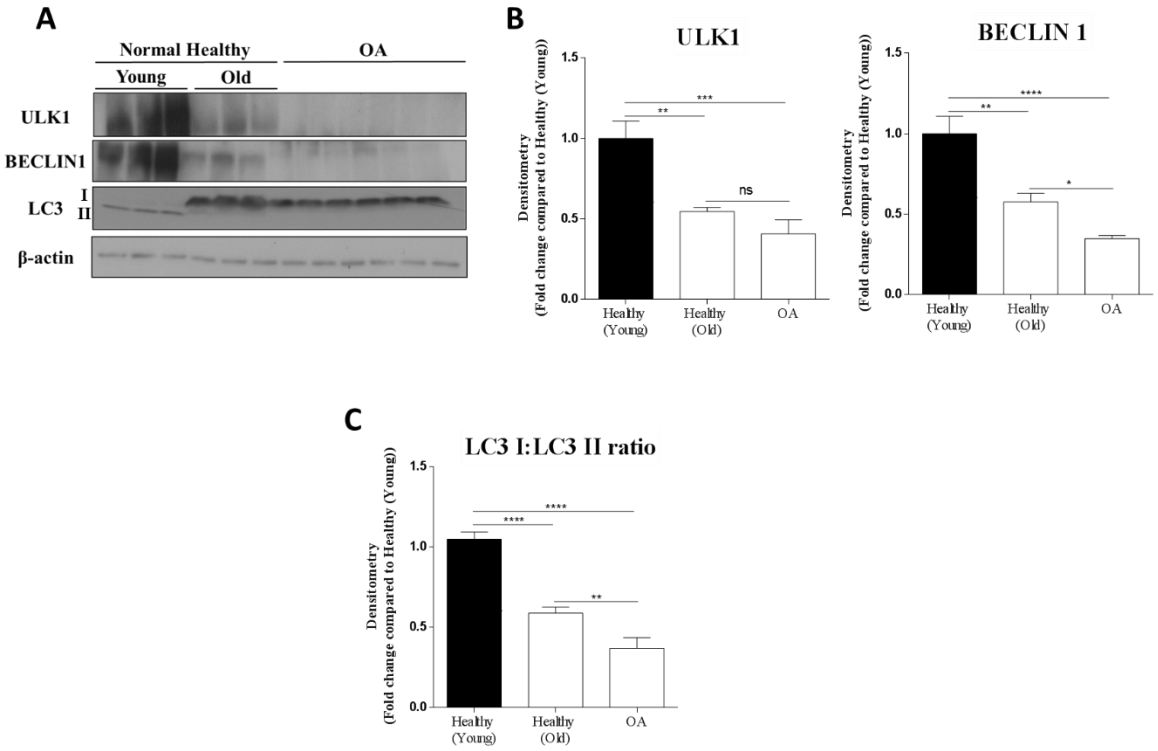

Figure 5.1: Autophagy protein expression in HACs. (A) ULK, BELCIN 1 and LC3 protein expression in isolated chondrocytes from young (21-37yrs) (*n*=3), old (62-68yrs) (*n*=3) and OA (49-86yrs) (*n*=6) knee joints. **(B)** Densitometry quantification of ULK and BECLIN1 protein expression from HACs. **(C)** Densitometry quantification of LC3 I to LC3 II protein conversion from HACs. ULK1: 130 kDa; BECLIN 1: 60 kDa; LC3 I: 19kDa; LC3 II: ~17 kDa. β-actin: 42 kDa. Graphs show S.E.M.; ANOVA Tukeys multiple comparison test; ns=non-significant; * *P*< 0.05, ** *P*< 0.01, *** *P*< 0.001 or **** *P*<0.0001.

5.3.2 Effects of SIRT1 mRNA silencing on autophagy markers

After observing the decrease in SIRT1 and autophagy markers in HACs with increasing, age I went on to examine the effect of silencing SIRT1 on autophagy markers in HTB-94 cells. *ULK1* (43.73%; *P*=0.007), *BECN1* (57.70%; *P*=0.002) and *LC3* (69.67% *P*=0.006) significantly decreased when SIRT1 (88.98%; *P*=0.0001) was silenced (Figure 5.2 A). In addition, the protein expression of ULK1 (40.19%; *P*=0.017), BECLIN 1 (43.53%; *P*=0.012) and LC3 I to LC3 II conversion (35.97%; *P*=0.043) significantly decreased when SIRT1 (51.15%; *P*=0.003) was silenced (Figure 5.2 B and C).

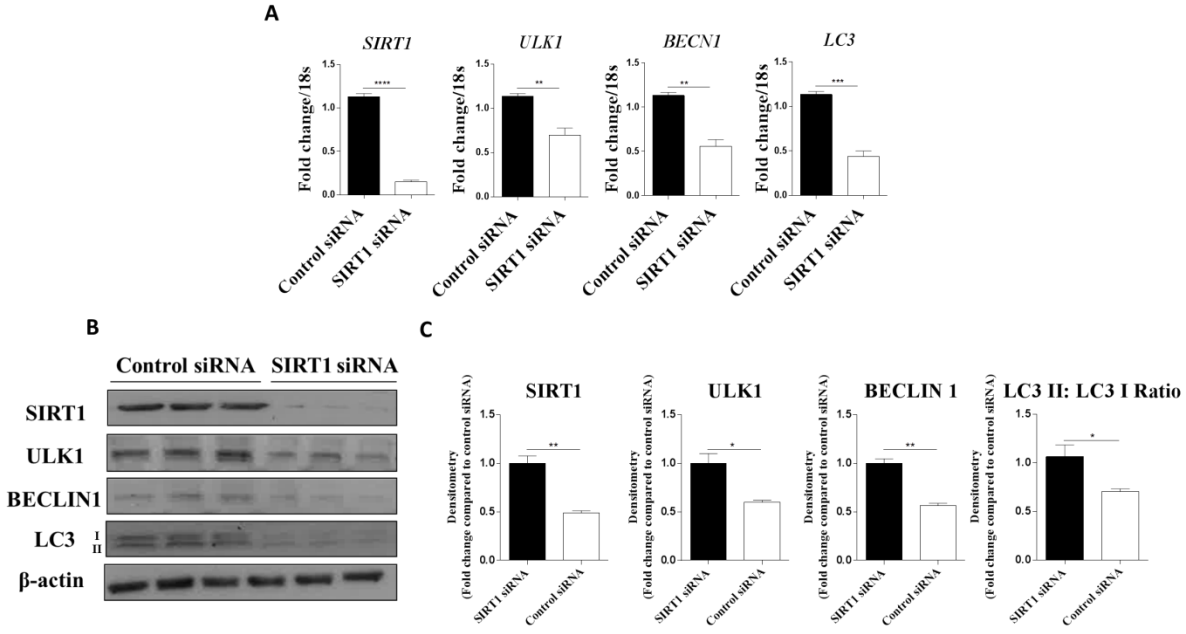

Figure 5.2: Effects of SIRT1 mRNA silencing on autophagy markers. (A) RT-qPCR analysis of autophagy marker expression in HTB-94 chondrocytic cells following SIRT1 siRNA or control siRNA transfection (*n*=3). Data normalised to the endogenous level of *18S*. **(B)** Protein expression of autophagy markers in HTB-94 cells transfected with SIRT1 siRNA or control siRNA (*n*=3). **(C)** Densitometry quantification of protein expression of autophagy markers in HTB-94 cells transfected with SIRT1 siRNA or control siRNA (n=3). ULK1: 130 kDa; BECLIN 1: 60 kDa; LC3 I: 19kDa; LC3 II: ~17 kDa. β-actin: 42 kDa. Graphs show the mean ± S.E.M; unpaired t-test; ns=non-significant, * *P*< 0.05, ** *P*< 0.01, *** *P*< 0.001 or **** *P*<0.0001.

5.3.3 Effects of pharmacologically manipulating SIRT1 activity on autophagy markers

I now wanted to examine if I could alter the gene and protein expression of key autophagy markers by manipulating SIRT1 activity. The gene expressions of autophagy markers of *ULK1* (79.60%; *P*=0.01), *BECN1* (90.77%; *P*=0.05) and *LC3* (79.60%; *P*=0.05) significantly decreased when SIRT1 activity was inhibited (61.28%; *P*=0.05) by EX-527 (Figure 5.3 A). Protein expression of ULK1 (56.11%; *P*=0.001), BECLIN 1 (46.01%; *P*=0.001) and LC3 I to LC3 II conversion (63.98%; *P*=0.05) also significantly decreased when SIRT1 activity was inhibited (30.81%; *P*=0.001) by EX-527 (Figure 5.3 B and C). In comparison, the gene expressions of *ULK1* (98.57%; *P*=0.01), *BECN1* (128.5%; *P*=0.05) and *LC3* (501.3%; *P*=0.0001) significantly increased when SIRT1 activity was stimulated (86.99%; *P*=0.01) by SRT1720 (Figure 5.3 A). Protein expression of ULK1 (25.97%; *P*=0.05), BECLIN 1 (60.24%; *P*=0.0001), and LC3 I to LC3 II conversion (22.56%; *P*=0.05) also significantly increased when SIRT1 activity was increased (66.07%; *P*=0.0001) by SRT1720 (Figure 5.3 B and C).

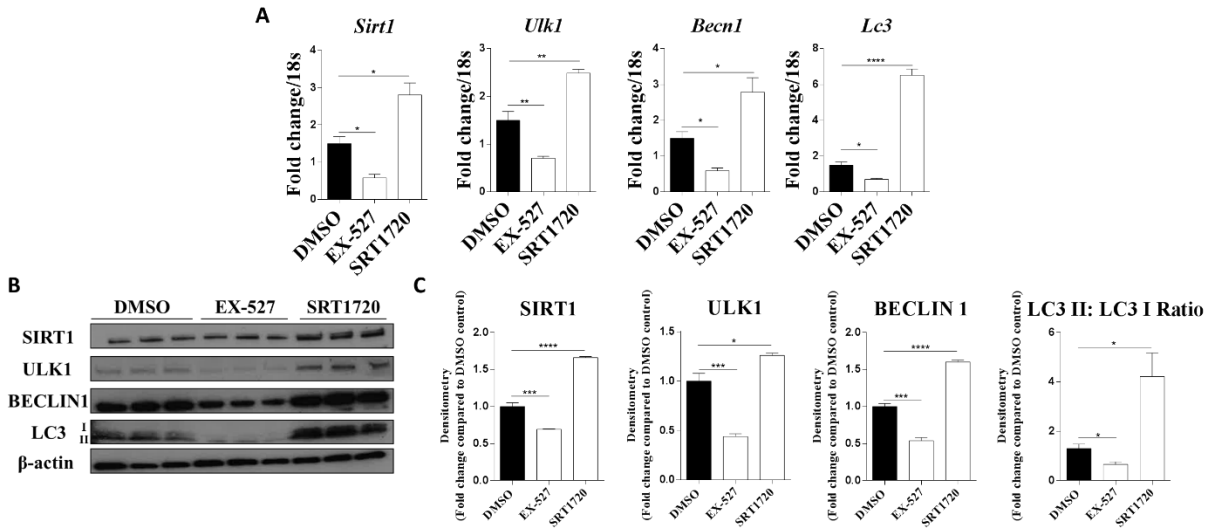

Figure 5.3: Effects of pharmacologically manipulating SIRT1 activity on autophagy markers. (A) RT-qPCR analysis of autophagy marker expressions in HTB-94 cells treated with DMSO control or EX-527 (100nM) or SRT1720 (500nM) (*n*=3). **(B)** Protein expression of autophagy marker expressions in HTB-94 cells with DMSO control or EX-527 (100nM) or SRT1720 (500nM) (*n*=3). **(C)** Densitometry quantification of protein expression of autophagy markers in HTB-94 cells treated with DMSO control or EX-527 (100nM) or SRT1720 (500nM) (*n*=3). ULK1: 130 kDa; BECLIN 1: 60 kDa; LC3 I: 19kDa; LC3 II: ~17 kDa. β-actin: 42 kDa. Graphs show the S.E.M.; ANOVA Tukeys multiple comparison test; * *P*< 0.05, ** *P*< 0.01, *** *P*<0.001 or **** *P*<0.001.

After observing gene and protein expressions of key autophagy markers were altered by changes in SIRT1 activity, I wanted to further validate this finding with a complimentary method. I used FACs and a selective antibody against LC3 II to measure the protein expression of this key autophagy marker in HTB-94 cells treated with EX-527, SRT1720 or the control of DMSO. All groups were treated with BAF except the untreated control. BAF treatment arrests autophagy and allows LC3 II levels to accumulate thus being a positive control. As expected BAF treatment increased LC3 II mean fluorescence intensity (54.97%; *P*=0.05) compared to untreated cells. There was no significant difference in LC3 II mean fluorescence intensity between BAF treated cells compared to DMSO treated cells (22.86%; *P*=0.05). LC3 II mean

fluorescence intensity significantly decreased in cells when SIRT1 activity was inhibited by EX-527 compared to DMSO treated cells (-42.17%; *P*=0.01). In comparison, LC3 II mean fluorescence intensity significantly increased in cells when SIRT1 activity was stimulated by SRT1720 compared to DMSO treated cells (213.51%; *P*=0.0001) (Figure 5.4 A and B).

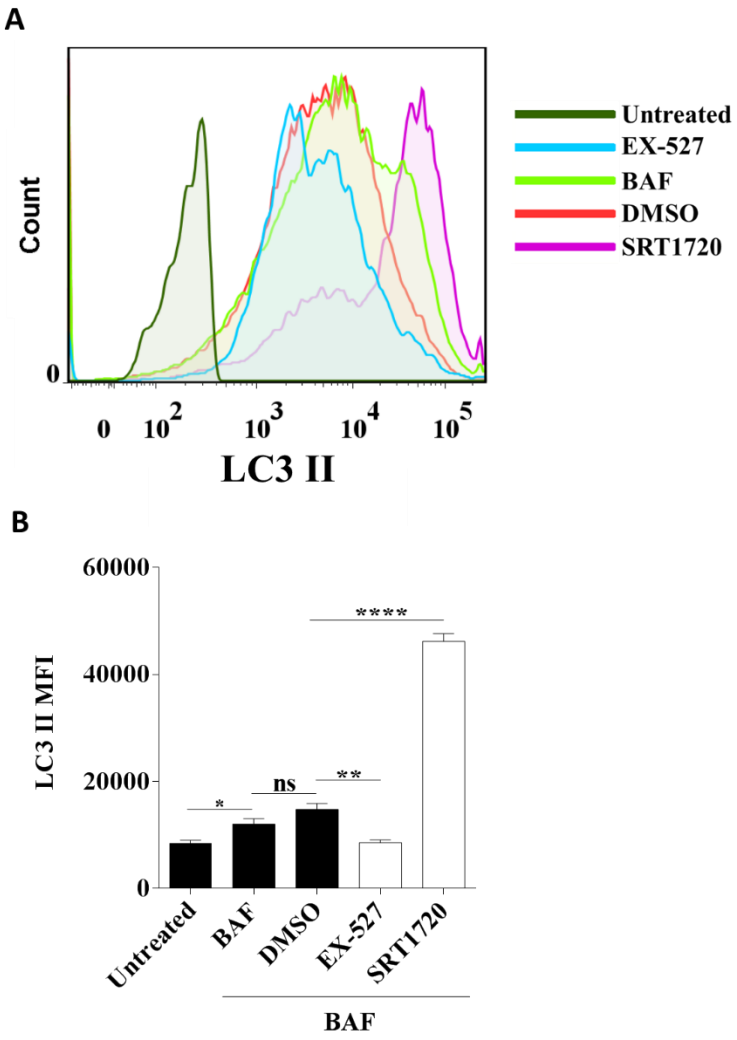

Figure 5.4: Effect of pharmacologically manipulating SIRT1 activity on LC3 II (A) Histogram and **(B)** quantification mean fluorescence intensity of LC3 II in HTB-94 cells either untreated or treated with BAF, alongside DMSO or EX-527 (100nM) or SRT1720 (500nM) (*n*=3). Graphs show the S.E.M.; ANOVA Tukeys multiple comparison test; ns=non-significant, * *P*< 0.05, ** *P*< 0.01 or **** *P*<0.0001.

5.3.4 Effects of manipulating SIRT1 on chondrocyte autophagy markers in vivo

After observing the inhibition or activation of SIRT1 directly affected autophagy *in vitro*, I wanted to confirm these findings *in vivo*. I used a customised array analysis to measure a panel of autophagy-related genes from micro-dissected cartilage of SIRT1^{Agg} mice compared to control mice. There was a significant downregulation of 10 autophagy genes, increase in *p62* (cargo molecule; increase indicates impaired autophagy) and no difference in *Atg4a* and *Atg16* (Table 5.1).

Table 5.1: Gene Expression changes of autophagy-related genes in SIRT1^{Agg} KO mice

Gene	Expression change	Percentage fold change	*P=*
Atg10	↓	54.60%	0.02
Atg12	↓	99.25%	0.02
Atg13	↓	77.52%	0.006
Atg14	↓	49.47%	0.02
Atg16	–	8.47%	N/S
Atg4A	–	8.50%	N/S
Atg5	↓	54.03%	0.02
Atg7	↓	70.30%	0.04
Atg9	↓	46.11%	0.04
Becn1	↓	78.33%	0.004
Map1lca	↓	61.37%	0.002
Map1lcb	↓	61.13%	0.009
Sqstm1 (p62)	↑	+29.86%	0.005
Ulk1	↓	31.81%	0.02

Expression changes of autophagy-related genes in SIRT1^{Agg} KO mice. RNA was extracted from articular cartilage microdissected from the joints of SIRT1$^{fl/fl}$ or SIRT1^{Agg} mice. RT-PCR was performed using TaqMan microfluidic cards. Fold changes were normalized to ribosomal protein *18S* and expressed relative to levels in SIRT1$^{fl/fl}$ mice. (*n*=8 mice per group). Unpaired t-test. NS = not significant.

Upon seeing the decrease in gene expressions of autophagy markers *in vivo* I wanted to validate this finding on the protein expression level. I measured the protein expression of P62 and LC3 in young cartilaginous avulsed hips from SIRT1^{Agg} mice compared to SIRT1$^{fl/fl}$ mice. P62 protein expression significantly increased (36.96%; *P*=0.002) in protein lysates from SIRT1^{Agg} mice compared to SIRT1$^{fl/fl}$ mice (Figure 5.5 A and B). LC3 I to LC3 II conversion was decreased (46.66%; *P*=0.05) in avulsed hips from SIRT1^{Agg} mice compared to SIRT1$^{fl/fl}$ mice (Figure 5.5 C and D). As expected LC3 I to LC3 II conversion increased (47.71;*P*=0.04) in avulsed hips treated *ex vivo* with BAF (increase autophagic flux) from SIRT1$^{fl/fl}$ mice compared to avulsed hips not treated with BAF from SIRT1$^{fl/fl}$ mice (Figure 5.5 C and D). However, even with BAF treatment; avulsed hips from SIRT1^{Agg} mice displayed a decrease (46.62%; *P*=0.0001) in LC3 I to LC3 II conversion compared to avulsed hips from SIRT1$^{fl/fl}$ mice treated with BAF (Figure 5.5 C and D).

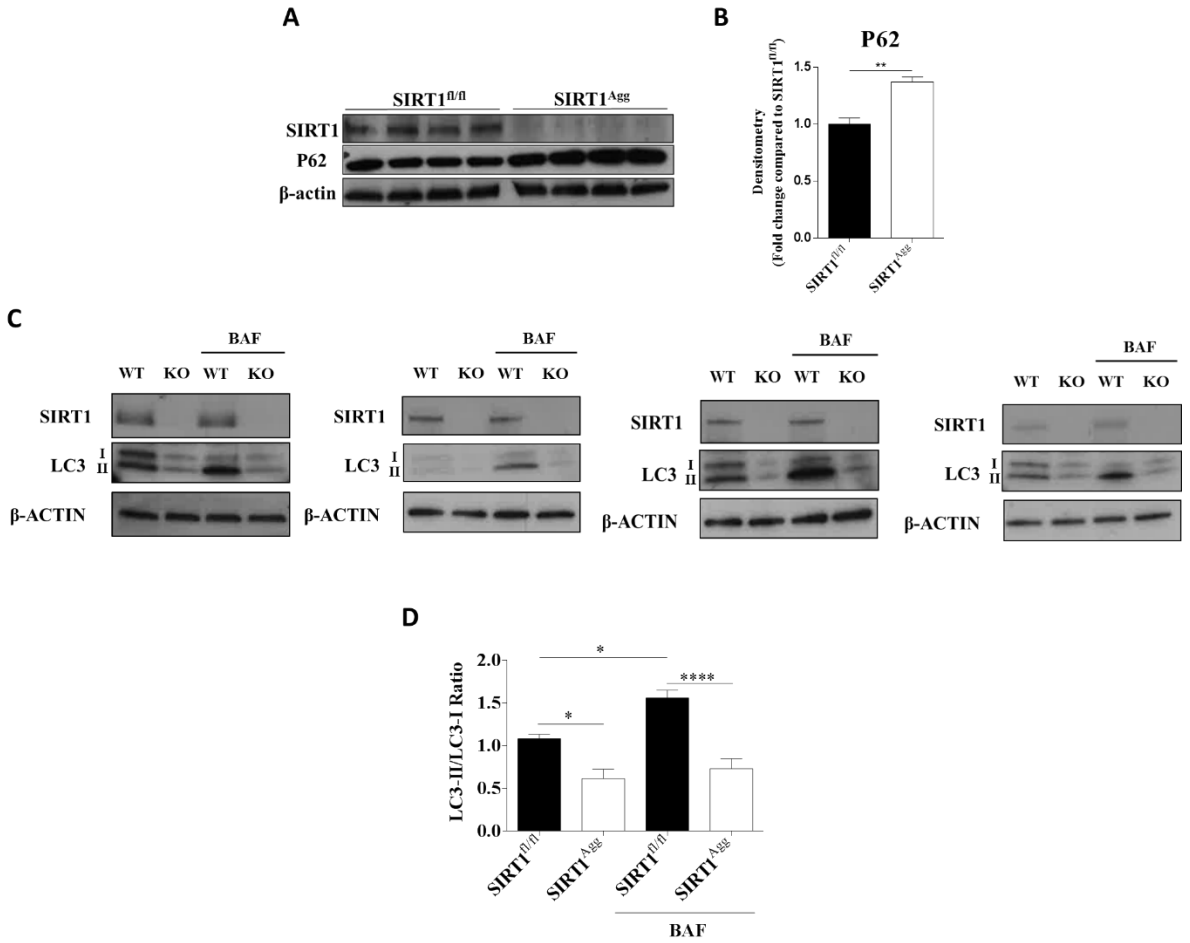

Figure 5.5: Effects of manipulating SIRT1 on P62 and LC3 in chondrocytes *in vivo*: (A) P62 protein expression from cartilaginous hips which were avulsed from young (aged week 6) SIRT1$^{fl/fl}$ or SIRT1^{Agg} mice (*n*=4). **(B)** Densitometry quantification of protein expression of P62 from cartilaginous hips which were avulsed from young (aged week 6) SIRT1$^{fl/fl}$ or SIRT1^{Agg} mice (*n*=4). **(C)** Results shown are of 4 independent experiments. LC3 protein expression from cartilaginous hips which were avulsed from young (aged week 6) SIRT1$^{fl/fl}$ or SIRT1^{Agg} mice either treated or not treated with BAF *ex vivo* for 2hrs (*n*=4). **(D)** Densitometry quantification of LC3 protein expression from cartilaginous hips which were avulsed from young (aged week 6) SIRT1$^{fl/fl}$ or SIRT1^{Agg} mice either treated or not treated with BAF *ex vivo* for 2hrs (*n*=4). SIRT1: 110 kDa; P62: 60 kDa; LC3 I: 19 kDa; LC3 II: ~17 kDa; β-actin: 42 kDa. Graphs show the S.E.M.; unpaired t-test (p62 protein analysis) or ANOVA Tukeys multiple comparison test (LC2 protein analysis); ns=non-significant, * *P*< 0.05, ** *P*< 0.01 or **** *P*<0.0001.

5.3.5 Effects of manipulating SIRT1 activity on LC3-GFP ex vivo

Thus far I systematically investigated the effect of manipulating SIRT1 on chondrocyte autophagy markers *in vitro* and *in vivo*. I next wanted to robustly validate the effect of manipulating SIRT1 activity on autophagy using another *in vivo* method. I avulsed young cartilaginous hips from LC3-GFP mice and treated them with either EX-527 or SRT1720 or DMSO *ex vivo* then measured LC3 puncta and intensity. Less chondrocytes showed decreased LC3-GFP puncta (77.17%; *P*=0.01) and staining intensity per cell (54.37%; *P*=0.0001) following SIRT1 inhibition by EX-527 (Figure 5.6 A, B and C). In comparison more chondrocytes displayed an increase in LC3-GFP puncta (126.8%; *P*=0.001) and LC3 intensity (20.53%; *P*=0.001) per cell upon stimulation by SRT1720 (Figure 5.6 A, B and C).

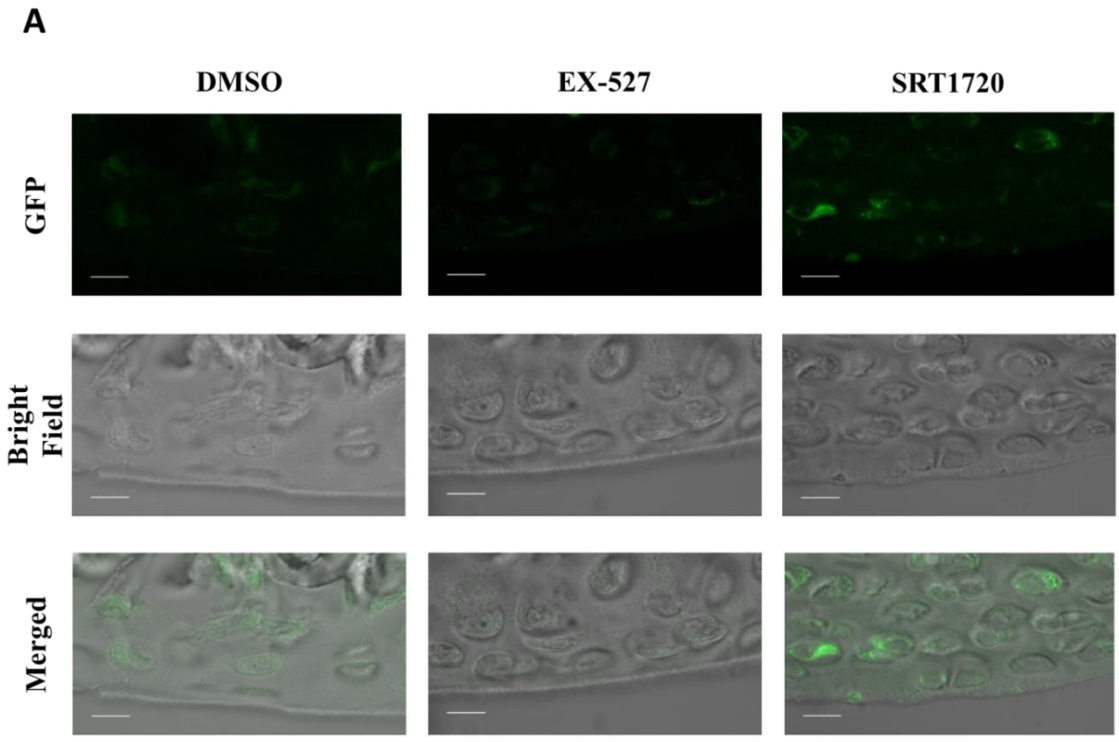

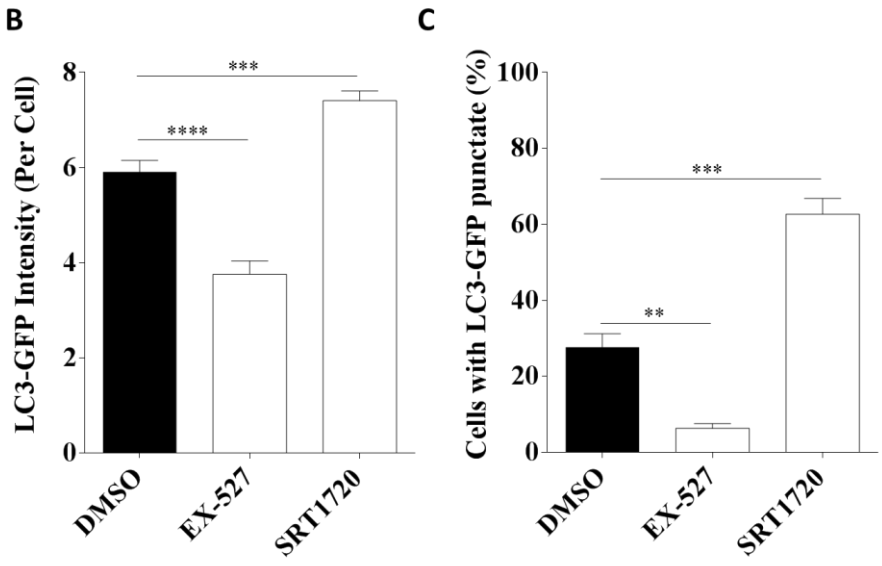

Figure 5.6: Effect of manipulating SIRT1 activity on LC3-GFP *ex vivo*. (A) Representative images of LC3-GFP chondrocytes from cartilaginous hips from young (6 weeks old) mice were captured in bright field and GFP in fluorescent channel using confocal microscopy then merged. Quantification of percentage of chondrocytes with **(B)** LC3 positive puncta and **(C)** total LC3-GFP intensity per chondrocyte from cartilaginous hips from young (6 weeks old) mice. Hips were treated with either DMSO control or EX-527 (100nM) or SRT1720 (500nM) for 2hrs before fixation (*n*=30-50 cells from 3 mice). Quantification was counted and analysed throughout each z stack by two blinded operators. Graphs show the S.E.M.; ANOVA Tukeys multiple comparison test; ns=non-significant, ** *P*< 0.01, *** *P*<0.001 or **** *P*<0.0001.

5.3.6 The functional effect of SIRT1 deletion on chondrocyte autophagy in vivo

After observing the loss of SIRT1 resulted in decreased autophagy markers I wanted to examine if the loss of SIRT1 will affect functional components of autophagy. The autophagosome is a double membrane structure (Figure 5.7 A) which engulfs cytoplasmic debris and damaged organelles and thereafter fuses with lysosomes to degrade the contents within. Hence, counting the number of autophagosomes in cells is a functional readout to robustly confirm the level of autophagy in cells. There was a significant decrease (69.21%; *P*=0.0001) in autophagosome count, indicative of reduced functional autophagy in $SIRT1^{Agg}$ mice compared with $SIRT1^{fl/fl}$ control mice (Figure 5.7 B and C).

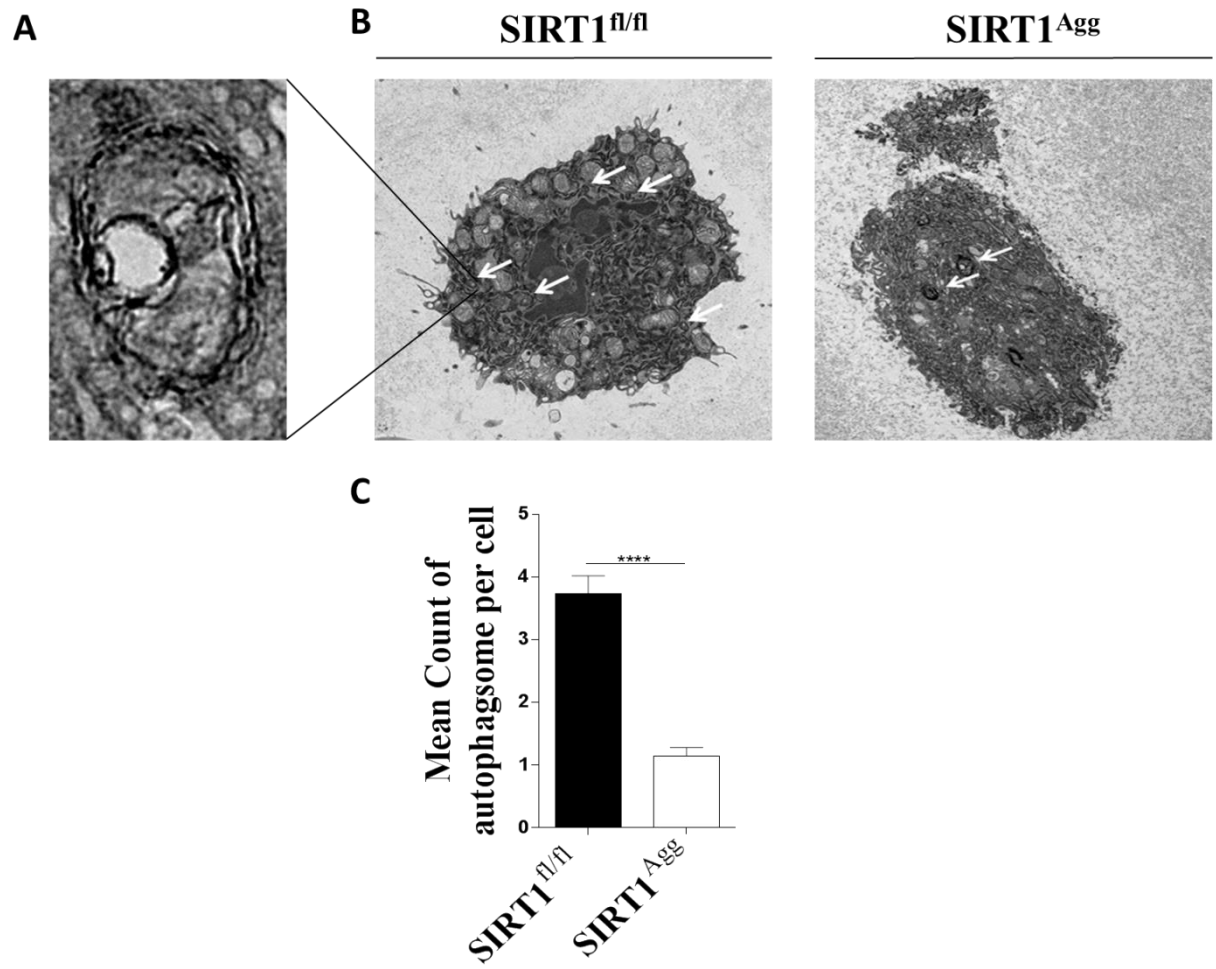

Figure 5.7: The effect of SIRT1 loss on autophagosomes count in murine chondrocytes. (A) Representative TEM image of autophagosome in a murine chondrocyte. **(B)** Representative TEM image of murine chondrocyte from SIRT1$^{fl/fl}$ or SIRT1^{Agg} mice (10 weeks of age). Arrows point towards autophagosomes. **(C)** Blinded quantification of autophagosomes from micro-dissected cartilage obtained from SIRT1$^{fl/fl}$ or SIRT1^{Agg} mice using EM (*n*=3). Graphs show the S.E.M; unpaired t-test; **** *P*<0.0001.

5.3.7 In vivo effects of SIRT1 knockout on autophagy in ageing murine cartilage

I next wanted to examine if declining levels of SIRT1 over time will also result in the loss of chondrocyte autophagy in ageing murine cartilage. LC3 protein expression decreased in joint sections from $SIRT1^{Agg}$ mice at 2 months (99.75 ± 11.65 vs 58.00 ± 6.481; *P*=0.02), 6 months (99.60 ± 13.88 vs 52.20 ± 12.66; *P*=0.03) and 12 months (100.2 ± 3.184 vs 39.80 ± 2.437; *P*=0.0001) compared to $SIRT1^{fl/fl}$ mice (Figure 5.8 A and B).

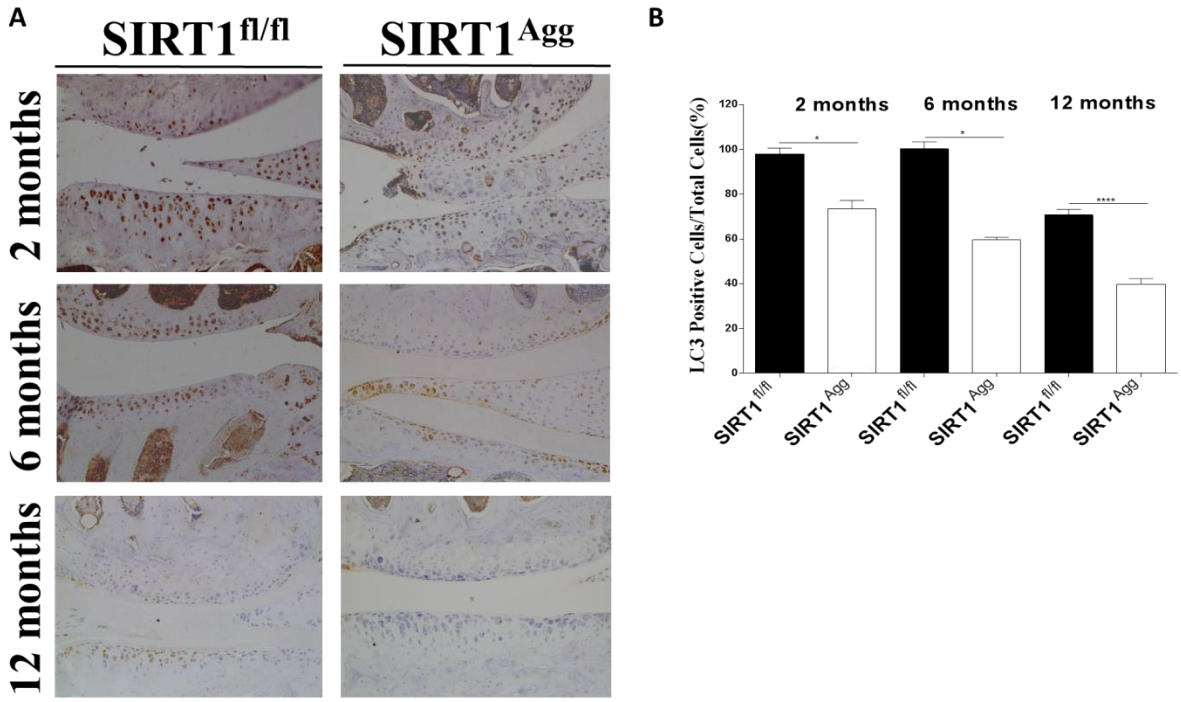

Figure 5.8: Effect of SIRT1 deletion on chondrocyte autophagy in ageing murine cartilage. (A) Representative images of LC3 protein expression of the medial femoral condyle and tibial plateau from control $SIRT1^{fl/fl}$ or $SIRT1^{Agg}$ mice at 2 months, 6 months and 12 months of age stained using anti-LC3, biotinylated anti-rabbit secondary with DAB visualisation **(B)** Quantification of LC3 positive cells/total cells assessed by two blinded operators (*n*=4-8). Data was analysed by ANOVA with Bonferroni post hoc. Graphs show the S.E.M.; * *P*< 0.05 or **** *P*<0.0001.

5.3.8 The direct regulation of autophagy proteins by SIRT1 in chondrocytes

At this stage it was unclear whether SIRT1 was directly interacting with key autophagy proteins or the decrease in autophagy was occurring independently. To investigate this, I used immunoprecipitation analysis in HTB-94 cells to determine which autophagy-related proteins directly interact with SIRT1. Several autophagy proteins including BECLIN1, ATG5, ATG7 and LC3, but not ULK1, were shown to bind to SIRT1 (Figure 5.9).

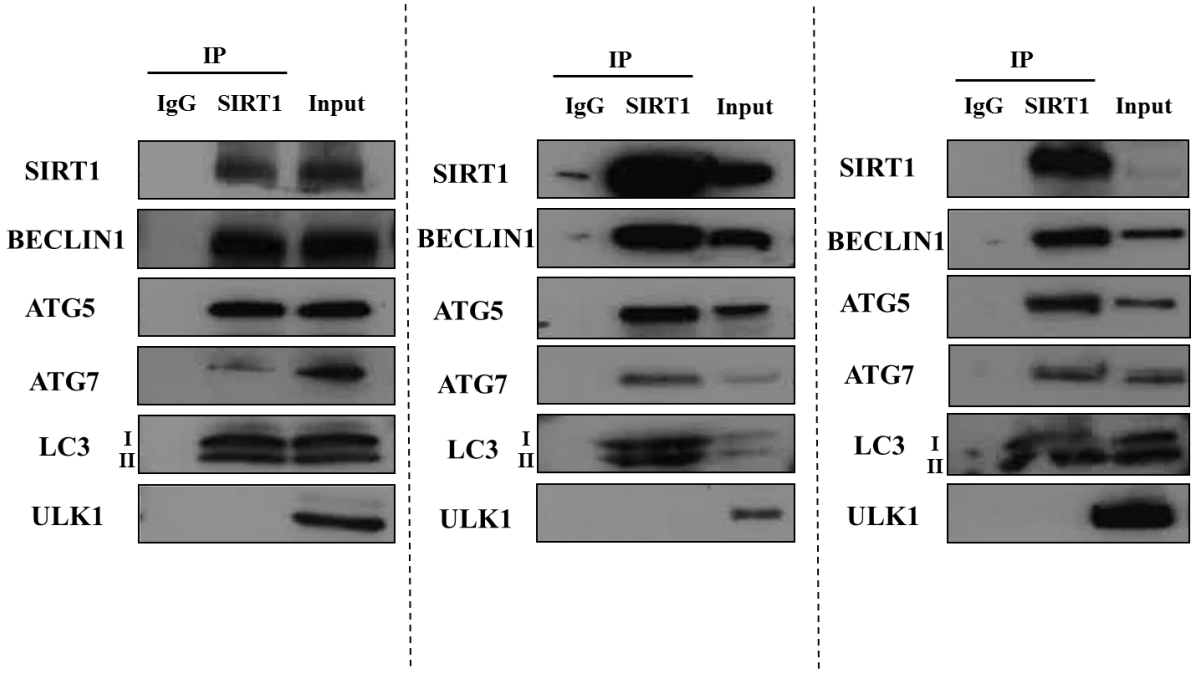

Figure 5.9: The direct regulation of autophagy proteins by SIRT1 in chondrocytes. Western blots showing the binding of autophagy markers using immunoprecipitation assays against SIRT1 in HTB-94 cells. Each blot panel is a repeat of the immunoprecipitation experiment (*n*=3). SIRT1: 110 kDa; BECLIN 1: 60 kDa; ATG5: 55 kDa; ATG7 75 kDa; LC3 I: 19 kDa; LC3 II: ~17 kDa. ULK1; 130 kDa ; β-actin: 42 kDa.

After observing the direct binding of SIRT1 to autophagy proteins in chondrocytes I wanted to examine if the deacetylate activity of SIRT1 has a direct functional effect on these proteins. Acetyl lysine is a common deacetylation target for SIRT1. Examining total acetyl lysine residue expression on immunoprecipitated autophagy proteins when SIRT1 activity is pharmacologically blocked (EX-527; 100nM) or activated (SRT1720; 500nM) would elucidate if SIRT1 functionally modifies autophagy proteins.

BECLIN 1 was functionally modified through its interaction with SIRT1 demonstrated by increased (104.2%; P=0.05) ratio of acetyl lysine protein expression/total BECLIN 1 protein expression when SIRT1 was pharmacologically blocked (Figure 5.10 A and B). Whereas, SIRT1 activation caused a decrease in (50.64%; P=0.05) the ratio of acetyl lysine protein expression/total BECLIN 1 protein expression (Figure 5.10 A and B).

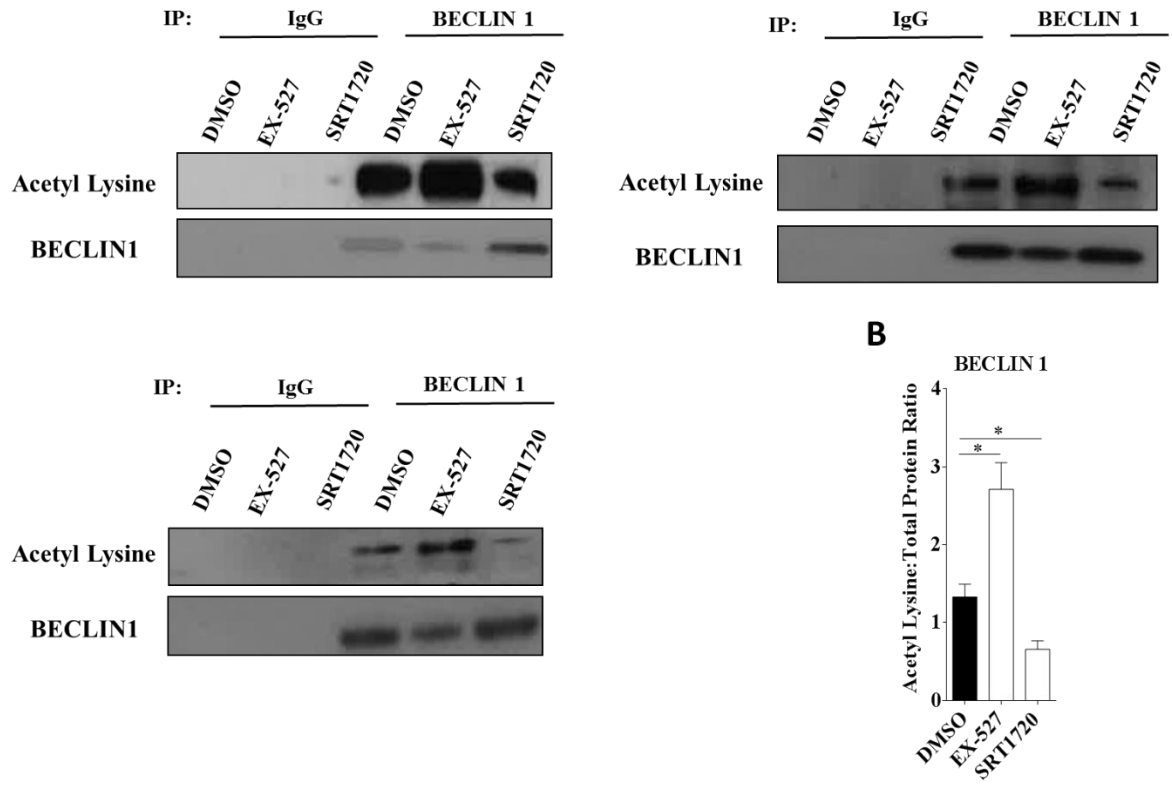

Figure 5.10: SIRT1 interaction and functional modification of BECLIN 1. (A) Results shown are of 3 independent experiments. Western blot analysis of acetyl lysine and total protein of BECLIN 1 in HTB-94 cells treated with DMSO (control), EX-527 (100nM) or SRT1720 (500nM) (*n*=3). **(B)** Densitometric analysis of acetyl lysine compared to total protein ratio of BECLIN 1 in HTB-94 cells treated with DMSO (control), EX-527 (100nM) or SRT1720 (500nM) (*n*=3). Acetyl lysine: 76 kDa; BECLIN 1: 60 kDa. Graphs show the S.E.M.; ANOVA Tukeys multiple comparison test; * $P< 0.05$.

ATG5 was functionally modified through its interaction with SIRT1 demonstrated by increased (55.97%; *P*=0.05) ratio of acetyl lysine protein expression/total ATG5 protein expression when SIRT1 was pharmacologically blocked (Figure 5.11 A and B). Conversely, SIRT1 activation caused a decrease in (58.17%; *P*=0.05) ratio of acetyl lysine protein expression/total ATG5 protein expression (Figure 5.11 A and B).

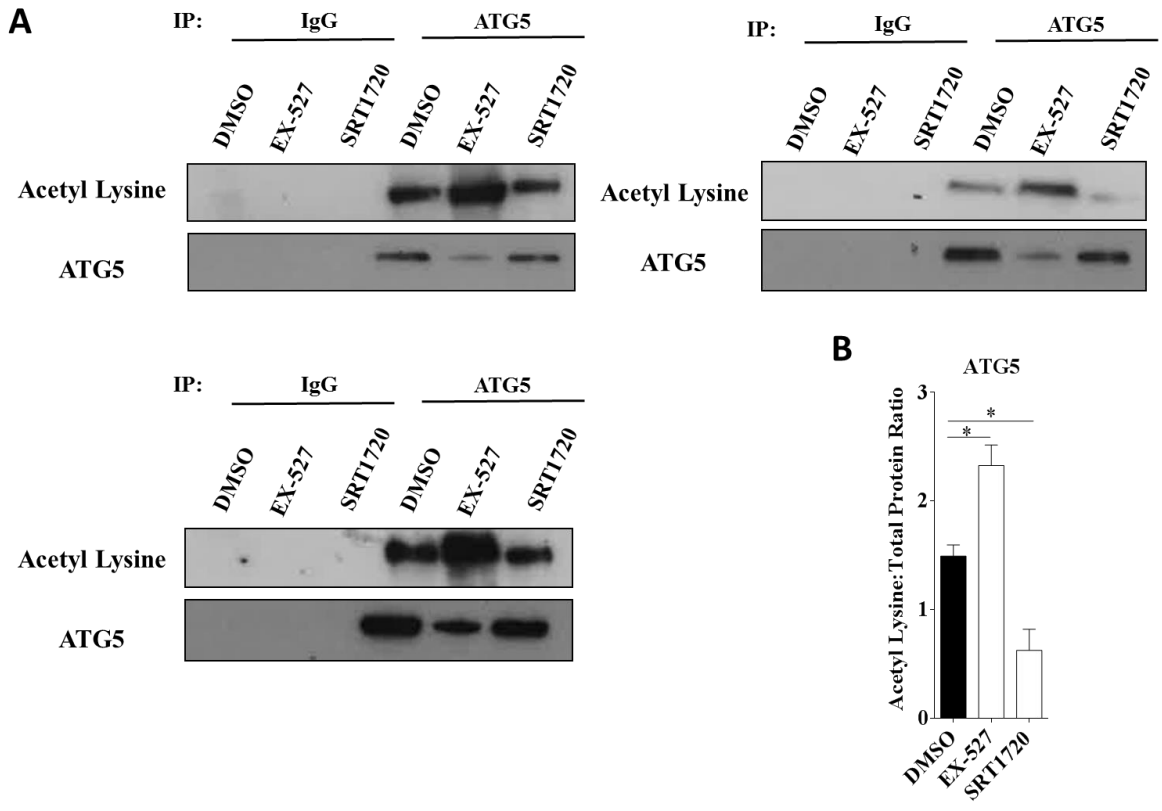

Figure 5.11: SIRT1 interaction and functional modification of ATG5. (A) Results shown are of 3 independent experiments. Western blot analysis of acetyl lysine and total protein of ATG5 in HTB-94 cells treated with DMSO (control), EX-527 (100nM) or SRT1720 (500nM) (n=3). **(B)** Densitometric analysis of acetyl lysine compared to total protein ratio of ATG5 in HTB-94 cells treated with DMSO (control), EX-527 (100nM) or SRT1720 (500nM) (*n*=3). Acetyl lysine: 76 kDa; ATG5: 55 kDa. Graphs show the S.E.M.; ANOVA Tukeys multiple comparison test; * *P*< 0.05.

ATG7 was functionally modified through its interaction with SIRT1 demonstrated by increased (107.1%; *P*=0.0013) ratio of acetyl lysine protein expression/total ATG7 protein expression when SIRT1 was pharmacologically blocked (Figure 5.12 A and B). Whereas, SIRT1 activation caused a decrease in (64.74%; *P*=0.0076) ratio of acetyl lysine protein expression/total ATG7 protein expression (Figure 5.12 A and B).

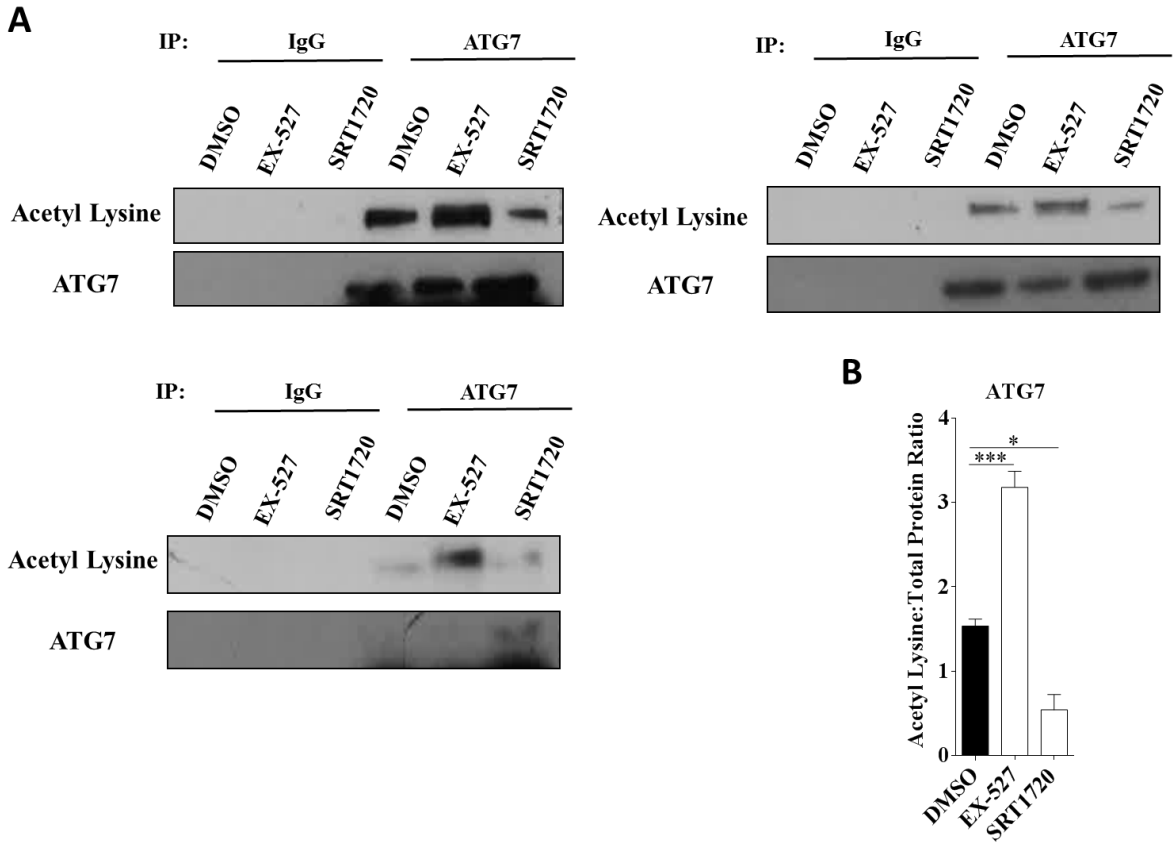

Figure 5.12: SIRT1 interaction and functional modification of ATG7. (A) Results shown are of 3 independent experiments. Western blot analysis of acetyl lysine and total protein of ATG7 in HTB-94 cells treated with DMSO (control), EX-527 (100nM) or SRT1720 (500nM) (n=3). **(B)** Densitometric analysis of acetyl lysine compared to total protein ratio of ATG7 in HTB-94 cells treated with DMSO (control), EX-527 (100nM) or SRT1720 (500nM) (*n*=3). Acetyl lysine: 76 kDa; ATG7: 75 kDa. Graphs show the S.E.M.; ANOVA Tukeys multiple comparison test; * *P*< 0.05 or *** *P*< 0.001.

LC3 I was functionally modified through its interaction with SIRT1 demonstrated by increased (130.99%; *P*=0.01) ratio of acetyl lysine protein expression/total LC3 I protein expression when SIRT1 was pharmacologically blocked (Figure 5.13 A and B). SIRT1 activation caused a decrease in (38.87%; *P*=0.05) ratio of acetyl lysine protein expression/total LC3 I protein expression (Figure 5.13 A and B).

LC3 II was functionally modified through its interaction with SIRT1 demonstrated by increased (82.11%; *P*=0.05) ratio of acetyl lysine protein expression/total LC3 II protein expression when SIRT1 was pharmacologically blocked (Figure 5.13 A and B). Conversely, SIRT1 activation caused a decrease in (57.05%; *P*=0.05) ratio of acetyl lysine protein expression/total LC3 II protein expression (Figure 5.13 A and B).

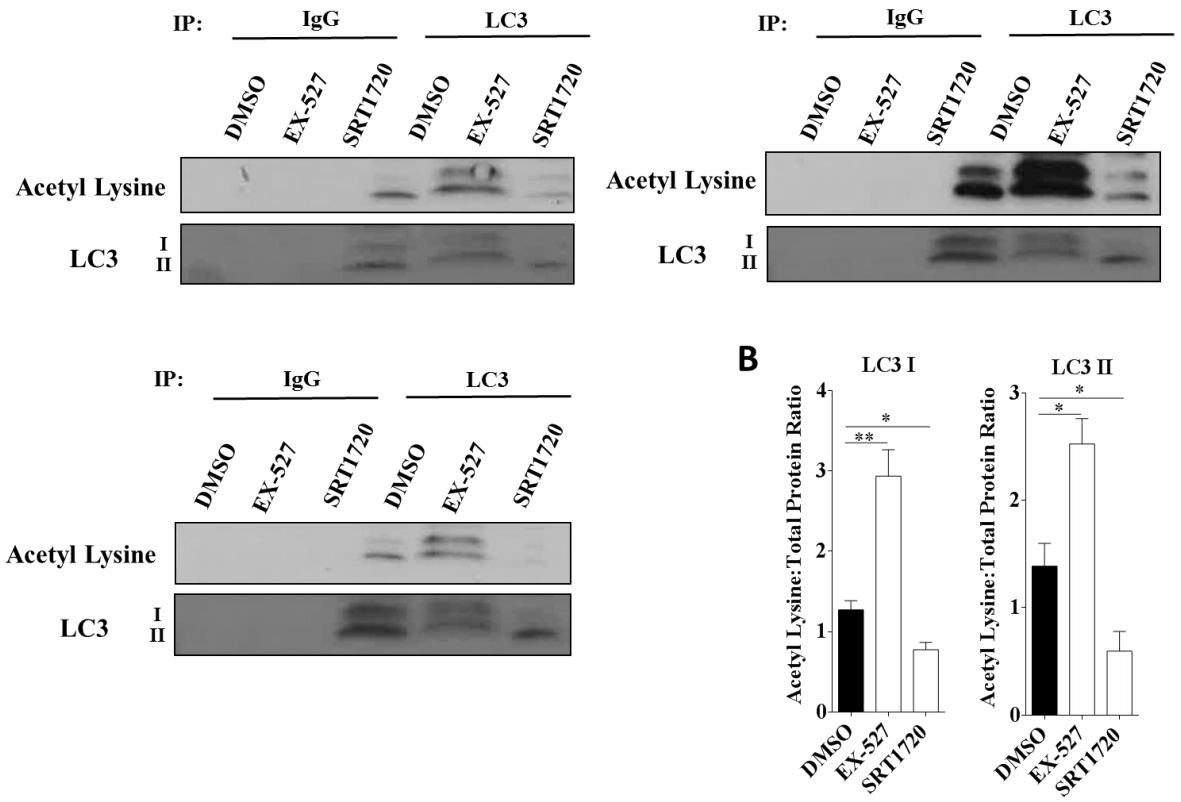

Figure 5.13: SIRT1 interaction and functional modification of LC3 I and LC3 II. (A) Results shown are of 3 independent experiments. Western blot analysis of acetyl lysine and total protein of LC3 I and LC3 II in HTB-94 cells treated with DMSO (control), EX-527 (100nM) or SRT1720 (500nM) (n=3). **(B)** Densitometric analysis of acetyl lysine compared to total protein ratio of LC3 I AND LC3 II in HTB-94 cells treated with DMSO (control), EX-527 (100nM) or SRT1720 (500nM) (*n*=3). Acetyl lysine: 76 kDa; LC3 I: 19 kDa; LC3 II: ~17 kDa. Graphs show the S.E.M.; ANOVA Tukeys multiple comparison test * *P*< 0.05 or ** *P*<0.01.

5.3.9 Targeting SIRT1-autophagy interaction in chondrocytes in vivo

After observing the direct link between SIRT1 and autophagy I wanted to test whether stimulating autophagy pharmacologically in cartilage *in vivo* would require SIRT1. I supplemented the drinking water of $SIRT1^{fl/fl}$ mice and $SIRT1^{Agg}$ mice with the autophagy activator spermidine for 2 weeks. As observed before $SIRT1^{Agg}$ mice displayed decreased (51.17%; *P*=0.03) LC3 I to LC3 II conversion in cartilaginous avulsed hips compared to $SIRT1^{fl/fl}$ control mice (Figure 5.14 A and B). As expected spermidine treatment increased (51.29%; *P*=0.001) LC3 I to LC3 II conversion in $SIRT1^{fl/fl}$ mice compared to $SIRT1^{fl/fl}$ mice without spermidine treatment (Figure 5.14 A and B). However, the increase in LC3 I to LC3 II conversion was not observed in $SIRT1^{Agg}$ mice treated with spermidine compared to $SIRT1^{fl/fl}$ mice treated with spermidine (-69.56%; *P*=0.0001) (Figure 5.14 A and B).

To further validate my finding, I avulsed hips from mice and cultured them with media containing BAF *ex vivo.* Avulsed hips from $SIRT1^{fl/fl}$ mice treated with spermidine and cultured with media containing BAF displayed a further increase (134.28%; *P*=0.0001) in LC3 I to LC3 II conversion than avulsed hips from $SIRT1^{fl/fl}$ mice treated with spermidine without *ex vivo* BAF treatment (Figure 5.14 A and B). Avulsed hips from $SIRT1^{Agg}$ mice treated with spermidine then cultured with BAF displayed a decrease (296.22%; *P*=0.0001) LC3 I to LC3 II conversion compared to avulsed hips from $SIRT1^{Agg}$ mice treated with spermidine then cultured with DMSO (Figure 5.14 A and B).

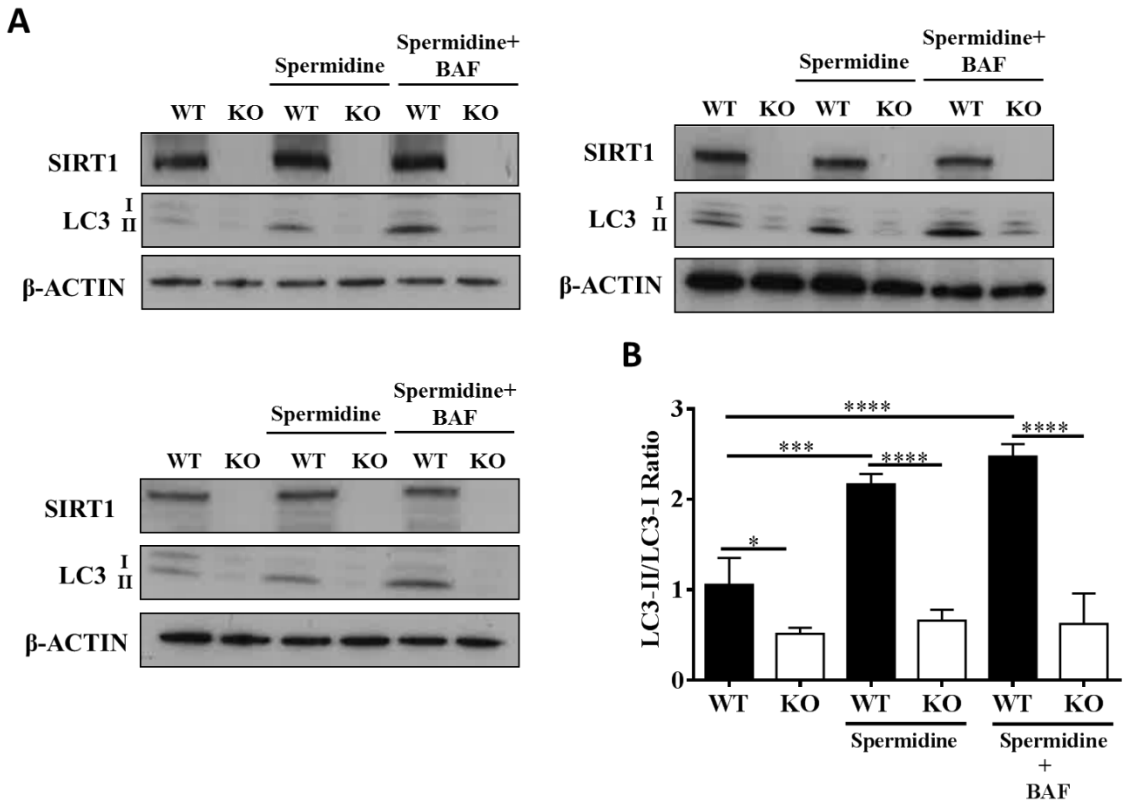

Figure 5.14: Targeting SIRT1-autophagy interaction in chondrocytes *in vivo:* (A) Results shown are of 3 independent experiments. Protein expression and **(B)** Densitometric qualification of LC3 I to II conversion from cartilaginous hips avulsed from young (6 weeks old) $SIRT1^{fl/fl}$ or $SIRT1^{Agg}$ mice treated with spermidine in drinking water (5mM) or vehicle control of water. After avulsion a group of hips were treated with BAF for positive control (*n*=3). SIRT1: 110 kDa; LC3 I: 19 kDa; LC3 II: ~17 kDa; β-actin: 42 kDa. Graphs show the S.E.M.; ANOVA Tukeys multiple comparison test; * *P*< 0.05, *** *P*<0.001 or **** *P*<0.0001.

5.3.10 Targeting SIRT1-autophagy interaction in an experimental OA model

After observing spermidine increased autophagy *ex vivo* avulsed hips, I wanted to test whether stimulating autophagy pharmacologically may represent a viable approach to reduce or prevent the cartilage degradation seen in OA *in vivo*. I also wanted to test if the chondroprotective effect of stimulating autophagy would require SIRT1.

There was no significant difference (2.25 ± 0.62 vs 1.75 ± 0.47; *P*=0.5504) in disease score between $SIRT1^{fl/fl}$ mice with sham surgery and $SIRT1^{fl/fl}$ mice with sham treated with spermidine (Figure 5.15 A and B). As expected there was an increase (2.25 ± 0.62, vs 9.36 ± 1.32; *P*=0.0080) in disease score between $SIRT1^{fl/fl}$ mice with sham surgery and $SIRT1^{fl/fl}$ mice with DMM surgery (Figure 5.15 A and B). Interestingly, a significant decrease (9.36 ± 1.32 vs 3.58 ± 0.48; *P*=0.0004) in disease score was observed in $SIRT1^{fl/fl}$ mice with DMM surgery treated with spermidine compared to $SIRT1^{fl/fl}$ mice with DMM surgery (Figure 5.15 A and B).

There was no significant difference (5.50 ± 1.84 vs 4.75 ± 0.47; *P*=0.7080) in disease score between $SIRT1^{Agg}$ mice with sham surgery and $SIRT1^{Agg}$ mice with sham treated with spermidine (Figure 5.15 A and B). There was an increase (17.68 ± 1.83 vs 9.36 ± 1.32; *P*=0.0020) in disease score in $SIRT1^{Agg}$ mice with DMM surgery compared to $SIRT1^{fl/fl}$ mice with DMM surgery (Figure 5.15 A and B). Interestingly, there was no significant difference (17.68 ± 1.83 vs 19.91 ± 2.81; *P*=0.4975) in disease score between $SIRT1^{Agg}$ mice with DMM surgery treated with spermidine compared to $SIRT1^{Agg}$ mice with DMM surgery and not treated with spermidine (Figure 5.15 A and B).

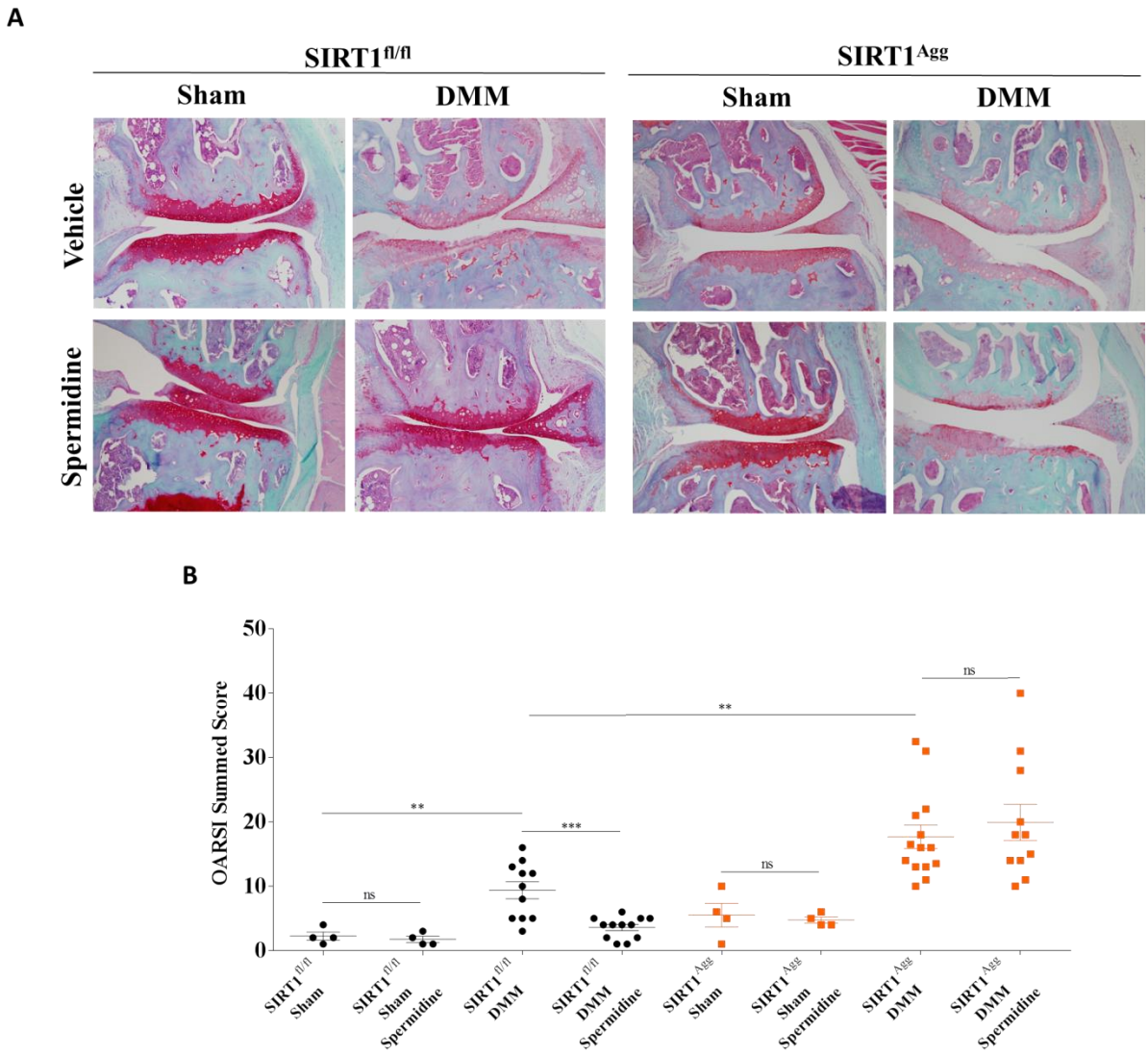

Figure 5.15: Targeting SIRT1-autophagy interaction in an experimental OA model (A) Representative images of Safranin-O–fast green staining of the medial femoral condyle and tibial plateau of control SIRT1$^{fl/fl}$ or SIRT1^{Agg} mice treated with either vehicle control (water) or spermidine (5mM) 8 weeks post-surgical DMM. **(B)** OA disease score of SIRT1$^{fl/fl}$ or SIRT1^{Agg} mice treated with either vehicle control or spermidine 8 weeks post-surgical DMM assessed by two blinded operators (*n*=4-12). ANOVA with Bonferroni post hoc test was used for disease score analysis. ns=non-significant, ** *P*< 0.01 or *** *P*<0.001.

There was no significant difference (3.10%; *P*=0.0972) in LC3 protein expression between $SIRT1^{fl/fl}$ mice with sham surgery and $SIRT1^{fl/fl}$ mice with sham treated with spermidine (Figure 5.16 A and B). There was a decrease (-38.50%; *P*=0.0041) in LC3 protein expression between $SIRT1^{fl/fl}$ mice with sham surgery and $SIRT1^{fl/fl}$ mice with DMM surgery (Figure 5.16 A and B). A significant increase (63.86%; *P*<0.0001) in LC3 protein expression was observed in $SIRT1^{fl/fl}$ mice with DMM surgery treated with spermidine compared to $SIRT1^{fl/fl}$ mice with DMM surgery and not treated with spermidine (Figure 5.16 A and B).

There was no significant difference (0.65%; *P*=0.9024) in LC3 protein expression between $SIRT1^{Agg}$ mice with sham surgery and $SIRT1^{Agg}$ mice with sham treated with spermidine (Figure 5.16 A and B). There was a decrease (-35.65%; *P*=0.0165) in LC3 protein expression in $SIRT1^{Agg}$ mice with DMM surgery compared to $SIRT1^{fl/fl}$ mice with DMM surgery (Figure 5.16 A and B). Interestingly, there was no significant difference (8.40%; *P*=0.5379) in LC3 protein expression between $SIRT1^{Agg}$ mice with DMM surgery treated with spermidine compared to $SIRT1^{Agg}$ mice with DMM surgery and not treated with spermidine (Figure 5.16 A and B).

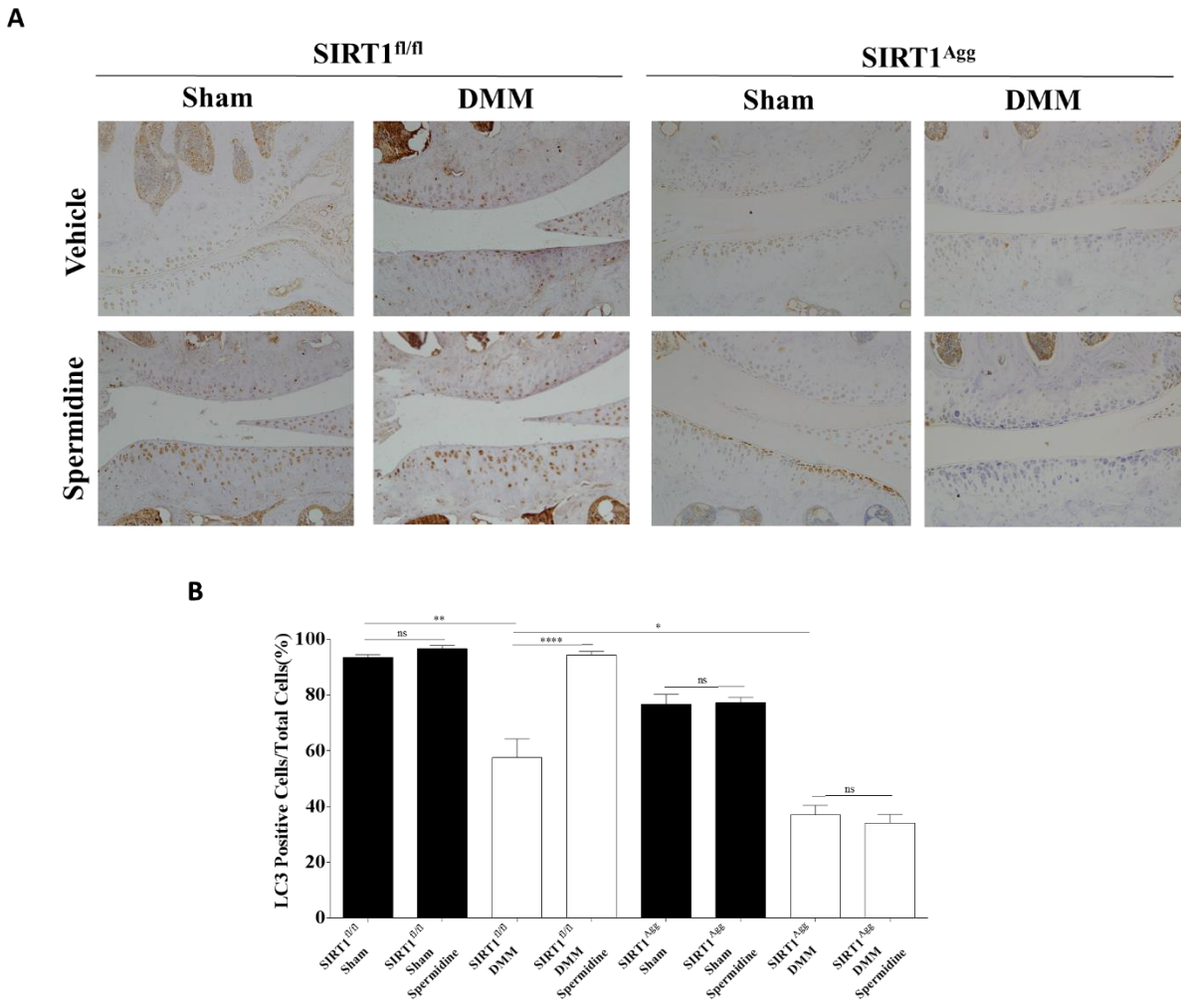

Figure 5.16: LC3 protein expression in mice treated with spermidine in an experimental OA model (A) Representative images of LC3 protein expression of the medial femoral condyle and tibial plateau of control SIRT1$^{fl/fl}$ or SIRT1^{Agg} mice treated with either vehicle control (water) or spermidine 8 weeks post-surgical DMM. **(B)** Quantification of LC3 positive cells/total cells in the medial femoral condyle and tibial plateau of SIRT1$^{fl/fl}$ or SIRT1^{Agg} mice treated with either vehicle control (water) or spermidine 8 weeks post-surgical DMM scored counted by two blinded operators (*n*=4-8); Data was analysed by ANOVA with Bonferroni post hoc. All data are S.E.M. ns=non-significant, * *P*< 0.05, ** *P*< 0.01 or **** *P*<0.0001.

5.4 Discussion

I wanted to investigate a precise mechanism though which SIRT1 could be chondroprotective after observing that SIRT1 positively regulated chondrocyte markers *in vitro*, and that loss of SIRT1 lead to cartilage degradation *in vivo*. Likewise the cellular process of autophagy as also been shown to decrease with age. Studies have reported autophagy to decrease in ageing human and murine cartilage (Caramés et al. 2010). In addition, mice deficient in the key autophagy protein ATG5 have been shown to develop premature OA (Bouderlique et al. 2015). Despite these observations, the mechanism through which autophagy in chondrocytes is regulated is not clear. So I investigated if the loss of SIRT1 during ageing impaired autophagy and leads to OA.

At first I examined autophagy protein expressions in young, aged and OA HACs. There was a decrease in ULK1, BECLIN 1 and LC3 I to LC3 II conversion in ageing and OA HACs compared to young HACs. Caramés *et al.* (2010) showed a decrease in ULK1, BECLIN1 and LC3 in OA and mild OA cartilage compared to normal healthy cartilage. My data confirms these results but also for the first time, shows a decrease in the autophagy markers in old HACs compared to young HACs. The decrease in autophagy markers in aged and OA HACs compared to young samples also correlated with a decrease in SIRT1 observed earlier in the same HACs. Hence, I manipulated SIRT1 using siRNA and pharmacological drugs to determine an effect on autophagy proteins. The gene and protein (determined by WB and FACs) expression of critical autophagy-related genes ULK1, BECLIN1 and LC3, were regulated in line with molecular and pharmacological alteration of SIRT1. Inhibition of SIRT1 by EX-527 and silencing of SIRT1 has been shown to reduce autophagy in dendritic cells leading to increased lung pathology in mice with lower respiratory tract infection (Owczarczyk *et al.* 2015). Conversely, neuroblastic cells

(PC12 cell line) treated with resveratrol, a first generation SIRT1 activator demonstrated an increase in LC3 I to LC3 II conversion and autophagosome count, compared to cells not treated with resveratrol (Deng and Mi 2016). Interestingly, my data showed increases in autophagy markers at the mRNA expression level. This indicates SIRT1 might have an effect on the transcription of autophagy genes alongside post-translational modifications. Transcriptional control of autophagy genes by SIRT1 might be explained by the direct deacetylation of Transcription factor EB (TFEB). TFEB is a master transcription factor for autophagy (Settembre *et al.* 2011). SIRT1 deacetylation has been shown to promote TFEB activity thus increasing autophagy (Bao *et al.* 2016). It would be of interest in the future to examine the interaction between SIRT1 and TFEB in the control of the transcription of autophagy genes in chondrocytes.

I went on to examine the role of SIRT loss on autophagy *in vivo*. Similar to my *in vitro* data a customised array analysis targeting a panel of autophagy-related genes, from micro-dissected cartilage of $SIRT1^{Agg}$ animals revealed a significant down regulation in over ten autophagy genes. In support of this data, a similar dysregulation of LC3 protein was observed in avulsed hips from $SIRT1^{Agg}$ mice, where decreased levels LCI-LC3II conversion were seen compared with control animals. This is particularly apparent when autophagy was arrested following BAF treatment and LC3 II levels were allowed to accumulate. The decrease in LC3 I to LC3 II conversion in the absence of SIRT1 have been reported before in monocytes (Takeda-Watanabe *et al.* 2012), HEK293 cells (Huang *et al.* 2015) and *ex vivo* cultured murine embryonic fibroblasts (MEFs) (Lee *et al.* 2008). Both mRNA and protein expression of P62 were increased in articular cartilage from $SIRT1^{Agg}$ mice compared to control mice. P62 acts as an adaptor protein which binds to cytotoxic protein aggregates, damaged mitochondria

and invasive microbes and then attaches to the forming autophagosome (Katsuragi *et al.* 2015). Hence, an increase in P62 indicates an increase in accumulation of dysfunctional protein aggregates and impaired autophagy (Katsuragi *et al.* 2015). Takeda-Watanabe *et al.* (2012) also reported a similar increase in P62 protein expression when SIRT1 was inhibited by EX-527 in a monocyte cell line. The decrease in LC3 I to LC3 II conversion was also supported by the use of LC3-GFP reporter mice. LC3-GFP puncta count and intensity decreased or increased in avulsed hips treated with EX-527 or SRT1720 respectively. Lee *et al.* (2008) also showed SIRT1 deficient MEFs had decreased levels of LC3 puncta per cell compared to controls with normal SIRT1 levels. I now wanted to confirm whether there was a decrease in autophagy on a functional level in the absence of SIRT1. TEM analysis demonstrated for the first time a decrease in autophagosome count in murine chondrocytes due to SIRT1 deficiency. Thereafter I wanted to investigate if SIRT1 loss will lead to reduced autophagy in ageing cartilage. Immunohistochemistry staining showed decreased LC3 positive stained cells/total cells in $SIRT1^{Agg}$ knee joint cartilage compared $SIRT1^{fl/fl}$ controls. The decline of autophagy is known to occur within cells of ageing individuals (García-Prat *et al.* 2016). Other studies have shown ULK1 and BECLIN1, ATG5 and LC3 to decrease in ageing murine cartilage (Caramés *et al.* 2010; Caramés *et al.* 2015).

At this stage it was unclear whether the effects of SIRT1 and autophagy were linked or occurring indirectly. To investigate this, I conducted immunoprecipitation analysis to determine which autophagy-related proteins directly interact with SIRT1 in chondrocytes. Several autophagy mediators including BECLIN1, ATG5, ATG7 and LC3, but excluding ULK1, were shown to bind to SIRT1. However, future experiments should be conducted to pull-down autophagy proteins to detect if SIRT1 binds to them. In addition, future experiments should

confirm if SIRT1 is directing binding to the autophagy proteins individually or via secondary and tertiary complex formation. Each autophagy protein was functionally modified through its interaction with SIRT1 demonstrated by increased acetylation of lysine residues when SIRT1 was pharmacologically blocked, and by decreased acetylation in the presence of a SIRT1 activator. Other studies have shown SIRT1 to directly bind to and modify autophagy proteins in other cell types; BECLIN1 (HEK293; Sun *et al.* 2015), ATG5 (MEFs; Lee *et al.* 2008), ATG7 (MEFs; Lee *et al.* 2008), LC3 (HEK293; Huang *et al.* 2015). Interestingly, SIRT1 did not bind to ULK1 which may indicate SIRT1 only controls downstream targets of the autophagy pathway. ULK1 activation by the inhibition of mTOR has been shown to be important in the control of autophagy in cartilage (Zhang *et al.* 2014) but no other regulation of chondrocyte autophagy has been reported. In addition, post-translational modifications of autophagy proteins have been reported to exert significant control over autophagic activity in other settings (Popelka and Klionsky 2015). Specifically, elevated acetylation of BECLIN1 reduced autophagosome maturation in cancer cells (Sun *et al.* 2015), whilst increased deacetylation of LC3 promoted autophagy following caloric restriction (Huang and Brumell 2014). Interestingly, CR is also an established experimental intervention for lifespan extension, and shown to be dependent on SIRT1 (Mercken *et al.* 2014; Qiu *et al.* 2015). Therefore, my findings show increased acetylation of key autophagy proteins brought about by an age-related decline in the SIRT1 would impair autophagy. However, at this stage I did not know if these events would lead to OA.

This led me to test whether stimulating autophagy pharmacologically may represent a viable approach to reduce OA and I wanted to determine if this protective effect of autophagy in OA will be lost if SIRT1 is deficient. I tested the effect of the naturally occurring non-toxic

autophagy activator spermidine, to protect against DMM induced OA. Spermidine has previously been used *in vivo* to enhance autophagy in a dose-dependent manner and protect against myopathy (Chrisam *et al.* 2015), neurodegeneration (Büttner *et al.* 2014), and age-related defects in T cell response (Puleston *et al.* 2014). As anticipated, spermidine treatment elevated autophagy in cartilage isolated from wild-type mice, evidenced by increased LC3 II protein levels. However, spermidine treatment did not activate autophagy in $SIRT1^{Agg}$ chondrocytes suggesting that the presence of SIRT1 is necessary for efficient autophagy activation. DMM led to significant cartilage degradation, as measured by the OARSI disease score. However, wild-type mice treated with spermidine were significantly protected from cartilage degradation; suggesting that activation of autophagy by spermidine confers a protective effect against OA. Similar to my results, Carames *et al.* (2012) reported mice administered with Rapamycin (an mTOR inhibitor) to increase autophagy had decreased disease scores compared to wild-type controls. However, rapamycin has many off-target mechanisms and shown to be immunosuppressive in humans (Li *et al.* 2014; Baroja-Mazo *et al.* 2016). Hence, spermidine might be a better naturally occurring alternative. Most importantly, in support of my data indicating SIRT1 as a key regulator of autophagy in chondrocytes, spermidine failed to protect $SIRT1^{Agg}$ mice against the development of OA. Morselli *et al.* (2011) showed spermidine and resveratrol (first generation SIRT1 activator) induce autophagy by distinct pathways converging on the acetylproteome. However, resveratrol has been shown not be a very specific activator of SIRT1 and to have multiple effects in cells (Beher et al. 2009; Hubbard and Sinclair 2014). Hence, the studies of Morselli *et al.* (2011) should be repeated with more specific SRT1 activators in the future.

In summary, in this chapter I showed that both SIRT1 and autophagy are dysregulated in human chondrocytes of ageing and OA cartilage. The loss of SIRT1 *in vitro* decreased chondrocyte and autophagy makers and in mature articular cartilage *in vivo* lead to accelerated OA. I have identified direct interactions between SIRT1 and autophagy-related proteins where functional modifications and changes in autophagic flux are dependent upon SIRT1 expression. Moreover, pharmacological activation of autophagy is protective against early OA development, but not in the absence of SIRT1. These data demonstrate that declining expression of SIRT1 with increasing age predisposes the cartilage to the development of OA by impairing autophagy.

6. The regulation of joint inflammation by SIRT1

6.1 Introduction

The role of inflammation and its mediators in OA pathogenesis has been well established (Goldring and Otero 2011; Liu-Bryan and Terkeltaub 2015). IL-1β and TNFα are capable of inducing and activating catabolic enzymes such as MMP-13 and ADAMTS5 to degrade cartilage (Saklatvala 1981; Saklatvala 1986). However, there is scant evidence that these cytokines are central in driving disease *in vivo* (Clements *et al.* 2003; Glasson 2007; Fukai *et al.* 2012). Catabolic enzymes can be induced rapidly upon surgical joint destabilization in a highly mechano-sensitive manner as well; gene regulation and disease is abrogated if the joint is immobilized following surgery. This suggests that mechanical factors can also initiate pathogenic pathways (Burleigh *et al.*, 2012). This accords well with epidemiological evidence that OA may principally be driven by mechanical joint overload and injury (Brandt, Dieppe, and Radin, 2009). The significance of joint inflammation in contributing to tissue breakdown is unclear. Infiltration of mononuclear cells into the synovial membrane is observed in human OA (Scanzello and Goldring 2012) and there is much evidence to support activation of the innate immune system in disease (Orlowsky and Kraus, 2015). It seems likely that inflammation, when present, will exacerbate tissue breakdown and contribute to painful episodes of disease.

SIRT1 has been shown to negatively regulate inflammation by deacetylation of NF-κB, thereby preventing its translocation to the nucleus and halting the transcription of pro-inflammatory genes (Rothgiesser et al. 2010). SIRT1 KO mice show increased levels of inflammatory cytokines in serum and an autoimmune phenotype (Sequeira *et al.* 2008). I wanted to investigate whether a whole body deletion of SIRT1 using $SIRT1^{ROSA}$ mice would cause an increased inflammatory response and exacerbate OA compared to $SIRT1^{Agg}$ mice and control

SIRT1$^{fl/fl}$ mice. Results from these studies may address if the inflammatory response initiated from the cartilage is more important than the systemic inflammation in OA pathogenesis.

6.2 Hypothesis

SIRT1^{ROSA} mice would display an increased inflammatory response in joints leading to increased OA compared to SIRT1^{Agg} mice and SIRT1$^{fl/fl}$ control mice.

6.3 Results

6.3.1 Effect of whole body vs cartilage specific SIRT1 deficiency on the gene expression of cartilage and OA markers

At first I wanted to examine inflammatory markers associated with OA pathogenesis in both SIRT1 cKO lines. Gene expressions of inflammatory cytokines (*Il-1β*, *Il-6*, *Il-18*, *Tnfα* and *Tnfaip6*) and proteases (*Adamts1, Adamts4, Adamts5, Mmp3, MMP-13 and Timp1)* were significantly increased in in knee joints from $SIRT1^{ROSA}$ mice compared to knee joints from $SIRT1^{fl/fl}$ mice (Table 6.1). There was no difference in gene expression of *Acan*, *Adamts15*, *Col2a1* and *Ctgf* in knee joints from $SIRT1^{ROSA}$ mice compared to knee joints from $SIRT1^{fl/fl}$ mice (Table 6.1).

In comparison, there was no difference in gene expression of inflammatory cytokines (*Il-1β*, *Il-6*, *Il-18*, *Tnfα* and *Tnfaip6*) and proteases (*Adamts1, Adamts15, Adamts4, Adamts5, Mmp3, MMP-13 and Timp1)* in knee joints from $SIRT1^{Agg}$ mice compared to knee joints from $SIRT1^{fl/fl}$ mice (Table 6.1). However, the gene expression of *Acan*, *Col2a1* and *Ctgf* were significantly decreased in knee joints from $SIRT1^{Agg}$ mice compared to knee joints from $SIRT1^{fl/fl}$ mice (Table 6.1). Baseline synovitis was checked using histology and was not present in both SIRT1 cKO lines and control mice.

Table 6.1: Gene expression of inflammatory markers in $SIRT1^{fl/fl}$, $SIRT1^{ROSA}$ and $SIRT1^{Agg}$ murine knee joints at 10 weeks of age.

	$SIRT1^{ROSA}$ vs $SIRT1^{fl/fl}$			$SIRT1^{Agg}$ vs $SIRT1^{fl/fl}$		
Gene	**Expression change**	**Fold Change**	***P=***	**Expression change**	**Fold Change**	***P=***
Acan	–	0.91	NS	↓	0.5	0.01
Adamts1	↑	1.57	0.02	–	0.88	NS
Adamts15	–	0.66	NS	–	1.12	NS
Adamts4	↑	4.62	0.0002	–	1	0.04
Adamts5	–	0.77	NS	–	1.01	NS
Col2a1	–	1.12	NS	↓	0.54	0.03
Ctgf	–	0.94	NS	↓	0.5	0.02
Il18	↑	3.27	0.01	–	0.66	NS
Il1b	↑	1.95	0.01	–	0.77	NS
Il6	↑	3.17	0.01	–	0.8	NS
Mmp3	↑	2.14	0.02	–	1.05	NS
MMP-13	↑	2.78	0.03	–	1.8	NS
Timp1	↑	1.86	0.05	–	1.3	NS
Tnfα	↑	1.61	0.05	–	1.1	NS
Tnfaip6	↑	2.38	0.02	–	1.23	NS

RNA was extracted from articular cartilage microdissected from murine joints. RT-PCR was performed using TaqMan microfluidic cards. Fold changes were normalized to ribosomal protein *18S* and expressed relative to levels in $SIRT1^{fl/fl}$ mice. (*n*=4 mice per group). Unpaired t-test. NS = not significant.

6.3.2 Effect of whole body vs cartilage specific SIRT1 deficiency on the gene expression of cartilage and OA markers 6hrs, 24hrs and 72hrs post DMM

After observing increased gene expression of inflammatory markers in naive joints of $SIRT1^{ROSA}$ mice compared to $SIRT1^{Agg}$ mice I now wanted to investigate the immediate response in inflammatory gene expression post mechanical injury (DMM). I chose three short time points; 6, 24 and 72hrs post DMM to validate the gene expression response of inflammatory markers.

At 6hrs post DMM, the gene expression of inflammatory cytokines (*Il-1β*, *Il-6*, *Il-18*, *Tnfα* and *Tnfaip6*) and proteases (*Adamts1, Adamts4, Mmp3, MMP-13 and Timp1)* were significantly increased in knee joints from $SIRT1^{ROSA}$ mice compared to knee joints from $SIRT1^{fl/fl}$ mice (Table 6.2). There was no difference in gene expression of *Acan*, *Adamts15*, *Adamts5*, *Col2a1* and *Ctgf* in knee joints from $SIRT1^{ROSA}$ mice compared to knee joints from $SIRT1^{fl/fl}$ mice (Table 6.2).

In comparison, there was no difference in gene expression of inflammatory cytokines (*Il-1β*, *Il-6*, *Il-18*, *Tnfα* and *Tnfaip6*) and proteases (*Adamts1, Adamts4, Adamts15, Adamts5, Mmp3, MMP-13 and Timp1)* in knee joints from $SIRT1^{Agg}$ mice compared to knee joints from $SIRT1^{fl/fl}$ mice (Table 6.2). The gene expression of *Acan*, *Col2a1* and *Ctgf* were significantly decreased in knee joints from $SIRT1^{Agg}$ mice compared to knee joints from $SIRT1^{fl/fl}$ mice (Table 6.2).

Table 6.2: Gene expression of inflammatory markers in $SIRT1^{fl/fl}$, $SIRT1^{ROSA}$ and $SIRT1^{Agg}$ murine knee joints at 6hrs post DMM.

	$SIRT1^{ROSA}$ vs $SIRT1^{fl/fl}$			$SIRT1^{Agg}$ vs $SIRT1^{fl/fl}$		
Gene	**Expression change**	**Fold Change**	***P=***	**Expression change**	**Fold Change**	***P=***
Acan	–	0.99	NS	↓	0.57	0.01
Adamts1	↑	2.38	0.01	–	0.96	NS
Adamts15	–	1.42	NS	–	1.16	NS
Adamts4	↑	2.33	0.0002	–	1.10	NS
Adamts5	–	1.25	NS	–	0.24	NS
Col2a1	–	1.05	NS	↓	0.13	0.0001
Ctgf	–	0.94	NS	↓	0.31	0.02
Il18	↑	2.77	0.05	–	1.36	NS
Il1b	↑	4.45	0.01	–	1.16	NS
Il6	↑	2.30	0.01	–	1.11	NS
Mmp3	↑	3.05	0.05	–	1.43	NS
MMP-13	↑	3.82	0.02	–	1.35	NS
Timp1	↑	3.84	0.05	–	1.06	NS
Tnfα	↑	2.97	0.001	–	1.34	NS
Tnfaip6	↑	1.86	0.02	–	0.90	NS

RNA was extracted from articular cartilage microdissected from murine joints. RT-PCR was performed using TaqMan microfluidic cards. Fold changes were normalized to ribosomal protein *18S* and expressed relative to levels in $SIRT1^{fl/fl}$ mice. (*n*=4 mice per group). Unpaired t-test. NS = not significant.

At 24hrs post DMM, the gene expression of inflammatory cytokines (*Il-1β*, *Il-6*, *Il-18*, *Tnfα* and *Tnfaip6*) and proteases (*Adamts1, Adamts15, Adamts4, Mmp3, MMP-13 and Timp1)* were significantly increased in knee joints from SIRT1^{ROSA} mice compared to knee joints from SIRT1$^{fl/fl}$ mice (Table 6.3). There was no difference in gene expression of *Adamts5* in knee joints from SIRT1^{ROSA} mice compared to knee joints from SIRT1$^{fl/fl}$ mice (Table 6.3). *Acan*, *Col2a1* and *Ctgf* were significantly increased in knee joints from SIRT1^{ROSA} mice compared to knee joints from SIRT1$^{fl/fl}$ mice (Table 6.3).

In comparison, gene expression of inflammatory cytokines (*Il-1β*, *Il-6*, *Il-18*, *Tnfα* and *Tnfaip6*) and proteases (*Adamts1, Adamts15, Adamts4, Mmp3 and MMP-13)* significantly decreased in knee joints from SIRT1^{Agg} mice compared to knee joints from SIRT1$^{fl/fl}$ mice (Table 6.3). The gene expression of *Acan*, *Col2a1* and *Ctgf* were significantly decreased in knee joints from SIRT1^{Agg} mice compared to knee joints from SIRT1$^{fl/fl}$ mice (Table 6.3). There was no change in gene expression of *Adamts5* in knee joints from SIRT1^{Agg} mice compared to knee joints from SIRT1$^{fl/fl}$ mice (Table 6.3).

Table 6.3: Gene expression of inflammatory markers in $SIRT1^{fl/fl}$, $SIRT1^{ROSA}$ and $SIRT1^{Agg}$ murine knee joints at 24hrs post DMM.

	$SIRT1^{ROSA}$ vs $SIRT1^{fl/fl}$			$SIRT1^{Agg}$ vs $SIRT1^{fl/fl}$		
Gene	**Expression change**	**Fold Change**	***P=***	**Expression change**	**Fold Change**	***P=***
Acan	↑	6.66	0.0001	↓	0.04	0.0001
Adamts1	↑	5.88	0.0001	↓	0.59	0.001
Adamts15	↑	2.61	0.0001	↓	0.69	0.0001
Adamts4	↑	3.89	0.0001	↓	0.40	0.0001
Adamts5	–	0.83	NS	–	0.11	0.0001
Col2a1	↑	4.32	0.0001	↓	0.06	0.0001
Ctgf	↑	2.55	0.0001	↓	0.61	0.05
Il18	↑	4.41	0.01	↓	0.58	0.0001
Il1b	↑	9.10	0.0001	↓	0.51	0.0001
Il6	↑	7.96	0.0001	↓	0.51	0.0001
Mmp3	↑	4.65	0.0001	↓	0.44	0.001
MMP-13	↑	6.21	0.0001	↓	0.48	0.0001
Timp1	↑	5.28	0.0001	↓	0.22	0.0001
Tnfα	↑	10.17	0.0001	↓	0.74	0.05
Tnfaip6	↑	4.28	0.0001	↓	0.77	0.03

RNA was extracted from articular cartilage microdissected from murine joints. RT-PCR was performed using TaqMan microfluidic cards. Fold changes were normalized to ribosomal protein *18S* and expressed relative to levels in $SIRT1^{fl/fl}$ mice. (*n*=4 mice per group). Unpaired t-test. NS = not significant.

At 72hrs post DMM, the gene expression of inflammatory cytokines (*Il-1β*, *Il-6*, *Il-18*, *Tnfα* and *Tnfaip6*) and proteases (*Adamts1, Adamts15, Adamts4, Mmp3, MMP-13 and Timp1)* were significantly increased in knee joints from SIRT1^{ROSA} mice compared to SIRT1$^{fl/fl}$ mice (Table 6.4). There was no difference in gene expression of *Adamts5* in knee joints from SIRT1^{ROSA} mice compared to SIRT1$^{fl/fl}$ mice (Table 6.3). *Acan*, *Col2a1* and *Ctgf* were significantly increased in knee joints from SIRT1^{ROSA} mice compared to SIRT1$^{fl/fl}$ mice (Table 6.4).

In comparison, gene expression of inflammatory cytokines (*Il-1β*, *Il-6*, *Il-18*, *Tnfα* and *Tnfaip6*) and proteases (*Adamts1, Adamts15, Adamts4, Mmp3 and MMP-13)* significantly decreased in knee joints from SIRT1^{Agg} mice compared to SIRT1$^{fl/fl}$ mice (Table 6.4). The gene expression of *Acan*, *Col2a1* and *Ctgf* were significantly decreased in knee joints from SIRT1^{Agg} mice compared to knee joints from SIRT1$^{fl/fl}$ mice (Table 6.4). There was no change in gene expression of *Adamts5* and *Il-18* in knee joints from SIRT1^{Agg} mice compared to knee joints from SIRT1$^{fl/fl}$ mice (Table 6.4).

Table 6.4: Gene expression of inflammatory markers in $SIRT1^{fl/fl}$, $SIRT1^{ROSA}$ and $SIRT1^{Agg}$ murine knee joints at 72hrs post DMM.

	$SIRT1^{ROSA}$ vs $SIRT1^{fl/fl}$			$SIRT1^{Agg}$ vs $SIRT1^{fl/fl}$		
Gene	**Expression change**	**Fold Change**	***P=***	**Expression change**	**Fold Change**	***P=***
Acan	↑	4.48	0.001	↓	0.62	0.004
Adamts1	↑	1.50	0.01	↓	0.75	0.05
Adamts15	↑	2.00	0.001	↓	0.60	0.03
Adamts4	↑	1.69	0.05	↓	0.82	0.007
Adamts5	–	1.26	NS	–	1.18	NS
Col2a1	↑	2.58	0.043	↓	0.2	0.0001
Ctgf	↑	2.86	NS	↓	0.78	0.005
Il18	↑	1.46	0.002	–	1.13	NS
Il1b	↑	4.26	0.005	↓	0.65	0.005
Il6	↑	3.97	0.006	↓	0.65	0.001
Mmp3	↑	3.24	0.032	–	0.86	NS
MMP-13	↑	5.03	0.026	↓	0.69	0.003
Timp1	↑	3.90	0.001	–	1.07	NS
Tnfα	↑	6.97	0.004	↓	0.85	0.01
Tnfaip6	↑	1.57	0.02	–	1.23	NS

RNA was extracted from articular cartilage microdissected from murine joints. RT-PCR was performed using TaqMan microfluidic cards. Fold changes were normalized to ribosomal protein *18S* and expressed relative to levels in $SIRT1^{fl/fl}$ mice. (*n*=4 mice per group). Unpaired t-test. NS = not significant.

6.3.3 Effect of whole body vs cartilage specific SIRT1 deletion on synovitis 24hrs post DMM

I wanted to investigate synovitis of knee joints 24hrs post DMM in both SIRT1 cKO lines and to validate if synovitis correlates with inflammatory gene expression. $SIRT1^{ROSA}$ mice displayed increased hyperplasia (+90.38%; 0.250 vs 2.600; *P*=0.0001) of the synovium and increased inflammation (+82.14; 0.500 vs 2.800; *P*=0.001) compared to $SIRT1^{fl/fl}$ mice (Figure 6.1 A, B and C). In addition, $SIRT1^{ROSA}$ mice displayed increased hyperplasia (-96.92%; 0.08 vs 2.600; *P*=0.0001) of the synovium and increased inflammation (-73.21%; 0.7500 vs 2.800; *P*=0.001) compared to $SIRT1^{Agg}$ mice (Figure 6.1 A, B and C). There was no significant difference in hyperplasia (-28.12%; 0.08 vs 0.25; *P*=0.315) of the synovium and inflammation (-33.21%; 0.500 vs 0.750; *P*=0.5370) in $SIRT1^{Agg}$ mice compared to $SIRT1^{fl/fl}$ mice (Figure 6.1 A, B and C).

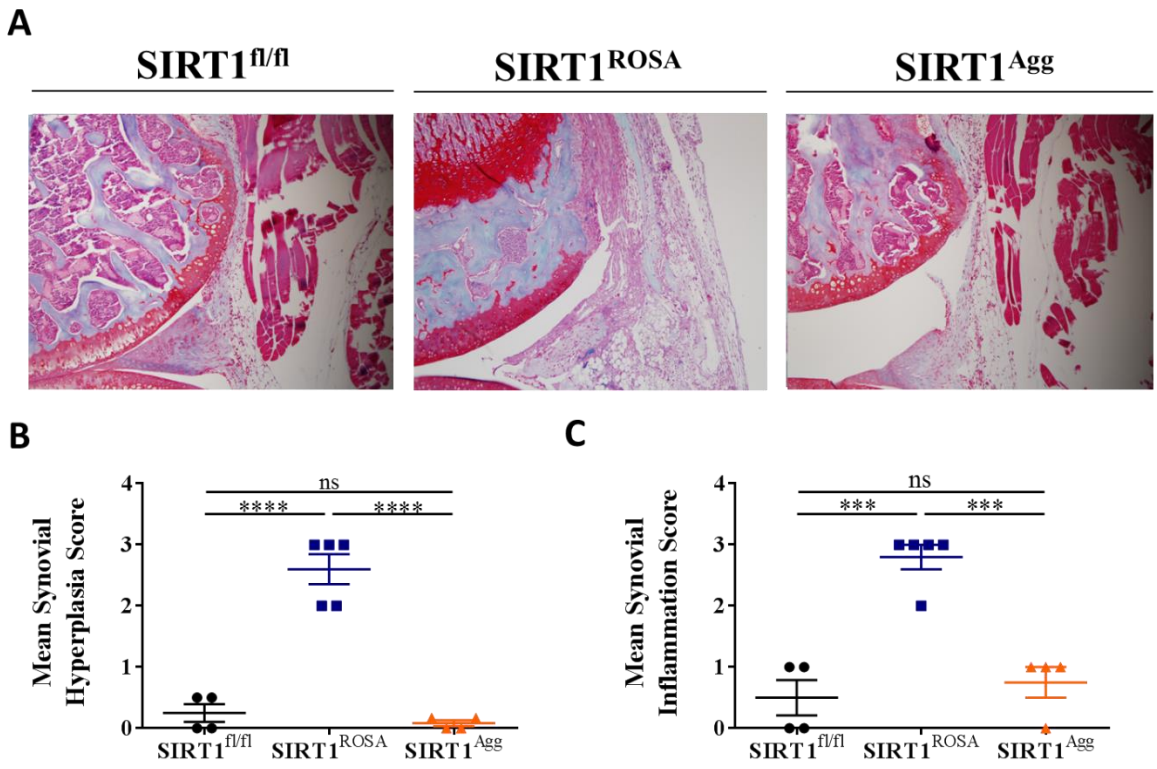

Figure 6.1: Synovitis scoring in SIRT1 cKO murine lines: (A) Representative images of sagittal sections of the medial femoral condyle and tibial plateau of SIRT1$^{fl/fl}$, SIRT1^{ROSA} or SIRT1^{Agg} mice to assess synovitis. Blinded scoring of **(B)** synovial hyperplasia and **(C)** inflammation scores in sagittal sections of the medial femoral condyle and tibial plateau of control SIRT1$^{fl/fl}$, SIRT1^{ROSA} or SIRT1^{Agg} mice (*n*=4-5). Graphs show the S.E.M.; ANOVA Tukeys multiple comparison test; ns: non-significant, *** $P< 0.001$ or **** $P<0.0001$.

6.3.4 Effect of whole body vs cartilage specific SIRT1 deficiency on cartilage degradation 8 and 12 weeks post DMM

After observing early increases in inflammatory gene expression and synovitis in joints of $SIRT1^{ROSA}$ mice at a short term time point post DMM, I wanted to determine if this increased inflammatory state would exacerbate cartilage damage at a long term time point.

At 8 weeks post, DMM $SIRT1^{ROSA}$ mice displayed decreased disease score (-51.62%; 10.00 vs 4.84; *P*=0.0109) compared to $SIRT1^{fl/fl}$ mice (Figure 6.2 A and B). In addition, $SIRT1^{ROSA}$ mice displayed decreased disease score (-72.62%; 17.68 vs 4.84; *P*=0.0001) compared to $SIRT1^{Agg}$ mice (Figure 6.2 A and B). $SIRT1^{Agg}$ mice displayed increased disease score (+76.8%; 17.68 vs 10.00; *P*=0.0040) compared to $SIRT1^{fl/fl}$ mice (Figure 6.2 A and B).

To further validate long term disease scores I repeated DMM experiments and assessed cartilage damage at 12 weeks DMM (Figure 6.2 A and B). $SIRT1^{ROSA}$ mice displayed decreased disease score (-71.36%; 4.46 vs 15.58; *P*=0.0001) compared to $SIRT1^{fl/fl}$ mice (Figure 6.2 A and B). In addition, $SIRT1^{ROSA}$ mice displayed decreased disease score (-82.26%; 4.46 vs 25.07; *P*=0.0001) compared to $SIRT1^{Agg}$ mice. $SIRT1^{Agg}$ mice displayed increased disease score (-60.91%; 15.58 vs 25.07; *P*=0.001) compared to $SIRT1^{fl/fl}$ mice (Figure 6.2 A and B).

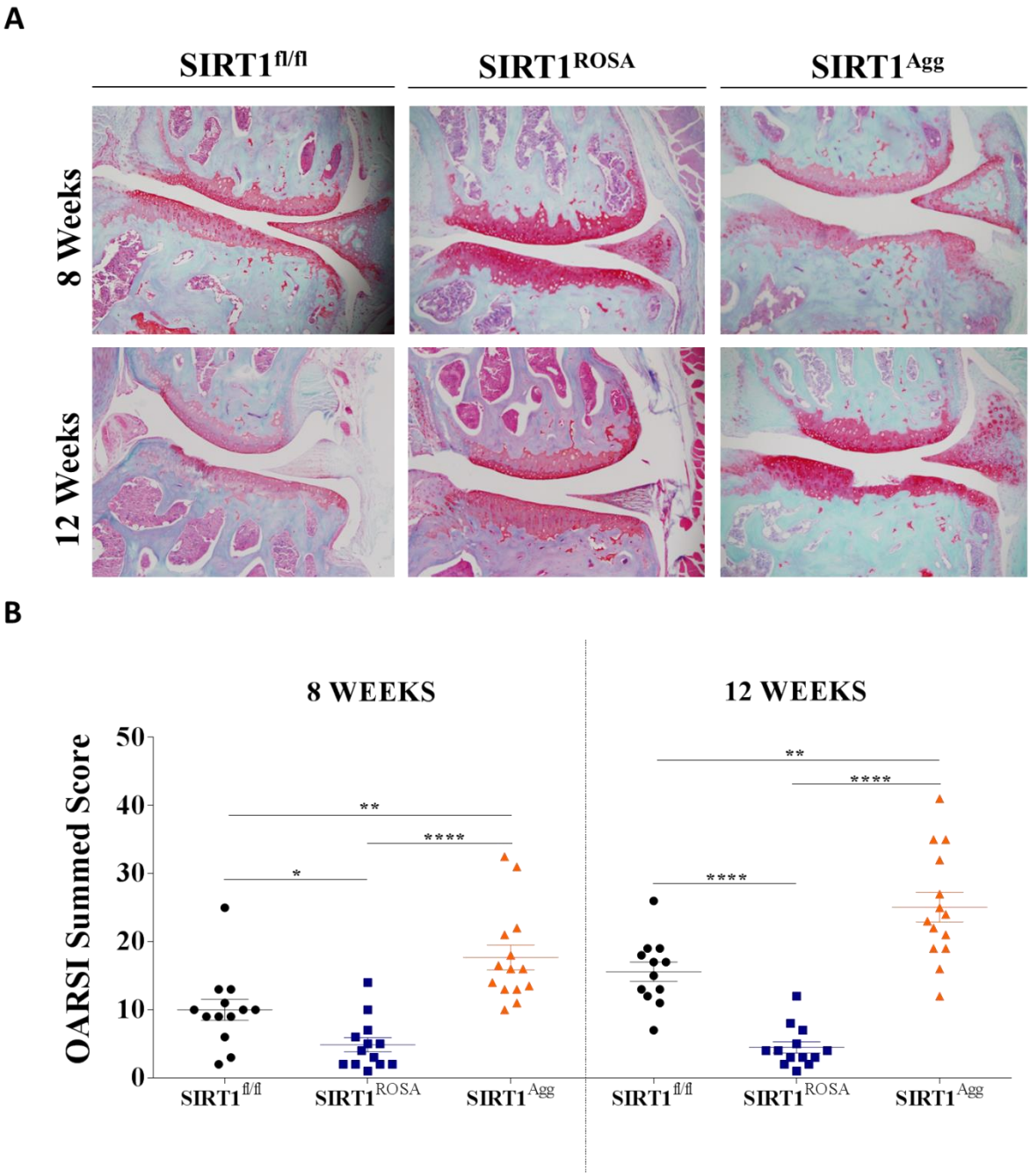

Figure 6.2: OARSI scoring of SIRT1 cKO mice 8 and 12 weeks post DMM. (A) Representative images of Safranin-O–fast green staining of the medial femoral condyle and tibial plateau of control SIRT1$^{fl/fl}$, SIRT1^{ROSA} or SIRT1^{Agg} mice 8 and 12 weeks post-surgical DMM. **(B)** OA disease score of SIRT1$^{fl/fl}$, SIRT1^{ROSA} or SIRT1^{Agg} mice 8 and 12 weeks post-surgical DMM (*n*=4-12). ANOVA with Bonferroni post hoc test was used for disease score analysis. * *P*< 0.05, ** *P*< 0.01, *** *P*<0.001 or **** *P*<0.0001.

6.4 Discussion

The role of inflammatory pathways in OA pathogenesis is well established. However, OA murine and human studies using biological treatments targeting inflammatory cytokines, such as IL-1β and TNFα have shown poor efficacy (Hunter 2011). It is not clear if persistent low grade joint inflammation will lead to exacerbated OA and how this process is regulated. SIRT1 has been shown to control inflammation by controlling NF-κB translocation into the nucleus (Rothgiesser *et al.* 2010). I hypothesized that SIRT1 cKO mice would display increased joint inflammation leading to exacerbated long term disease compared to control mice.

At first I examined the gene expression of inflammatory and protease markers associated with OA (Burleigh *et al.* 2012) at steady state. SIRT1^{ROSA} murine joints displayed increased expression of inflammatory and protease makers compared to control mice as hypothesized. This result is supported by other studies showing SIRT1 KO mice have elevated inflammatory status (Sequeira *et al.* 2008). In addition, SIRT1 activating compounds have been shown to reduce circulating inflammatory markers and systemic inflammation (Mitchell *et al.* 2014). SIRT1^{Agg} murine knee joints did not display any significant changes in inflammatory or protease gene expressions compared to control mice.

The gene expression level of *Mmp-13* and *Adamts5* increased in SIRT1^{ROSA} murine joints with higher inflammatory marker gene expression but not in SIRT1^{Agg} murine joints. This result supports my *in vitro* observations where *MMP-13* or *ADAMTS5* gene expressions in HTB-94 cells were not altered. This suggests the deletion of SIRT1 in chondrocytes does not affect *MMP-13* and *ADAMTS5* gene expression unless there is an inflammatory response present. Decreased gene expression of *Acan* and *Col2a1* were observed in knee joints of SIRT1^{Agg} mice.

Decreased gene expression of *Acan* and *Col2a1* has also been reported in cartilage from a mouse model with a point mutation in SIRT1 activity (Gabay *et al.* 2013). CTGF (shown to have a beneficial role in articular cartilage (Nishida *et al.* 2003)) was observed to decrease in $SIRT1^{Agg}$ murine joints and not in $SIRT1^{ROSA}$ mice. These results at this stage indicated a tissue-specific role of SIRT1 in the joint which has not been previously described.

I went on to examine if mechanical injury would exacerbate inflammatory and protease gene expression and change the tissue specific role of SIRT1 in murine joints. At 6hrs post DMM inflammatory and protease expression increased in $SIRT1^{ROSA}$ murine knee joints but not in knee joints of $SIRT1^{Agg}$ mice. However, inflammation and protease gene expression heightened at 24hrs post DMM in $SIRT1^{ROSA}$ murine knee joints, which may be caused by infiltrating immune cells into the knee joint. At 72hrs, inflammation and protease gene expression was elevated in $SIRT1^{ROSA}$ murine knee joints compared to control mice, however, the expression levels were not as high as 24hrs post DMM. This could be explained by the resolution of inflammation and decrease in infiltrating immune system cells 72hrs post injury. It was surprising to observe *Col2a1* and *Acan* gene expression in $SIRT1^{ROSA}$ murine joints increased compared to control mice. The increased inflammatory and protease gene expression in the knee joint may cause the chondrocytes to increase type 2 collagen and aggrecan synthesis to maintain ECM turnover. At this stage, I wanted to validate if the increase in inflammatory gene expression in $SIRT1^{ROSA}$ murine knee joints correlated with increased synovitis post injury. Indeed, $SIRT1^{ROSA}$ murine knee joints displayed increased synovial hyperplasia alongside increased numbers of infiltrating cells compared to $SIRT1^{Agg}$ mice and $SIRT1^{fl/fl}$ mice. The exacerbated synovitis in $SIRT1^{ROSA}$ mice post injury is in line with previous studies which reported SIRT1 KO mice to display systemic lupus erythmatosus-like

symptoms (Sequeira *et al.* 2008), hyper-activated T cell proliferation (Kwon *et al.* 2008) and increased macrophage numbers (Schug *et al.* 2010). Although, systemic SIRT1 deletion led to increased synovitis post injury, cartilage specific SIRT1 deletion did not show any difference in synovitis compared to control mice even after injury. This was surprising to observe and could be explained due to the fact at 24 hours post injury the $SIRT1^{Agg}$ murine joints displayed decreased levels of inflammatory cytokines which could lead to reduced levels of inflammatory signalling to attract infiltrating cells to the site of injury. At this stage it was evident that SIRT1 had a tissue specific role in cartilage and a protective role against synovitis in the knee joint. The question still remained to investigate if the exacerbated inflammation in the knee joints of the $SIRT1^{ROSA}$ mice or the lack of inflammation in the joints of $SIRT1^{Agg}$ would impact long term OA disease.

Surprisingly, long term disease was reduced in $SIRT1^{ROSA}$ mouse joints 8 weeks post injury and increased in $SIRT1^{Agg}$ mice. The impact of increased early inflammation did not make a difference in long term disease. It would be interesting to measure inflammatory cytokine and protease expression alongside synovitis at a long term time point. These experiments would elucidate if exacerbated inflammation was persistent at a longer disease point in $SIRT1^{ROSA}$ murine knee joints and if it had an impact on cartilage degradation. In addition, it was interesting to note increased *Col2a1* and *Acan* gene expression early on in $SIRT1^{ROSA}$ murine knee joints and these markers in the future should be measured at a long term DMM timepoint. In speculation, low grade chronic inflammation may be promoting increased type 2 collagen and aggrecan production or repair which then would inhibit cartilage loss. The innate immune response has been shown to activate inflammation resulting in repair in lung injury models (Tolle and Standiford 2013). It would also be interesting to check for fibrosis in

the murine knee joints which may result in the stabilisation of the knee joint leading to reduced mechanical loading and decreased cartilage loss. Another future experiment could be conducting bone marrow chimeras between $SIRT1^{ROSA}$ and $SIRT1^{fl/fl}$ mice. This will investigate if the 'hyperactive' immune cells derived from bone marrow $SIRT1^{ROSA}$ mice, will cause $SIRT1^{fl/fl}$ mice to display early increased joint inflammation and proceed to be protective at a later time point compared to control mice. The loss of cartilage in $SIRT1^{Agg}$ mice post DMM at a long time point correlated with my earlier findings. Matsuzaki and colleagues (2013) reported increased cartilage damage using a SIRT1 cKO (COL2A1 $CreER^{T2}$) only at 2 and 4 weeks post DMM and not at 8 weeks post DMM.

In summary, in this chapter I showed SIRT1 has both anti-inflammatory effects globally as well as pro-anabolic effects in cartilage. Increased chronic inflammation protected against long term OA. Moreover, I have highlighted the relative importance of the anti-inflammatory effect of SIRT1 post injury and the 'positive' role of chronic inflammation on disease progression.

7. Final Discussion

7.0 Final Discussion

The class three histone deacetylase SIRT1 was originally showen to increase lifespan in lower organisms (Nakagawa and Guarente 2011b). Later studies demonstrated SIRT1 to control multiple age-related pathways including inflammation, cellular apoptosis and cellular metabolism (Sacitharan et al. 2012). SIRT1 has been shown to decrease with age in multiple tissues (Gong et al. 2014). The decline has been reported to initiate or be involved in several age-related disorders such as cardiovascular disease, Alzheimer's disease and diabetes (Guarente 2011). The most common form of arthritis is OA and its primary risk factor is age (Glyn-Jones et al. 2015). The maintenance of the ECM by chondrocytes is lost over time resulting in cartilage loss and OA (Glyn-Jones et al. 2015). However, ageing mechanisms in chondrocytes are poorly understood. In this thesis I investigated the role of SIRT1 in cartilage homeostasis and OA.

I revealed that aged and OA HACs have reduced SIRT1 protein expression compared to young HACs. Further studies using pharmacological activation or inhibition of SIRT1 and SIRT1 siRNA showed key cartilage and chondrocyte markers (COL2A1, ACAN and SOX-9) were altered *in vitro*. Hence the loss of SIRT1 during ageing and OA may possibly dysregulates chondrocyte biology and leads to OA. Previous studies have shown SIRT1 to decrease in OA samples and SIRT1 siRNA treatment in chondrocytes decreased the gene expression of *COL2A1 and ACAN* (Dvir-Ginzberg et al. 2008). My studies have used pharmacological agents which are more specific to SIRT1 than traditional first generation drugs, such as resveratrol (Hubbard and Sinclair 2014). SRT1720 and next generation SIRT1 activating compounds have been shown to have promising beneficial effects in clinical trials in diseases such as diabetes (Morris 2013).

However, the efficacy and long term usage of histone deacetylation activators is unknown. The use of SRT1720 and other activating drugs still requires further testing in OA disease models and human trials. At this stage of my doctoral studies the *in vivo* role of SIRT1 using reliable SIRT1 cKO was still not known.

Therefore, I went on to successfully generate and validate two SIRT1 cKO mouse lines. Initial studies showed the SIRT1^{Agg} mice displayed increased cartilage degradation at 2, 6 and 12 months of age compared to control mice. A previous study showed SIRT1 cartilage-specific KO mice using the COL2A1 CREER^{T2} displayed increased cartilage loss at 12 months (Matsuzaki et al. 2013). However, the disease scores reported were very low compared to my findings in aged SIRT1^{Agg} mice and could be due to the inefficient function of the COL2A1 CREER^{T2} in adult articular cartilage (Nakamura et al. 2006). My studies also revealed COL2A1, ACAN and SOX-9 expression decreased in articular cartilage from SIRT1^{Agg} mice compared to control mice. These results alluded to the importance of SIRT1 in chondrocytes to maintain cartilage homoeostasis. It would have been interesting to further age the mice up to 18-24 months, which may be more representative of old age in humans (Dutta and Sengupta 2016). I would expect SIRT1^{Agg} mice to develop increased OA compared to control mice at these later time points. In addition, it would have been interesting to measure bone parameters such as density, volume and osteophyte formation in the SIRT1 cKO mice lines during the ageing process. The interaction of the cartilage and bone has been reported to be critical in providing stability to the joint (Yuan et al. 2014). Dissecting the biological cross-talk between the bone and cartilage tissue with premature loss of SIRT1 and an ageing phenotype would reveal the interesting adaptations of bone tissue to cartilage loss over time. At this point of my doctoral studies, my data pointed towards a critical role of SIRT1 in chondrocyte homoeostasis and a

protective role in OA. I went on to examine a precise mechanism of action of SIRT1 in regulating cartilage homoeostasis. Autophagy is another well-established ageing mechanism that has been shown to be regulated by SIRT1 (Lee et al. 2008; Rubinsztein et al. 2011). Hence, at first I examined the role of autophagy in aged and diseased cartilage, and its putative link with SIRT1. My data showed that both SIRT1 and autophagy were dysregulated in human chondrocytes of ageing and OA cartilage which is supported by other studies performed on similar samples (Caramés et al. 2010; Fujita et al. 2011). ATG5 cKO (COL2A1 Cre) mice also showed increased OA disease scores compared to control mice post DMM (Bouderlique et al. 2015). However, the exact mechanism of how chondrocyte autophagy is controlled remains unclear.

My data revealed that the loss of SIRT1 *in vitro* decreased autophagy markers, and in mature articular cartilage *in vivo* led to accelerated OA. The regulation of autophagy by SIRT1 has been shown in other cell types such as MEFs and HEK293 cells (Lee et al. 2008; Salminen and Kaarniranta 2009b). However, my work has identified a direct interaction between SIRT1 and autophagy-related proteins in chondrocytes, where functional modifications and changes in autophagic flux are dependent upon SIRT1 expression and acetylation status of crucial autophagy proteins. Interestingly, I found SIRT1 not to bind and have a functional effect on ULK1. In speculation, SIRT1 could have post-translational control over downstream autophagy proteins such as ATG5, ATG7 and LC3; whereas ULK1 is directly controlled by mTOR. The exact targets in the control of the autophagy pathway by SIRT1 which I found may have the same role in other cell types too. This may impact on other age-related disorders such as Alzheimer's disease which are characterized by defective autophagy (Rubinsztein et al. 2011). Other proteins in the autophagy pathway need to be investigated also to validate if

they are targets of SIRT1. It would also be of interest to examine and validate the direct lysine or other deacetylation targets of SIRT1 on these autophagy proteins. Experiments using mass spectrometry can reveal specific SIRT1 deacetylation targets which could selectively modulate autophagy in different disease settings for beneficial therapeutic outcomes.

More importantly, I showed pharmacological activation of autophagy was protective against early OA development, but not in the absence of SIRT1. Studies using rapamycin have shown to have beneficial effects in experimental OA models (Carames et al. 2012). However, the safety of rapamycin and its analogues are of concern (Li et al. 2014). Spermidine is a naturally occurring compound found in peas, wholegrain and cheese (Minois et al. 2011). Polyamine derivatives such as spermidine, decrease during ageing (Minois et al. 2011) and supplementation of spermidine has been shown to increase lifespan in lower organisms (Eisenberg et al. 2009). Hence, spermidine may be a cost-effective and safe option to increase autophagy in the elderly or patients with age-related diseases such as OA. It has been shown Spermidine induces autophagy by virtue of its capacity to inhibit EP300 (histone acetyltransferase) a repressor of autophagy proteins ATG5, ATG7, ATG12 and LC3 (Eisenberg et al. 2009). Future experiments should look at the role of EP300 and SIRT1 in chondrocytes post spermidine treatment. However, the safety and efficacy of the use of polyamines in disease is not fully evaluated (Gerner and Meyskens 2004). Early clinical trials have shown polyamine modulation to be a promising target in cancer treatment (Gerner and Meyskens 2004); however, further clinical trials are required in multiple disease settings over longer periods of time.

It would be interesting to examine inflammatory marker expression in mice treated with spermidine to elucidate its effect on joint inflammation and OA. A microglia cell line pretreated with spermidine prior to LPS treatment significantly inhibited production of IL-6 and TNF-α suggesting the polyamine to have anti-inflammatory properties (Choi and Park 2012). In addition, decreased disease scores observed in spermidine treated mice could be explained through the activation of repair pathways in chondrocytes. Wang and Johnson (1992) showed that spermine, a polyamine which is structurally similar to spermidine, increased repair of stress-induced intestinal mucosal damage in rats. Thus, it would be interesting to investigate the downstream protective effect of activating autophagy via spermidine in cartilage.

The relationship between impaired autophagy caused by SIRT1 and endoplasmic reticulum (ER) stress may also play a role in SIRT1 deficient mice. The ER is arranged in a dynamic tubular network and protein maturation at the ER is vital for the correct folding of proteins (Hetz 2012). Several feedback mechanisms are in place to cope with impaired protein folding which causes ER stress and may lead to apoptosis (Hetz 2012). *In vitro* studies have shown increased ER stress markers in OA articular chondrocytes (Liu-Bryan and Terkeltaub 2015). Overexpression of ER stress proteins in chondrocyte cell lines led to accelerated chondrocyte hypertrophy as shown by increased expression of COL10 (Husa et al. 2013). Increased ER stress in cells activates autophagy to clear unwanted misfolded proteins (Hetz 2012). Hence, the loss of autophagy might cause an increase in ER stress leading to the production of COL10 or even lead to the apoptosis of chondrocytes. Overall, my data demonstrated that declining expression of SIRT1 with increasing age predisposes the cartilage to the development of OA by impairing autophagy. However, SIRT1 has been shown to have multiple effects on different

cellular pathways and these other effects may also be chondroprotective and should not be ruled out.

The final part of my thesis examined the role of SIRT1 in the regulation of joint inflammation. It is well established that SIRT1 downregulates NFκB signalling in cells, thus decreasing inflammatory signalling (Rothgiesser et al. 2010). Increased joint inflammation was observed post injury in $SIRT1^{ROSA}$ mice joints compared to $SIRT1^{Agg}$ mice indicating the tissue-specific role of SIRT1. Short-term injury studies showed SIRT1 had both anti-inflammatory effects globally as well as pro-anabolic effects in cartilage. Surprisingly, increased chronic joint inflammation in $SIRT1^{ROSA}$ mice protected against long term OA disease scores. As previously discussed above, further studies will need to be conducted to elucidate if chronic inflammation is promoting fibrosis and stiffness of the joint, to increase stabilisation and/or promoting cartilage repair. Future experiments should use other OA disease models such as the focal cartilage injury repair model or an aggressive OA injury (i.e. ACL transection) model to further validate the protective nature of the chronic inflammation in $SIRT1^{ROSA}$ mice. In addition, pain readouts in both SIRT1 cKO mice were not performed, which in future could validate the differences in cartilage degradation scores in the mice. In speculation, the stabilisation of the knee joint due to fibrosis and stiffness in $SIRT1^{ROSA}$ mice could lead to less mechanical forces though the joint and less pain in mice. Moreover, the regulation of pain signalling over age and its connection to SIRT1 and ageing mechanisms has not been established yet.

As mentioned previously bone marrow chimeras between the SIRT1 cKO mouse lines should elucidate the role of the immune system in the role of disease and answer if the hyperactive

inflammation in the SIRT1^{ROSA} mice is protective in SIRT1^{Agg} mice or WT mice. Importantly, future experiments should phenotype the type of cells infiltrating into the joint at an early timepoint and a late timepoint post injury. A hyperactive immune phenotype in SIRT1^{ROSA} mice may induce an increase in the infiltration of neutrophils, macrophages or mesenchymal stem cells which may be contributing to changes in the local environment to promote cartilage repair. Phenotyping cell types or tracing cells during the disease time course might also reveal which type of cell may remain in the joint and be providing the beneficial effect in the SIRT1^{ROSA} mice compared to the SIRT1^{Agg} mice. Addressing these questions may allow us to modulate the beneficial repair capacity of certain cell types either intrinsic or extrinsic to the joint to prevent cartilage loss post injury or during OA development.

It would be interesting to measure autophagy in cartilage from SIRT1^{ROSA} mice too. These measurements may show differences in chondrocyte autophagy when chronic low grade inflammation is upregulated. Inflammatory-related signalling molecules such as pathogen-associated molecular patterns and damage-associated molecular patterns have been shown to positively regulate autophagy through toll-like receptor signalling (Levine et al. 2011). In addition, an increase in inflammation may be increasing autophagy in other cells types of the joint. For example, the deletion of autophagy genes in specific lymphocyte cell types in mice has revealed a crucial role for autophagy proteins in the maintenance of normal numbers of T and B cells and hematopoietic stem cells (Levine et al. 2011). It would also be interesting to use other tissue- or cell-specific Cre lines to delete SIRT1 in cells such as macrophages, neutrophils, osteoblasts, osteoclasts, synovial fibroblasts and mesenchymal stem cells. These experiments may elucidate which cell type is providing the cartilage protective effect seen in the SIRT1^{ROSA} mice and validate the importance of autophagy in the ageing phenotype of

these specific cells. Although my thesis has concentrated on the role of SIRT1 in chondrocyte autophagy and joint inflammation other mechanisms could also be playing a role in the protective or defective phenotypes of the $SIRT1^{ROSA}$ or $SIRT1^{Agg}$ mice. For example, the regulation of cellular metabolism by SIRT1 is well established (Houtkooper et al. 2012). SIRT1 has been shown to directly deacetylate Peroxisome proliferator-activated receptor gamma coactivator-1α (PGC-1α) and increase cellular metabolism (Houtkooper et al. 2012). More studies are required to unravel the larger interconnecting pathways and interactions of SIRT1 in metabolism and the control of chondrocyte autophagy and inflammatory signalling.

In conclusion, in my thesis I have shown that SIRT1 declines with age and OA in human articular cartilage. The loss of SIRT1 impairs autophagy and dysregulates normal chondrocyte biology during ageing and experimental OA *in vivo*. Activation of autophagy by spermidine can prevent the development of OA in a SIRT1 dependent manner *in vivo*. My data has shown SIRT1 to have a global anti-inflammatory role and anabolic role in cartilage. The chronic low grade inflammation caused by systemic SIRT1 loss was protective in experimental OA and provides critical insight which challenges the paradigm of inflammation being deleterious in the disease. More importantly, my data suggests SIRT1 regulated chondrocyte autophagy and inflammatory pathways can be targeted to treat osteoarthritis.

8. Awards and Publications

The following awards and publications have been the result of my D.Phil work:

8.1 Publications

Sacitharan P.K, Zarebska J, Vincent TL and Edwards JR. Spermidine stimulates SIRT1-dependent autophagy to protect against osteoarthritis. Under review at ***Annals of the Rheumatic Diseases.***

Sacitharan P.K, and Vincent TL. Cellular Ageing Mechanisms in Osteoarthritis. ***Mammalian Genome.*** 2016; 27 (7); 421-429.

Driscoll C*, Chanalaris A*, Knights C, Ismail H, **Sacitharan P.K**, Gentry C, Bevan S, TL Vincent. Nociceptive sensitizers are regulated in damaged joint tissues, including the articular cartilage, when osteoarthritic mice display pain behavior. ***Arthritis & Rheumatology***. 2015; 12 (67).

Sacitharan P.K, Snelling SJB, Edwards JR. Aging mechanisms in arthritic disease. ***Discovery Medicine***. 2012;14 (78).

8.2 Awards

- European Institute of Innovation & Technology Transitional Fellowship
- American Society for Bone and Mineral Research New Investigator Award
- European Calcified Tissue Society New Investigator Award
- British Bone Research Society New Investigator Award
- Nature Reviews Rheumatology International Best Talk Award
- British Bone Research Society Best Oral Communication Award
- University of Oxford Medical Sciences Divisional 3 Minute Thesis Champion

9. References

Akiyama H, Kim J-E, Nakashima K, et al (2005) Osteo-chondroprogenitor cells are derived from Sox9 expressing precursors. Proc Natl Acad Sci U S A 102:14665–70. doi: 10.1073/pnas.0504750102

Alcendor RR, Gao S, Zhai P, et al (2007) Sirt1 regulates aging and resistance to oxidative stress in the heart. Circ Res 100:1512–1521. doi: 10.1161/01.RES.0000267723.65696.4a

Alvarez J, Balbin M, Fernandez M, Lopez JM (2001) Collagen metabolism is markedly altered in the hypertrophic cartilage of growth plates from rats with growth impairment secondary to chronic renal failure. J Bone Miner Res 16:511–524.

Amat R, Planavila A, Chen SL, et al (2009) SIRT1 controls the transcription of the peroxisome proliferator-activated receptor-?? co-activator-1??(PGC-1??) gene in skeletal muscle through the PGC-1?? autoregulatory loop and interaction with MyoD. J Biol Chem 284:21872–21880. doi: 10.1074/jbc.M109.022749

Ameye LG, Young MF (2006) Animal models of osteoarthritis: lessons learned while seeking the “Holy Grail”. Curr Opin Rheumatol 18:537–547. doi: 10.1097/01.bor.0000240369.39713.af

Amin AR (1999) Regulation of tumor necrosis factor-alpha and tumor necrosis factor converting enzyme in human osteoarthritis. Osteoarthr Cartil 7:392–394.

Amin AR, Abramson SB (1998) The role of nitric oxide in articular cartilage breakdown in osteoarthritis. Curr Opin Rheumatol 10:263–8. doi: 10.1097/00002281-199805000-00018

Appleton CTG, Pitelka V, Henry J, Beier F (2007) Global analyses of gene expression in early experimental osteoarthritis. Arthritis Rheum 56:1854–1868. doi: 10.1002/art.22711

Archer CW, Francis-West P (2003) The chondrocyte. Int J Biochem Cell Biol 35:401–404.

Arden NK, Lane NE, Parimi N, et al (2009) Defining incident radiographic hip osteoarthritis for epidemiologic studies in women. Arthritis Rheum 60:1052–1059. doi: 10.1002/art.24382

Autiero I, Costantini S, Colonna G (2009) Human Sirt-1: Molecular Modeling and Structure-Function Relationships of an Unordered Protein. PLoS One. doi: 10.1371/journal.pone.0007350

Banks AS, Kon N, Knight C, et al (2008) SirT1 Gain of Function Increases Energy Efficiency and Prevents Diabetes in Mice. Cell Metab 8:333–341. doi: 10.1016/j.cmet.2008.08.014

Bao J, Zheng L, Zhang Q, et al (2016) Deacetylation of TFEB promotes fibrillar Aβ degradation by upregulating lysosomal biogenesis in microglia. Protein Cell 7:417–433. doi: 10.1007/s13238-016-0269-2

Bar Oz M, Kumar A, Elayyan J, et al (2016) Acetylation reduces SOX9 nuclear entry and ACAN gene transactivation in human chondrocytes. Aging Cell 15:499–508. doi: 10.1111/acel.12456

Baroja-Mazo A, Revilla-Nuin B, Ramirez P, Pons JA (2016) Immunosuppressive potency of mechanistic target of rapamycin inhibitors in solid-organ transplantation. World J Transplant 6:183–192. doi: 10.5500/wjt.v6.i1.183

Beher D, Wu J, Cumine S, et al (2009) Resveratrol is not a direct activator of sirt1 enzyme activity. Chem Biol Drug Des 74:619–624. doi: 10.1111/j.1747-0285.2009.00901.x

Bell DM, Leung KK, Wheatley SC, et al (1997) SOX9 directly regulates the type-II collagen gene. Nat Genet 16:174–178. doi: 10.1038/ng0697-174

Bijlsma JWJ, Berenbaum F, Lafeber FPJG (2011) Osteoarthritis: an update with relevance for clinical practice. Lancet 377:2115–26. doi: 10.1016/S0140-6736(11)60243-2

Blaney Davidson EN, Vitters EL, van Beuningen HM, et al (2007) Resemblance of

osteophytes in experimental osteoarthritis to transforming growth factor beta-induced osteophytes: limited role of bone morphogenetic protein in early osteoarthritic osteophyte formation. Arthritis Rheum 56:4065–73. doi: 10.1002/art.23034

Blom AB, van Lent PLEM, Holthuysen AEM, et al (2004) Synovial lining macrophages mediate osteophyte formation during experimental osteoarthritis. Osteoarthr Cartil 12:627–635. doi: 10.1016/j.joca.2004.03.003

Bordone L, Cohen D, Robinson A, et al (2007) SIRT1 transgenic mice show phenotypes resembling calorie restriction. Aging Cell 6:759–767. doi: 10.1111/j.1474-9726.2007.00335.x

Bouderlique T, Vuppalapati KK, Newton PT, et al (2015) Targeted deletion of Atg5 in chondrocytes promotes age-related osteoarthritis. Ann Rheum Dis annrheumdis-2015-207742. doi: 10.1136/annrheumdis-2015-207742

Bouras T, Fu M, Sauve AA, et al (2005) SIRT1 deacetylation and repression of p300 involves lysine residues 1020/1024 within the cell cycle regulatory domain 1. J Biol Chem 280:10264–10276. doi: 10.1074/jbc.M408748200

Boya P, Reggiori F, Codogno P (2013) Emerging regulation and functions of autophagy. Nat Cell Biol 15:1017–1017. doi: 10.1038/ncb2815

Brandt KD, Dieppe P, Radin E (2009) Etiopathogenesis of Osteoarthritis. Med. Clin. North Am. 93:1–24.

Brook MS, Wilkinson DJ, Phillips BE, et al (2015) Skeletal muscle homeostasis and plasticity in youth and ageing: impact of nutrition and exercise. Acta Physiol n/a-n/a. doi: 10.1111/apha.12532

Brunet A, Sweeney LB, Sturgill JF, et al (2004) Stress-dependent regulation of FOXO transcription factors by the SIRT1 deacetylase. Science 303:2011–5. doi:

10.1126/science.1094637

Buckingham JC (2006) Glucocorticoids: exemplars of multi-tasking. Br J Pharmacol 147 Suppl:S258-68. doi: 10.1038/sj.bjp.0706456

Buckwalter JA, Mankin HJ (1998) Articular cartilage: tissue design and chondrocyte-matrix interactions. Instr Course Lect 47:477–486.

Burleigh A, Chanalaris A, Gardiner MD, et al (2012) Joint immobilization prevents murine osteoarthritis and reveals the highly mechanosensitive nature of protease expression in vivo. Arthritis Rheum 64:2278–88. doi: 10.1002/art.34420

Büttner S, Broeskamp F, Sommer C, et al (2014) Spermidine protects against α-synuclein neurotoxicity. Cell Cycle 13:3903–3908. doi: 10.4161/15384101.2014.973309

Calich ALG, Domiciano DS, Fuller R (2010) Osteoarthritis: Can anti-cytokine therapy play a role in treatment? Clin Rheumatol 29:451–455. doi: 10.1007/s10067-009-1352-3

Carames B, Hasegawa A, Taniguchi N, et al (2012) Autophagy activation by rapamycin reduces severity of experimental osteoarthritis. Ann Rheum Dis 71:575–581. doi: 10.1136/annrheumdis-2011-200557

Caramés B, Olmer M, Kiosses WB, Lotz MK (2015) The Relationship of Autophagy Defects to Cartilage Damage During Joint Aging in a Mouse Model. Arthritis Rheumatol 67:1568–1576. doi: 10.1002/art.39073

Caramés B, Taniguchi N, Otsuki S, et al (2010) Autophagy is a protective mechanism in normal cartilage, and its aging-related loss is linked with cell death and osteoarthritis. Arthritis Rheum 62:791–801. doi: 10.1002/art.27305

Carlsén S, Hansson AS, Olsson H, et al (1998) Cartilage oligomeric matrix protein (COMP)-induced arthritis in rats. Clin Exp Immunol 114:477–484. doi: 10.1046/j.1365-2249.1998.00739.x

Chakravarti S (2002) Functions of lumican and fibromodulin: Lessons from knockout mice. Glycoconj. J. 19:287–293.

Chen D, Bruno J, Easlon E, et al (2008) Tissue-specific regulation of SIRT1 by calorie restriction. Genes Dev 22:1753–1757. doi: 10.1101/gad.1650608

Chen D, Steele AD, Lindquist S, Guarente L (2005) Increase in activity during calorie restriction requires Sirt1. Science 310:1641. doi: 10.1126/science.1118357

Chen FH, Rousche KT, Tuan RS (2006) Technology Insight: adult stem cells in cartilage regeneration and tissue engineering. Nat Clin Pract Rheumatol 2:373–382. doi: 10.1038/ncprheum0216

Chen M, Lichtler AC, Sheu T-J, et al (2007) Generation of a Transgenic Mouse Model With Chondrocyte-Specific and Tamoxifen-Inducible Expression of Cre Recombinase. Genesis 45:44–50. doi: 10.1002/dvg

Cheng DS, Visco CJ (2012) Pharmaceutical therapy for osteoarthritis. PM R 4:S82-8. doi: 10.1016/j.pmrj.2012.02.009

Chevalier X, Eymard F, Richette P (2013) Biologic agents in osteoarthritis: hopes and disappointments. Nat Rev Rheumatol 9:400–410. doi: 10.1038/nrrheum.2013.44

Chia SL, Sawaji Y, Burleigh A, et al (2009) Fibroblast growth factor 2 is an intrinsic chondroprotective agent that suppresses ADAMTS-5 and delays cartilage degradation in murine osteoarthritis. Arthritis Rheum 60:2019–2027. doi: 10.1002/art.24654

Choi AMK, Ryter SW, Levine B (2013) Autophagy in human health and disease. N Engl J Med 368:651–62. doi: 10.1056/NEJMra1205406

Choi YH, Park HY (2012) Anti-inflammatory effects of spermidine in lipopolysaccharide-stimulated BV2 microglial cells. J Biomed Sci 19:31. doi: 10.1186/1423-0127-19-31

Chrisam M, Pirozzi M, Castagnaro S, et al (2015) Reactivation of autophagy by spermidine

ameliorates the myopathic defects of collagen VI-null mice. Autophagy 11:2142–2152. doi: 10.1080/15548627.2015.1108508

Christensen R, Bartels EM, Astrup A, Bliddal H (2007) Effect of weight reduction in obese patients diagnosed with knee osteoarthritis: a systematic review and meta-analysis. Ann Rheum Dis 66:433–439. doi: 10.1136/ard.2006.065904

Cicuttini FM, Wluka AE (2014) Osteoarthritis: Is OA a mechanical or systemic disease? Nat Rev Rheumatol 10:1–2. doi: 10.1038/nrrheum.2014.114

Cirillo DJ, Wallace RB, Wu L, Yood RA (2006) Effect of hormone therapy on risk of hip and knee joint replacement in the women's health initiative. Arthritis Rheum 54:3194–3204. doi: 10.1002/art.22138

Clements KM, Price JS, Chambers MG, et al (2003) Gene Deletion of Either Interleukin-1??, Interleukin-1?? -Converting Enzyme, Inducible Nitric Oxide Synthase, or Stromelysin 1 Accelerates the Development of Knee Osteoarthritis in Mice after Surgical Transection of the Medial Collateral Ligament and Part. Arthritis Rheum 48:3452–3463. doi: 10.1002/art.11355

Cohen DE, Supinski AM, Bonkowski MS, et al (2009) Neuronal SIRT1 regulates endocrine and behavioral responses to calorie restriction. Genes Dev 23:2812–2817. doi: 10.1101/gad.1839209

Coussens M, Maresh JG, Yanagimachi R, et al (2008) Sirt1 deficiency attenuates spermatogenesis and germ cell function. PLoS One. doi: 10.1371/journal.pone.0001571

Daans M, Luyten FP, Lories RJU (2011) GDF5 deficiency in mice is associated with instability-driven joint damage, gait and subchondral bone changes. Ann Rheum Dis 70:208–213. doi: 10.1136/ard.2010.134619

Dagenais S, Garbedian S, Wai EK (2009) Systematic review of the prevalence of radiographic

primary hip Osteoarthritis. In: Clinical Orthopaedics and Related Research. pp 623–637

Dang H, Le W (2012) The Relation between Resveratrol , Sirt1 , mTOR and Autophagy.

De Crombrugghe B, Lefebvre V, Behringer RR, et al (2000) Transcriptional mechanisms of chondrocyte differentiation. Matrix Biol. 19:389–394.

DeLise AM, Fischer L, Tuan RS (2000) Cellular interactions and signaling in cartilage development. Osteoarthr Cartil 8:309–334. doi: 10.1053/joca.1999.0306

Denechaud PD, Bossard P, Lobaccaro JMA, et al (2008) ChREBP, but not LXRs, is required for the induction of glucose-regulated genes in mouse liver. J Clin Invest 118:956–964. doi: 10.1172/JCI34314

Deng H, Mi M (2016) Resveratrol Attenuates Aβ25–35 Caused Neurotoxicity by Inducing Autophagy Through the TyrRS-PARP1-SIRT1 Signaling Pathway. Neurochem Res 41:2367–2379. doi: 10.1007/s11064-016-1950-9

Deretic V, Saitoh T, Akira S (2013) Autophagy in infection, inflammation and immunity. Nat Rev Immunol 13:722–737. doi: 10.1038/nri3532

Donmez G, Wang D, Cohen DE, Guarente L (2010) SIRT1 suppresses beta-amyloid production by activating the alpha-secretase gene ADAM10. Cell 142:320–32. doi: 10.1016/j.cell.2010.06.020

Drissi H, Zuscik M, Rosier R, O'Keefe R (2005) Transcriptional regulation of chondrocyte maturation: Potential involvement of transcription factors in OA pathogenesis. Mol. Aspects Med. 26:169–179.

Dutta S, Sengupta P (2016) Men and mice: Relating their ages. Life Sci 152:244–248. doi: 10.1016/j.lfs.2015.10.025

Dvir-Ginzberg M, Gagarina V, Lee E-J, Hall DJ (2008) Regulation of cartilage-specific gene expression in human chondrocytes by SirT1 and nicotinamide

phosphoribosyltransferase. J Biol Chem 283:36300–10. doi: 10.1074/jbc.M803196200

Eades G, Yang M, Yao Y, et al (2011) miR-200a regulates Nrf2 activation by targeting Keap1 mRNA in breast cancer cells. J Biol Chem 286:40725–40733. doi: 10.1074/jbc.M111.275495

Eisenberg T, Knauer H, Schauer A, et al (2009) Induction of autophagy by spermidine promotes longevity. Nat Cell Biol 11:1305–14. doi: 10.1038/ncb1975

Ekenstedt KJ, Sonntag WE, Loeser RF, et al (2006) Effects of chronic growth hormone and insulin-like growth factor 1 deficiency on osteoarthritis severity in rat knee joints. Arthritis Rheum 54:3850–8. doi: 10.1002/art.22254

El Marjou F, Janssen KP, Chang BHJ, et al (2004) Tissue-specific and inducible Cre-mediated recombination in the gut epithelium. Genesis 39:186–193. doi: 10.1002/gene.20042

Englund M, Guermazi A, Gale D, et al (2008) Incidental meniscal findings on knee MRI in middle-aged and elderly persons. N Engl J Med 359:1108–15. doi: 10.1056/NEJMoa0800777

Fang H, Beier F (2014) Mouse models of osteoarthritis: modelling risk factors and assessing outcomes. Nat Rev Rheumatol 10:413–21. doi: 10.1038/nrrheum.2014.46

Fang W, Wu P, Hu R, Huang Z (2003) Environmental Se-Mo-B deficiency and its possible effects on crops and Keshan-beck disease (KBD) in the Chousang area, Yao County, Shaanxi Province, China. Environ Geochem Health 25:267–280. doi: 10.1023/A:1023271403310

Feil R, Wagner J, Metzger D, Chambon P (1997) Regulation of Cre recombinase activity by mutated estrogen receptor ligand-binding domains. Biochem Biophys Res Commun 237:752–7. doi: 10.1006/bbrc.1997.7124

Feil S, Valtcheva N, Feil R (2009a) Gene Knockout Protocols. 530:343–363. doi: 10.1007/978-

1-59745-471-1

Feil S, Valtcheva N, Feil R (2009b) Inducible cre mice. Methods Mol Biol 530:343–363. doi: 10.1007/978-1-59745-471-1_18

Feldmann M, Maini RN (2001) Anti-TNF alpha therapy of rheumatoid arthritis: what have we learned? Annu Rev Immunol 19:163–196. doi: 19/1/163 [pii]\r10.1146/annurev.immunol.19.1.163

Felson DT, Naimark a, Anderson J, et al (1987) The prevalence of knee osteoarthritis in the elderly. The Framingham Osteoarthritis Study. Arthritis Rheum 30:914–8. doi: 10.1002/art.1780300811

Felson DT, Zhang Y, Anthony JM, et al (1992) Weight loss reduces the risk for symptomatic knee osteoarthritis in women: The framingham study. Ann Intern Med 116:535–539. doi: 10.1059/0003-4819-116-7-535

Ferguson MA, Kinoshita T, Hart GW (2009) Essentials of Glycobiology. 2nd edition.

Ford J, Ahmed S, Allison S, et al (2008) JNK2-dependent regulation of SIRT1 protein stability. Cell Cycle 7:3091–3097. doi: 10.4161/cc.7.19.6799

Fortier L a, Mohammed HO, Lust G, Nixon a J (2002) Cell-Based Repair of Articular Cartilage. J Bone Jt Surg Br 84:276–88.

Frye R a (1999) Characterization of five human cDNAs with homology to the yeast SIR2 gene: Sir2-like proteins (sirtuins) metabolize NAD and may have protein ADP-ribosyltransferase activity. Biochem Biophys Res Commun 260:273–9. doi: 10.1006/bbrc.1999.0897

Fujimaki R, Hayashi K, Watanabe N, et al (2005) Expression of Cre recombinase in the mouse developing chondrocytes driven by the mouse ??2(XI) collagen promoter. J Bone Miner Metab 23:270–273. doi: 10.1007/s00774-004-0595-y

Fujita N, Matsushita T, Ishida K, et al (2011) Potential involvement of SIRT1 in the pathogenesis of osteoarthritis through the modulation of chondrocyte gene expressions. J Orthop Res 29:511–5. doi: 10.1002/jor.21284

Fukai A, Kamekura S, Chikazu D, et al (2012) Lack of a chondroprotective effect of cyclooxygenase 2 inhibition in a surgically induced model of osteoarthritis in mice. Arthritis Rheum 64:198–203. doi: 10.1002/art.33324

Fukumoto T, Sperling JW, Sanyal a, et al (2003) Combined effects of insulin-like growth factor-1 and transforming growth factor-beta1 on periosteal mesenchymal cells during chondrogenesis in vitro. Osteoarthritis Cartilage 11:55–64. doi: 10.1053/joca.2002.0869

Funk JA, Odejinmi S, Schnellmann RG (2010) SRT1720 induces mitochondrial biogenesis and rescues mitochondrial function after oxidant injury in renal proximal tubule cells. J Pharmacol Exp Ther 333:593–601. doi: 10.1124/jpet.109.161992

Gabay O, Oppenheimer H, Meir H, et al (2012a) Increased apoptotic chondrocytes in articular cartilage from adult heterozygous SirT1 mice. 1:613–616. doi: 10.1136/annrheumdis-2011-200504

Gabay O, Oppenhiemer H, Meir H, et al (2012b) NIH Public Access. 71:613–616. doi: 10.1136/ard.2011.200504.Increased

Gabay O, Sanchez C, Dvir-Ginzberg M, et al (2013) Sirtuin 1 enzymatic activity is required for cartilage homeostasis in vivo in a mouse model. Arthritis Rheum 65:159–66. doi: 10.1002/art.37750

Gagarina V, Gabay O, Dvir-Ginzberg M, et al (2010) SirT1 enhances survival of human osteoarthritic chondrocytes by repressing protein tyrosine phosphatase 1B and activating the insulin-like growth factor receptor pathway. Arthritis Rheum 62:1383–

92. doi: 10.1002/art.27369

Gao J, Wang W-Y, Mao Y-W, et al (2010) A novel pathway regulates memory and plasticity via SIRT1 and miR-134. Nature 466:1105–9. doi: 10.1038/nature09271

García-Prat L, Martínez-Vicente M, Perdiguero E, et al (2016) Autophagy maintains stemness by preventing senescence. Nature 529:37–42. doi: 10.1038/nature16187

Gendron C, Kashiwagi M, Hughes C, et al (2003) TIMP-3 inhibits aggrecanase-mediated glycosaminoglycan release from cartilage explants stimulated by catabolic factors. FEBS Lett 555:431–436. doi: 10.1016/S0014-5793(03)01295-X

Gerner EW, Meyskens FL (2004) Polyamines and cancer: old molecules, new understanding. Nat Rev Cancer 4:781–792. doi: 10.1038/nrc1454

Giblin W, Skinner ME, Lombard DB (2014) Sirtuins: guardians of mammalian healthspan. Trends Genet 30:271–286. doi: 10.1016/j.tig.2014.04.007

Glasson SS (2007) In vivo osteoarthritis target validation utilizing genetically-modified mice. Curr Drug Targets 8:367–376. doi: 10.2174/138945007779940061

Glasson SS, Askew R, Sheppard B, et al (2004) Characterization of and osteoarthritis susceptibility in ADAMTS-4-knockout mice. Arthritis Rheum 50:2547–2558. doi: 10.1002/art.20558

Glasson SS, Blanchet TJ, Morris E a (2007) The surgical destabilization of the medial meniscus (DMM) model of osteoarthritis in the 129/SvEv mouse. Osteoarthritis Cartilage 15:1061–9. doi: 10.1016/j.joca.2007.03.006

Glick D, Barth S, Macleod KF (2010) Autophagy: cellular and molecular mechanisms. J Pathol 221:3–12. doi: 10.1002/path.2697

Glyn-Jones S, Palmer AJR, Agricola R, et al (2015) Osteoarthritis. Lancet 386:376–387. doi: 10.1016/S0140-6736(14)60802-3

Goldring MB (2012) Chondrogenesis, chondrocyte differentiation, and articular cartilage metabolism in health and osteoarthritis. Ther Adv Musculoskelet Dis 4:269–85. doi: 10.1177/1759720X12448454

Goldring MB, Otero M (2011) Inflammation in osteoarthritis. Curr Opin Rheumatol 23:471–8. doi: 10.1097/BOR.0b013e328349c2b1

Gong H, Pang J, Han Y, et al (2014) Age-dependent tissue expression patterns of Sirt1 in senescence-accelerated mice. Mol Med Rep 10:3296–3302. doi: 10.3892/mmr.2014.2648

Goodrich LR, Hidaka C, Robbins PD, et al (2007) Genetic modification of chondrocytes with insulin-like growth factor-1 enhances cartilage healing in an equine model. J Bone Jt Surg - Br Vol 89–B:672–685. doi: 10.1302/0301-620X.89B5.18343

Guarente L (2011) Sirtuins, Aging, and Medicine. 2235–2244.

Gudbergsen H, Lohmander LS, Jones G, et al (2013) Correlations between radiographic assessments and MRI features of knee osteoarthritis - a cross-sectional study. Osteoarthr Cartil 21:535–543. doi: 10.1016/j.joca.2012.12.010

Guo X, Williams JG, Schug TT, Li X (2010) DYRK1A and DYRK3 promote cell survival through phosphorylation and activation of SIRT1. J Biol Chem 285:13223–13232. doi: 10.1074/jbc.M110.102574

Hajji N, Wallenborg K, Vlachos P, et al (2010) Opposing effects of hMOF and SIRT1 on H4K16 acetylation and the sensitivity to the topoisomerase II inhibitor etoposide. Oncogene 29:2192–2204. doi: 10.1038/onc.2009.505

Hall BK, Miyake T (1992) The membranous skeleton: the role of cell condensations in vertebrate skeletogenesis. Anat. Embryol. (Berl). 186:107–124.

Hamilton DL, Abremski K (1984) Site-specific recombination by the bacteriophage P1 lox-Cre

system. Cre-mediated synapsis of two lox sites. J Mol Biol 178:481–486. doi: 10.1016/0022-2836(84)90154-2

Han L, Zhou R, Niu J, et al (2010) SIRT1 is regulated by a PPAR??-SIRT1 negative feedback loop associated with senescence. Nucleic Acids Res 38:7458–7471. doi: 10.1093/nar/gkq609

Hansen TE, Johansen T (2011) Following autophagy step by step. BMC Biol 9:39. doi: 10.1186/1741-7007-9-39

He W, Wang Y, Zhang MZ, et al (2010) Sirt1 activation protects the mouse renal medulla from oxidative injury. J Clin Invest 120:1056–1068. doi: 10.1172/JCI41563

Heinegard D, Inerot S, Olsson SE, Saxne T (1987) Cartilage proteoglycans in degenerative joint disease. J Rheumatol 14:110–112.

Heinegård D, Saxne T (2011) The role of the cartilage matrix in osteoarthritis. Nat Rev Rheumatol 7:50–6. doi: 10.1038/nrrheum.2010.198

Henry SP, Jang CW, Deng JM, et al (2009) Generation of aggrecan-CreERT2 knockin mice for inducible Cre activity in adult cartilage. Genesis 47:805–814. doi: 10.1002/dvg.20564

Herranz D, Muñoz-Martin M, Cañamero M, et al (2010) Sirt1 improves healthy ageing and protects from metabolic syndrome-associated cancer. Nat Commun 1:3. doi: 10.1038/ncomms1001

Hetz C (2012) The unfolded protein response: controlling cell fate decisions under ER stress and beyond. Nat Publ Gr 13:89–102. doi: 10.1038/nrm3270

Hiligsmann M, Cooper C, Guillemin F, et al (2014) A reference case for economic evaluations in osteoarthritis: An expert consensus article from the European Society for Clinical and Economic Aspects of Osteoporosis and Osteoarthritis (ESCEO). Semin. Arthritis Rheum. 44:271–282.

Hilton MJ, Tu X, Long F (2007) Tamoxifen-inducible gene deletion reveals a distinct cell type associated with trabecular bone, and direct regulation of PTHrP expression and chondrocyte morphology by Ihh in growth region cartilage. Dev Biol 308:93–105. doi: 10.1016/j.ydbio.2007.05.011

Hiramatsu K, Iwai T, Yoshikawa H, Tsumaki N (2011) Expression of dominant negative TGF-?? receptors inhibits cartilage formation in conditional transgenic mice. J Bone Miner Metab 29:493–500. doi: 10.1007/s00774-010-0248-2

Hochberg MC, Altman RD, April KT, et al (2012) American College of Rheumatology 2012 recommendations for the use of nonpharmacologic and pharmacologic therapies in osteoarthritis of the hand, hip, and knee. Arthritis Care Res 64:465–474. doi: 10.1002/acr.21596

Hofmann C, Gropp R, von der Mark K (1992) Expression of anchorin CII, a collagen-binding protein of the annexin family, in the developing chick embryo. Dev Biol 151:391–400. doi: 10.1016/0012-1606(92)90179-K

Houtkooper RH, Pirinen E, Auwerx J (2012) Sirtuins as regulators of metabolism and healthspan. Nat Rev Mol Cell Biol 13:225–38. doi: 10.1038/nrm3293

Hsu DC (2008) JANEWAY'S IMMUNOBIOLOGY, 7TH EDITION. Shock 29:770.

Huang J, Brumell JH (2014) Bacteria-autophagy interplay: a battle for survival. Nat Rev Microbiol 12:101–14. doi: 10.1038/nrmicro3160

Huang J, Gan Q, Han L, et al (2008) SIRT1 overexpression antagonizes cellular senescence with activated ERK/S6k1 signaling in human diploid fibroblasts. PLoS One 3:e1710. doi: 10.1371/journal.pone.0001710

Huang R, Xu Y, Wan W, et al (2015) Deacetylation of nuclear LC3 drives autophagy initiation under starvation. Mol Cell 57:456–467. doi: 10.1016/j.molcel.2014.12.013

Hubbard BP, Sinclair D a (2014) Small molecule SIRT1 activators for the treatment of aging and age-related diseases. Trends Pharmacol Sci 35:146–154. doi: 10.1016/j.tips.2013.12.004

Huffman DM, Grizzle WE, Bamman MM, et al (2007) SIRT1 is significantly elevated in mouse and human prostate cancer. Cancer Res 67:6612–6618. doi: 10.1158/0008-5472.CAN-07-0085

Hunter DJ (2011) Pharmacologic therapy for osteoarthritis--the era of disease modification. Nat Rev Rheumatol 7:13–22. doi: 10.1038/nrrheum.2010.178

Hunter DJ, Demissie S, Cupples LA, et al (2004) A genome scan for joint-specific hand osteoarthritis susceptibility: The framingham study. Arthritis Rheum 50:2489–2496. doi: 10.1002/art.20445

Husa M, Petursson F, Lotz M, et al (2013) C/EBP homologous protein drives pro-catabolic responses in chondrocytes. Arthritis Res Ther 15:R218. doi: 10.1186/ar4415

Hwang J woong, Chung S, Sundar IK, et al (2010) Cigarette smoke-induced autophagy is regulated by SIRT1-PARP-1-dependent mechanism: Implication in pathogenesis of COPD. Arch Biochem Biophys 500:203–209. doi: 10.1016/j.abb.2010.05.013

Imai S, Armstrong CM, Kaeberlein M, Guarente L (2000a) Transcriptional silencing and longevity protein Sir2 is an NAD-dependent histone deacetylase. Nature 403:795–800. doi: 10.1038/35001622

Imai S, Armstrong CM, Kaeberlein M, Guarente L (2000b) Transcriptional silencing and longevity protein Sir2 is an NAD-dependent histone deacetylase. Nature 403:795–800. doi: 10.1038/35001622

Imai S, Yoshino J (2013) The importance of NAMPT/NAD/SIRT1 in the systemic regulation of metabolism and ageing. Diabetes, Obes. Metab. 15:26–33.

Jaeger P a, Wyss-Coray T (2009) All-you-can-eat: autophagy in neurodegeneration and neuroprotection. Mol Neurodegener 4:16. doi: 10.1186/1750-1326-4-16

Järvinen T a, Jozsa L, Kannus P, et al (1999) Mechanical loading regulates tenascin-C expression in the osteotendinous junction. J Cell Sci 112 Pt 18:3157–3166.

Jazrawi LM, Alaia MJ, Chang G, et al (2011) Advances in magnetic resonance imaging of articular cartilage. J Am Acad Orthop Surg 19:420–429.

Jensen LK, Eenberg W (1996) Occupation as a risk factor for knee disorders. Scand. J. Work. Environ. Heal. 22:165–175.

Jeong H, Cohen DE, Cui L, et al (2012) Sirt1 mediates neuroprotection from mutant huntingtin by activation of the TORC1 and CREB transcriptional pathway. Nat Med 18:159–165. doi: 10.1038/nm.2559

Jiang W, Zhang X, Hao J, et al (2014) SIRT1 protects against apoptosis by promoting autophagy in degenerative human disc nucleus pulposus cells. Sci Rep 4:7456. doi: 10.1038/srep07456

Jin Q, Zhang F, Yan T, et al (2010) C/EBPalpha regulates SIRT1 expression during adipogenesis. Cell Res 20:470–479. doi: 10.1038/cr.2010.24

Jordan JM, Helmick CG, Renner JB, et al (2009) Prevalence of hip symptoms and radiographic and symptomatic hip osteoarthritis in African Americans and Caucasians: The Johnston County osteoarthritis project. J Rheumatol 36:809–815. doi: 10.3899/jrheum.080677

Jung HS, Lee MS (2010) Role of autophagy in diabetes and mitochondria. In: Annals of the New York Academy of Sciences. pp 79–83

Kaeberlein M, Mcvey M, Guarente L (1999) Saccharomyces cerevisiae by two different mechanisms promote longevity in Saccharomyces cerevisiae by two different

mechanisms. 2570–2580.

Kang H, Jung JW, Kim MK, Chung JH (2009) CK2 is the regulator of SIRT1 substrate-binding affinity, deacetylase activity and cellular response to DNA-damage. PLoS One. doi: 10.1371/journal.pone.0006611

Karlson EW, Mandl LA, Aweh GN, et al (2003) Total hip replacement due to osteoarthritis: The importance of age, obesity, and other modifiable risk factors. Am J Med 114:93–98. doi: 10.1016/S0002-9343(02)01447-X

Kashiwagi M, Tortorella M, Nagase H, Brew K (2001) TIMP-3 Is a Potent Inhibitor of Aggrecanase 1 (ADAM-TS4) and Aggrecanase 2 (ADAM-TS5). J Biol Chem 276:12501–12504. doi: 10.1074/jbc.C000848200

Katsuragi Y, Ichimura Y, Komatsu M (2015) P62/SQSTM1 functions as a signaling hub and an autophagy adaptor. FEBS J 282:4672–4678. doi: 10.1111/febs.13540

Keene DR, Jordan CD, Reinhardt DP, et al (1997) Fibrillin-1 in human cartilage: developmental expression and formation of special banded fibers. J Histochem Cytochem 45:1069–1082. doi: 10.1177/002215549704500805

Kellendonk C, Tronche F, Monaghan AP, et al (1996) Regulation of Cre recombinase activity by the synthetic steroid RU 486. Nucleic Acids Res 24:1404–1411. doi: 10.1093/nar/24.8.1404

Kellgren J, Lawrence J (1957) Radiological assessment of osteoarthritis. Ann Rheum Dis 16:494.

Kenific CM, Debnath J (2015) Cellular and metabolic functions for autophagy in cancer cells. Trends Cell Biol. 25:37–45.

Kim EJ, Kho JH, Kang MR, Um SJ (2007) Active Regulator of SIRT1 Cooperates with SIRT1 and Facilitates Suppression of p53 Activity. Mol Cell 28:277–290. doi:

10.1016/j.molcel.2007.08.030

Kim HJ, Braun HJ, Dragoo JL (2014) The effect of resveratrol on normal and osteoarthritic chondrocyte metabolism. Bone Joint Res 3:51–9. doi: 10.1302/2046-3758.33.2000226

Kim JE, Chen J, Lou Z (2008) DBC1 is a negative regulator of SIRT1. Nature 451:583–586. doi: 10.1038/nature06500

King LK, March L, Anandacoomarasamy A (2013) Obesity & osteoarthritis. Indian J. Med. Res. 138:185–193.

Knudson CB, Knudson W (2001) Cartilage proteoglycans. Semin Cell Dev Biol 12:69–78. doi: 10.1006/scdb.2000.0243

Knudson W, Aguiar DJ, Hua Q, Knudson CB (1996) CD44-anchored hyaluronan-rich pericellular matrices: an ultrastructural and biochemical analysis. Exp Cell Res 228:216–228. doi: 10.1006/excr.1996.0320

Kwon HS, Brent MM, Getachew R, et al (2008) Human Immunodeficiency Virus Type 1 Tat Protein Inhibits the SIRT1 Deacetylase and Induces T Cell Hyperactivation. Cell Host Microbe 3:158–167. doi: 10.1016/j.chom.2008.02.002

Lane NE, Gore LR, Cummings SR, et al (1999) Serum vitamin D levels and incident changes of radiographic hip osteoarthritis: a longitudinal study. Study of Osteoporotic Fractures Research Group. Arthritis Rheum 42:854–860. doi: 10.1002/1529-0131(199905)42:5<854::AID-ANR3>3.0.CO;2-I

Lee IH, Cao L, Mostoslavsky R, et al (2008) A role for the NAD-dependent deacetylase Sirt1 in the regulation of autophagy. Proc Natl Acad Sci U S A 105:3374–9. doi: 10.1073/pnas.0712145105

Levine B, Mizushima N, Virgin HW (2011) Autophagy in immunity and inflammation. Nature 469:323–35. doi: 10.1038/nature09782

Lewandoski M (2001) Conditional control of gene expression in the mouse. Nat Rev Genet 2:743–55. doi: 10.1038/35093537

Leyland KM, Hart DJ, Javaid MK, et al (2012) The natural history of radiographic knee osteoarthritis: A fourteen-year population-based cohort study. Arthritis Rheum 64:2243–2251. doi: 10.1002/art.34415

Li J, Kim SG, Blenis J (2014) Rapamycin: One Drug, Many Effects. Cell Metab 19:373–379. doi: 10.1016/j.cmet.2014.01.001

Li L, Gao P, Zhang H, et al (2011) SIRT1 inhibits angiotensin II-induced vascular smooth muscle cell hypertrophy. Acta Biochim Biophys Sin (Shanghai) 43:103–109. doi: 10.1093/abbs/gmq104

Li X, Zhang S, Blander G, et al (2007) SIRT1 Deacetylates and Positively Regulates the Nuclear Receptor LXR. Mol Cell 28:91–106. doi: 10.1016/j.molcel.2007.07.032

Little C, Smith M (2008) Animal Models of Osteoarthritis. Curr Rheumatol Rev 4:175–182. doi: 10.2174/157339708785133523

Little CB, Barai A, Burkhardt D, et al (2009) Matrix metalloproteinase 13-deficient mice are resistant to osteoarthritic cartilage erosion but not chondrocyte hypertrophy or osteophyte development. Arthritis Rheum 60:3723–3733. doi: 10.1002/art.25002

Little CB, Hunter DJ (2013) Post-traumatic osteoarthritis: from mouse models to clinical trials. Nat Rev Rheumatol 9:485–97. doi: 10.1038/nrrheum.2013.72

Liu-Bryan R, Terkeltaub R (2015) Emerging regulators of the inflammatory process in osteoarthritis. Nat Rev Rheumatol 11:35–44. doi: 10.1038/nrrheum.2014.162

Liu W, Hong Q, Bai XY, et al (2010) High-affinity Na+-dependent dicarboxylate cotransporter promotes cellular senescence by inhibiting SIRT1. Mech Ageing Dev 131:601–613. doi: 10.1016/j.mad.2010.08.006

Liu Y, Dentin R, Chen D, et al (2008) A fasting inducible switch modulates gluconeogenesis via activator/coactivator exchange. Nature 456:269–273. doi: 10.1038/nature07349

Lo Cascio L, Liu K, Nakamura H, et al (2014) Generation of a mouse line harboring a Bi-transgene expressing luciferase and tamoxifen-activatable creER(T2) recombinase in cartilage. Genesis 52:110–9. doi: 10.1002/dvg.22734

Loeser RF (2012a) NIH Public Access. 23:492–496. doi: 10.1097/BOR.0b013e3283494005.Aging

Loeser RF (2012b) Aging processes and the development of osteoarthritis. Curr Opin Rheumatol 25:1. doi: 10.1097/BOR.0b013e32835a9428

Loeser RF, Olex A, Mcnulty MA, et al (2013) Microarray analysis reveals age-related diferrences in gene expression during the development of osteoarthritis in mice. Arthritis Rheum 64:705–717. doi: 10.1002/art.33388.Microarray

Loeser RF, Shanker G, Carlson CS, et al (2000) Reduction in the chondrocyte response to insulin-like growth factor 1 in aging and osteoarthritis: Studies in a non-human primate model of naturally occurring disease. Arthritis Rheum 43:2110–2120. doi: 10.1002/1529-0131(200009)43:9<2110::AID-ANR23>3.0.CO;2-U

Logan M, Martin JF, Nagy A, et al (2002) Expression of Cre Recombinase in the developing mouse limb bud driven by a Prxl enhancer. Genesis 33:77–80. doi: 10.1002/gene.10092

Lotz M, Loeser RF (2012) Effects of aging on articular cartilage homeostasis. Bone 51:241–8. doi: 10.1016/j.bone.2012.03.023

Lotz MK, Caramés B (2011) Autophagy and cartilage homeostasis mechanisms in joint health, aging and OA. Nat Rev Rheumatol 7:579–87. doi: 10.1038/nrrheum.2011.109

Loughlin J (2001) Genetic epidemiology of primary osteoarthritis. Curr Opin Rheumatol 13:111–6. doi: 10.1097/00002281-200103000-00004

Loughlin J (2005) The genetic epidemiology of human primary osteoarthritis: current status. Expert Rev Mol Med 7:1–12. doi: 10.1017/S1462399405009257

Luo G, D'Souza R, Hogue D, Karsenty G (1995) The matrix Gla protein gene is a marker of the chondrogenesis cell lineage during mouse development. J Bone Miner Res 10:325–34. doi: 10.1002/jbmr.5650100221

Maroudas A, Bullough P (1968) Permeability of articular cartilage. Nature 219:1260–1261. doi: 10.1038/2191260a0

Massagué J (2012) TGFβ signalling in context. Nat Rev Mol Cell Biol 13:616–30. doi: 10.1038/nrm3434

Matsushita T, Sasaki H, Takayama K, et al (2013) The overexpression of SIRT1 inhibited osteoarthritic gene expression changes induced by interleukin-1β in human chondrocytes. J Orthop Res 31:531–7. doi: 10.1002/jor.22268

Matsuzaki T, Matsushita T, Takayama K, et al (2013) Disruption of Sirt1 in chondrocytes causes accelerated progression of osteoarthritis under mechanical stress and during ageing in mice. Ann Rheum Dis. doi: 10.1136/annrheumdis-2012-202620

McAlindon TE, Felson DT, Zhang Y, et al (1996a) Relation of dietary intake and serum levels of vitamin D to progression of osteoarthritis of the knee among participants in the Framingham Study. Ann Intern Med 125:353–359. doi: 10.7326/0003-4819-125-5-199609010-00001

McAlindon TE, Jacques P, Zhang Y, et al (1996b) Do antioxidant micronutrients protect against the development and progression of knee osteoarthritis? Arthritis Rheum 39:648–656. doi: 10.1002/art.1780390417

Mcburney MW, Yang X, Jardine K, et al (2003) The Mammalian SIR2 ␣ Protein Has a Role in Embryogenesis and Gametogenesis. 23:38–54. doi: 10.1128/MCB.23.1.38

McInnes IB, Schett G (2007) Cytokines in the pathogenesis of rheumatoid arthritis. Nat Rev Immunol 7:429–42. doi: 10.1038/nri2094

McMillan G, Nichols L (2005) Osteoarthritis and meniscus disorders of the knee as occupational diseases of miners. Occup Environ Med 62:567–75. doi: 10.1136/oem.2004.017137

Melchiorri C, Meliconi R, Frizziero L, et al (1998) Enhanced and coordinated in vivo expression of inflammatory cytokines and nitric oxide synthase by chondrocytes from patients with osteoarthritis. Arthritis Rheum 41:2165–2174. doi: 10.1002/1529-0131(199812)41:12<2165::AID-ART11>3.0.CO;2-O

Menghini R, Casagrande V, Cardellini M, et al (2009) MicroRNA 217 modulates endothelial cell senescence via silent information regulator 1. Circulation 120:1524–1532. doi: 10.1161/CIRCULATIONAHA.109.864629

Mercken EM, Hu J, Krzysik-Walker S, et al (2014) SIRT1 but not its increased expression is essential for lifespan extension in caloric-restricted mice. Aging Cell 13:193–196. doi: 10.1111/acel.12151

Messier SP, Loeser RF, Miller GD, et al (2004) Exercise and Dietary Weight Loss in Overweight and Obese Older Adults with Knee Osteoarthritis: The Arthritis, Diet, and Activity Promotion Trial. Arthritis Rheum 50:1501–1510. doi: 10.1002/art.20256

Michán S, Li Y, Chou MM-H, et al (2010) SIRT1 is essential for normal cognitive function and synaptic plasticity. J Neurosci 30:9695–707. doi: 10.1523/JNEUROSCI.0027-10.2010

Miller RL (2011) Transgenic mice: beyond the knockout. Am J Physiol Renal Physiol 300:F291–F300. doi: 10.1152/ajprenal.00082.2010

Milner JM, Rowan AD, Cawston TE, Young D a (2006) Metalloproteinase and inhibitor expression profiling of resorbing cartilage reveals pro-collagenase activation as a

critical step for collagenolysis. Arthritis Res Ther 8:R142. doi: 10.1186/ar2034

Min SW, Cho SH, Zhou Y, et al (2010) Acetylation of tau inhibits its degradation and contributes to tauopathy. Neuron 67:953–966. doi: 10.1016/j.neuron.2010.08.044

Minois N, Carmona-Gutierrez D, Madeo F (2011) Polyamines in aging and disease. Aging (Albany NY) 3:716–732. doi: 10.1016/S0044-8486(03)00351-X

Mintz G, Fraga A (1973) Severe Osteoarthritis of the Elbow in Foundry Workers. Arch Environ Heal An Int J 27:78–80. doi: 10.1080/00039896.1973.10666322

Mitchell SJ, Martin-Montalvo A, Mercken EM, et al (2014) The SIRT1 activator SRT1720 extends lifespan and improves health of mice fed a standard diet. Cell Rep 6:836–43. doi: 10.1016/j.celrep.2014.01.031

Miyamoto Y, Mabuchi A, Shi DQ, et al (2007) A functional polymorphism in the 5 â€™ UTR of GDF5 is associated with susceptibility to osteoarthritis. Nat Genet 39:529–533. doi: Doi 10.1038/Ng2005

Mizushima N (2007) Autophagy: Process and function. Genes Dev. 21:2861–2873.

Mizushima N, Levine B (2010) Autophagy in mammalian development and differentiation. Nat Cell Biol 12:823–830. doi: 10.1038/ncb0910-823

Mizushima N, Yoshimori T, Levine B (2010) Methods in mammalian autophagy research. Cell 140:313–26. doi: 10.1016/j.cell.2010.01.028

Moon M-H, Jeong J-K, Lee Y-J, et al (2013) SIRT1, a class III histone deacetylase, regulates TNF-α-induced inflammation in human chondrocytes. Osteoarthritis Cartilage 21:470–80. doi: 10.1016/j.joca.2012.11.017

Moos V, Fickert S, Müller B, et al (1999) Immunohistological analysis of cytokine expression in human osteoarthritic and healthy cartilage. J Rheumatol 26:870–879.

Morales TI (2008) The quantitative and functional relation between insulin-like growth

factor-I (IGF) and IGF-binding proteins during human osteoarthritis. J Orthop Res 26:465–74. doi: 10.1002/jor.20549

Moreno-Reyes R, Mathieu F, Boelaert M, et al (2003) Selenium and iodine supplementation of rural Tibetan children affected by Kashin-Beck osteoarthropathy. Am J Clin Nutr 78:137–144.

Morris BJ (2013) Seven sirtuins for seven deadly diseases of aging. Free Radic Biol Med 56:133–71. doi: 10.1016/j.freeradbiomed.2012.10.525

Morselli E, Maiuri MC, Markaki M, et al (2010) Caloric restriction and resveratrol promote longevity through the Sirtuin-1-dependent induction of autophagy. Cell Death Dis 1:e10. doi: 10.1038/cddis.2009.8

Morselli E, Mariño G, Bennetzen M V., et al (2011) Spermidine and resveratrol induce autophagy by distinct pathways converging on the acetylproteome. J Cell Biol 192:615–629. doi: 10.1083/jcb.201008167

Nagase H, Kashiwagi M (2003) Aggrecanases and cartilage matrix degradation. 5:94–103. doi: 10.1186/ar630

Nagase H, Visse R, Murphy G (2006) Structure and function of matrix metalloproteinases and TIMPs. Cardiovasc Res 69:562–573. doi: 10.1016/j.cardiores.2005.12.002

Nakagawa T, Guarente L (2011a) Sirtuins at a glance. J Cell Sci 124:833–8. doi: 10.1242/jcs.081067

Nakagawa T, Guarente L (2011b) Sirtuins at a glance. J. Cell Sci. 124:833–8.

Nakamura E, Nguyen MT, Mackem S (2006) Kinetics of tamoxifen-regulated Cre activity in mice using a cartilage-specific CreERT to assay temporal activity windows along the proximodistal limb skeleton. Dev Dyn 235:2603–2612. doi: 10.1002/dvdy.20892

Nasrin N, Kaushik VK, Fortier E, et al (2009) JNK1 phosphorylates SIRT1 and promotes its

enzymatic activity. PLoS One. doi: 10.1371/journal.pone.0008414

Nayagam VM, Wang X, Tan YC, et al (2006) SIRT1 modulating compounds from high-throughput screening as anti-inflammatory and insulin-sensitizing agents. J Biomol Screen Off J Soc Biomol Screen 11:959–967. doi: 10.1177/1087057106294710

Nelson F, Billinghurst RC, Pidoux RT, et al (2006) Early post-traumatic osteoarthritis-like changes in human articular cartilage following rupture of the anterior cruciate ligament. Osteoarthr Cartil 14:114–119. doi: 10.1016/j.joca.2005.08.005

Nemoto S, Fergusson MM, Finkel T (2004) Nutrient Availability Regulates SIRT1 Through a Forkhead-Dependent Pathway. Science (80-) 306:2105–2108. doi: 10.1126/science.1101731

Neogi T, Felson DT, Sarno R, Booth SL (2008) Vitamin K in hand osteoarthritis: results from a randomised clinical trial. Ann Rheum Dis 67:1570–1573. doi: 10.1136/ard.2008.094771

Neogi T, Zhang Y (2013) Epidemiology of Osteoarthritis. Rheum. Dis. Clin. North Am. 39:1–19.

Neuhold LA, Killar L, Zhao W, et al (2001) Postnatal expression in hyaline cartilage of constitutively active human collagenase-3 (MMP-13) induces osteoarthritis in mice. J Clin Invest 107:35–44. doi: 10.1172/JCI10564

Nevitt MC, Felson DT, Williams EN, Grady D (2001) The effect of estrogen plus progestin on knee symptoms and related disability in postmenopausal women: The Heart and Estrogen/Progestin Replacement Study, a randomized, double-blind, placebo-controlled trial.

Ng F, Tang BL (2013) Sirtuins' modulation of autophagy. J Cell Physiol 228:2262–70. doi: 10.1002/jcp.24399

Nishida T, Kubota S, Fukunaga T, et al (2003) CTGF/Hcs24, hypertrophic chondrocyte-

specific gene product, interacts with perlecan in regulating the proliferation and differentiation of chondrocytes. J Cell Physiol 196:265–75. doi: 10.1002/jcp.10277

Øiestad BE, Engebretsen L, Storheim K, Risberg MA (2009) Knee osteoarthritis after anterior cruciate ligament injury: a systematic review. Am J Sports Med 37:1434–43. doi: 10.1177/0363546509338827

Oldberg A, Antonsson P, Lindblom K, Heinegård D (1992) COMP (cartilage oligomeric matrix protein) is structurally related to the thrombospondins. J Biol Chem 267:22346–50.

Olin AI, Mörgelin M, Sasaki T, et al (2001) The proteoglycans aggrecan and versican form networks with fibulin-2 through their lectin domain binding. J Biol Chem 276:1253–1261. doi: 10.1074/jbc.M006783200

Oliveria S a, Felson DT, Reed JI, et al (1995) Incidence of symptomatic hand, hip, and knee osteoarthritis among patients in a health maintenance organization. Arthritis Rheum 38:1134–1141. doi: 10.1002/art.1780380817

Oppenheimer H, Gabay O, Meir H, et al (2012) 75-Kd Sirtuin 1 Blocks Tumor Necrosis Factor A-Mediated Apoptosis in Human Osteoarthritic Chondrocytes. Arthritis Rheum 64:718–28. doi: 10.1002/art.33407

Oppenheimer H, Kumar A, Meir H, et al (2014) Set7/9 impacts COL2A1 expression through binding and repression of SirT1 histone deacetylation. J Bone Miner Res 29:348–60. doi: 10.1002/jbmr.2052

Ota H, Eto M, Kano MR, et al (2008) Cilostazol inhibits oxidative stress-induced premature senescence via upregulation of Sirt1 in human endothelial cells. Arterioscler Thromb Vasc Biol 28:1634–1639. doi: 10.1161/ATVBAHA.108.164368

Owczarczyk AB, Schaller MA, Reed M, et al (2015) Sirtuin 1 Regulates Dendritic Cell Activation and Autophagy during Respiratory Syncytial Virus-Induced Immune

Responses. J Immunol 1500326. doi: 10.4049/jimmunol.1500326

Page-McCaw A, Ewald AJ, Werb Z (2007) Matrix metalloproteinases and the regulation of tissue remodelling. Nat Rev Mol Cell Biol 8:221–33. doi: 10.1038/nrm2125

Peach CA, Carr AJ, Loughlin J (2005) Recent advances in the genetic investigation of osteoarthritis. Trends Mol. Med. 11:186–191.

Pearle AD, Warren RF, Rodeo S a (2005) Basic science of articular cartilage and osteoarthritis. Clin Sports Med 24:1–12. doi: 10.1016/j.csm.2004.08.007

Pelletier JP, Caron JP, Evans C, et al (1997) In vivo suppression of early experimental osteoarthritis by interleukin-1 receptor antagonist using gene therapy. Arthritis Rheum 40:1012–1019. doi: 10.1002/1529-0131(199706)40:6<1012::AID-ART3>3.0.CO;2-#

Pettipher ER, Higgs G a, Henderson B (1986) Interleukin 1 induces leukocyte infiltration and cartilage proteoglycan degradation in the synovial joint. Proc Natl Acad Sci U S A 83:8749–8753. doi: 10.1073/pnas.83.22.8749

Pfander D, Heinz N, Rothe P, et al (2004) Tenascin and aggrecan expression by articular chondrocytes is influenced by interleukin 1beta: a possible explanation for the changes in matrix synthesis during osteoarthritis. Ann Rheum Dis 63:240–244. doi: 10.1136/ard.2002.003749

Popelka H, Klionsky DJ (2015) Post-translationally-modified structures in the autophagy machinery: An integrative perspective. FEBS J 282:3474–3488. doi: 10.1111/febs.13356

Pradhan AK, Kuila N, Singh S, Chakraborty S (2011) EVI1 up-regulates the stress responsive gene SIRT1 which triggers deacetylation and degradation of EVI1. Biochim Biophys Acta - Gene Regul Mech 1809:269–275. doi: 10.1016/j.bbagrm.2011.04.007

Pruitt K, Zinn RL, Ohm JE, et al (2006) Inhibition of SIRT1 reactivates silenced cancer genes without loss of promoter DNA hypermethylation. PLoS Genet 2:0344–0352. doi:

10.1371/journal.pgen.0020040

Puleston DJ, Zhang H, Powell TJ, et al (2014) Autophagy is a critical regulator of memory CD8(+) T cell formation. Elife 3:e03706. doi: 10.7554/eLife.03706

Purushotham A, Schug TT, Xu Q, et al (2009) Hepatocyte-Specific Deletion of SIRT1 Alters Fatty Acid Metabolism and Results in Hepatic Steatosis and Inflammation. Cell Metab 9:327–338. doi: 10.1016/j.cmet.2009.02.006

Qiu G, Li X, Che X, et al (2015) SIRT1 is a regulator of autophagy: Implications in gastric cancer progression and treatment. FEBS Lett. 589:2034–2042.

Rees J a, Ali SY, Brown R a (1987) Ultrastructural localisation of fibronectin in human osteoarthritic articular cartilage. Ann Rheum Dis 46:816–22. doi: 10.1136/ard.46.11.816

Reynard LN, Bui C, Canty-laird EG, et al (2011) Expression of the osteoarthritis-associated gene GDF5 is modulated epigenetically by DNA methylation. Hum Mol Genet 20:3450–3460. doi: 10.1093/hmg/ddr253

Reynard LN, Loughlin J (2012) Genetics and epigenetics of osteoarthritis. Maturitas 71:200–4. doi: 10.1016/j.maturitas.2011.12.001

Rock MJ, Cain SA, Freeman LJ, et al (2004) Molecular basis of elastic fiber formation: Critical interactions and a tropoelastin-fibrillin-1 cross-link. J Biol Chem 279:23748–23758. doi: 10.1074/jbc.M400212200

Rodgers JT, Lerin C, Haas W, et al (2005) Nutrient control of glucose homeostasis through a complex of PGC-1a and SIRT1. Nature 434:113–118. doi: 10.1038/nature03314.1.

Rogina B, Helfand SL (2004) Sir2 mediates longevity in the fly through a pathway related to calorie restriction. Proc Natl Acad Sci U S A 101:15998–6003. doi: 10.1073/pnas.0404184101

Rosenberg K, Olsson H, Mörgelin M, Heinegård D (1998) Cartilage oligomeric matrix protein shows high affinity zinc-dependent interaction with triple helical collagen. J Biol Chem 273:20397–20403. doi: 10.1074/jbc.273.32.20397

Rothgiesser KM, Erener S, Waibel S, et al (2010) SIRT2 regulates NF-κB dependent gene expression through deacetylation of p65 Lys310. J Cell Sci 123:4251–8. doi: 10.1242/jcs.073783

Rountree RB, Schoor M, Chen H, et al (2004) BMP receptor signaling is required for postnatal maintenance of articular cartilage. PLoS Biol. doi: 10.1371/journal.pbio.0020355

Rubinsztein DC, Mariño G, Kroemer G (2011) Autophagy and aging. Cell 146:682–95. doi: 10.1016/j.cell.2011.07.030

Ryan MC, Sandell LJ (1990) Differential expression of a cysteine-rich domain in the amino-terminal propeptide of type II (cartilage) procollagen by alternative splicing of mRNA. J Biol Chem 265:10334–10339.

Sacitharan PK, Snelling SJB, Edwards JR (2012) Aging mechanisms in arthritic disease. Discov Med 14:345–52.

Sah R., Chen A.C., Grodzinsky A. J., Trippel S. (1994) Differential Effect of bFGF and IGF-I on Matrix Metabolism in Calf and Adult Bovine Cartilage Explants. Arch. Biochem. Biophys. 308:137–147.

Sakai K, Hiripi L, Glumoff V, et al (2001) Stage-and tissue-specific expression of a Col2a1-Cre fusion gene in transgenic mice. Matrix Biol 19:761–767. doi: 10.1016/S0945-053X(00)00122-0

Saklatvala J (1981) Characterization of catabolin, the major product of pig synovial tissue that induces resorption of cartilage proteoglycan in vitro. Biochem J 199:705–714.

Saklatvala J (1986) Tumour necrosis factor alpha stimulates resorption and inhibits synthesis of proteoglycan in cartilage. Nature 322:547–549. doi: 10.1038/322547a0

Salminen A, Kaarniranta K (2009a) Regulation of the aging process by autophagy. Trends Mol Med 15:217–24. doi: 10.1016/j.molmed.2009.03.004

Salminen A, Kaarniranta K (2009b) SIRT1: regulation of longevity via autophagy. Cell Signal 21:1356–60. doi: 10.1016/j.cellsig.2009.02.014

Salmon WD, Daughaday WH (1957) A hormonally controlled serum factor which stimulates sulfate incorporation by cartilage in vitro. J Lab Clin Med 49:825–836. doi: 10.5555/uri:pii:0022214357900914

Sandell LJ, Morris N, Robbins JR, Goldring MB (1991) Alternatively spliced type II procollagen mRNAs define distinct populations of cells during vertebral development: Differential expression of the amino-propeptide. J Cell Biol 114:1307–1319. doi: 10.1083/jcb.114.6.1307

Sasaki T, Maier B, Bartke A, Scrable H (2006) Progressive loss of SIRT1 with cell cycle withdrawal. Aging Cell 5:413–422. doi: 10.1111/j.1474-9726.2006.00235.x

Sauer B, Henderson N (1989) Cre-stimulated recombination at loxP-containing DNA sequences placed into the mammalian genome. Nucleic Acids Res 17:147–161. doi: 10.1093/nar/17.1.147

Saunders LR, Sharma AD, Tawney J, et al (2010) miRNAs regulate SIRT1 expression during mouse embryonic stem cell differentiation and in adult mouse tissues. Aging (Albany NY) 2:415–431.

Scanzello CR, Goldring SR (2012) The role of synovitis in osteoarthritis pathogenesis. Bone 51:249–57. doi: 10.1016/j.bone.2012.02.012

Schug TT, Xu Q, Gao H, et al (2010) Myeloid deletion of SIRT1 induces inflammatory

signaling in response to environmental stress. Mol Cell Biol 30:4712–4721. doi: 10.1128/MCB.00657-10

Sequeira J, Boily G, Bazinet S, et al (2008) sirt1-null mice develop an autoimmune-like condition. Exp Cell Res 314:3069–3074. doi: 10.1016/j.yexcr.2008.07.011

Serra R, Johnson M, Filvaroff EH, et al (1997) Expression of a truncated, kinase-defective TGF-?? type II receptor in mouse skeletal tissue promotes terminal chondrocyte differentiation and osteoarthritis. J Cell Biol 139:541–552. doi: 10.1083/jcb.139.2.541

Settembre C, Di Malta C, Polito VA, et al (2011) TFEB links autophagy to lysosomal biogenesis. Science 332:1429–33. doi: 10.1126/science.1204592

Shane Anderson A, Loeser RF (2010) Why is osteoarthritis an age-related disease? Best Pract. Res. Clin. Rheumatol. 24:15–26.

Shen J, Li J, Wang B, et al (2013) Deletion of the transforming growth factor β receptor type II gene in articular chondrocytes leads to a progressive osteoarthritis-like phenotype in mice. Arthritis Rheum 65:3107–19. doi: 10.1002/art.38122

Shen J, Li S, Chen D (2014) TGF-β signaling and the development of osteoarthritis. Bone Res 2:14002. doi: 10.1038/boneres.2014.2

Shoulders MD, Raines RT (2010) Collagen Structure and Stability. Annu Rev Biochem 78:929–958. doi: 10.1146/annurev.biochem.77.032207.120833.COLLAGEN

Singh D, Srivastava SK, Chaudhuri TK, Upadhyay G (2015) Multifaceted role of matrix metalloproteinases (MMPs). Front Mol Biosci 2:19. doi: 10.3389/fmolb.2015.00019

Smith MD, Triantafillou S, Parker a, et al (1997) Synovial membrane inflammation and cytokine production in patients with early osteoarthritis. J. Rheumatol. 24:365–71.

Sock E, Pagon R a, Keymolen K, et al (2003) Loss of DNA-dependent dimerization of the transcription factor SOX9 as a cause for campomelic dysplasia. Hum Mol Genet

12:1439–1447. doi: 10.1093/hmg/ddg158

Song T, Yang L, Kabra N, et al (2013) The NAD+ synthesis enzyme nicotinamide mononucleotide adenylyltransferase (NMNAT1) regulates ribosomal RNA transcription. J Biol Chem 288:20908–20917. doi: 10.1074/jbc.M113.470302

Sophia Fox AJ, Bedi A, Rodeo SA (2009) The basic science of articular cartilage: structure, composition, and function. Sports Health 1:461–8. doi: 10.1177/1941738109350438

Spector TD, Cicuttini F, Baker J, et al (1996) Genetic influences on osteoarthritis in women: a twin study. BMJ 312:940–943. doi: 10.1136/bmj.312.7036.940

Srikanth VK, Fryer JL, Zhai G, et al (2005) A meta-analysis of sex differences prevalence, incidence and severity of osteoarthritis. Osteoarthr Cartil 13:769–781. doi: 10.1016/j.joca.2005.04.014

Stanton H, Melrose J, Little CB, Fosang AJ (2011) Proteoglycan degradation by the ADAMTS family of proteinases. Biochim. Biophys. Acta - Mol. Basis Dis. 1812:1616–1629.

Stefan L, Martin P, Stefan Lohmander OL, et al (2007) The Long-Term Consequence of ACL and Meniscus Injuries. Am J Sport Med 35:1756–69. doi: 10.1177/0363546507307396

Stockwell RA (1978) Chondrocytes. J Clin Pathol (Royal Coll Pathol 12:7–13.

Stockwell R a. (1991) Cartilage failure in osteoarthritis: Relevance of normal structure and function. A review. Clin Anat 4:161–191. doi: 10.1002/ca.980040303

Styrkarsdottir U, Thorleifsson G, Helgadottir HT, et al (2014) Severe osteoarthritis of the hand associates with common variants within the ALDH1A2 gene and with rare variants at 1p31. Nat Genet 46:498–502. doi: 10.1038/ng.2957

Sun T, Li X, Zhang P, et al (2015) Acetylation of Beclin 1 inhibits autophagosome maturation and promotes tumour growth. Nat Commun 6:7215. doi: 10.1038/ncomms8215

Takata T, Ishikawa F (2003) Human Sir2-related protein SIRT1 associates with the bHLH

repressors HES1 and HEY2 and is involved in HES1- and HEY2-mediated transcriptional repression. Biochem Biophys Res Commun 301:250–257. doi: 10.1016/S0006-291X(02)03020-6

Takayama K, Ishida K, Matsushita T, et al (2009) SIRT1 regulation of apoptosis of human chondrocytes. Arthritis Rheum 60:2731–40. doi: 10.1002/art.24864

Takeda-Watanabe A, Kitada M, Kanasaki K, Koya D (2012) SIRT1 inactivation induces inflammation through the dysregulation of autophagy in human THP-1 cells. Biochem Biophys Res Commun 427:191–196. doi: 10.1016/j.bbrc.2012.09.042

Tanida I (2011) Autophagy basics. Microbiol. Immunol. 55:1–11.

Tanno M, Sakamoto J, Miura T, et al (2007) Nucleocytoplasmic shuttling of the NAD+-dependent histone deacetylase SIRT1. J Biol Chem 282:6823–6832. doi: 10.1074/jbc.M609554200

Tepper S, Hochberg MC (1993) Factors associated with hip osteoarthritis: data from the First National Health and Nutrition Examination Survey (NHANES-I). Am J Epidemiol 137:1081–1088.

Thirunavukkarasu K, Pei Y, Wei T (2007) Characterization of the human ADAMTS-5 (aggrecanase-2) gene promoter. Mol Biol Rep 34:225–231. doi: 10.1007/s11033-006-9037-3

Thomas JT, Ayad S, Grant ME (1994) Cartilage collagens: strategies for the study of their organisation and expression in the extracellular matrix. Ann Rheum Dis 53:488–96. doi: 10.1136/ard.53.8.488

Tissenbaum H a, Guarente L (2001) Increased dosage of a sir-2 gene extends lifespan in Caenorhabditis elegans. Nature 410:227–30. doi: 10.1038/35065638

Tolle LB, Standiford TJ (2013) Danger-associated molecular patterns (DAMPs) in acute lung

injury. J. Pathol. 229:145–156.

Tortorella MD, Burn TC, Pratta MA, et al (1999) Purification and cloning of aggrecanase-1: a member of the ADAMTS family of proteins. Science (80-) 284:1664–1666. doi: 10.1126/science.284.5420.1664

Tsukazaki T, Matsumoto T, Enomoto H, Usa T, Ohtsuru A, Namba H, Iwasaki K YS (1994) Growth hormone directly and indirectly stimulates articular chondrocyte cell growth. Osteoarthr Cartil 2:259–67.

Uthman O a, van der Windt D a, Jordan JL, et al (2013) Exercise for lower limb osteoarthritis: systematic review incorporating trial sequential analysis and network meta-analysis. BMJ 347:f5555. doi: 10.1136/bmj.f5555

Valdes AM, Spector TD (2014) Genetics of osteoarthritis. In: Rheumatology: Sixth Edition. pp 1477–1482

Valdes AM, Spector TD (2009) The Contribution of Genes to Osteoarthritis. Med. Clin. North Am. 93:45–66.

van Saase JL, van Romunde LK, Cats a, et al (1989) Epidemiology of osteoarthritis: Zoetermeer survey. Comparison of radiological osteoarthritis in a Dutch population with that in 10 other populations. Ann Rheum Dis 48:271–280. doi: 10.1136/ard.48.4.271

Verdin E (2014) The many faces of sirtuins: Coupling of NAD metabolism, sirtuins and lifespan. Nat Med 20:25–7. doi: 10.1038/nm.3447

Verma RP, Hansch C (2007) Matrix metalloproteinases (MMPs): Chemical-biological functions and (Q)SARs. Bioorganic Med. Chem. 15:2223–2268.

Vincent TL, Watt FE (2014) Osteoarthritis. Medicine (Baltimore) 42:213–219. doi: 10.1016/j.mpmed.2014.01.010

Vincent TL, Williams RO, Maciewicz R, et al (2012) Mapping pathogenesis of arthritis through small animal models. Rheumatology (Oxford) 51:1931–41. doi: 10.1093/rheumatology/kes035

Vinciguerra M, Fulco M, Ladurner A, et al (2010) SirT1 in muscle physiology and disease: lessons from mouse models. Dis Model Mech 3:298–303. doi: 10.1242/dmm.004655

Wang C, Chen L, Hou X, et al (2006) Interactions between E2F1 and SirT1 regulate apoptotic response to DNA damage. Nat Cell Biol 8:1025–1031. doi: 10.1038/ncb1468

Wang JY, Johnson LR (1992) Luminal polyamines substitute for tissue polyamines in duodenal mucosal repair after stress in rats. Gastroenterology 102:1109–1117.

Wang RH, Li C, Deng CX (2010) Liver steatosis and increased ChREBP expression in mice carrying a liver specific SIRT1 null mutation under a normal feeding condition. Int J Biol Sci 6:682–690. doi: 10.7150/ijbs.6.682

Westling J, Fosang AJ, Last K, et al (2002) ADAMTS4 cleaves at the aggrecanase site (Glu373-Ala374) and secondarily at the matrix metalloproteinase site (Asn341-Phe342) in the aggrecan interglobular domain. J Biol Chem 277:16059–16066. doi: 10.1074/jbc.M108607200

Wieland H a, Michaelis M, Kirschbaum BJ, Rudolphi K a (2005) Osteoarthritis - an untreatable disease? Nat Rev Drug Discov 4:331–44. doi: 10.1038/nrd1693

Wluka AE, Cicuttini FM, Spector TD (2000) Menopause, oestrogens and arthritis. Maturitas 35:183–199.

Wong E, Cuervo AM (2010) Autophagy gone awry in neurodegenerative diseases. Nat Neurosci 13:805–11. doi: 10.1038/nn.2575

Woolf AD, Pfleger B (2003) Burden of major musculoskeletal conditions. Bull World Health Organ 81:646–656. doi: S0042-96862003000900007 [pii]

Wu Q, Huang JH, Sampson ER, et al (2009) Smurf2 induces degradation of GSK-3?? and upregulates ??-catenin in chondrocytes: A potential mechanism for Smurf2-induced degeneration of articular cartilage. Exp Cell Res 315:2386–2398. doi: 10.1016/j.yexcr.2009.05.019

Xiong S, Salazar G, Patrushev N, Alexander RW (2011) FoxO1 mediates an autofeedback loop regulating SIRT1 expression. J Biol Chem 286:5289–5299. doi: 10.1074/jbc.M110.163667

Yamakuchi M (2012) MicroRNA regulation of SIRT1. Front. Physiol. 3 MAR:

Yang X, Chen L, Xu X, et al (2001) TGF-??/Smad3 signals repress chondrocyte hypertrophic differentiation and are required for maintaining articular cartilage. J Cell Biol 153:35–46. doi: 10.1083/jcb.153.1.35

Yang Y, Fu W, Chen J, et al (2007) SIRT1 sumoylation regulates its deacetylase activity and cellular response to genotoxic stress. Nat Cell Biol 9:1253–1262. doi: 10.1038/ncb1645

Yuan XL, Meng HY, Wang YC, et al (2014) Bone-cartilage interface crosstalk in osteoarthritis: Potential pathways and future therapeutic strategies. Osteoarthr. Cartil. 22:1077–1089.

Zhang QJ, Wang Z, Chen HZ, et al (2008) Endothelium-specific overexpression of class III deacetylase SIRT1 decreases atherosclerosis in apolipoprotein E-deficient mice. Cardiovasc Res 80:191–199. doi: 10.1093/cvr/cvn224

Zhang Y, Niu J, Kelly-Hayes M, et al (2002) Prevalence of symptomatic hand osteoarthritis and its impact on functional status among the elderly: The framingham study. Am J Epidemiol 156:1021–1027. doi: 10.1093/aje/kwf141

Zhang Y, Vasheghani F, Li Y-H, et al (2014) Cartilage-specific deletion of mTOR upregulates autophagy and protects mice from osteoarthritis. Ann Rheum Dis 1–9. doi:

10.1136/annrheumdis-2013-204599

Zhao T, Li J, Chen AF (2010) MicroRNA-34a induces endothelial progenitor cell senescence and impedes its angiogenesis via suppressing silent information regulator 1. Am J Physiol Endocrinol Metab 299:E110–E116. doi: 10.1152/ajpendo.00192.2010

Zhen G, Wen C, Jia X, et al (2013) Inhibition of TGF-β signaling in mesenchymal stem cells of subchondral bone attenuates osteoarthritis. Nat Med 19:704–12. doi: 10.1038/nm.3143

Zhu H, Yang Y, Wang Y, et al (2011) MicroRNA-195 promotes palmitate-induced apoptosis in cardiomyocytes by down-regulating Sirt1. Cardiovasc Res 92:75–84. doi: 10.1093/cvr/cvr145